HIGHWAY RESEARCH BOARD

Bulletin 168

Fundamental and Practical Concepts of Soil Freezing

National Academy of Sciences—
National Research Council

publication 52

HIGHWAY RESEARCH BOARD

Officers and Members of the Executive Committee

1957

OFFICERS

REX M. WHITTON, *Chairman* C. H. SCHOLER, *First Vice Chairman*

HARMER E. DAVIS, *Second Vice Chairman*

FRED BURGGRAF, *Director* ELMER M. WARD, *Assistant Director*

Executive Committee

C. D. CURTISS, *Commissioner, Bureau of Public Roads*

A. E. JOHNSON, *Executive Secretary, American Association of State Highway Officials*

LOUIS JORDAN, *Executive Secretary, Division of Engineering and Industrial Research, National Research Council*

R. R. BARTELSMEYER, *Chief Highway Engineer, Illinois Division of Highways*

J. E. BUCHANAN, *President, The Asphalt Institute*

W. A. BUGGE, *Director of Highways, Washington State Highway Commission*

HARMER E. DAVIS, *Director, Institute of Transportation and Traffic Engineering, University of California*

DUKE W. DUNBAR, *Attorney General of Colorado*

FRANCIS V. DU PONT, *Consulting Engineer, Washington, D. C.*

PYKE JOHNSON, *Consultant, Automotive Safety Foundation*

KEITH F. JONES, *County Engineer, Jefferson County, Washington*

G. DONALD KENNEDY, *President, Portland Cement Association*

BURTON W. MARSH, *Director, Traffic Engineering and Safety Department, American Automobile Association*

GLENN C. RICHARDS, *Commissioner, Detroit Department of Public Works*

C. H. SCHOLER, *Head, Applied Mechanics Department, Kansas State College*

WILBUR S. SMITH, *Wilbur Smith and Associates*

REX M. WHITTON, *Chief Engineer, Missouri State Highway Department*

K. B. WOODS, *Head, School of Civil Engineering and Director, Joint Highway Research Project, Purdue University*

Editorial Staff

FRED BURGGRAF ELMER M. WARD HERBERT P. ORLAND

2101 Constitution Avenue Washington 25, D. C.

HIGHWAY RESEARCH BOARD

Bulletin 168

Fundamental and Practical Concepts of Soil Freezing

PRESENTED AT THE
Thirty-Sixth Annual Meeting
January 7-11, 1957

1957
Washington, D. C.

Department of Soils, Geology and Foundations

Frank R. Olmstead, Chairman
Chief, Soils Branch
Bureau of Public Roads

COMMITTEE ON FROST HEAVE AND FROST ACTION IN SOIL

George W. McAlpin, Chairman
Assistant Deputy Chief Engineer (Research)
New York State Department of Public Works

Dr. Harl P. Aldrich, Jr., Massachusetts Institute of Technology, Cambridge
Charles W. Allen, Research Engineer, Ohio Department of Highways, Columbus
Earl F. Bennett, c/o Koppers Company, Tar Products Division, Koppers Building, Pittsburgh 19, Pennsylvania
F. C. Brownridge, Materials and Research Engineer, Department of Highways, Parliament Buildings, Toronto, Ontario, Canada
C. B. Crawford, Soil Mechanics Section, Division of Building Research, National Research Council, Ottawa, Canada
Professor Ellis Danner, University of Illinois, Urbana
Dr. Hamilton Gray, Chairman, Department of Civil Engineering, Ohio State University, Columbus
L. E. Gregg, L. E. Gregg & Associates, Consulting Engineers, P.O. Box 1325, Lexington 29, Kentucky
Frank B. Hennion, Office, Chief of Engineers, Department of the Army, Washington, D. C.
Alfreds R. Jumikis, Professor of Civil Engineering, Rutgers University, New Brunswick, N. J.
Dr. Miles S. Kersten, University of Minnesota, Minneapolis
O. L. Lund, Assistant Engineer of Materials and Tests, Nebraska Department of Roads and Irrigation, Lincoln
A. E. Matthews, Engineer of Soils, Testing and Research Division, Michigan State Highway Department, Lansing
P. L. Melville, Soils Section, Airfields Branch, Engineering Division, Military Construction, Office, Chief of Engineers, Department of the Army, Washington, D.C.
Lloyd H. Morgan, Supervising Highway Engineer, Washington Department of Highways, Olympia
Paul S. Otis, Materials and Research Engineer, New Hampshire Department of Public Works & Highways, Concord
Andrew W. Potter, Materials Engineer, South Dakota Department of Highways, Pierre
C. K. Preus, Engineer of Materials and Research, Minnesota Department of Highways, St. Paul
James R. Schuyler, Assistant District Engineer, Soils, Soils and Subdrainage Section, New Jersey State Highway Department, Trenton
H. R. Smith, Manager, Calcium Chloride Section, Solvay Process Division, Allied Chemical and Dye Corporation, New York
K. B. Woods, Head, School of Civil Engineering and Director, Joint Highway Research Project, Purdue University, Lafayette, Indiana

Contents

Calculation of Maximum Pavement Temperatures From Weather Reports

EDWARD S. BARBER, Highway Physical Research Engineer
Bureau of Public Roads, Physical Research Branch

Pavement temperatures are of interest in connection with stabilization of bituminous surfaces, curing and curling of portland cement concrete, and moisture movements in any type of pavement.

This paper presents a relation between pavement temperature and wind, precipitation, air temperature, and solar radiation, as controlled by the thermal properties of the pavements.

● PAVEMENT temperatures are of interest in connection with stability of bituminous surfaces, curing and curling of portland cement concrete, and moisture movements in any type of pavement.

In order to extrapolate directly observed temperatures to other localities and times, it would be convenient if pavement temperatures were correlated with standard weather reports.

The following discussion presents a relation between pavement temperatures and the wind, precipitation, air temperature, and solar radiation as controlled by the thermal properties of the pavement.

THEORY

For a semi-infinite mass in contact with air at a temperature $T_M + T_V \sin 0.262\,t$, the 24-hour periodic temperature of the mass is (1):

$$T = T_M + T_V \frac{H e^{-xC}}{\sqrt{(H+C)^2 + C^2}} \sin\left(0.262t - xC - \arctan\frac{C}{H+C}\right) \quad \ldots\ldots (1)$$

in which

T = temperature of mass;
T_M = mean effective air temperature, F;
T_V = maximum variation in temperature from mean, F;
t = time from beginning of cycle, hours;
x = depth below surface, feet;
$H = h/k$;
h = surface coefficient, BTU per sq ft per hour, F;
k = conductivity, BTU per sq ft per hour, F per ft;
$C = \sqrt{0.131 \text{ per } c}$;
c = diffusivity, ft sq per hour $= \frac{k}{sw}$;
s = specific heat, BTU per pound F; and
w = density, pounds per cu ft.

Figure 1 shows how the surface temperature varies with the air temperature.

For forced convection including average reradiation (2)

$$h = 1.3 + 0.62v^{3/4} \quad \ldots\ldots (2)$$

where v = wind velocity, mph, the average wind velocity is about 7.2 mph giving $h = 4.0$.

The surface also receives heat by solar radiation as indicated in Figure 2. The effective air temperature to include solar radiation (3) may be taken as:

$$T_E = T_a + \frac{b\,I}{h} \quad \ldots\ldots (3)$$

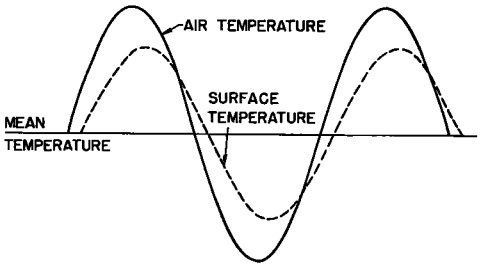

Figure 1. Surface temperature without radiation.

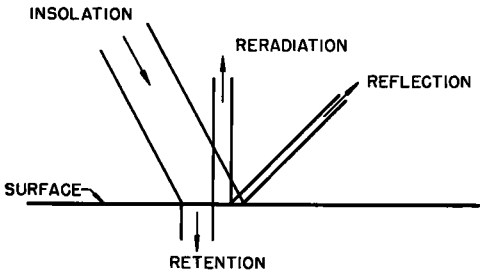

Figure 2. Distribution of insolation.

where T_E = effective air temperature, F;

T_a = air temperature, F;

b = absorptivity of surface to solar radiation;

I = solar radiation, BTU per sq ft hour.

The solar radiation received on a horizontal surface is reported in langleys per day or calories per square centimeter day, L, which is 3.69 BTU per sq ft day. There is an average net loss by long-wave reradiation (4) of about ⅓, so that R, the average contribution to effective air temperature, is:

$$R = 0.67b\ 3.69\,L/24\ h \quad \ldots\ldots (4)$$

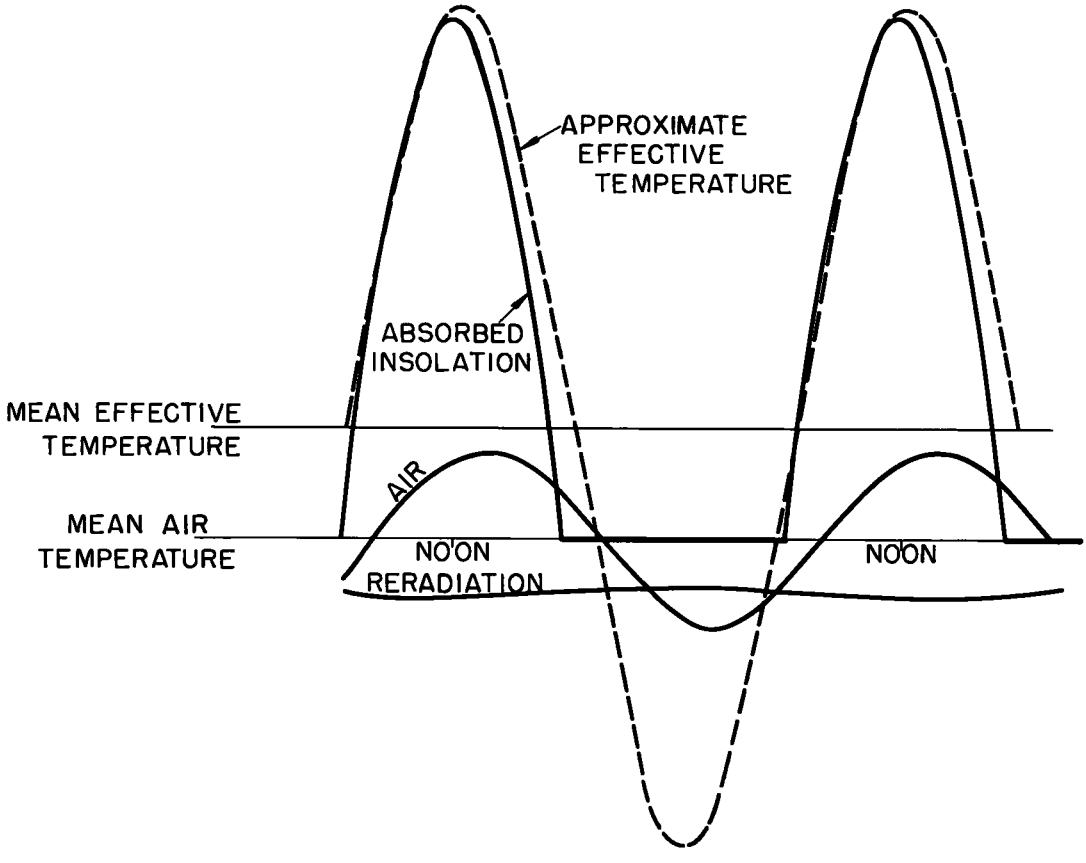

Figure 3. Effective temperature above horizontal surface.

The deviation of the radiation from this average may be roughly approximated by a sine wave with a half amplitude of 3R. Combining this with the air temperature, which is approximated by a sine wave with amplitude equal to the daily range in temperature, gives a sinusoidal effective temperature (see Figure 3). (A different curve is required for minimum temperature.) The maximum pavement temperature may then be calculated from equation 1, using

$$T_M = T_A + R \quad \ldots\ldots (5)$$

where T_A = average air temperature, F;

and

$$T_V = 0.5\, T_R + 3R \quad \ldots\ldots (6)$$

where T_R = daily range in air temperature, F.

After a rain the evaporation of water would considerably decrease the maximum temperatures due to insolation. For instance, the evaporation of 0.1 in. of water requires 0.1 x 2.54 x 539 = 137 calories per sq centimeter which is a considerable portion of a summer day's radiation.

COMPARISONS FOR BITUMINOUS PAVEMENT

Calculated values will be compared with those observed on the surface of a bituminous concrete pavement at Hybla Valley, Virginia, with the following considered assumptions:

h = 3.6 for a sheltered area;
k = 0.7 average value from texts;
s = 0.22 for dry stone plus asphalt;
w = 140 from field data; and
b = 0.95 for black surface.

These values give H = 5.14, c = 0.0227, C = 2.40 and R = 0.027 L. Substituting in equation 1, using equations 5 and 6, the maximum surface temperature (when sine function is one and x is zero) is

$$T_A + R + F(0.5\, T_R + 3R) \quad \ldots\ldots (7)$$

where $F = \dfrac{H}{\sqrt{(H+C)^2 + C^2}} = \dfrac{H \text{ per } C}{\sqrt{(H \text{ per } C+1)^2 + 1}}$ as tabulated below:

H per C	F
1	0.447
1.5	0.557
2	0.633
2.5	0.686
3	0.727
3.5	0.759
4	0.784
4.5	0.804
5	0.822

For H per C = 5.14 per 2.40 = 2.14, F = 0.65.

Table 1 shows the ambient conditions, the observed surface temperature and values calculated from the above formula. The agreement as shown in Figure 4 is generally good considering that L was measured 20 miles from the pavement. Where local temperatures are not available, more day to day deviation should be expected. In the present case, a weather station at another inland location reported similar temperatures, whereas one near the river reported consistently different temperatures.

Since equation 1 assumes that the cycle of temperatures has prevailed for a long time, a lag may be expected after a sudden change in T_M. Thus, when T_M changes

TABLE 1

CALCULATION OF MAXIMUM SURFACE TEMPERATURE OF BITUMINOUS PAVEMENT, HYBLA VALLEY, VIRGINIA

Date	Ambient Condition T_A	Ambient Condition T_R	L	Observed Surface Temp.	Calculated Values R	Calculated Values 0.65 (0.5 T_R + 3R)	Calculated Values Surface Temperature
1953	F	F	Lang.	F	F	F	F
May 21	69	28	526	122	14	37	120
22	71	18	270	103	7	20	98
23	70	7	616	118	17	35	122
24	61	31	479	113	13	35	109
25	68	25	268	104	7	22	97
26	74	29	462	122	12	34	120
27	60	12	494	106	13	30	103
28	50	32	747	116	20	50	120
29	56	37	715	126	19	50	125
30	64	30	381	118	10	30	104
July 31	84	20	526	133	14	34	132
Aug. 1	92	16	430	134	12	29	132
2	92	18	423	131	11	28	131
3	87	26	396	127	11	30	128
4	82	7	222	109	6	14	102
5	92	21	435	131	12	30	134

from 69 + 14 = 83 on May 21 to 71 + 7 = 78 on May 22, the observed temperature in Table 1 does not drop as much as calculated. Considering a sudden change in temperature, the lag, T_L, for large t and small x is (5):

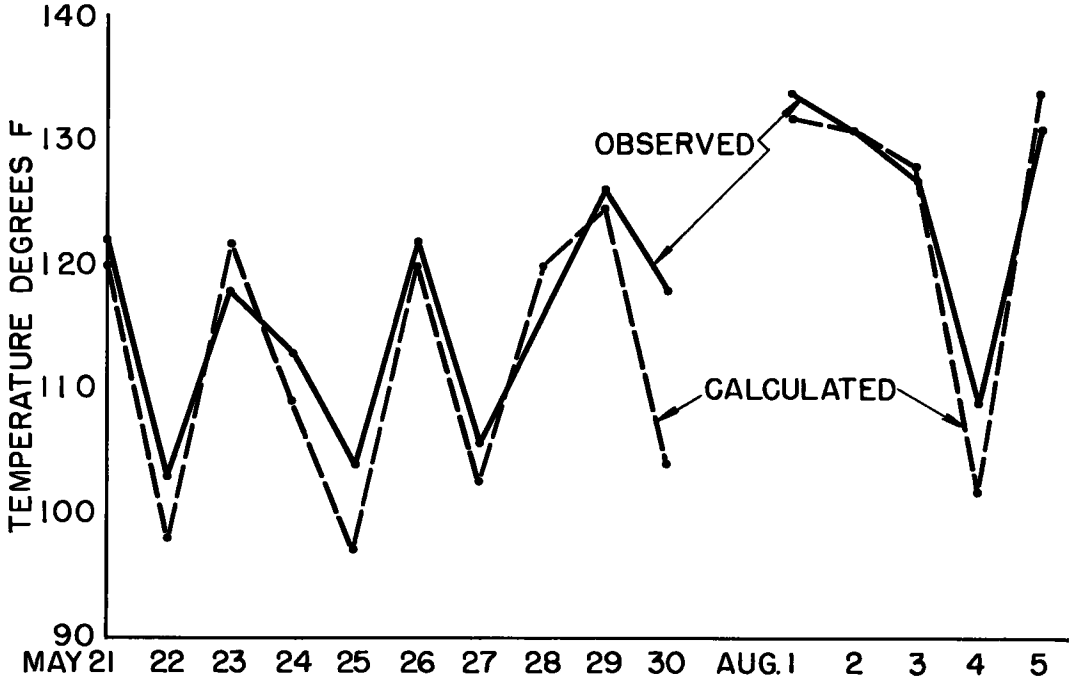

Figure 4. Bituminous pavement surface temperatures.

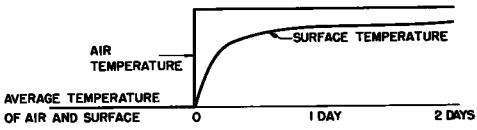

Figure 5. Lag in surface temperature.

$$T_L = \frac{x + 0.25}{\sqrt{\pi\, ct}} \quad \ldots\ldots\ldots\ldots (8)$$

At the surface after 24 hours, the lag is about $\frac{1}{5}$ the change in the mean, as illustrated in Figure 5, or 1 degree in the present case.

The larger deviations on May 25 and August 4 are probably due to less reradiation than the average because of clouds indicated by the low solar radiation received. The excessive deviation on May 30 is due to the fact that the radiation is averaged over the day in the calculations, whereas it was actually received before a rainstorm which started at 2:00 p. m.

TABLE 2

CALCULATED AND OBSERVED TEMPERATURES OF BITUMINOUS PAVEMENT IN IDAHO

Date	Ambient Condition T_A	Ambient Condition T_R	Ambient Condition L	Maximum Temperature ¼ in Below Surface Observed	Maximum Temperature ¼ in Below Surface Calculated
1953	F	F	Lang.	F	F
Sept 11	68	56	467	120	117
Oct. 19	52	21	325	68	80
Nov 19	22	30	233	48	48
Dec. 8	25	26	104	37	40
1954					
May 17	66	47	722	127	129

Using the same coefficients as above, except h = 4.4 for a bituminous pavement in an exposed location in Idaho, temperatures at a depth of ¼ in. were calculated and are shown in Table 2 compared to observed temperatures. From equation 1 the depth reduces the cyclic contribution by the factor $e^{-xC} = e^{-2.40 \text{ per } 48} = 0.95$, a reduction of 5 percent. The discrepancy in October is accounted for by clouds over the pavement which were not present at the nearest radiation station. The December calculated temperature is high because long-wave reradiation is under-estimated for winter months.

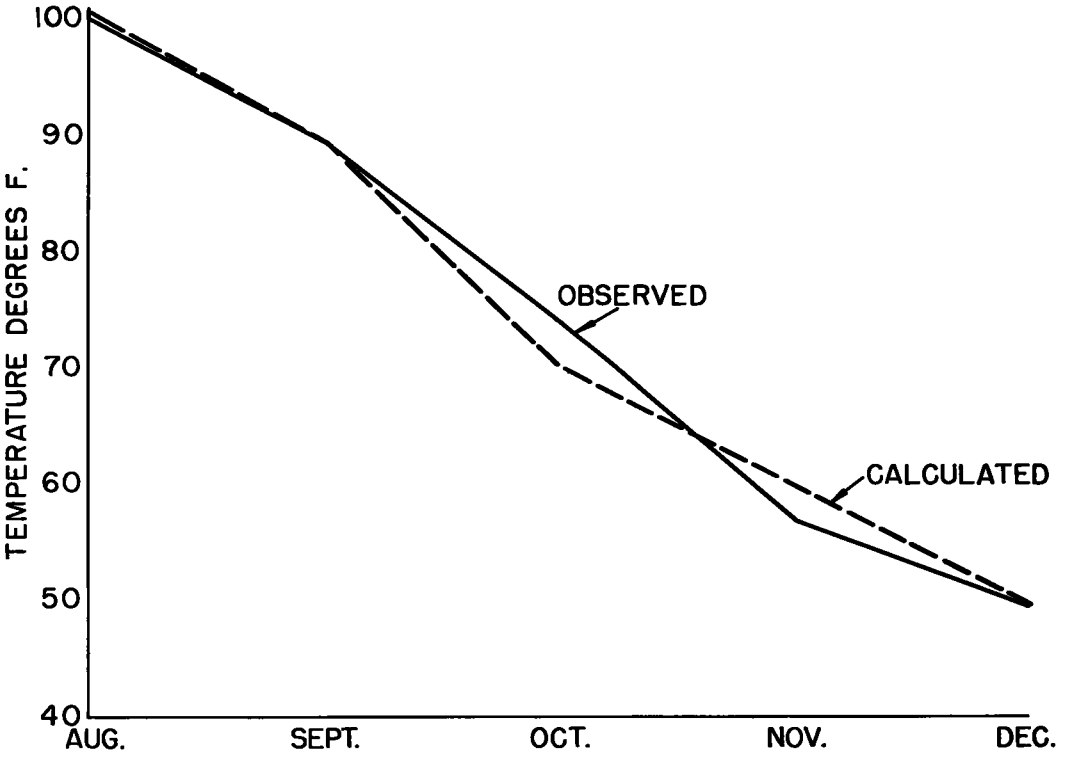

Figure 6. Average maximum temperatures--Bates road.

COMPARISON FOR CONCRETE PAVEMENT

Further comparison is available for two 6-in. portland cement concrete slabs at Langley, Virginia, to which the following values are assigned:

h = 4.4 for an exposed site;
s = 0.2 for good drainage; and
w = 150.

For sand and gravel concrete

k = 0.9 giving c = 0.030
b = 0.65 giving R = 0.015 L

For slag concrete

k = 0.45 giving c = 0.015
b = 0.70 giving R = 0.016 L.

TABLE 3

CALCULATION OF SURFACE TEMPERATURE OF PORTLAND CEMENT CONCRETE LANGLEY, VIRGINIA

	Ambient Conditions			Maximum Surface Temperature: Observed [a]		Maximum Surface Temperature: Calculated	
Date	T_A	T_R	L	Sand & Gravel	Slag	Sand & Gravel	Slag
1953	F	F	Lang	F	F	F	F
Aug 20	71	19	505	106	108	101	105
25	78	26	507	106	113	110	115
Sept 23	58	10	522	83	89	85	90

[a] 2 degrees added to off-peak readings

For the surface temperature equation 1 gives:

$T_A + R + 0.67\ (0.5\ T_R + 3R)$ for sand and gravel; and

$T_A + R + 0.75\ (0.5\ T_R + 3R)$ for slag.

Table 3 shows a reasonable correlation between observed and computed surface temperatures.

Table and Figure 6 show calculated and observed maximum temperatures for the Bates Road using locally observed temperatures (6) and monthly radiation values taken from published maps (7). The insolation is a function of season and latitude as

TABLE 4

CALCULATED AND OBSERVED MAXIMUM TEMPERATURES ON BATES ROAD

	Average Temperature for Normal Days						Calculated Pavement Temperature	
	Air			Pavement Maximum		Average		
Month	Max.	Min.	Ave.	Surface	3.5 in. Deep	Radiation	Surface	3.5 in. Deep
1922	F	F	F	F	F	Langleys	F	F
Aug.	87	59	73	100	95	470	100.5	92
Sept.	80	52	66	89.5	85	320	89.5	82
Oct.	65	36	50.5	74.5	69.5	270	70.5	63.5
Nov.	58	33	45.5	57	54	170	60	55
Dec.	49	29	39	49.5	45.5	120	50	46

shown in Figure 7 but modified by local atmospheric conditions. The radiation for "normal" days is taken as the average monthly radiation.

It is assumed that h = 4.8, c = 0.04, k = 1.2, b = 0.6 for poorly drained portland cement concrete, giving R = 0.013 L and maximum surface temperature equal

$$T_A + R + 0.66\ (0.5\ T_R + 3R)$$

Although equation 1 assumed homogeneous material, numerical calculations (8) indicate that a change of conductivity of as much as 50 percent below 7 in. (bottom of slab) has only a small effect on the temperature difference between the surface and a depth of 3.5 inches.

Table 5 shows a similar comparison for a concrete road in Kansas (9) using the same coefficients as assumed for sand and gravel concrete in Table 3.

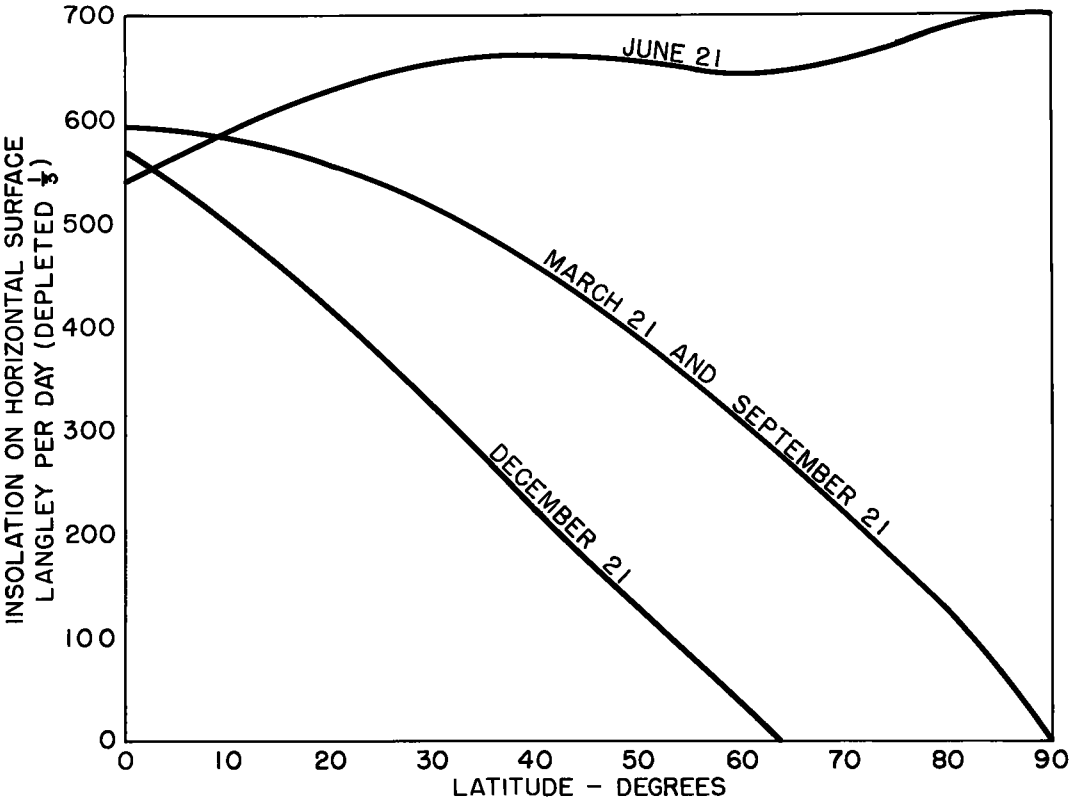

Figure 7. Insolation vs latitude.

TABLE 5

CALCULATED TEMPERATURE 1 INCH BELOW CONCRETE SURFACE IN KANSAS

Date 1940	T_A	T_R	L	Temp 1 in Below Surface, F	
				Observed	Calculated
	F	F	Lang		
July 30	89	22	750	126	126
Sept 20	74	18	540	105	101
Oct 17	58	26	420	83	82
Apr 27	63	22	690	96	97
June 26	83	18	790	120	120

CONCLUSIONS

The foregoing calculations indicate the possibility of roughly correlating surface temperatures with values reported by the Weather Bureau so that means are available to extrapolate field observed temperatures to other times and places. To calculate exact temperatures for a given structure, exact values of its thermal properties and the ambient conditions must be known.

REFERENCES

1. Carslaw, H.S. and Jaeger, J.C., "Conduction of Heat in Solids," Oxford Press, 1947, p. 56 Eq. 4.

2. Alford, T.S., Ryan, J.E., and Urban, F.O., "Effect of Heat Storage and Variation in Outdoor Temperature and Solar Intensity on Heat Transfer through Walls." Transactions, ASH & VE, Vol. 45, 1939, p. 384.

3. Mackey, C.O. and Wright, Jr., L.T., "Summer Comfort Factors as Influenced by the Thermal Properties of Building Materials," Transactions, ASH & VE, 1943, p. 150.

4. Johnson, J.C., "Physical Metereorology." John Wiley, 1954, p. 167.

5. Carslaw, H.S. and Jaeger, J.C., "Conduction of Heat in Solids," Oxford Press, 1947, p. 53.

6. "Report on the Bates Experimental Road Highway Research," State of Illinois, Department of Public Works, Division of Highways, May 1925.

7. "Heating and Ventilating," July 1949, p. 62, for average days; January 1949, p. 72, for cloudless days.

8. Dusinberre, G.M., "Numerical Analysis of Heat Flow," McGraw-Hill, 1949.

9. "Lawrence Experimental Concrete Pavement," State Highway Commission of Kansas, 1949.

Loss and Recovery of Bearing Capacity of 30 New Jersey Soil Materials as Determined by Field CBR Tests 1954-5

K. A. TURNER, JR., Assistant Research Specialist in Instrumentation, Bureau of Engineering Research, Rutgers University, New Brunswick, N. J.

During the winter of 1954-5 a study was made of the effects of frost action resulting from exposure to natural freeze-thaw conditions of prepared specimens of 30 New Jersey soil and subbase materials. This research was conducted by the Joint Highway Research Project, under the co-sponsorship of Rutgers University and the New Jersey State Highway Department.

One phase of this study was the determination of the loss of bearing capacity of each soil during the winter and its subsequent recovery during the following spring and summer.

The materials studied consisted of 22 soils, representing approximately 75 percent of the soil areas of New Jersey, and 8 subbase materials in use in highway construction. These materials had been compacted in 9-ft square pits, the soils to a depth of 2 ft and the subbase materials to a depth of 1 ft.

Because of the limited size of the soil specimens, the field CBR test was selected for the purpose of the bearing capacity study. The initial bearing ratio of each material was the average of three tests performed on each material after compaction in October. After the completion of these tests a 4-ft by 4-ft by 6-in. concrete slab was poured on each material for the frost-heave study and six 1-ft by 1-ft by 6-in. slabs for bearing test purposes. The small slabs were intended for removal at proper intervals to allow the performance of the field CBR tests on the soil beneath. Sufficient material was added to produce shoulders flush with the slab surfaces.

The program of field CBR testing was started in March. One small slab was removed from each material and three bearing tests performed on the soil beneath. Soil moisture contents were also determined. Two weeks were required to perform three tests on each of the 30 materials. At approximately one-month intervals additional sets of slabs were removed and tests performed. The last group of tests was completed in August.

Results showed little correlation between HRB classification and loss of bearing capacity expressed as percent of initial bearing capacity. A better correlation existed between HRB classification and the actual spring bearing capacity. Little correlation was noted between HRB classification and percent recovery of bearing capacity.

Variable climatic conditions during the two-week period required for each group of tests may make comparison among all of the materials unreliable.

During the recovery period the relationship between decreasing moisture content and increasing bearing capacity was apparent; the bearing ratios of many of the materials increased to a point considerably higher than their initial values.

The lack of control over natural climatic conditions evidenced in this study shows the desirability of conducting further bearing tests on soil specimens frozen and thawed under controlled laboratory conditions.

●DURING the winter of 1954-5 a study was made of the effects of frost action resulting from exposure to natural freeze-thaw conditions of 30 New Jersey soil and subbase

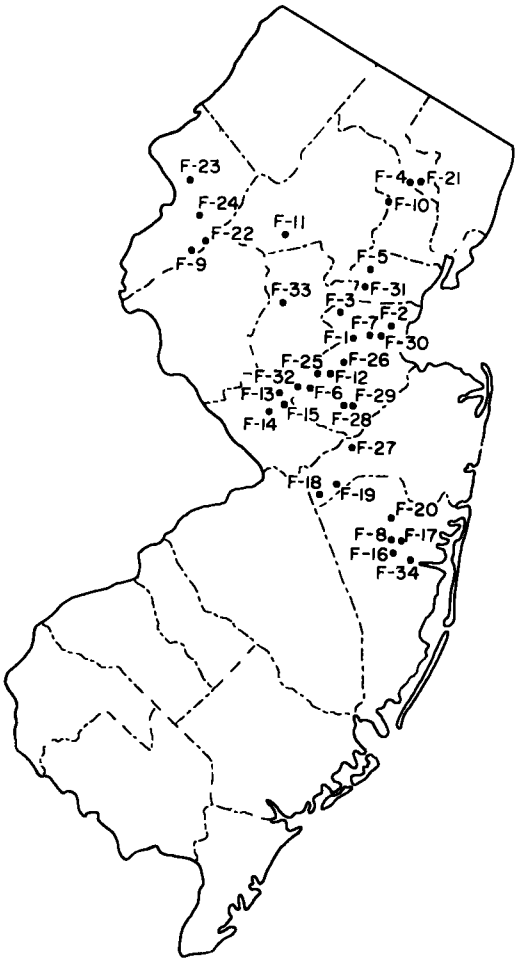

Figure 1. Map of New Jersey showing sample locations of soil and subbase materials used for frost action investigation.

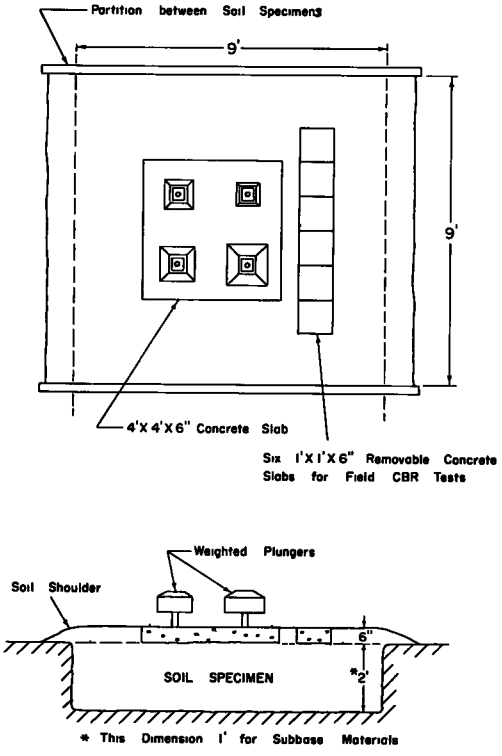

Figure 2. Soil installation.

materials. To simulate pavement conditions, concrete slabs were poured on prepared specimens of the materials under investigation. Daily vertical movement of the slabs during the winter was a measure of frost heave. Daily penetration of statically weighted plungers indicated loss of bearing capacity. Subsurface temperatures and moisture contents were measured in several of the soil materials.

To determine by an accepted method the total loss of bearing capacity of each material during the winter and the recovery of bearing capacity during the ensuing spring and summer, provision was made for the performance of field bearing tests. Because of the relatively limited size of the soil specimens and because of the availability of the required equipment, the field CBR test was selected for this purpose. An analysis of the data obtained from the performance of these tests is presented in this report.

DESCRIPTION OF FIELD INSTALLATION

Twenty-six soil materials, representing approximately 75 percent of the soil areas of New Jersey, were selected from various sites throughout the state. In addition, eight subbase materials in use in highway construction were suggested by the New Jersey State Highway Department (see Fig. 1 and Table 1). In order that all of the materials could be studied under similar environmental conditions a sample of each was brought to the field installation at Rutgers University.

A representative fraction of each sample was tested in the soil mechanics laboratory to determine its physical properties (Table 2). Grain size distribution curves of the materials have been given in HRB Bulletin 135 (1956), paper by K. A. Turner, Jr., and A. R. Jumikis, Appendix A to "Loss of Bearing Capacity and Vertical Displacements

TABLE 1

DESCRIPTION OF SOILS TESTED

F-1	A well-graded mixture of friable shale fragments from gravel to clay sizes Derived from Triassic shales The angular fragments might easily have been broken up by compacting them in the pits during placement of the sample
F-2	A sandy silt-clay mixture with considerable gravel Derived from glacial material of Triassic shale and sandstone origin
F-3	A silty sand with traces of gravel Derived from stratified glacial outwash, mostly Triassic rock fragments
F-4	A clay-silt-sand mixture with considerable gravel Derived from glacial drift, primarily gneiss and traprock
F-5	A sandy silt-clay mixture Derived from old glacial lake bed sediments
F-6	A silty, clayey sand with some gravel Derived from Coastal Plain sands and gravels
F-7	A gravelly sand with small amounts of silt and clay Derived from Coastal Plain sands and gravels
F-8	A fine sand with traces of silt and clay Derived from Coastal Plain sands and gravels
F-9	A clayey silt containing much sand Derived mostly from Kittatinny limestone
F-10	A mixture of coarse medium and fine sands, containing considerable gravel and some silt and clay Derived from gneissic glacial materials which have been reworked by water
F-11	A well-graded mixture of gravel, sand, silt and clay Derived from granitoid gneiss
F-12	A silt and clay mixture containing considerable sand with traces of gravel Derived from marine clays
F-13	A sandy gravel with considerable silt and clay Derived from basalt and diabase (Gravel is large angular fragments.)
F-14	A well-graded mixture of gravel, sand, silt and clay Derived from Triassic shale, sandstone and argillite
F-15	A well-graded sand-silt-clay mixture containing considerable gravel Derived from underlying Triassic shale, sandstone and argillite
F-16	A mixture of sands Derived from Coastal Plain sediments
F-17	A mixture of coarse, medium and fine sands with traces of gravel, silt and clay Derived from Coastal Plain sediments.
F-18	Medium fine sand containing considerable clay and silt Derived from the glauconitic formations of the upper Coastal Plain
F-19	A gravelly, silty, clayey sand Derived from the glauconitic upper Coastal Plain deposits
F-20	Sand containing considerable gravel and some silt and clay Derived from poorly drained Coastal Plain sediments (This material had a very high organic content)
F-21	A sand, silt and clay mixture with traces of gravel Derived from glacial deposits of basalt and diabase
F-22	A sandy silt-clay mixture containing considerable gravel Derived from early glacial drift
F-23	A well-graded gravel-sand-silt-clay mixture Derived from glaciated Martinsburg shale (Gravel consists of large, flat shale fragments)
F-24	A well-graded mixture of gravel, sands, silt and clay Derived from till containing much limestone
F-25	Coarse and medium sands containing considerable fine gravel and some silt and clay Subbase material
F-26	A medium sand with considerable gravel and some silt and clay Subbase material
F-27	Gravel containing considerable sand and some silt and clay Subbase material
F-28	A gravelly sand Subbase material
F-29	A sandy gravel Subbase material
F-30	A gravel and sand mixture containing numerous rounded shale particles Subbase material
F-31	A sandy gravel, essentially shale and sandstone Subbase material
F-32	Traprock screenings
F-33	A sandy gravel Subbase material
F-34	A sandy gravel Subbase material

of New Jersey Soils." Existing soil at the field installation was Penn soil, a predominantly silty soil classed as A-2-4 in the Highway Research Board classification because of a considerable percentage of soft shale fragments. Depth of soil to the parent material, Brunswick shale, was approximately 20 in.

The 26 soil materials were compacted in 6-in. layers in separate pits 9 ft square by 24 in. deep, the estimated maximum depth of frost penetration. The 8 subbase materials were compacted in similar pits 12 in. deep, as suggested by current construction practice. During the winter of 1954-5 only 22 of the soil materials and the 8 subbase materials were tested.

Three field CBR tests were performed on the surface of each of the materials. The initial bearing ratio of each material was the average value determined by the three tests. On each soil specimen was then poured a 4 ft by 4 ft by 6 in. thick concrete slab for the frost heave study and six 1 ft by 1 ft by 6 in. thick concrete slabs for bearing test purposes. The small slabs were intended for removal at proper intervals to allow the performance of the field CBR tests on the soil beneath. Sufficient material was added and compacted to produce shoulders flush with the concrete slabs. A completed soil installation is shown in Figure 2.

CLIMATIC CONDITIONS

A general evaluation, based on temperature, of the severity of the winter of 1954-5 was made by means of cold quantity determined by a degree-day method. U. S. Weather Bureau climatological data for the New Brunswick, N. J., weather station were used. The differences between the daily mean temperature and 32 F for the days that the mean was lower than 32 F were totaled for the period from September 1954 to April 1955. A cold quantity of 285 degree-days resulted. By comparison, the winter of 1947-8, a recent outstanding example of severity from the viewpoint of resulting extensive frost damage to pavements, had a cold quantity of 528 degree-days (Fig. 3). The winter of 1954-5 may be considered medium severe.

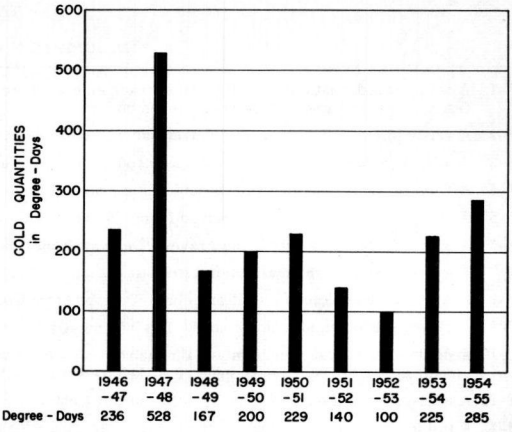

Figure 3. Cold quantities - New Brunswick weather station.

January and early February were characterized by an extended cold period having abnormally low precipitation. Subsurface temperature studies indicated the presence of frozen soil during this entire period. Rains and general thawing occurred in mid-February.

BEARING TESTS

The program of field CBR testing was started March 2. One small slab was removed from each material and three bearing tests were performed on the soil area beneath, the bearing ratio being the average of the three tests. The soil moisture content was taken as the average of three determinations.

Approximately two weeks were required to perform the three tests on each of the 30 materials. The cavities formed by the removal of the small slabs were filled with the respective materials after completion of the tests.

At approximately one-month intervals, weather permitting, additional small slabs were removed and bearing tests were performed on each material. The last group of tests was completed in August 1955.

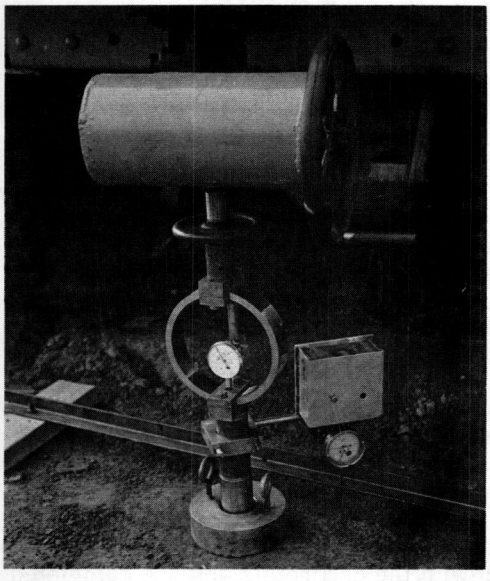

Figure 4. Field CBR test.

TEST PROCEDURE

Figure 4 shows a field CBR test in progress. Following is a description of the required equipment and the test procedure.

List of Equipment

1. CBR truck: A loaded vehicle equipped with spring locking clamps, stabilizers, and a jack mounting plate on the tailbeam.
2. Penetration jack: A screw-type jack equipped with a ball adjustment joint to provide for leveling and a handwheel for operation.
3. 5,000-lb test ring with 0.0001-in. dial indicator.
4. Penetration piston having a 3-sq in. circular face.
5. Assorted threaded extensions for the penetration piston.

6. 10-lb annular surcharge weight.
7. 0.001-in. penetration dial indicator equipped with clamp and timing device consisting of a clockwork-actuated pointer turning at a rate of ½ rpm which is superimposed over the face of the dial indicator.
8. Steel angle for reference point.
9. Wrenches for assembly of equipment.
10. Shovel and trowel for preparation of test area.
11. Data sheets.
12. Moisture content equipment.

TABLE 2

ENGINEERING SOIL PROPERTIES

Sample No.	Agronomic Name (as mapped 1917-27)	Soil Test Results: Sieve Analysis Percent Passing					Hyd Silt Sizes	Anal Clay Sizes	Atterberg Test		Proctor		Uniform. Coef. D_{60}/D_{10}	Eff. Grain Size	HRB Classification	
		¾	4	10	40	200			L.L	P.I	Max Dens	Opt M C			Sub-grade Group	Group Index
1	2	3	4	5	6	7	8	9	10	11	12	13	14	15	16	17
							%	%	%	%	pcf	%				
F-1	Penn	94	76	63	46	35	16	19	31	7	106	17	850.0	.002	A-2-4	0
F-2	Wethersfield	94	86	82	64	43	19	23	32	16	119	13	360.0	.001	A-6	3
F-3	Dunellen	100	98	95	76	27	--	--	16	0	120	12	33.3	--	A-2-4	0
F-4	Gloucester	100	90	86	79	56	31	21	25	6	109	16	73 3	.0015	A-4	4
F-5	Whippany	100	100	100	98	83	43	37	41	7	100	22	50 0	--	A-5	8
F-6	Sassafras	99	95	93	79	42	20	21	28	12	117	14	16.7	0015	A-6	2
F-7	Sassafras	88	67	61	28	7	--	--	NL	NP	120	12	12.0	.15	A-1-b	0
F-8	Sassafras	100	100	98	78	4	--	--	NL	NP	106	15	1 9	.16	A-3	0
F-9	Hagerstown	100	99	98	92	83	40	34	43	20	101	20	51.1	--	A-7-6	13
F-10	Merrimac	100	90	77	41	11	--	--	NL	NP	125	9	11 4	.07	A-1-b	0
F-11	Chester	89	74	70	55	46	26	16	33	11	109	18	30.4	023	A-6	2
F-12	Elkton	99	97	95	89	79	45	31	28	10	108	16	113.3	--	A-4	8
F-13	Montalto	91	80	58	46	28	9	19	32	9	114	17	360.0	.03	A-2-4	0
F-14	Croton	97	80	73	68	64	23	27	41	21	100	21	233.3	--	A-7-6	15
F-15	Lansdale	99	87	85	69	55	21	32	41	15	95	26	283.3	--	A-7-6	6
F-16	Lakewood	100	100	100	73	1	--	--	NL	NP	102	15	2.2	.16	A-3	0
F-17	Lakewood	100	99	98	64	3	--	--	NL	NP	106	14	2.8	15	A-3	0
F-18	Collington	100	100	100	80	26	10	15	32	8	105	23	166.7	.0018	A-2-4	0
F-19	Collington	96	91	87	69	39	12	18	48	14	97	27	113 7	--	A-7-5	2
F-20	Portsmouth	99	87	84	56	7	--	--	NL	NP	118	10	3.7	.13	A-3	0
F-21	Holyoke	99	98	96	89	60	32	20	27	12	116	14	40 0	.002	A-6	6
F-22	Washington	93	88	85	76	64	25	36	31	10	104	18	130.0	--	A-4	6
F-23	Dutchess	93	84	72	61	52	26	18	31	9	110	15	22.5	.0016	A-4	3
F-24	Dover	82	72	66	54	37	20	14	31	9	112	16	400 0	.0025	A-4	0
F-25	Subbase Sand Hills	97	96	93	54	6	--	--	NL	NP	106	15	2 7	.17	A-3	0
F-26	Subbase Farrington	93	86	78	36	10	--	--	NL	NP	120	12	8.8	.08	A-1-b	0
F-27	Subbase Perrinville	85	48	40	24	10	3	6	NL	NP	122	12	58.3	.12	A-1-a	0
F-28	Subbase Bot. Jamesburg	94	78	71	41	2	--	--	NL	NP	108	16	2 7	.26	A-1-b	0
F-29	Subbase Top Jamesburg	87	35	26	12	3	--	--	NL	NP	123	10	26.5	.4	A-1-a	0
F-30	Subbase Nixon	89	66	48	17	4	--	--	NL	NP	119	13	17.5	.2	A-1-a	0
F-31	Zimmerman Pit Westfield	74.5	53.6	46.4	9.3	2	--	--	NL	NP	112 3	13	26.5	.4	A-1-a	0
F-32	Kingston Traprock Screening	100	97.5	84.4	40 7	15	--	--	NL	NP	131.3	10	19	--	A-1-b	0
F-33	Franklin Pit North Branch	83.9	52.3	44 4	22	3	--	--	NL	NP	122.4	12	41.7	.24	A-1-a	0
F-34	Whitt Pit Toms River	97.4	55.6	39.4	8.7	1	--	--	NL	NP	115	13	14.4	.45	A-1-a	0

Preparation of Test Area

The test area was prepared by carefully smoothing and leveling an area at least 12 in. in diameter at the required depth in the soil to be tested. Soil might be removed to accomplish this, but none was added.

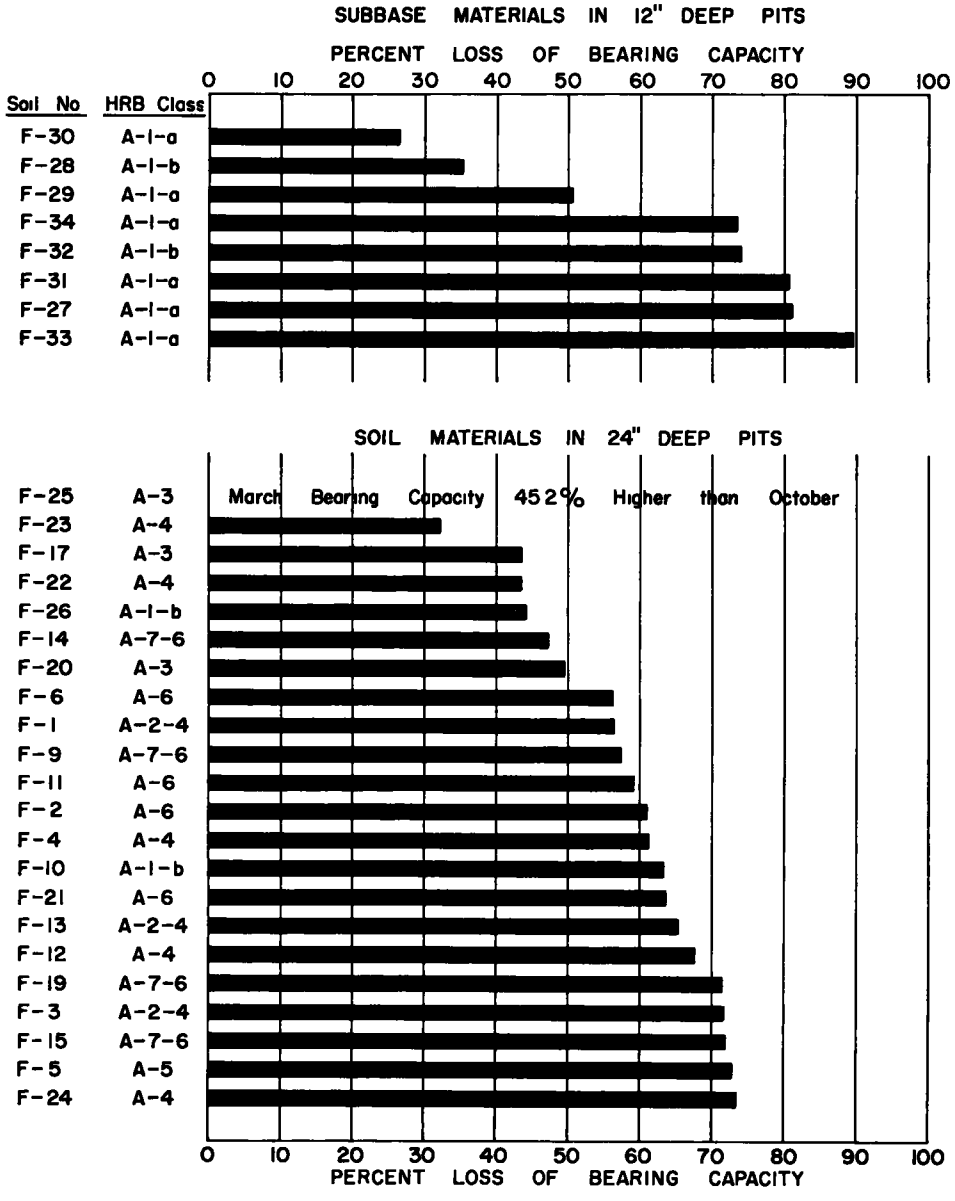

Figure 5. Percent loss of bearing capacity of subbase and soil materials during the winter of 1954-5.

Positioning of Vehicle

The CBR truck was backed into position so that the center of the jack mounting plate was over the center of the test area. The spring locking clamps were assembled and tightened with just enough tension to prevent expansion of the springs. The stabilizers were mounted and adjusted to prevent sideward movement of the truck.

Assembly of Test Equipment

The penetration jack was bolted to its mounting plate and the test ring screwed onto the jack spindle. The locking ring of the ball adjustment joint was loosened and the jack leveled so that the axis of its spindle was vertical. The locking ring was then tightened.

TABLE 3

PERCENT LOSS AND RECOVERY OF BEARING CAPACITY

Order No. Order No.	Soil No.	HRB Class.	October 1954 CBR (Initial)	March 1955 CBR	Percent Loss of Bearing Capacity
		(a) Subbase Materials in 12-in. Deep pits			
1	F-30	A-1-a	6.0	4.4	26.7
2	F-28	A-1-b	5.4	3.5	35.2
3	F-29	A-1-a	7.9	3.9	50.6
4	F-34	A-1-a	15.5	4.1	73.5
5	F-32	A-1-b	29.9	7.8	73.9
6	F-31	A-1-a	17.1	3.4	80.1
7	F-27	A-1-a	41.8	8.0	80.9
8	F-33	A-1-a	37.6	3.9	89.6
		(b) Soil Materials in 24-in. Deep Pits			
1	F-25	A-3	3 1	4.5	+45.2
2	F-23	A-4	6.5	4.4	32.3
3	F-17	A-3	6.2	3.5	43.6
4	F-22	A-4	5.5	3.1	43.6
5	F-26	A-1-b	12.7	7.1	44.1
6	F-14	A-7-6	3.6	1.9	47.2
7	F-20	A-3	9.3	4.7	49.8
8	F-6	A-6	5.5	2.4	56.3
9	F-1	A-2-4	6.2	2.7	56.4
10	F-9	A-7-6	4.2	1.8	57.2
11	F-11	A-6	7.7	3.1	59.7
12	F-2	A-6	4.1	1.6	61.0
13	F-4	A-4	6.2	2.4	61.3
14	F-10	A-1-b	10.7	3.9	63.5
15	F-21	A-6	6.9	2.5	63.8
16	F-13	A-2-4	14.3	5.0	65.1
17	F-12	A-4	5.6	1.8	67.8
18	F-19	A-7-6	8.1	2.3	71.6
19	F-3	A-2-4	11.0	3.1	71.8
20	F-15	A-7-6	8.2	2.3	71.9
21	F-5	A-5	4.8	3.1	72.9
22	F-24	A-4	8.4	1.4	83.3

The jack was retracted as far as possible. The proper combination of threaded extensions was selected and mounted on the test ring, leaving sufficient space for the penetration piston.

The penetration piston was inserted in the hole in the annular surcharge weight and the two placed carefully on the prepared soil area. The piston was then screwed up into the extension.

The test ring dial indicator was zeroed and the penetration piston lowered nearly into contact with the soil. Rapid movement of the jack was accomplished by releasing the spindle lock and rotating the spindle.

The timer was wound if necessary. The penetration dial indicator and timer were then clamped to the piston and the reference angle positioned so that the stem of the indicator was in proper contact.

The penetration piston was then seated on the soil with a 10-lb load (1.8 divisions of

the ring dial). Downward movement of the piston was produced by clockwise rotation of the jack handwheel. The penetration and ring dials were then zeroed.

Performance of Penetration Test

The penetration test was started when the red timer pointer reached the black penetration dial pointer. The jack handwheel was turned at such a rate as to keep the two pointers synchronized. This produced a penetration rate of 0.05 in. per minute.

The ring dial was read at penetrations of 0.025, 0.050, 0.075, 0.10, 0.20, 0.30, 0.40 and 0.50 inches. After a penetration of 0.50 in. had been reached, the piston was backed off by releasing the spindle lock. The moisture content of the soil at the test area was then determined.

Bearing Ratio Determination

The results of the penetration test were plotted as a curve with the piston load as ordinate and penetration as abscissa. A correction was made to the point of zero penetration if, as a result of surface irregularities of the soil, the initial portion of the curve was concave upward. The straight portion of the curve was extended downward, its intersection with the zero load line defining the corrected point of zero penetration.

TABLE 4

MARCH, 1955, BEARING RATIOS

Order No.	Soil No.	HRB Class.	March 1955 CBR
(a) Subbase Materials in 12-in. Deep Pits			
1	F-27	A-1-a	8.0
2	F-32	A-1-b	7.8
3	F-30	A-1-a	4.4
4	F-34	A-1-a	4.1
5	F-29	A-1-a	3.9
6	F-33	A-1-a	3.9
7	F-28	A-1-b	3.5
8	F-31	A-1-a	3.4
(b) Soil Materials in 24-in Deep Pits			
1	F-26	A-1-b	7.1
2	F-13	A-2-4	5.0
3	F-20	A-3	4.7
4	F-25	A-3	4 5
5	F-23	A-4	4.4
6	F-10	A-1-b	3.9
7	F-17	A-3	3.5
8	F-3	A-2-4	3.1
9	F-22	A-4	3.1
10	F-5	A-5	3 1
11	F-11	A-6	3.1
12	F-1	A-2-4	2.7
13	F-21	A-6	2.5
14	F-4	A-4	2.4
15	F-6	A-6	2.4
16	F-15	A-7-6	2 3
17	F-19	A-7-6	2.3
18	F-14	A-7-6	1.9
19	F-12	A-4	1.8
20	F-9	A-7-6	1.8
21	F-2	A-6	1.6
22	F-24	A-4	1.4

The bearing ratio was then determined at penetrations of 0.10 and 0.20 in., measured from the corrected zero point. The piston loads were divided by 1,000 and 1,500 psi, respectively, the accepted bearing values of crushed rock, and multiplied by 100 to give the bearing ratio in percent. The larger value was selected as the bearing ratio.

EVALUATION OF DATA

After completion of all bearing ratios and moisture content determinations, a chart was prepared for each soil (see Appendix) showing the relationship between time and the following:

1. Precipitation, presented as a bar graph. Data were obtained from the U.S. Weather Bureau climatological data for the New Brunswick, N.J., weather station.
2. Soil moisture content, the average of three determinations at the time of each bearing test.
3. CBR, the bearing ratio determined at approximately one-month intervals.
4. Percent of October (1954) bearing capacity. The initial bearing ratio determined in October was regarded as 100 percent bearing capacity, and the percentage bearing capacities from subsequent tests determined accordingly.

It should be noted that for convenience the period from December 1954 to February 1955, during which no tests were performed, has been condensed on the charts.

OBSERVATIONS

Comparison of the three tests used for each bearing capacity determination revealed that any error introduced by performing three tests within a 1-ft square area was ap-

TABLE 5

RECOVERY OF BEARING CAPACITY

Order No.	Soil No.	HRB Class.	October 1954 CBR (Initial)	July 1955 CBR	July Percentage of Initial
		(a) Subbase Materials in 12-in. Deep Pits			
1	F-29	A-1-a	7.9	9.5	120.2
2	F-33	A-1-a	37.6	26.3	69.9
3	F-28	A-1-b	5.4	3.6	66.7
4	F-31	A-1-a	17.1	9.8	57.3
5	F-32	A-1-b	29.9	16.8	56.2
6	F-30	A-1-a	6.0	3.3	55.0
7	F-34	A-1-a	15.5	5.3	34.2
8	F-27	A-1-a	41.8	11.2	26.8
		(b) Soil Materials in 24-in. Deep Pits			
1	F-2	A-6	4.1	7.7	187.8
2	F-1	A-2-4	6.2	11.1	179.0
3	F-9	A-7-6	4.2	6.6	157.2
4	F-5	A-5	4.8	7.4	154.1
5	F-14	A-7-6	3.6	5.4	150.0
6	F-12	A-4	5.6	8.1	144.7
7	F-26	A-1-b	12.7	15.3	120.5
8	F-21	A-6	6.9	8.1	117.4
9	F-13	A-2-4	14.3	16.3	114.0
10	F-25	A-3	3.1	3.4	109.7
11	F-4	A-4	6.2	6.5	104.9
12	F-6	A-6	5.5	5.7	103.6
13	F-23	A-4	6.5	6.7	103.1
14	F-10	A-1-b	10.7	9.4	87.8
15	F-22	A-4	5.5	4.4	80.0
16	F-15	A-7-6	8.2	6.5	79.3
17	F-19	A-7-6	8.1	5.4	66.7
18	F-20	A-3	9.3	5.9	63.4
19	F-17	A-3	6.2	3.9	62.8
20	F-11	A-6	7.7	3.8	49.4
21	F-3	A-2-4	11.0	4.8	43.7
22	F-24	A-4	8.4	3.4	40.5

parently less than that inherent in the soil itself as a result of existing non-homogeneity. Compaction of the surrounding soil, if caused by one test, should result in a higher bearing ratio of a subsequent test. As no such relation was found, it is felt that the procedure of performing three tests within such a small area is justified.

In Table 3 the materials are listed in order from the least to the greatest percentage loss of bearing capacity. The subbase materials and soil materials are grouped separately because of the environmental differences induced by the 12-in. and 24-in. deep pits. The percentage loss of bearing capacity of each material is shown in Figure 5. It is apparent that there is not much correlation between HRB classification and percentage loss of bearing capacity. The granular A-1-6 and A-3 materials in 24-in. deep pits show in general less loss than most of the other materials. F-25, HRB A-3, was the only material showing an increase in bearing ratio. This material had the lowest bearing ratio of all the materials in October as a result of its dry condition.

It should be noted, however, that the percentage losses of bearing capacity of the granular A-1-a and A-1-b subbase materials in 12-in. deep pits are greater than the losses of most of the materials in 24-in. deep pits. This is probably a result of the detrimental effect of poorer drainage conditions in the shallow pits.

In Table 4 the materials are presented in order from the greatest to the least bearing capacity as determined by their March 1955 bearing ratios. It is noted here that a better correlation exists between HRB classification and spring bearing capacity than between HRB classification and percent loss of bearing capacity.

Recovery of bearing capacity is indicated in Table 5. The materials are listed in order according to the July 1955 bearing ratio percentages of the initial October 1954 bearing ratios. Again, there is little apparent relationship between HRB classification and percent recovery of bearing capacity. Of interest is the fact that during the summer the bearing ratios of many of the materials increased to a point considerably higher than their initial values. It should be noted, however, that as a result of variable climatic conditions during the two-week period required for each group of field CBR tests a direct comparison among all of the materials may be unreliable.

The curves in the Appendix show the effect of moisture content upon bearing ratio, particularly during the recovery period. As moisture content decreased bearing ratio increased.

The effect of the heavy rains in early August is of particular note. Recorded precipitation during a six-day period was 10.95 in. Some of the August tests were performed prior to this period. As a result of a July drought, moisture contents were low and many bearing ratios showed great increases. Soil F-6, HRB A-6, showed the maximum increase, its August 1955 bearing ratio being 516 percent of its October 1954 bearing ratio. The soils tested after the rains showed increased moisture contents and bearing ratios reduced, in some cases considerably below their July values.

CONCLUSIONS

1. A considerable reduction in soil bearing capacity may occur during the winter as a result of the combined effects of freeze-thaw conditions and precipitation.
2. There is little correlation between HRB classification and percentage reduction in bearing capacity, but in general under equivalent conditions granular soils retain the highest bearing capacities.
3. The greater percentage reduction of bearing capacity in the shallow pits shows the importance of sufficient thickness of subbase material and of adequate facilities for drainage.
4. The recovery of bearing capacity is variable, showing little relation to HRB classifications. Many materials show a recovery of bearing capacity considerably greater than their initial values.
5. For any soil there is a definite relationship between moisture content and bearing capacity, the higher bearing capacities being associated with low moisture contents.
6. Considerable reduction of soil bearing capacity may result from excessive precipitation, even in summer.
7. Because of the lack of control of natural climatic conditions it would be desirable also to conduct bearing capacity tests on soil specimens frozen and thawed under controlled conditions in the laboratory.

ACKNOWLEDGMENT

The research covered by this report was conducted by the Joint Highway Research Project under the co-sponsorship of Rutgers University and the New Jersey State Highway Department. The author wishes to express his appreciation for the support and guidance of Alfreds R. Jumikis, Professor of Civil Engineering and Supervisor of the Joint Highway Research Project, and for the assistance of the members of the Project who performed many of the necessary tests.

Appendix

Curves showing precipitation, soil moisture content, and loss and recovery of bearing capacity of 39 New Jersey soil and subbase materials, 1954-5.

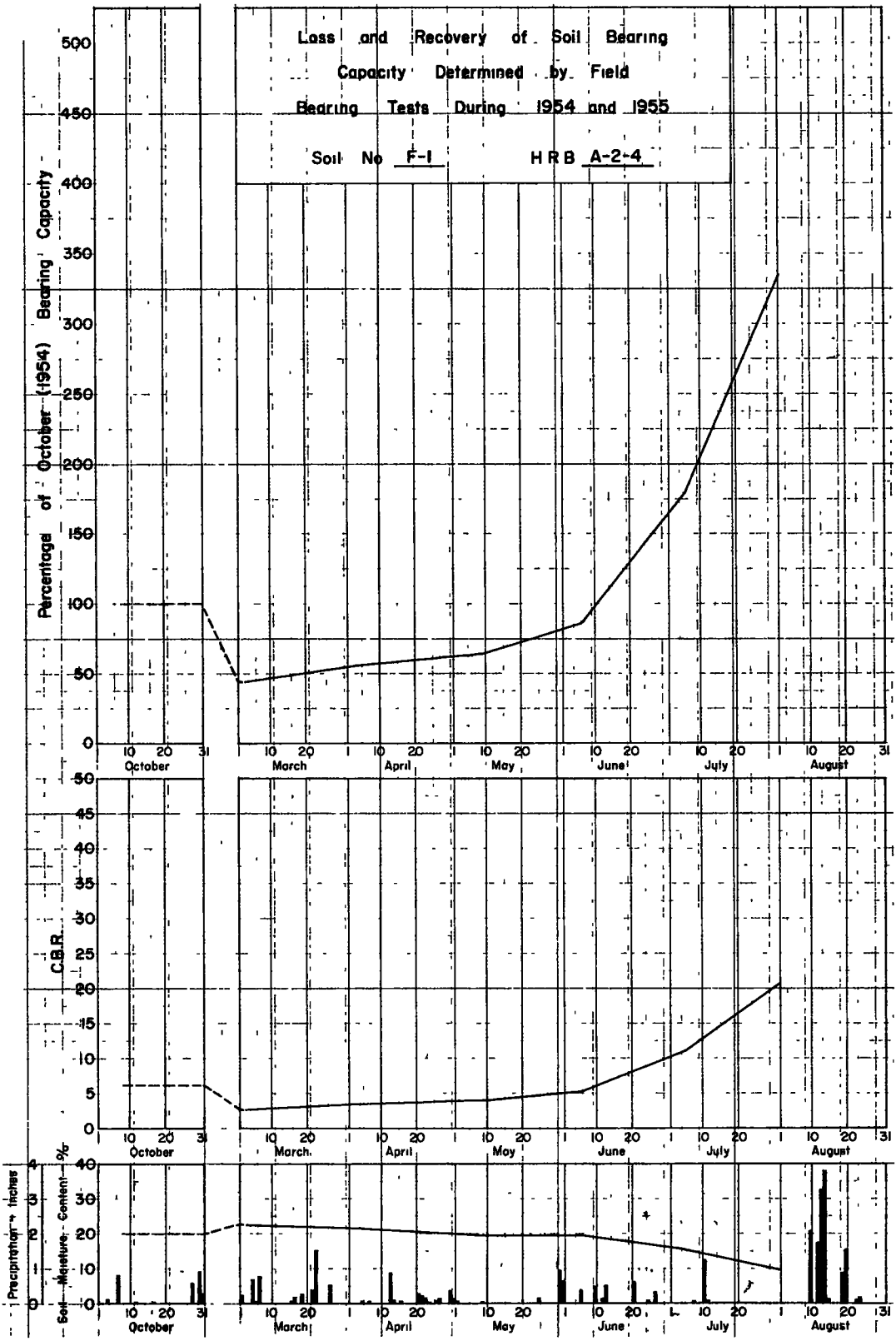
Loss and Recovery of Soil Bearing Capacity Determined by Field Bearing Tests During 1954 and 1955
Soil No F-1
H R B A-2-4
Percentage of October (1954) Bearing Capacity
C.B.R.
Precipitation - Inches
Soil Moisture Content - %
October
March
April
May
June
July
August

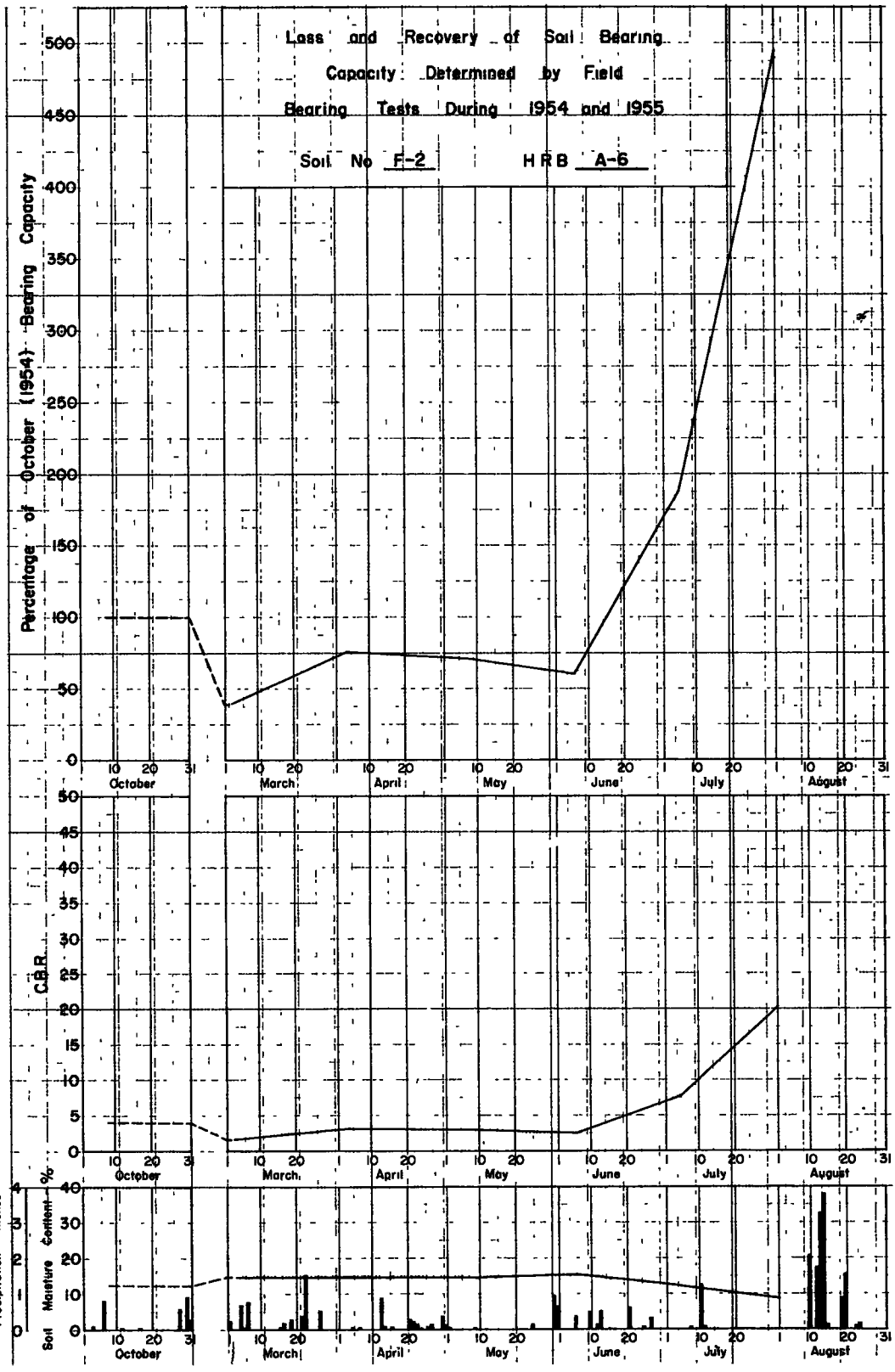
Loss and Recovery of Soil Bearing Capacity Determined by Field Bearing Tests During 1954 and 1955
Soil No F-2
HRB A-6
Percentage of October (1954) Bearing Capacity
C.B.R.
Soil Moisture Content—%
Precipitation — Inches
October
March
April
May
June
July
August

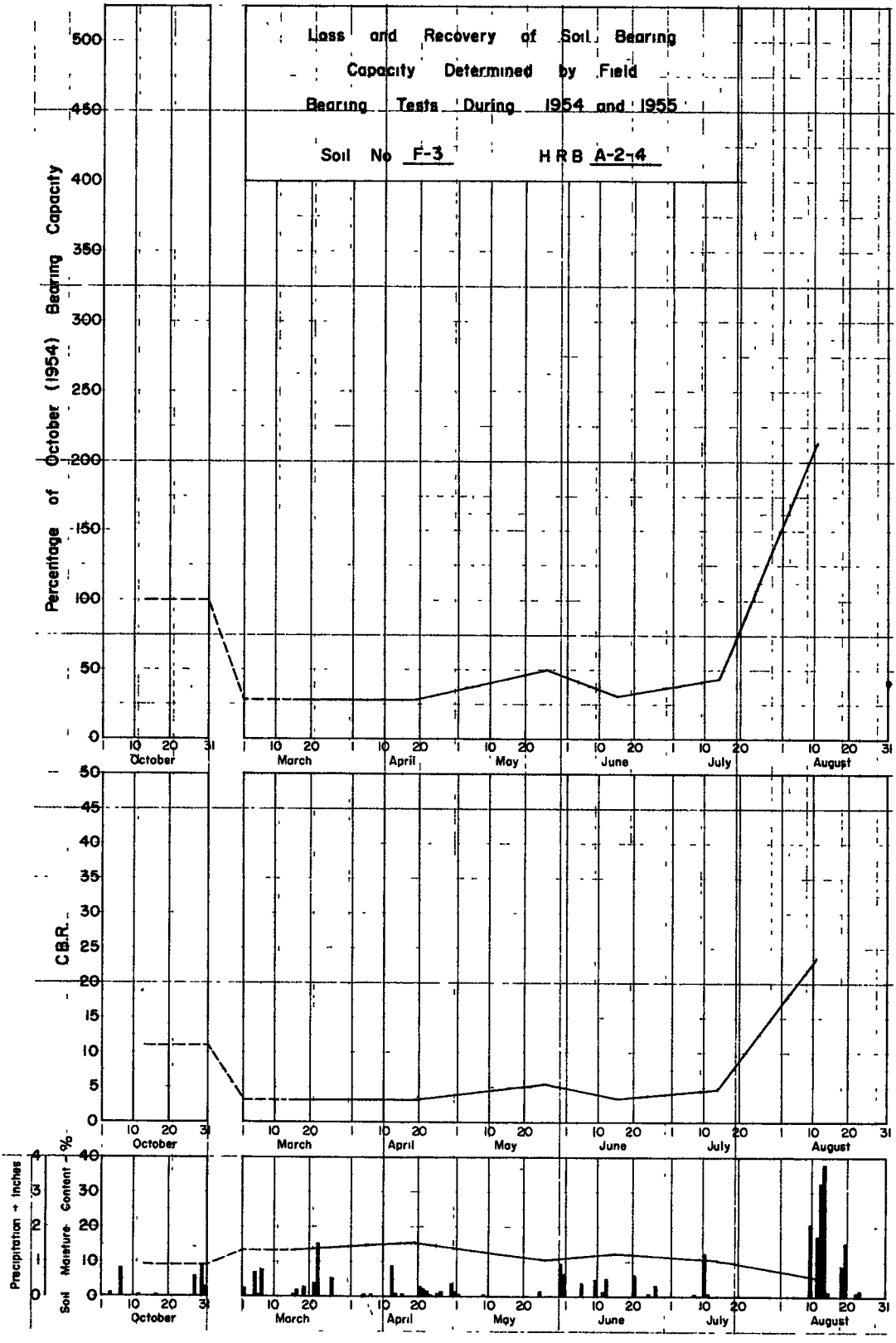
Loss and Recovery of Soil Bearing Capacity Determined by Field Bearing Tests During 1954 and 1955
Soil No F-3
HRB A-2-4
Percentage of October (1954) Bearing Capacity
C.B.R.
Precipitation - Inches
Soil Moisture Content - %
October
March
April
May
June
July
August

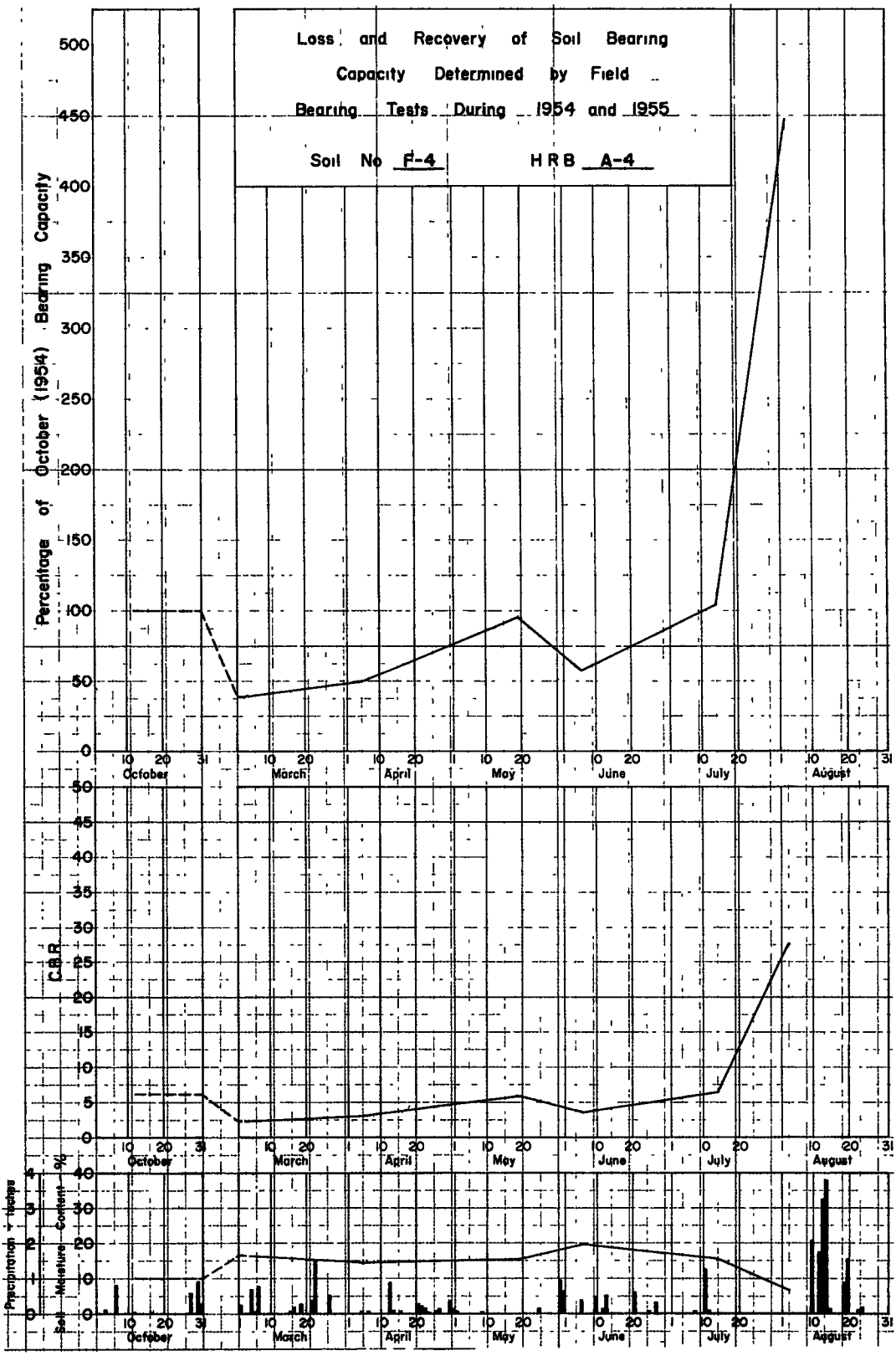
Loss and Recovery of Soil Bearing Capacity Determined by Field Bearing Tests During 1954 and 1955
Soil No F-4
H R B A-4
Percentage of October (1954) Bearing Capacity
C.B.R.
Precipitation + Inches
Soil Moisture Content %
October
March
April
May
June
July
August

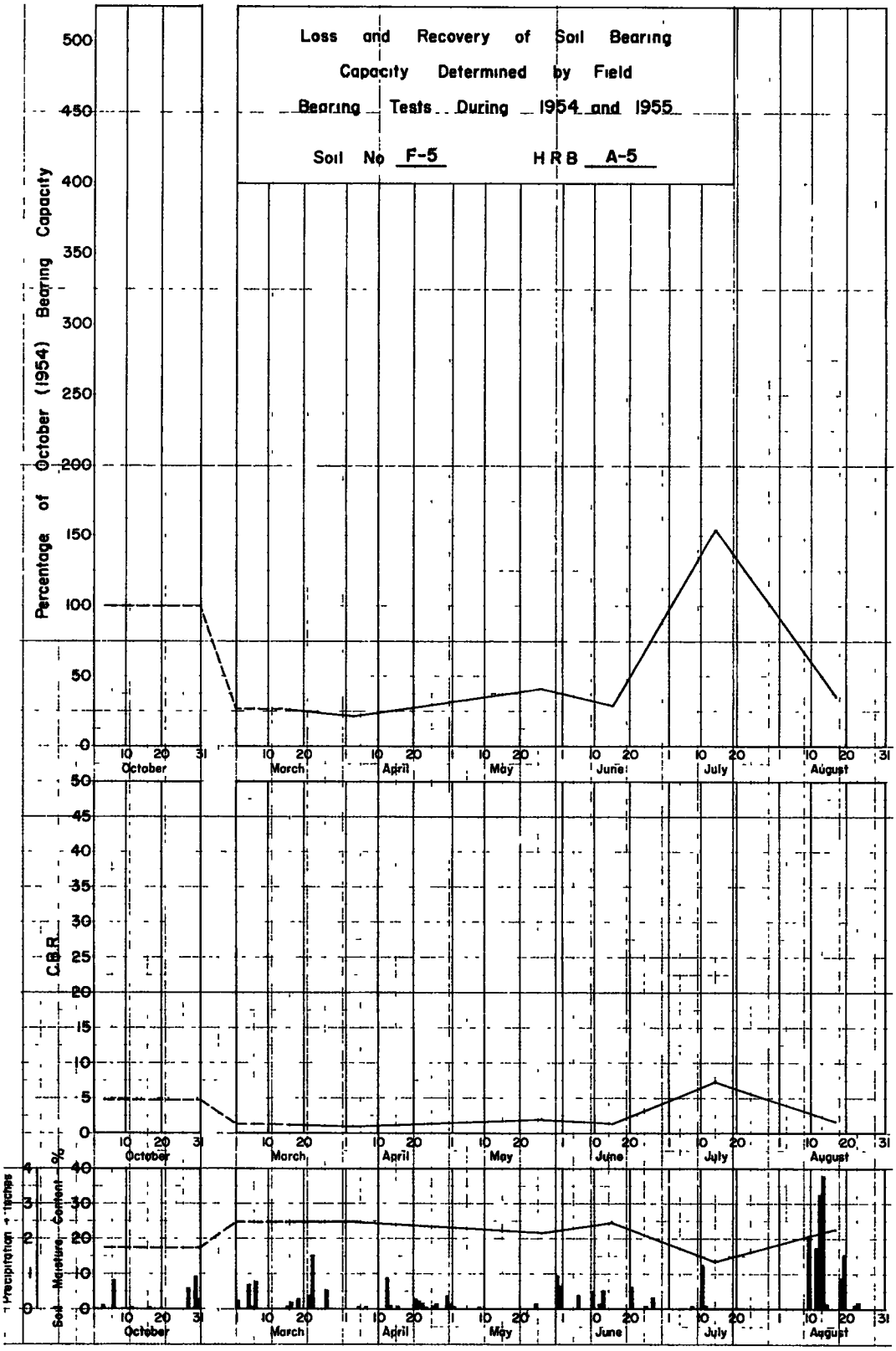
Loss and Recovery of Soil Bearing Capacity Determined by Field Bearing Tests During 1954 and 1955
Soil No F-5
H R B A-5
Percentage of October (1954) Bearing Capacity
C.B.R.
Soil Moisture Content %
Precipitation - Inches
October
March
April
May
June
July
August

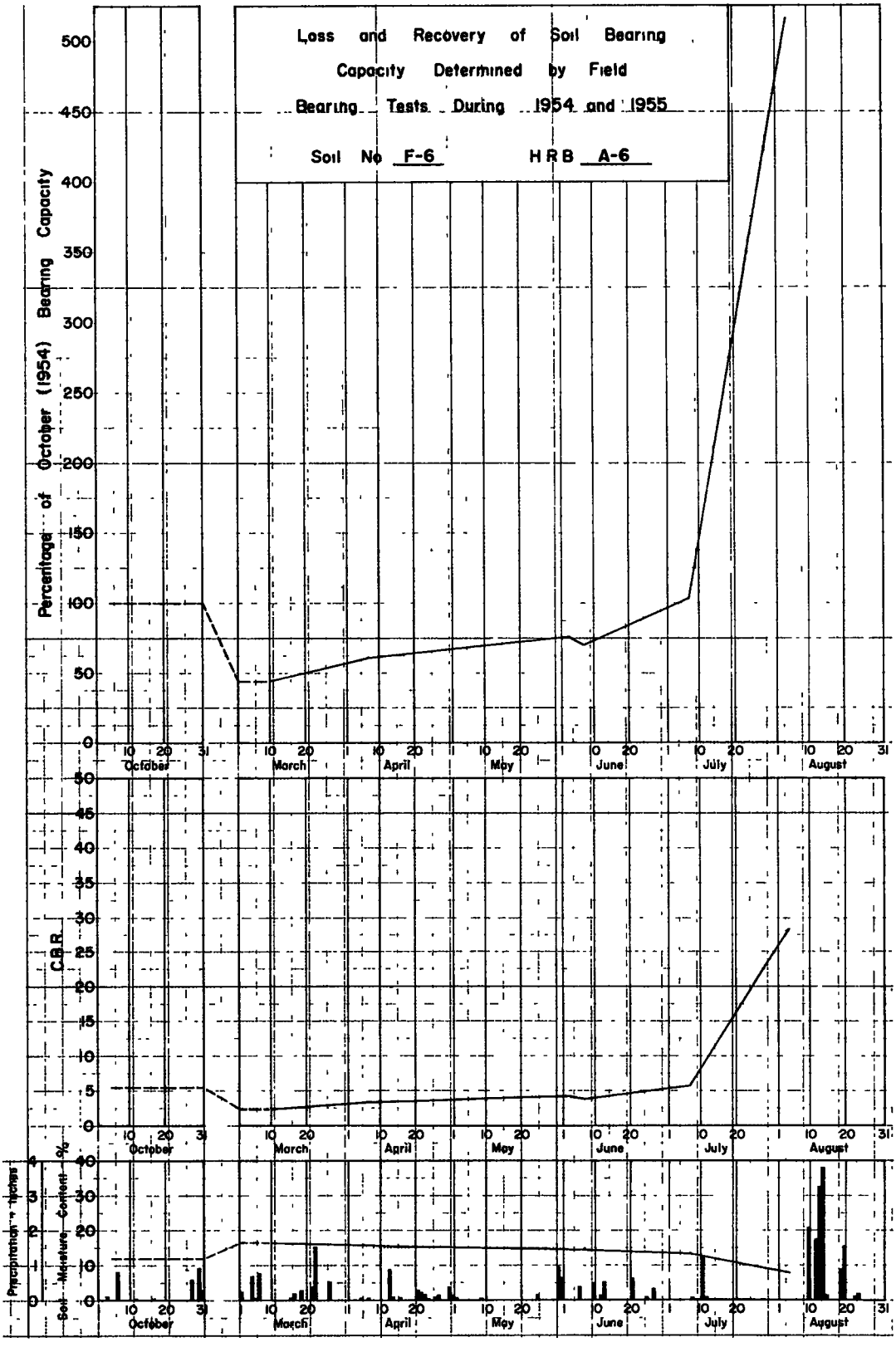
Loss and Recovery of Soil Bearing Capacity Determined by Field Bearing Tests During 1954 and 1955
Soil No F-6
HRB A-6
Percentage of October (1954) Bearing Capacity
C.B.R.
Soil Moisture Content %
Precipitation - Inches
October
March
April
May
June
July
August

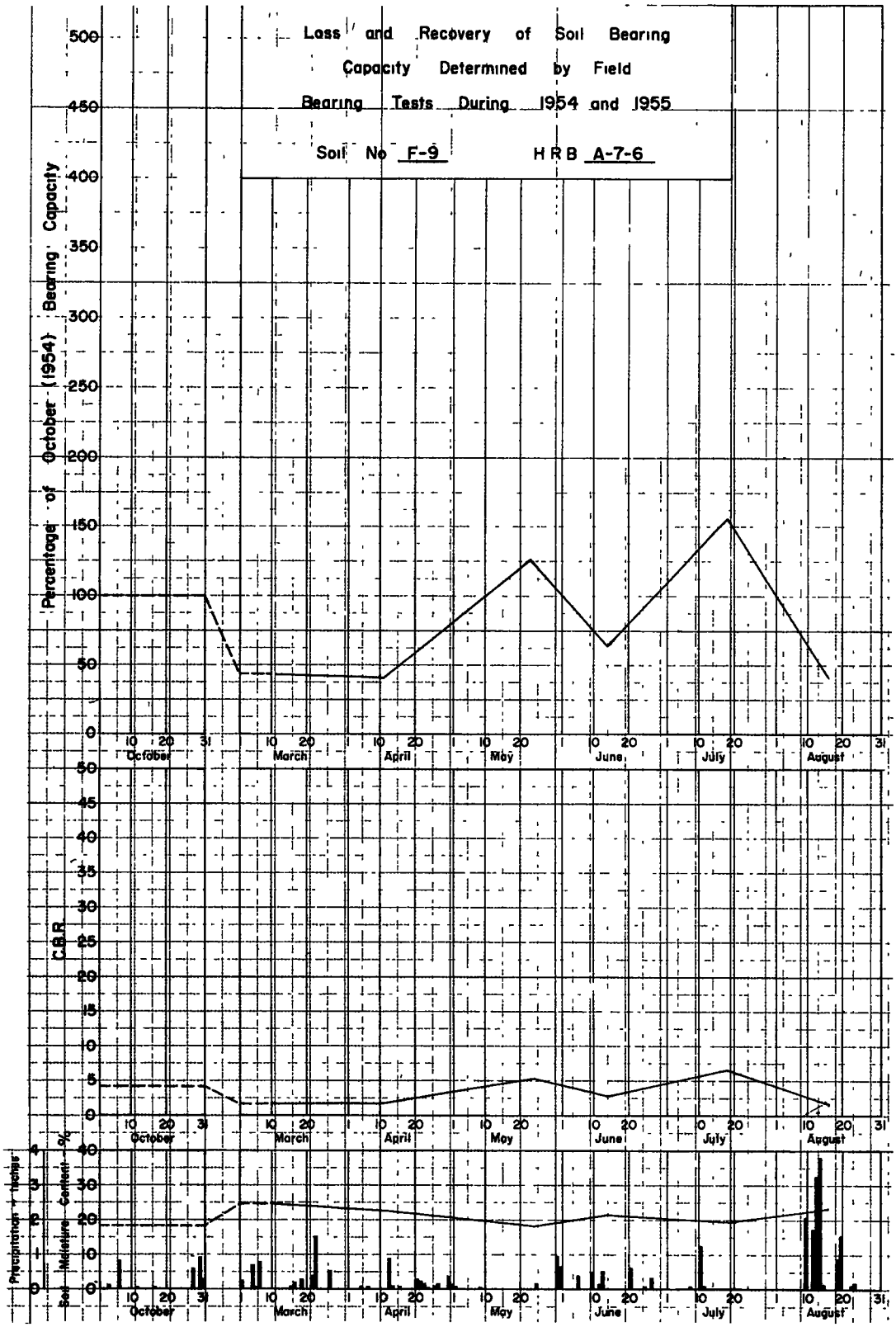
Loss and Recovery of Soil Bearing Capacity Determined by Field Bearing Tests During 1954 and 1955
Soil No F-9
H R B A-7-6
Percentage of October (1954) Bearing Capacity
C.B.R.
Precipitation - Inches
Soil Moisture Content - %
October
March
April
May
June
July
August

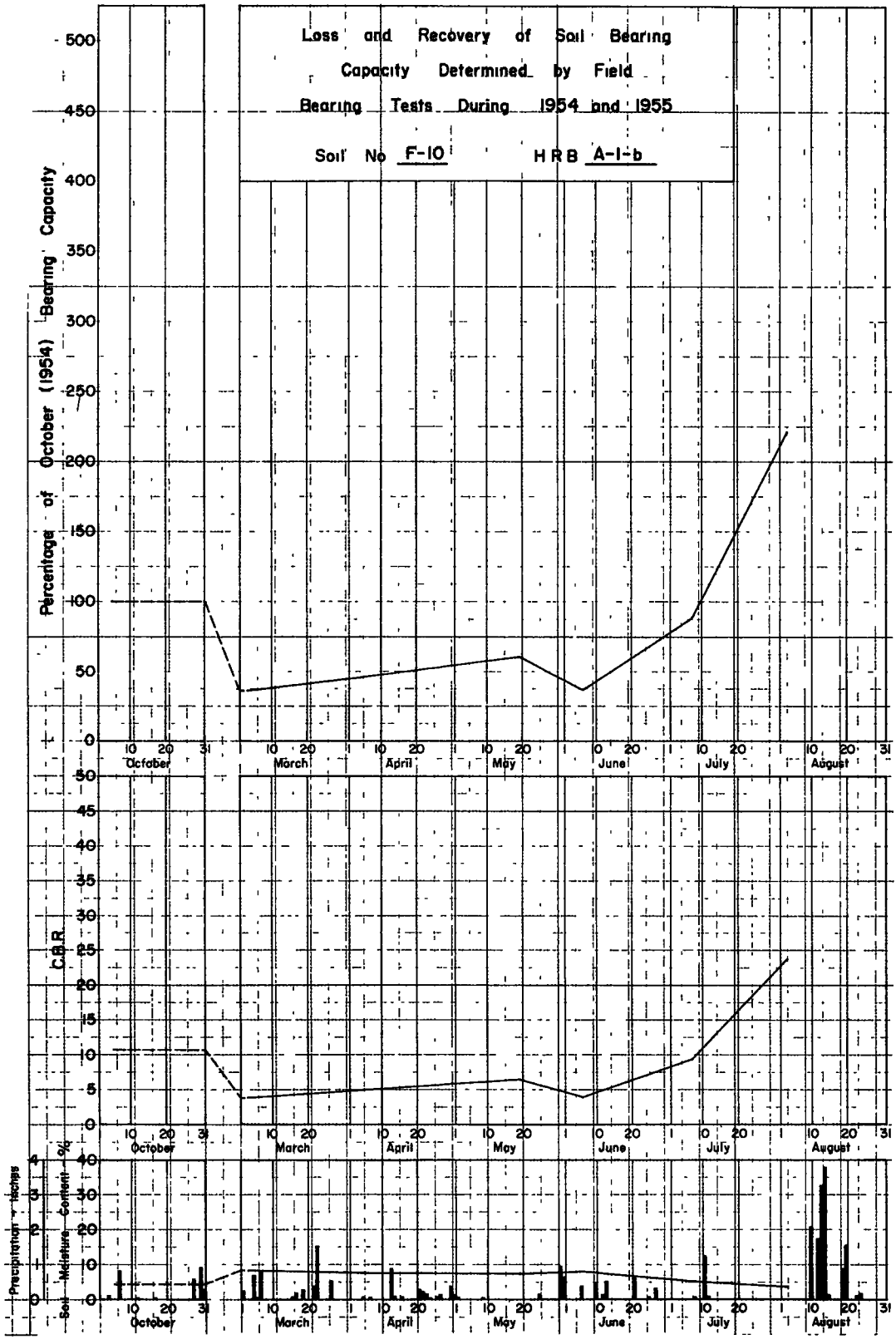
Loss and Recovery of Soil Bearing Capacity Determined by Field Bearing Tests During 1954 and 1955
Soil No F-10
H R B A-1-b
Percentage of October (1954) Bearing Capacity
C.B.R.
Precipitation - Inches
Soil Moisture Content %
October
March
April
May
June
July
August

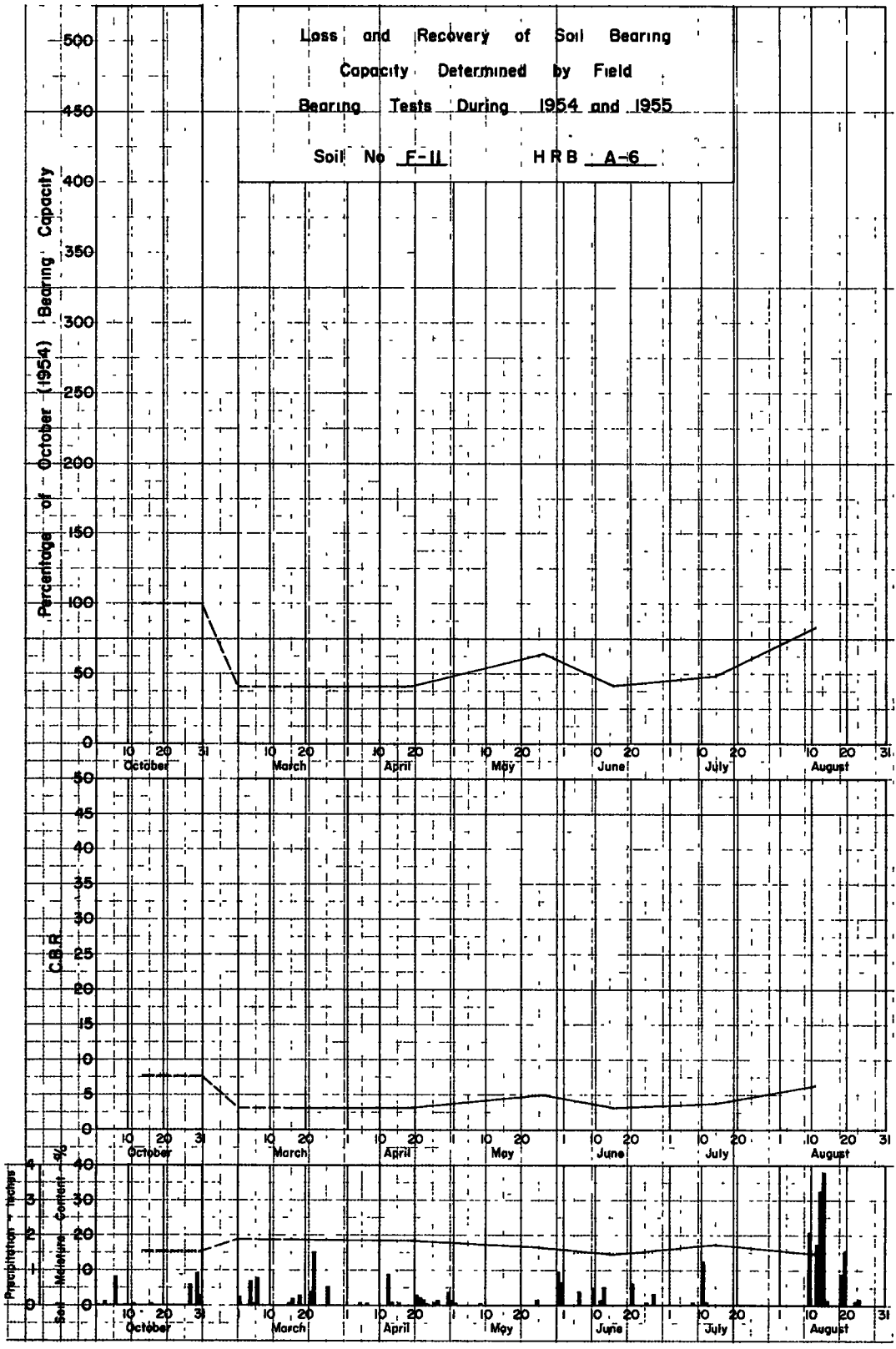
Loss and Recovery of Soil Bearing Capacity Determined by Field Bearing Tests During 1954 and 1955
Soil No F-11 HRB A-6
Percentage of October (1954) Bearing Capacity
C.B.R.
Precipitation - Inches
Soil Moisture Content - %
October
March
April
May
June
July
August

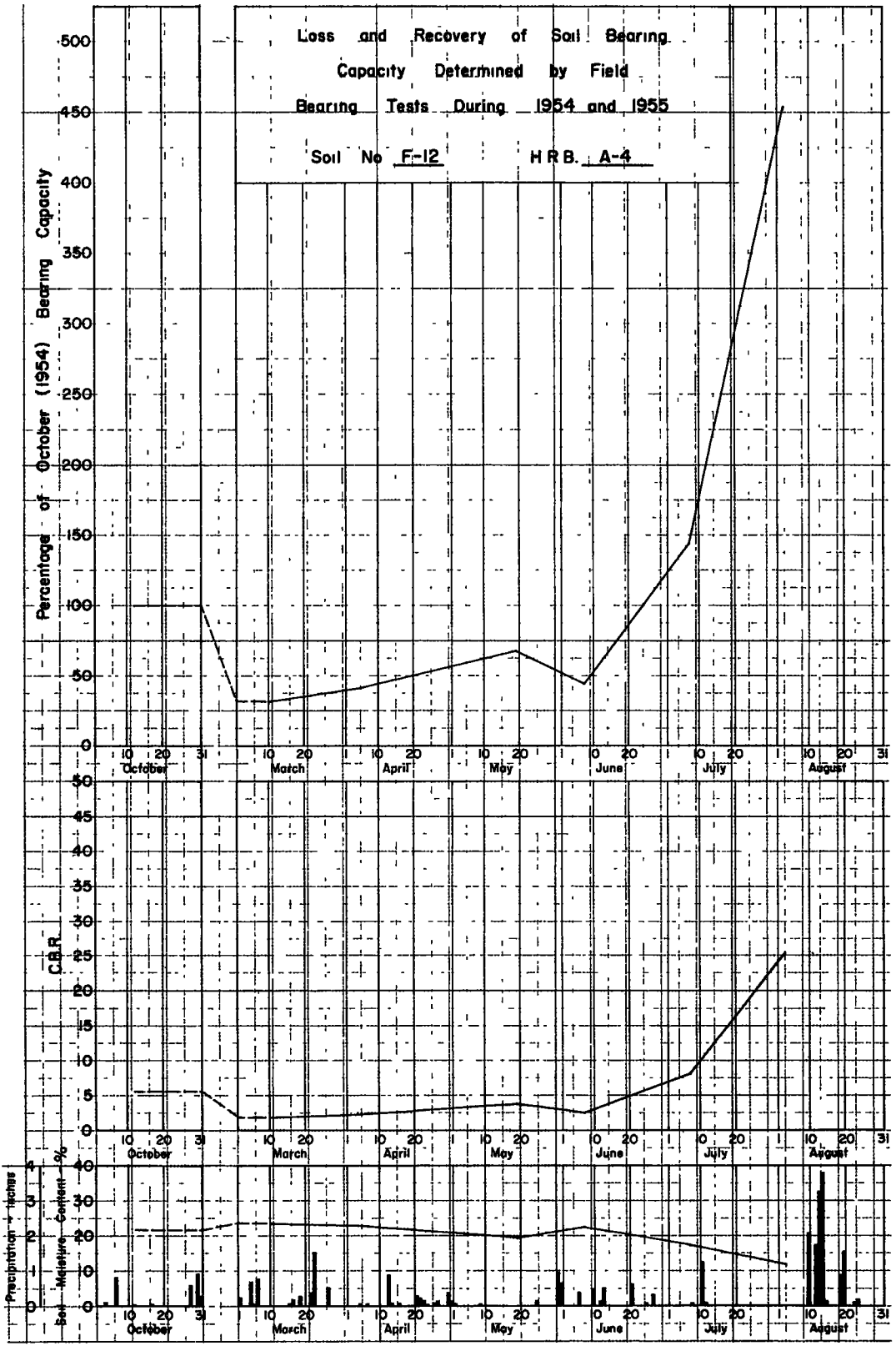
Loss and Recovery of Soil Bearing Capacity Determined by Field Bearing Tests During 1954 and 1955
Soil No F-12
H R B. A-4
Percentage of October (1954) Bearing Capacity
C.B.R.
Precipitation - Inches
Soil Moisture Content - %
October
March
April
May
June
July
August

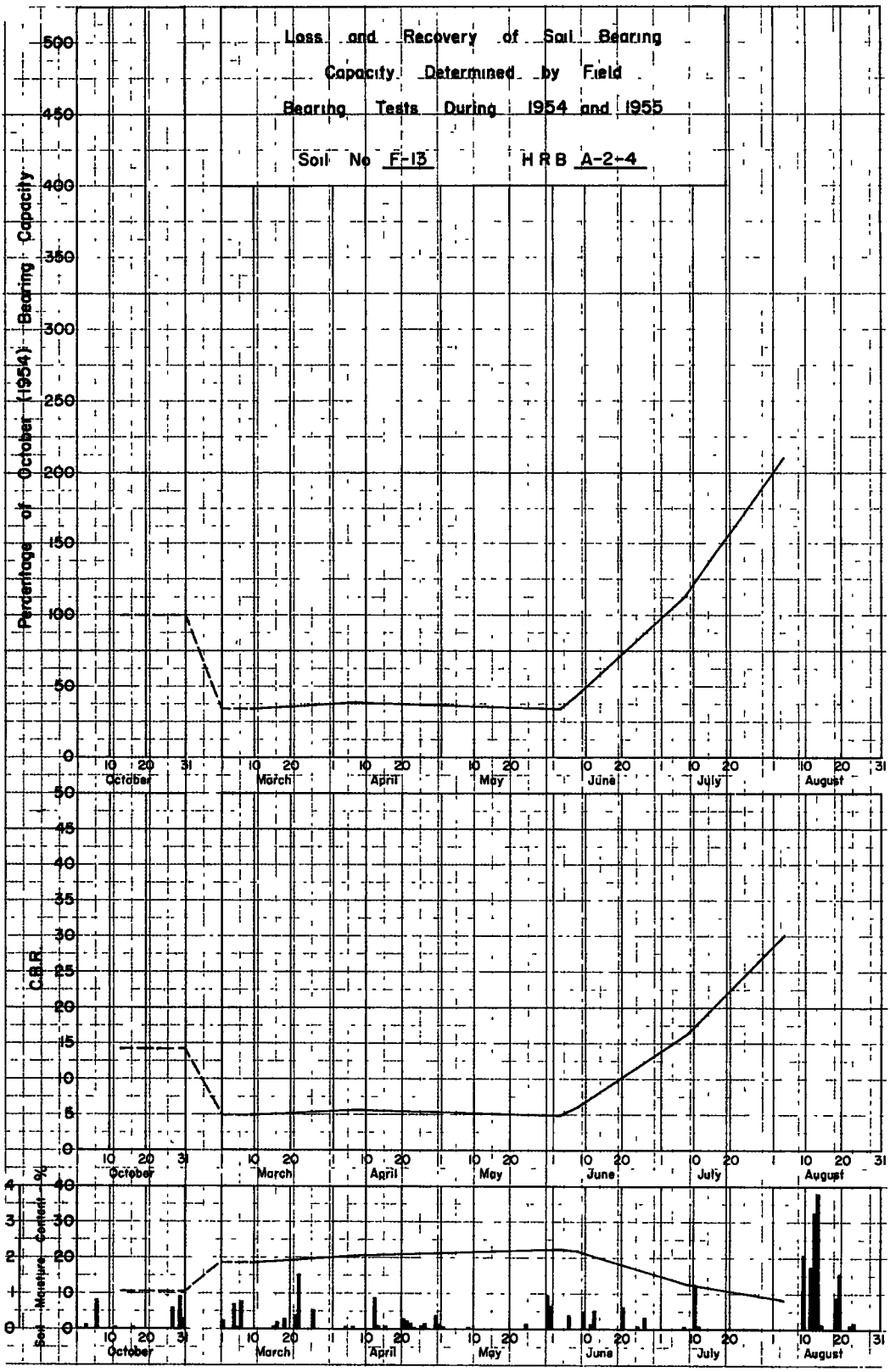
Loss and Recovery of Soil Bearing Capacity Determined by Field Bearing Tests During 1954 and 1955
Soil No F-13
H R B A-2-4
Percentage of October (1954) Bearing Capacity
C.B.R.
Soil Moisture Content %
October
March
April
May
June
July
August

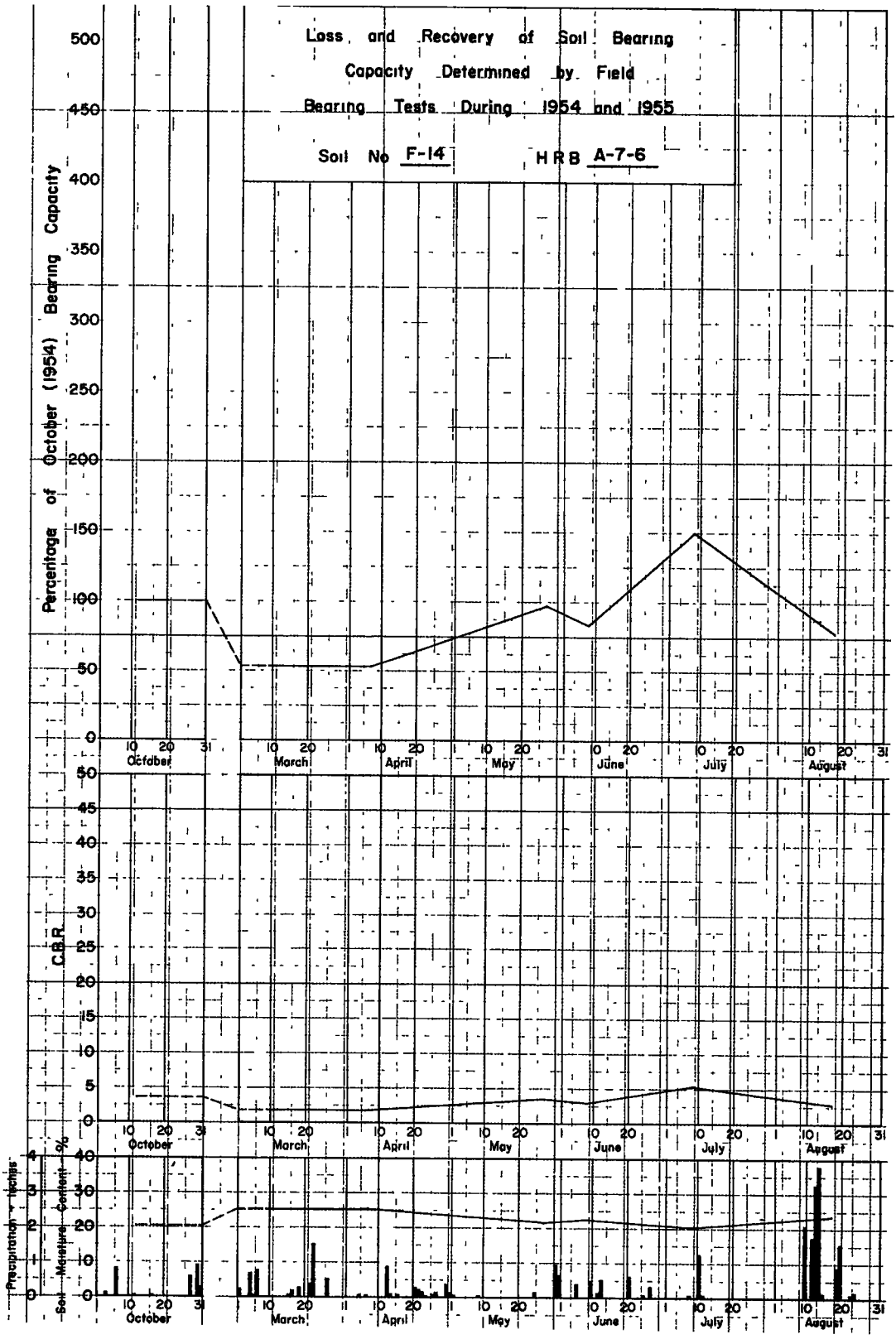
Loss and Recovery of Soil Bearing Capacity Determined by Field Bearing Tests During 1954 and 1955
Soil No F-14
HRB A-7-6
Percentage of October (1954) Bearing Capacity
C.B.R.
Precipitation - Inches
Soil Moisture Content - %
October
March
April
May
June
July
August

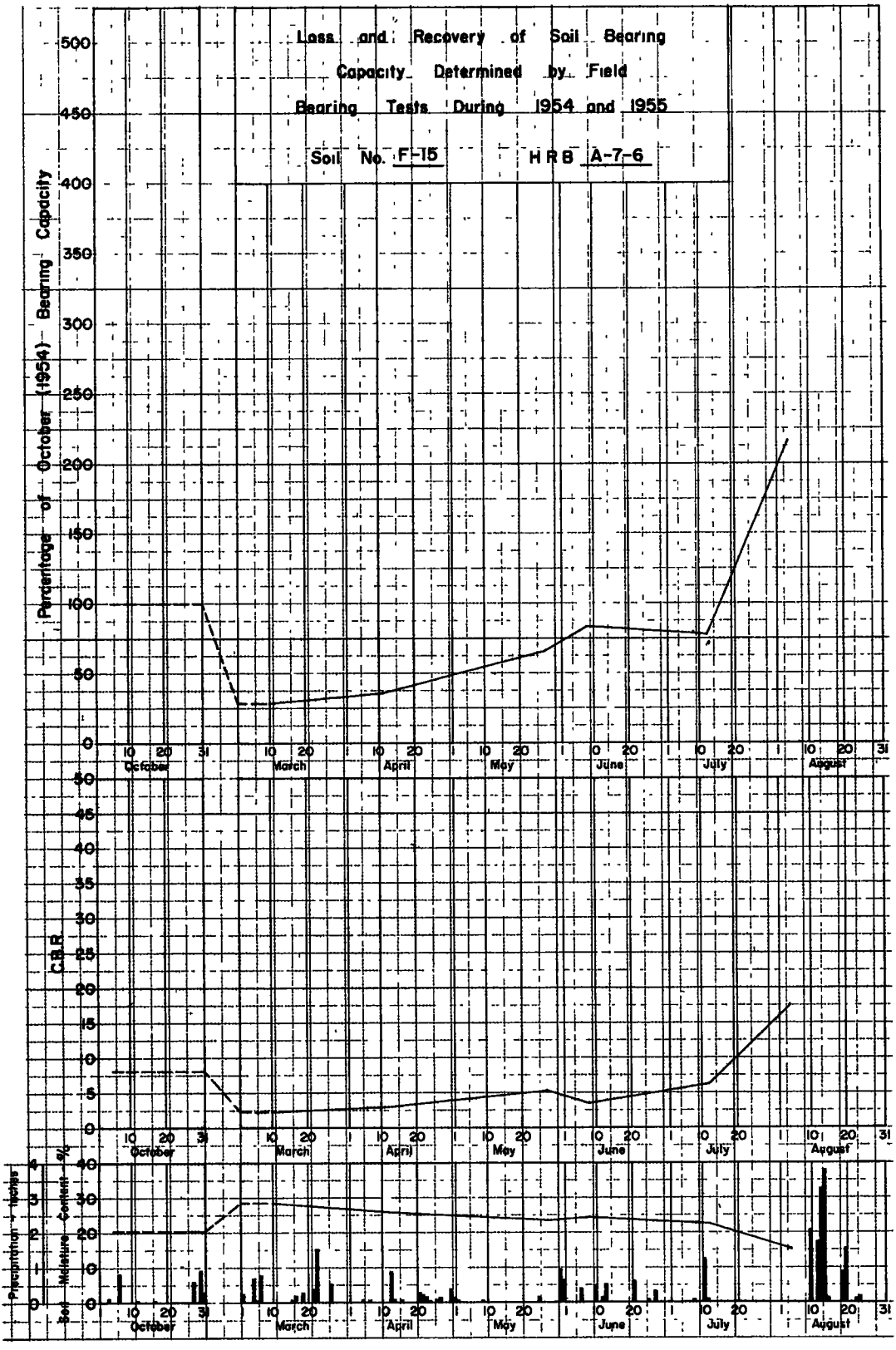
Loss and Recovery of Soil Bearing Capacity Determined by Field Bearing Tests During 1954 and 1955
Soil No. F-15 H R B A-7-6
Percentage of October (1954) Bearing Capacity
C.B.R.
Precipitation - Inches
Soil Moisture Content - %
October
March
April
May
June
July
August

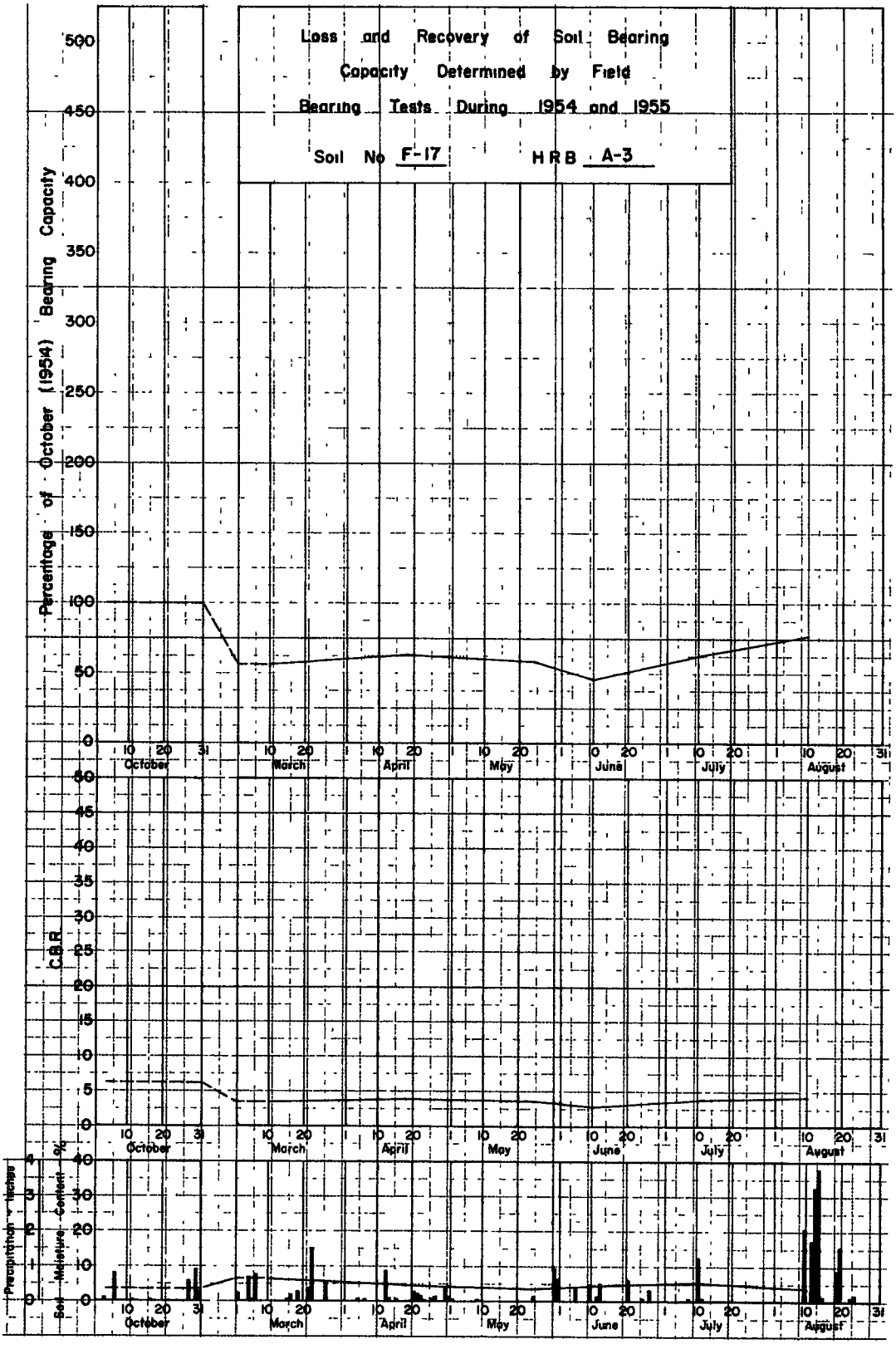
Loss and Recovery of Soil Bearing Capacity Determined by Field Bearing Tests During 1954 and 1955
Soil No F-17
HRB A-3
Percentage of October (1954) Bearing Capacity
500
450
400
350
300
250
200
150
100
50
0
C.B.R.
60
55
50
45
40
35
30
25
20
15
10
5
0
Precipitation - Inches
Soil Moisture Content - %
4
3
2
1
0
40
30
20
10
0
10 20 31
October
March
April
May
June
July
August

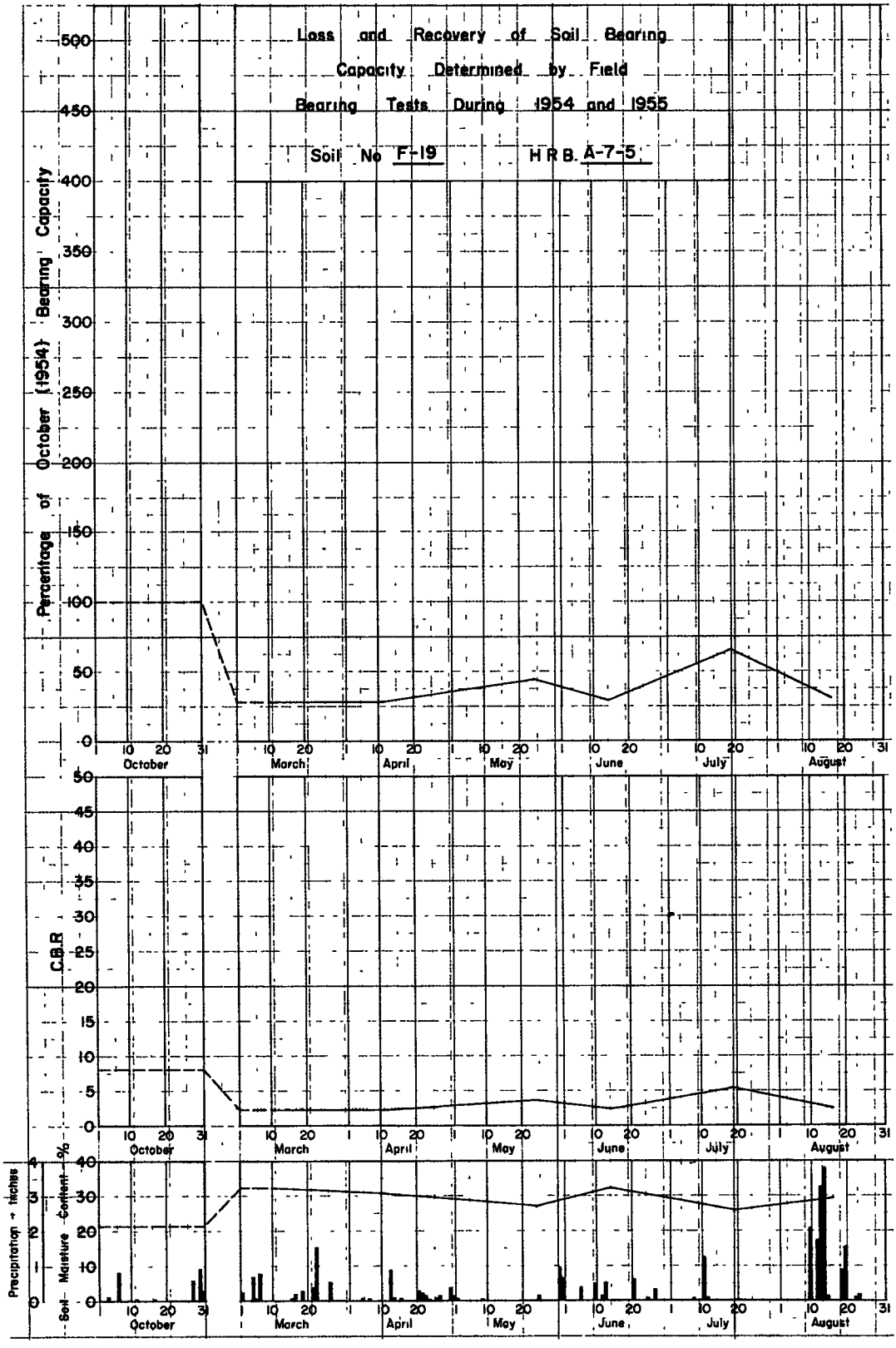
Loss and Recovery of Soil Bearing Capacity Determined by Field Bearing Tests During 1954 and 1955
Soil No F-19
H R B. A-7-5
Percentage of October (1954) Bearing Capacity
C.B.R.
Soil Moisture Content - %
Precipitation - Inches
October
March
April
May
June
July
August

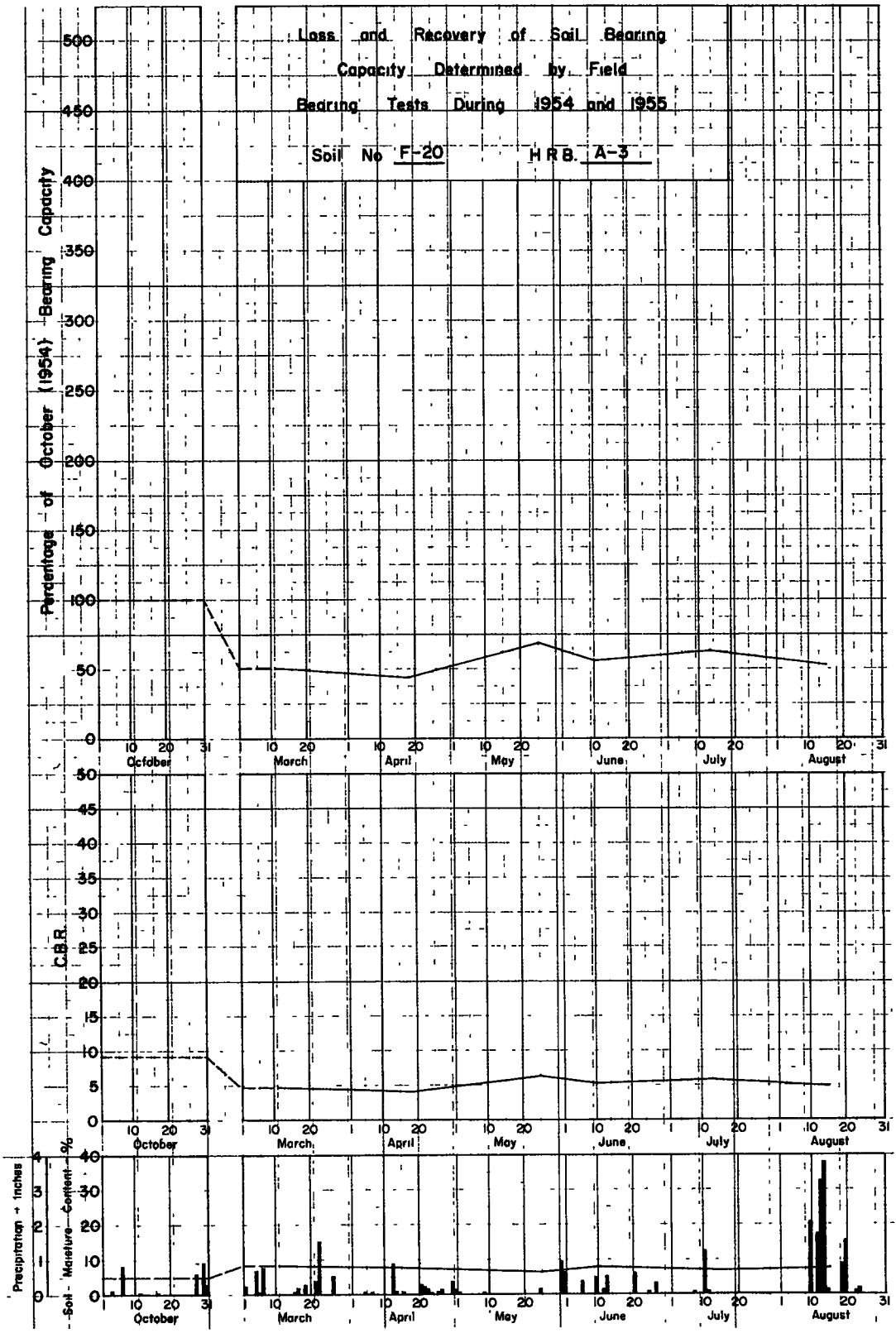
Loss and Recovery of Soil Bearing Capacity Determined by Field Bearing Tests During 1954 and 1955
Soil No F-20
H R B. A-3
Percentage of October (1954) Bearing Capacity
C.B.R.
Soil Moisture Content - %
Precipitation - Inches
October
March
April
May
June
July
August

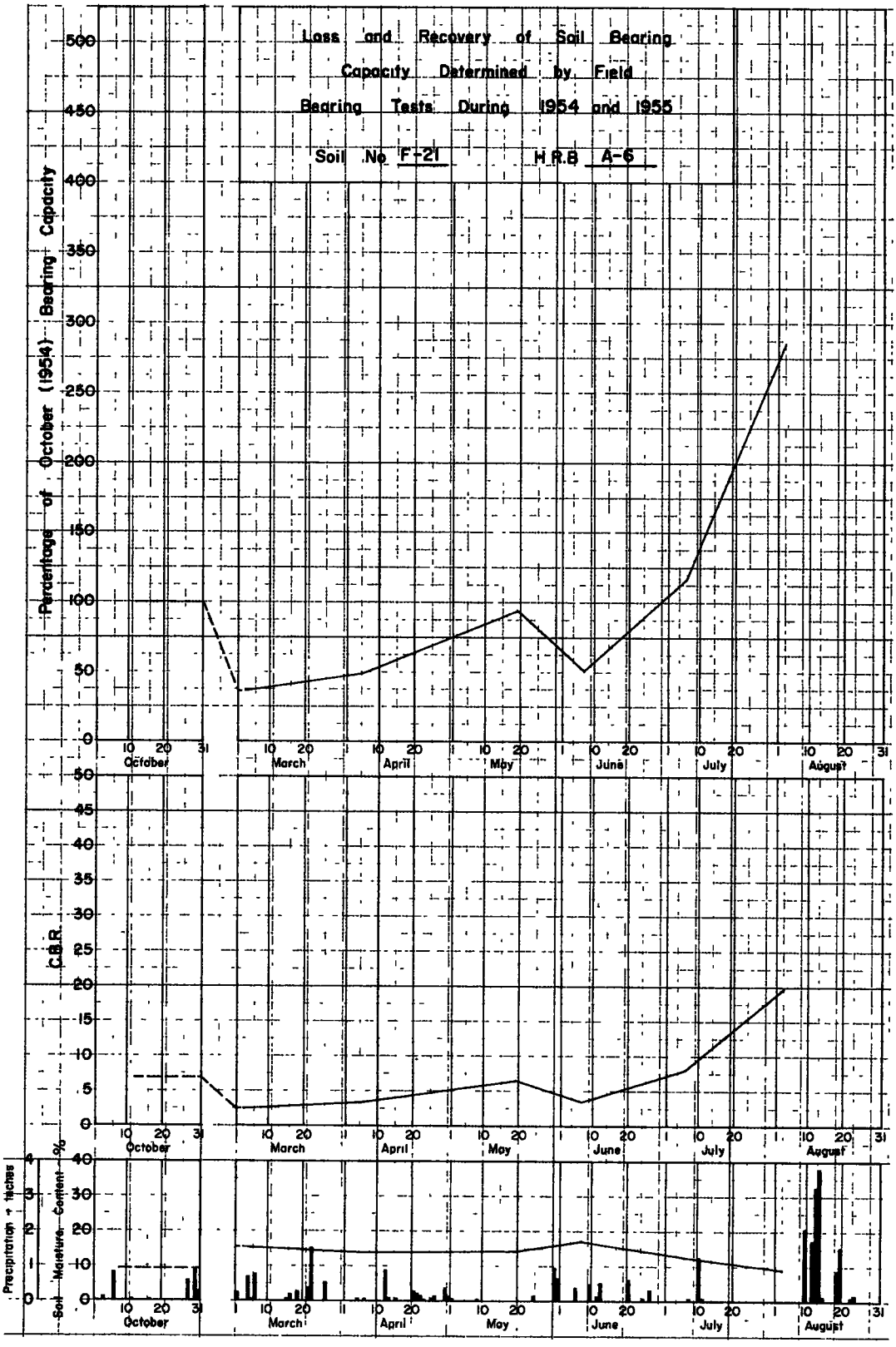
Loss and Recovery of Soil Bearing Capacity Determined by Field Bearing Tests During 1954 and 1955
Soil No F-21
H.R.B. A-6
Percentage of October (1954) Bearing Capacity
C.B.R.
Precipitation - Inches
Soil Moisture Content - %
October
March
April
May
June
July
August

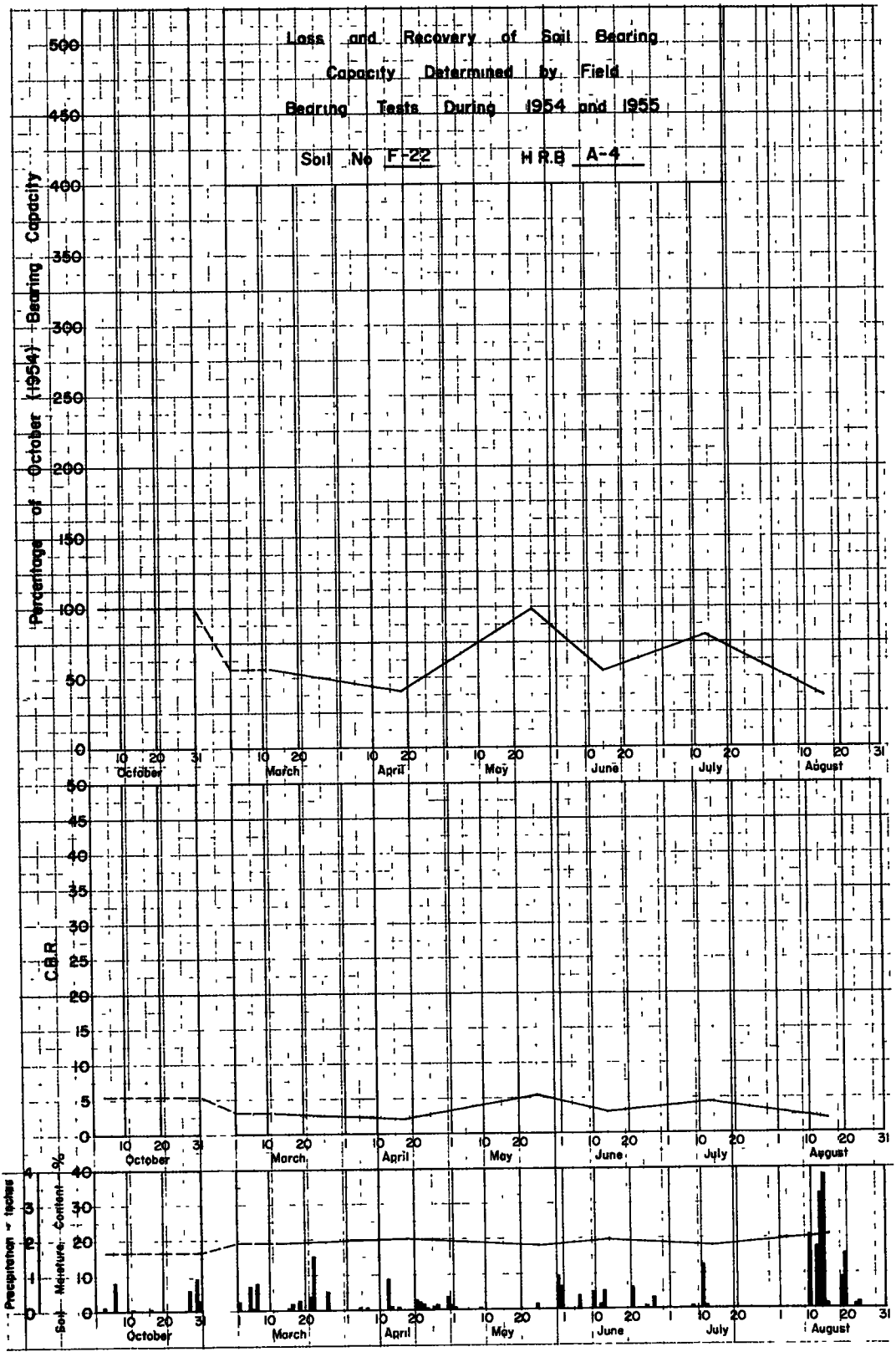
Loss and Recovery of Soil Bearing Capacity Determined by Field Bearing Tests During 1954 and 1955
Soil No F-22
H R B A-4
Percentage of October (1954) Bearing Capacity
C.B.R.
Precipitation - Inches
Soil Moisture Content %
October
March
April
May
June
July
August

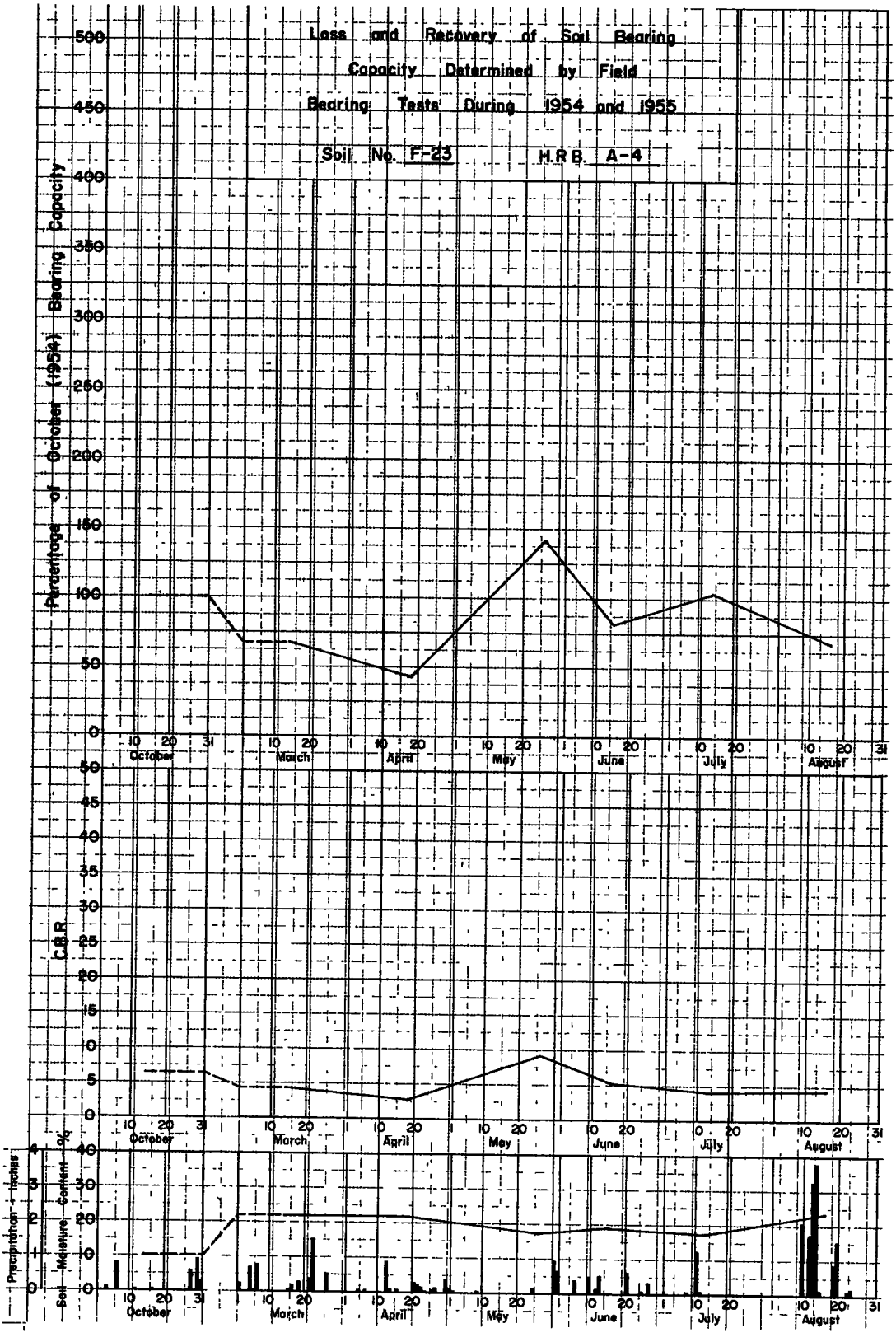
Loss and Recovery of Soil Bearing Capacity Determined by Field Bearing Tests During 1954 and 1955
Soil No. F-23
H.R.B. A-4
Percentage of October (1954) Bearing Capacity
C.B.R.
Precipitation - Inches
Soil Moisture Content - %
October
March
April
May
June
July
August

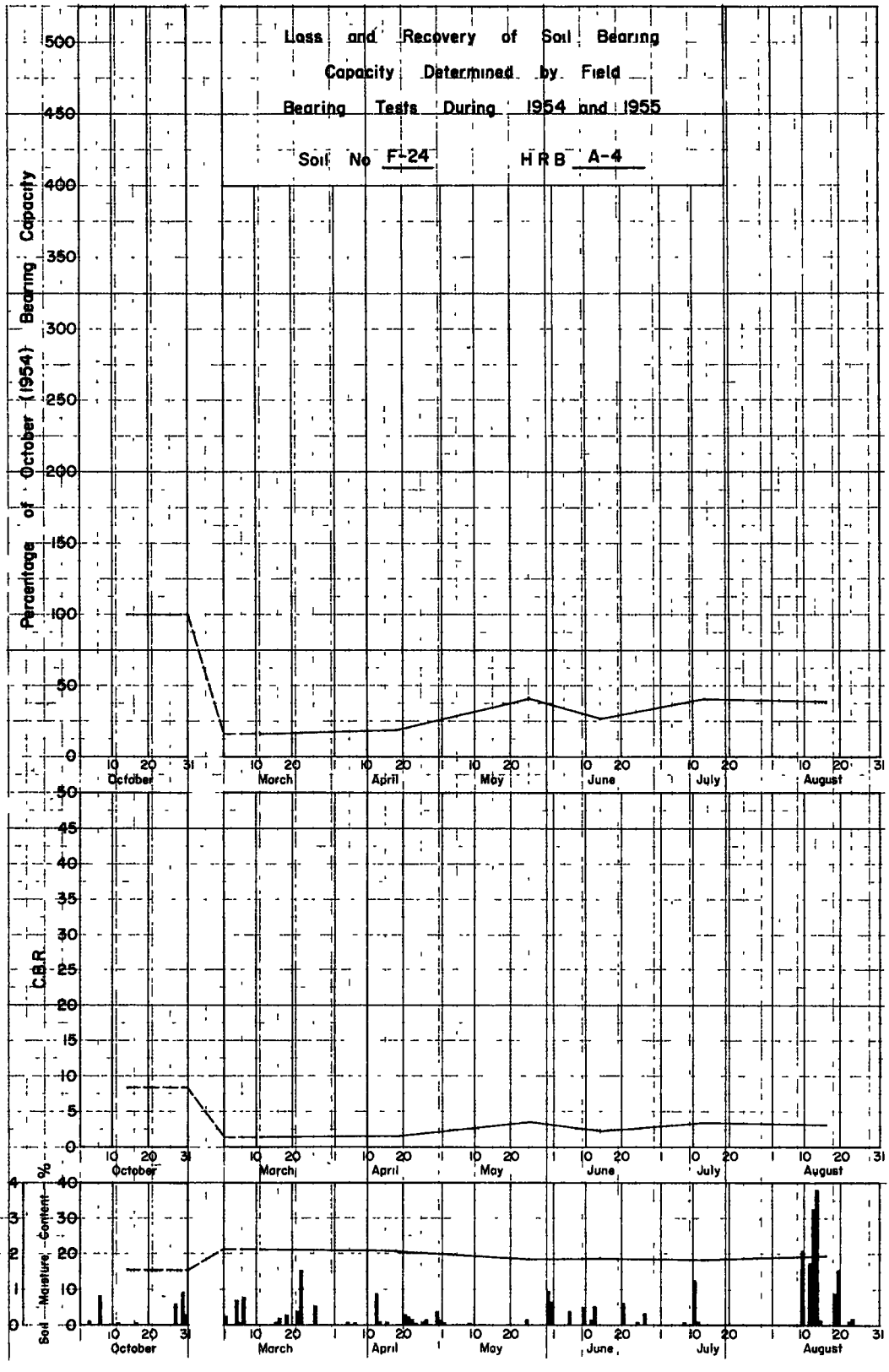
Loss and Recovery of Soil Bearing Capacity Determined by Field Bearing Tests During 1954 and 1955
Soil No F-24
H R B A-4
Percentage of October (1954) Bearing Capacity
C.B.R.
Soil Moisture Content %
Precipitation - Inches
October
March
April
May
June
July
August

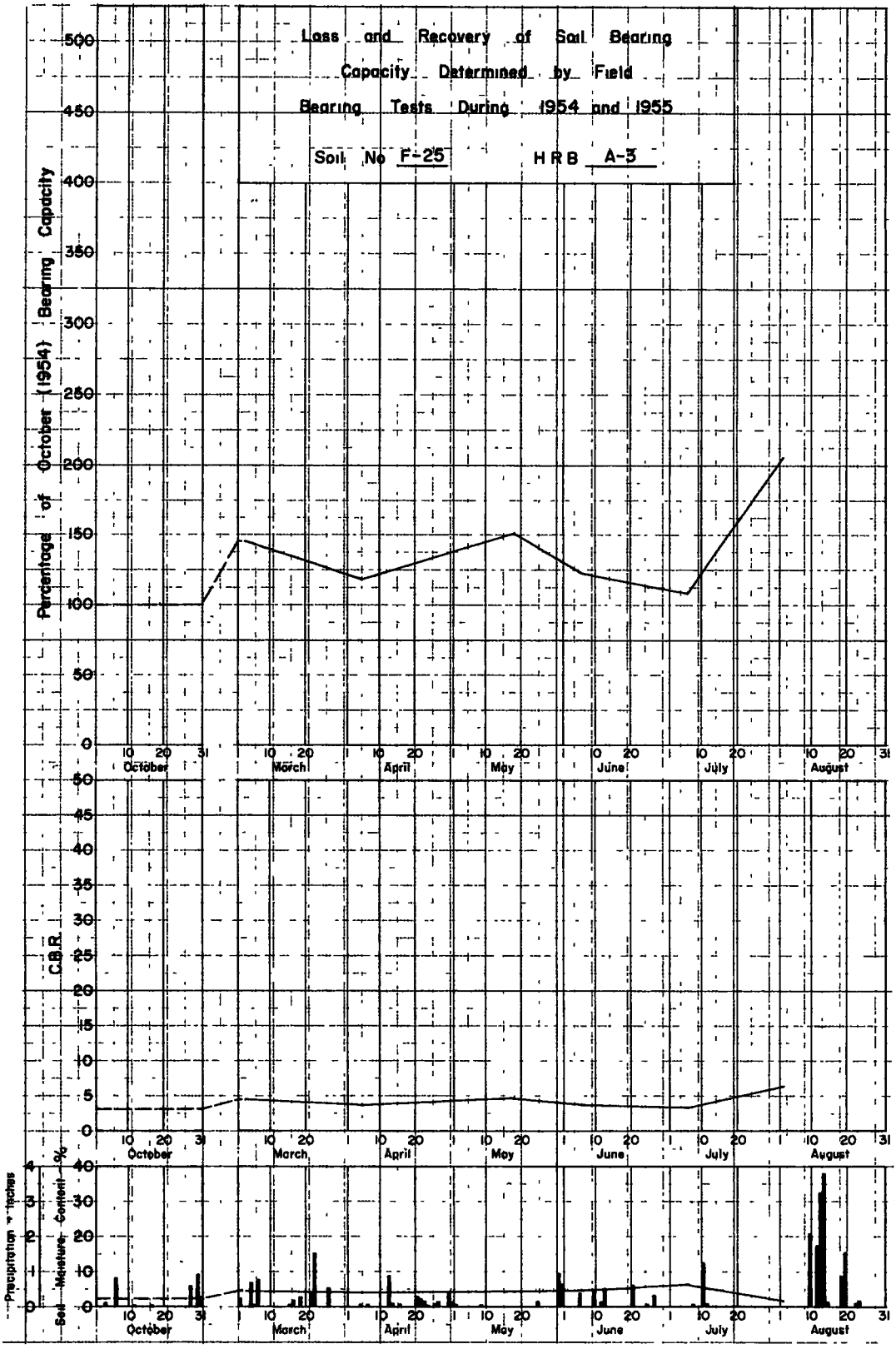
Loss and Recovery of Soil Bearing Capacity Determined by Field Bearing Tests During 1954 and 1955
Soil No F-25
H R B A-3
Percentage of October (1954) Bearing Capacity
C.B.R.
Soil Moisture Content %
Precipitation - Inches
October
March
April
May
June
July
August

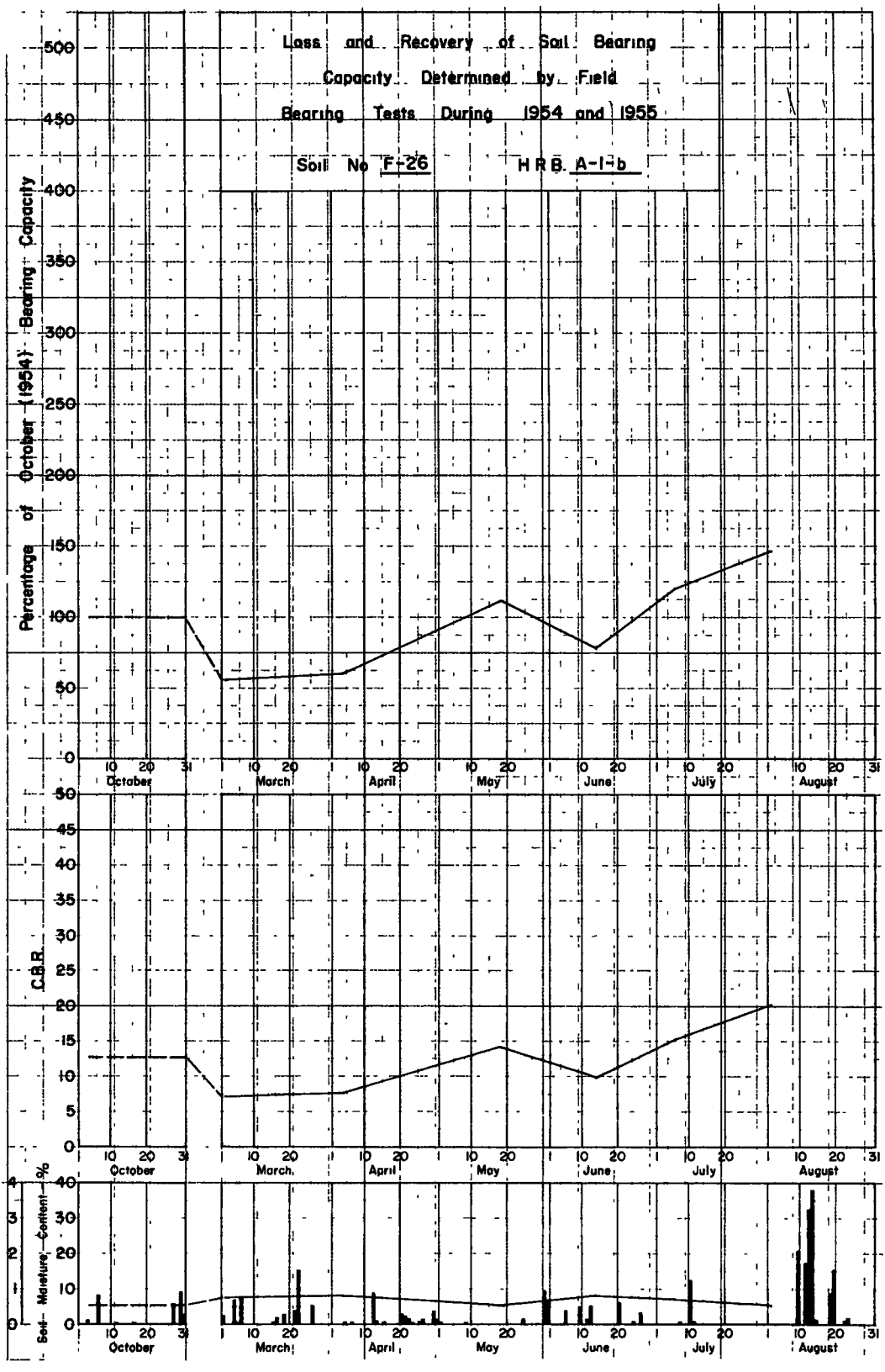
Loss and Recovery of Soil Bearing Capacity Determined by Field Bearing Tests During 1954 and 1955
Soil No F-26
H R B. A-1-b
Percentage of October (1954) Bearing Capacity
C.B.R.
Soil Moisture Content %
Precipitation - Inches
October
March
April
May
June
July
August

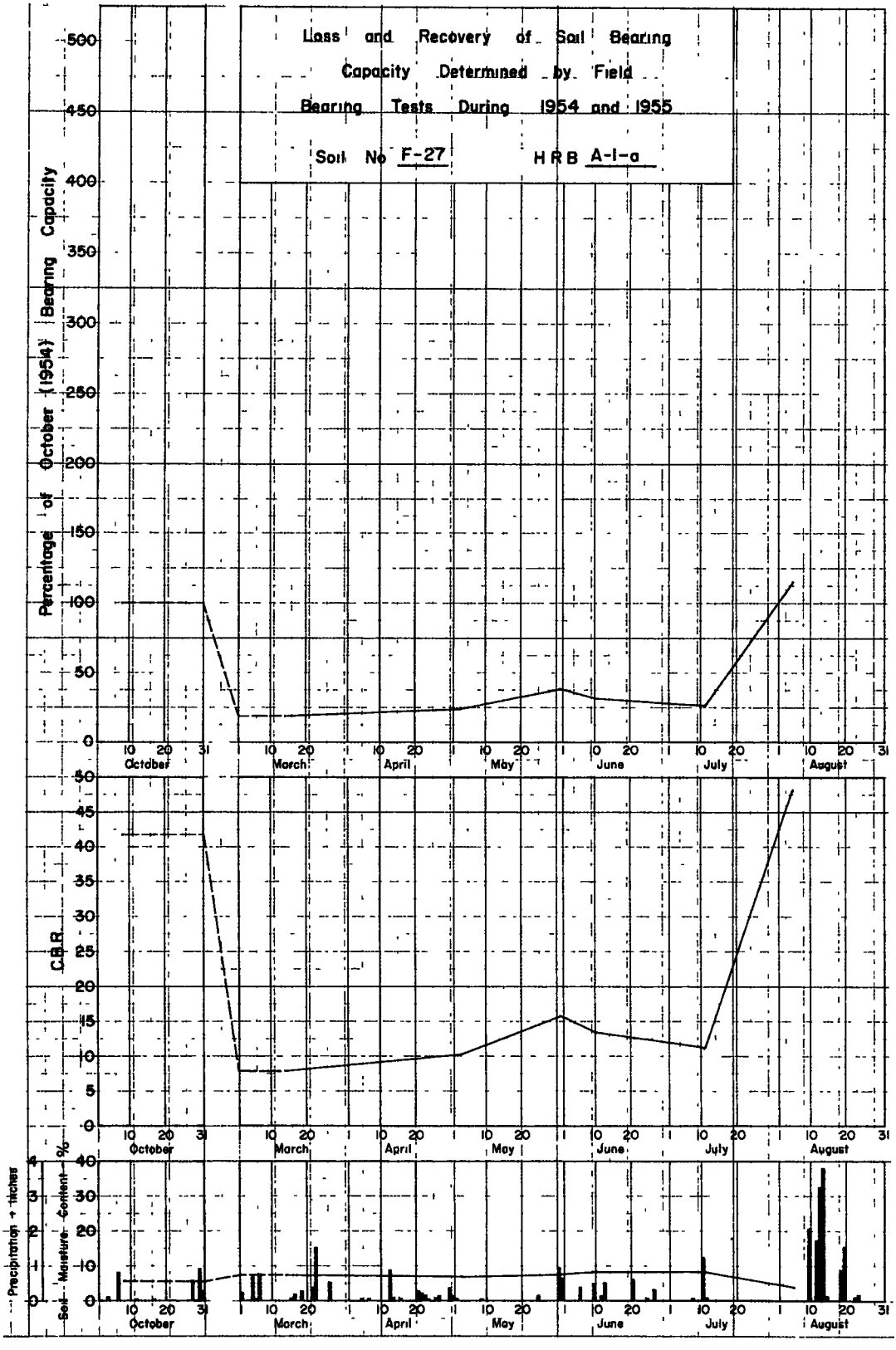
Loss and Recovery of Soil Bearing Capacity Determined by Field Bearing Tests During 1954 and 1955
Soil No F-27
HRB A-1-a
Percentage of October (1954) Bearing Capacity
C.B.R.
Soil Moisture Content - %
Precipitation - Inches
October
March
April
May
June
July
August

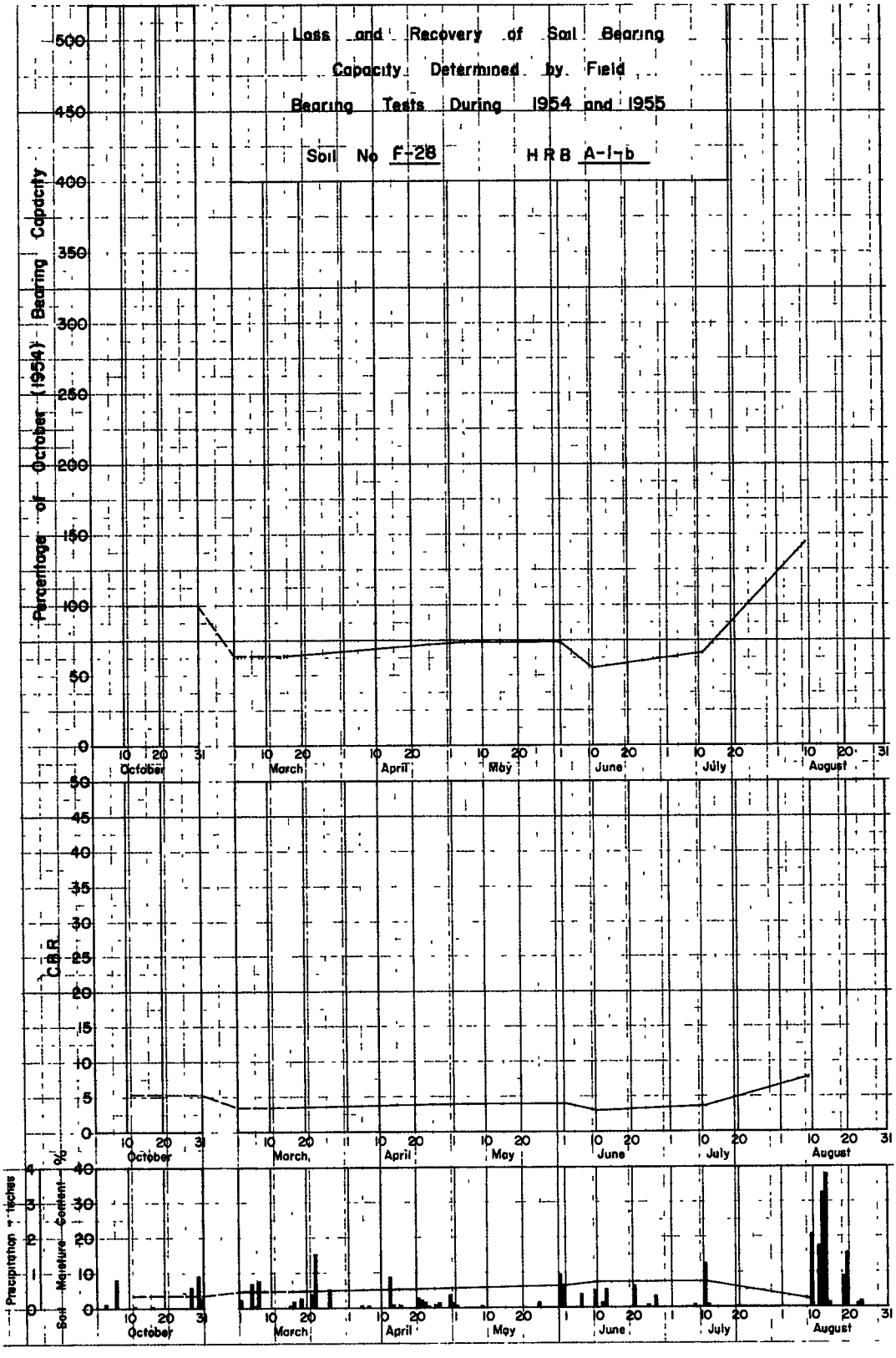
Loss and Recovery of Soil Bearing Capacity Determined by Field Bearing Tests During 1954 and 1955
Soil No F-28
H R B A-1-b
Percentage of October (1954) Bearing Capacity
C.B.R.
Soil Moisture Content %
Precipitation - Inches
October
March
April
May
June
July
August

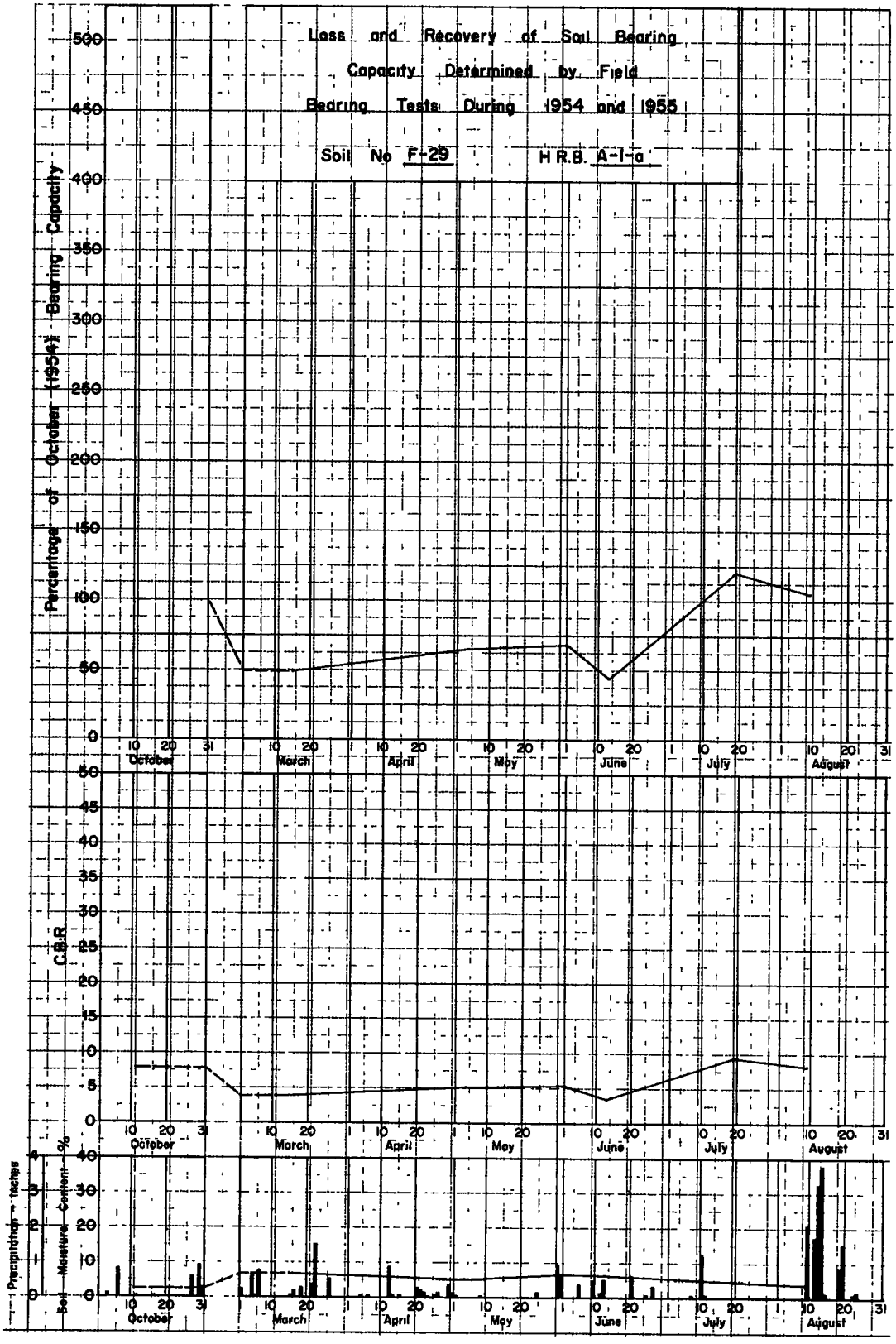
Loss and Recovery of Soil Bearing Capacity Determined by Field Bearing Tests During 1954 and 1955
Soil No F-29
H R.B. A-1-a
Percentage of October 1954 Bearing Capacity
C.B.R.
Soil Moisture Content - %
Precipitation - Inches
October
March
April
May
June
July
August

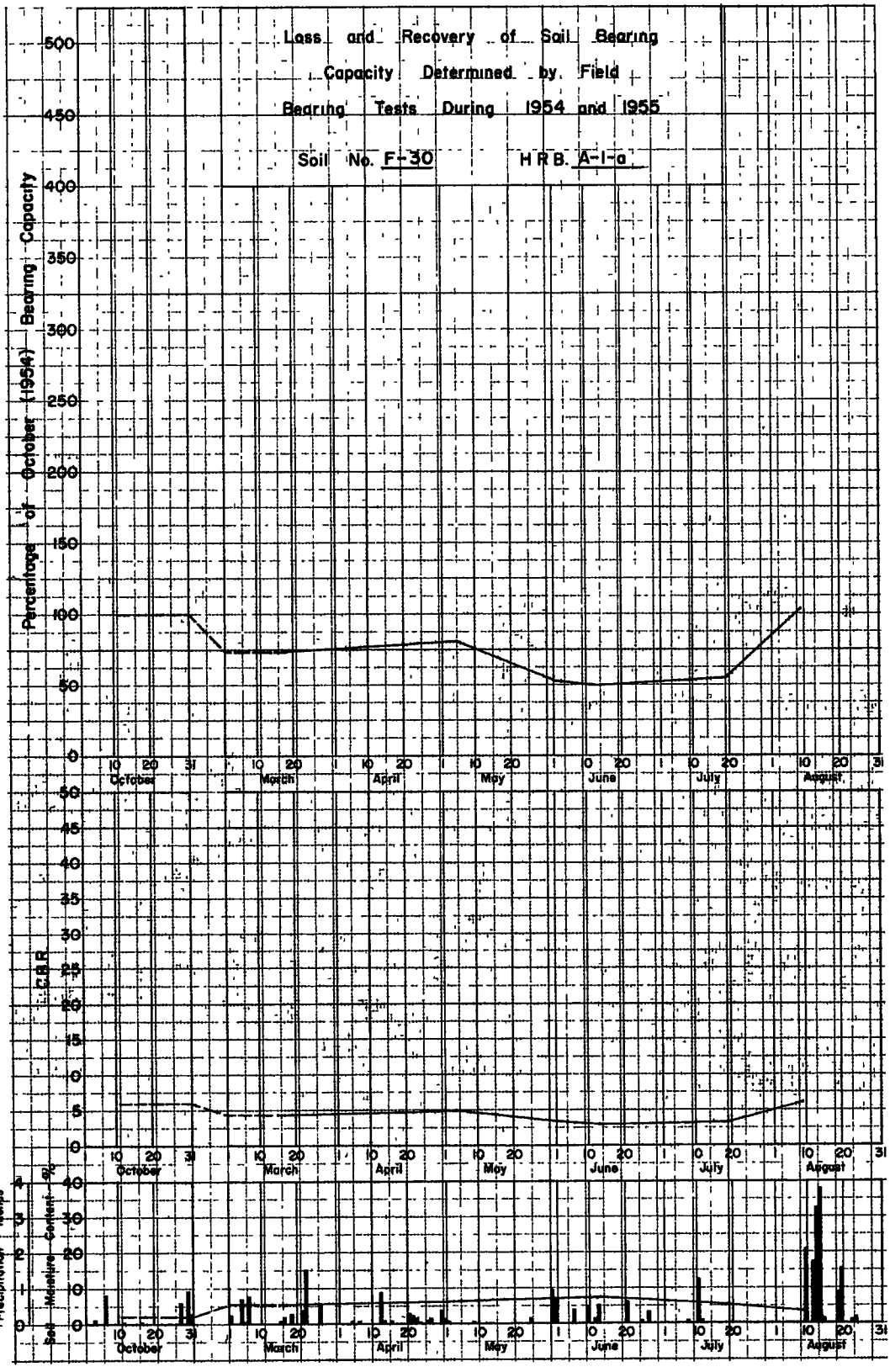
Loss and Recovery of Soil Bearing Capacity Determined by Field Bearing Tests During 1954 and 1955
Soil No. F-30
H R B. A-1-a
Percentage of October (1954) Bearing Capacity
C.B.R.
Soil Moisture Content - %
Precipitation - Inches
October
March
April
May
June
July
August

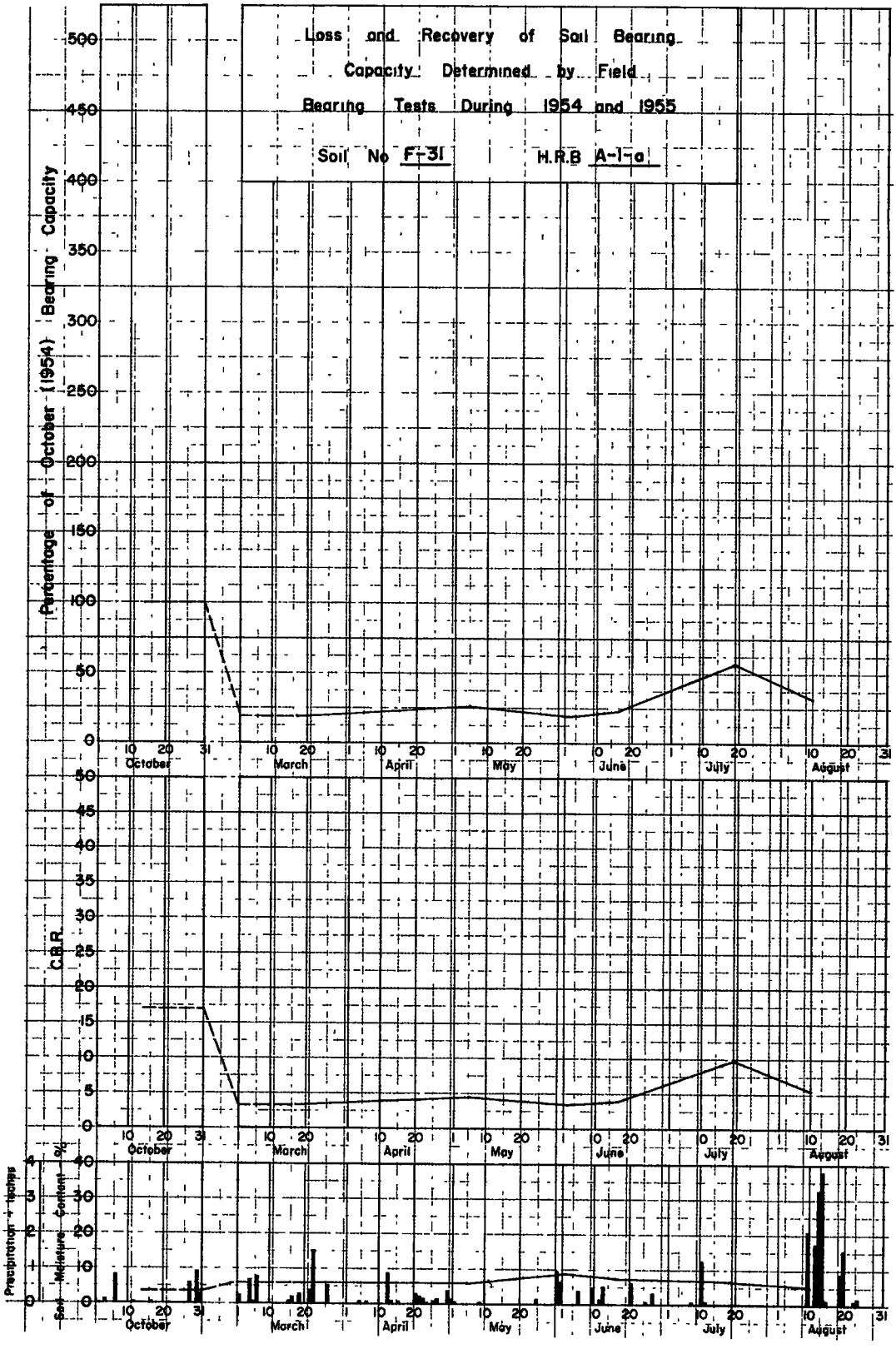
Loss and Recovery of Soil Bearing Capacity Determined by Field Bearing Tests During 1954 and 1955
Soil No F-31
H.R.B A-1-a
Percentage of October (1954) Bearing Capacity
C.B.R.
Precipitation + Inches
Soil Moisture Content %
October
March
April
May
June
July
August

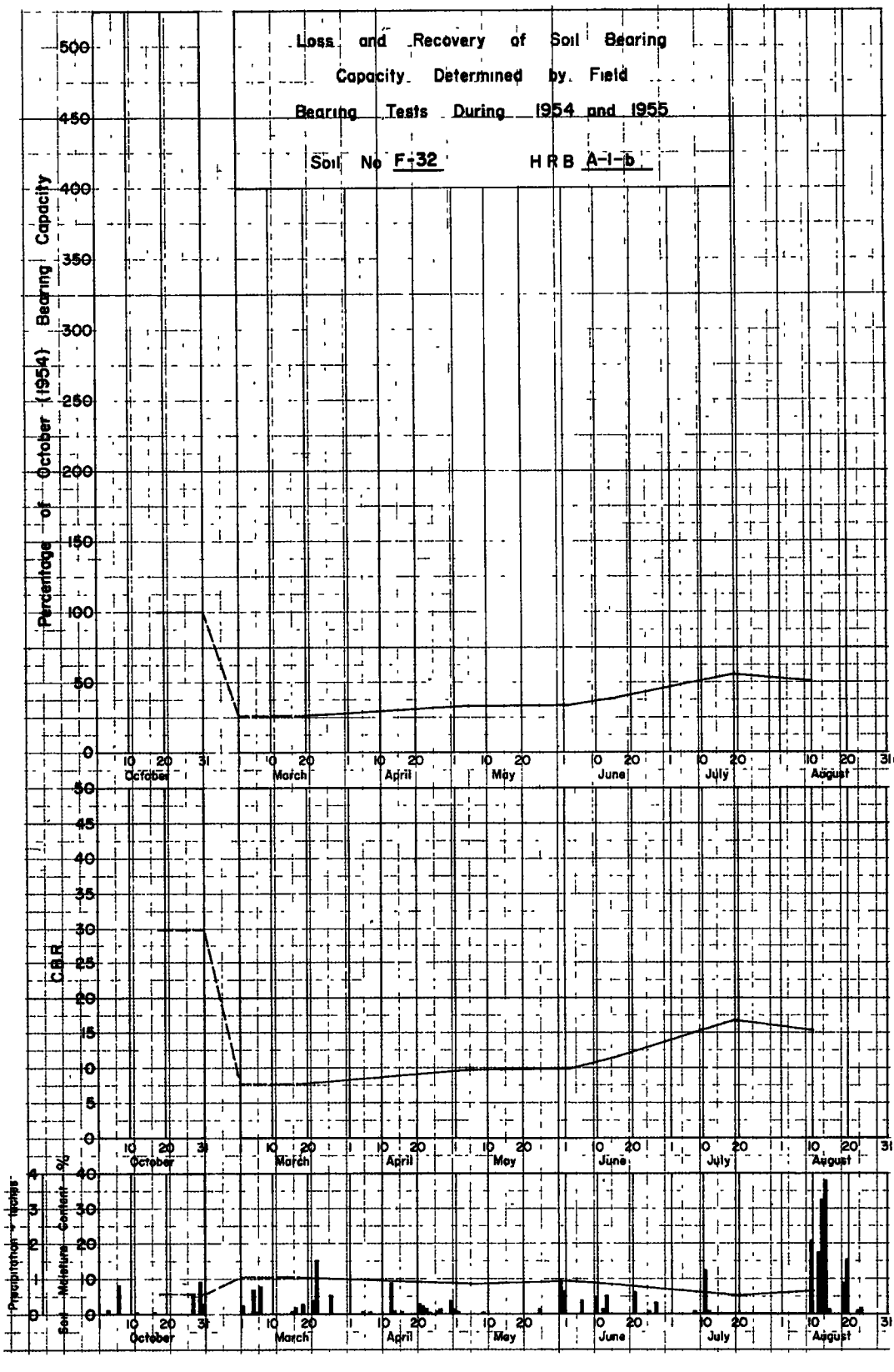
Loss and Recovery of Soil Bearing Capacity Determined by Field Bearing Tests During 1954 and 1955
Soil No F-32
H R B A-1-b
Percentage of October (1954) Bearing Capacity
C.B.R.
Precipitation - Inches
Soil Moisture Content - %
October
March
April
May
June
July
August

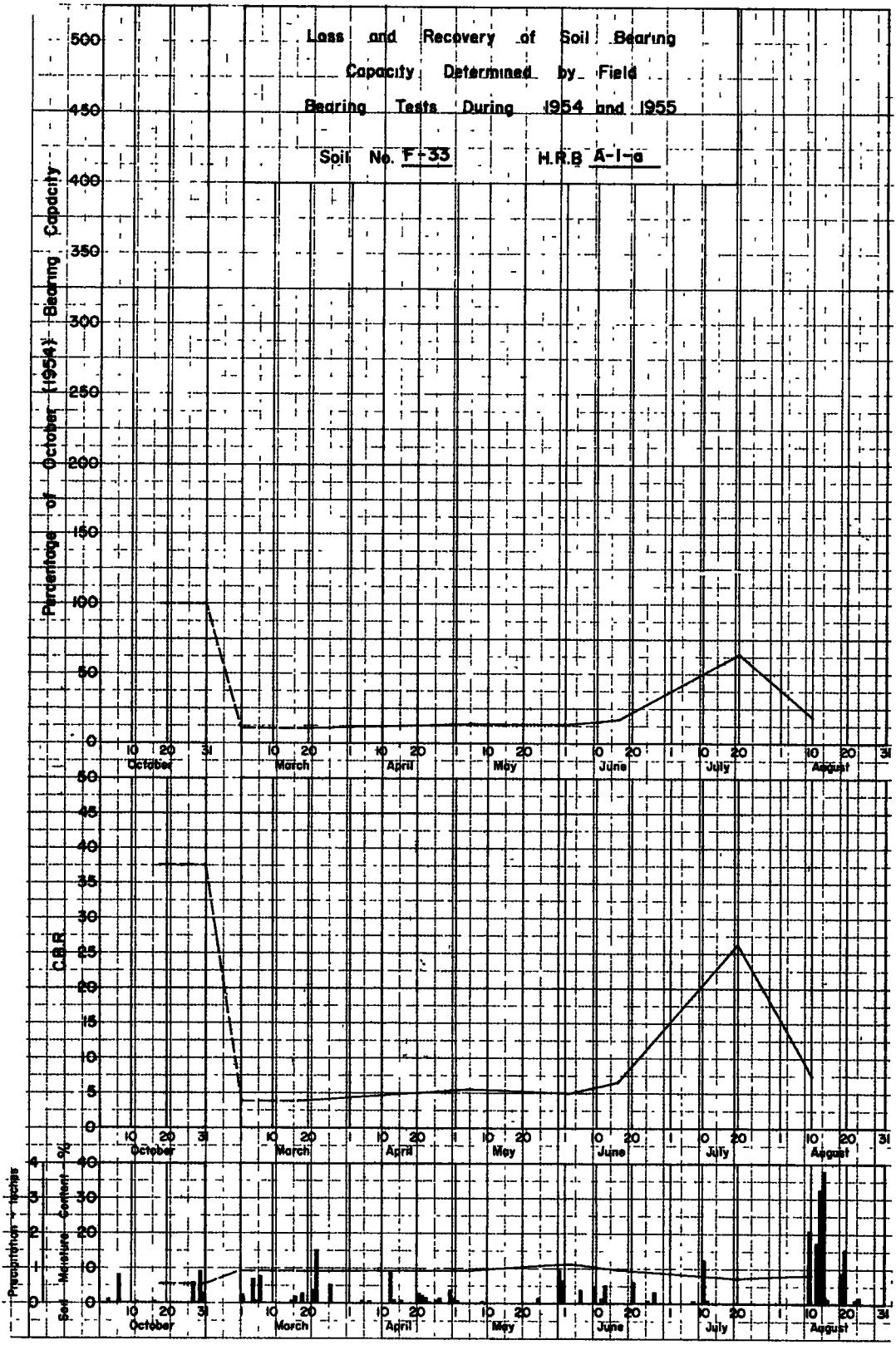
Loss and Recovery of Soil Bearing Capacity Determined by Field Bearing Tests During 1954 and 1955
Soil No. F-33
H.R.B A-1-a
Percentage of October (1954) Bearing Capacity
C.B.R
Soil Moisture Content %
Precipitation - Inches
October
March
April
May
June
July
August

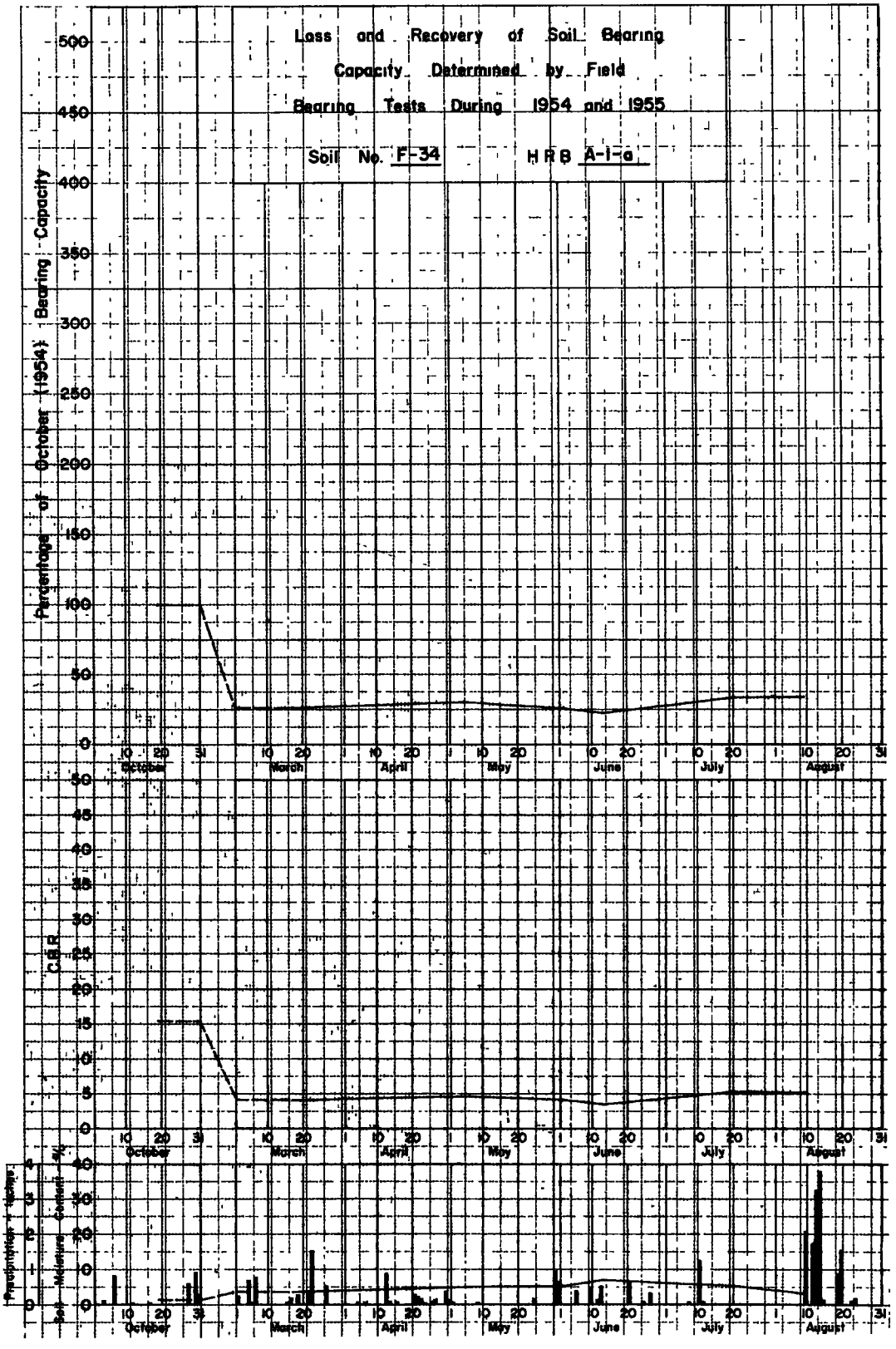
Loss and Recovery of Soil Bearing Capacity Determined by Field Bearing Tests During 1954 and 1955
Soil No. F-34
H R B A-1-a
Percentage of October (1954) Bearing Capacity
C B R
Precipitation + Melting
Soil Moisture Content %
October
March
April
May
June
July
August

Soil Moisture Tension and Ice Segregation

EDWARD PENNER, Soil Mechanics Section
Division of Building Research, National Research Council, Canada

This paper deals with some of the fundamental aspects of frost actions in soils. It is suggested that the freezing point depression at the ice-water interface determines the soil moisture tension which acts as the driving force during frost heaving. The dimensions of the soil pores are responsible, at least in part, for the induced freezing point depression when a saturated soil specimen is frozen unidirectionally.

Moisture tensions in excess of 8,000 cm of water have been measured in closed systems containing fine-grained soils after heaving approached zero, but are much less in coarse-grained soils. Blended soils covering a wide textural range as well as fine Ottawa sand were used to prepare a series of test specimens. In general, the experimental findings are in harmony with the suggested theory.

● THE PROBLEMS arising from frost action are well known to the soils engineer concerned with the construction and maintenance of highways and airports. The destructive action falls into two fairly distinct categories. One involves uniform or differential frost heaving as a result of ice segregation; the other concerns the loss of bearing strength when thawing occurs. A soil which exhibits either one or both of these conditions is known as a frost-susceptible soil.

The growth of ice lenses results from the migration of water to the freezing zone, from either a high water-table or the unfrozen portion of the soil which reduces its moisture content. The whole process of frost heaving, therefore, depends on the development of tension in the soil moisture at the freezing plane which acts as the driving force for moisture migration.

An investigation was undertaken to determine the dominant characteristics of the soil system responsible for the development of a moisture tension at the freezing plane. This paper reports soil moisture tension measurements under controlled freezing conditions for a number of soils, and also suggests a mechanism which is compatible with the experimental findings.

METHODS AND MATERIALS

Description of Frost Action Apparatus

The temperature conditioning apparatus has already been described (1). A modification was made to the frost cell containing the soil specimen to reduce further the frictional resistance to heaving. In place of a continuous sleeve around the upper portion of the soil specimen, a stack of lucite rings, each approximately ¼ in. in length, was used. A photograph of the frost cell is shown in Fig. 1. A sectional drawing of the frost cell incorporating the modification is shown in Fig. 2.

The temperature conditioning of the soil specimen is achieved by circulating temperature-controlled mixtures of ethylene-glycol and water through the compartments shown. The inlets and outlets to the compartments are set obliquely to the periphery of the cell but parallel to each other to facilitate the circulation of the cooling liquids, thus providing good heat exchange.

The frost cell was designed to give both a sharp temperature gradient at the frost line and a reasonably constant temperature over the lower two inches of the soil specimen. In this way, thermally activated vapour diffusion would be reduced to a minimum over the lower portion of the specimen. The characteristics of the moisture flow are interpreted in terms of liquid flow, recognizing some contribution to the total flow in the vapour phase.

Description of Soil and Sand Samples

The soil samples used in these experiments consisted of artifically blended soils.

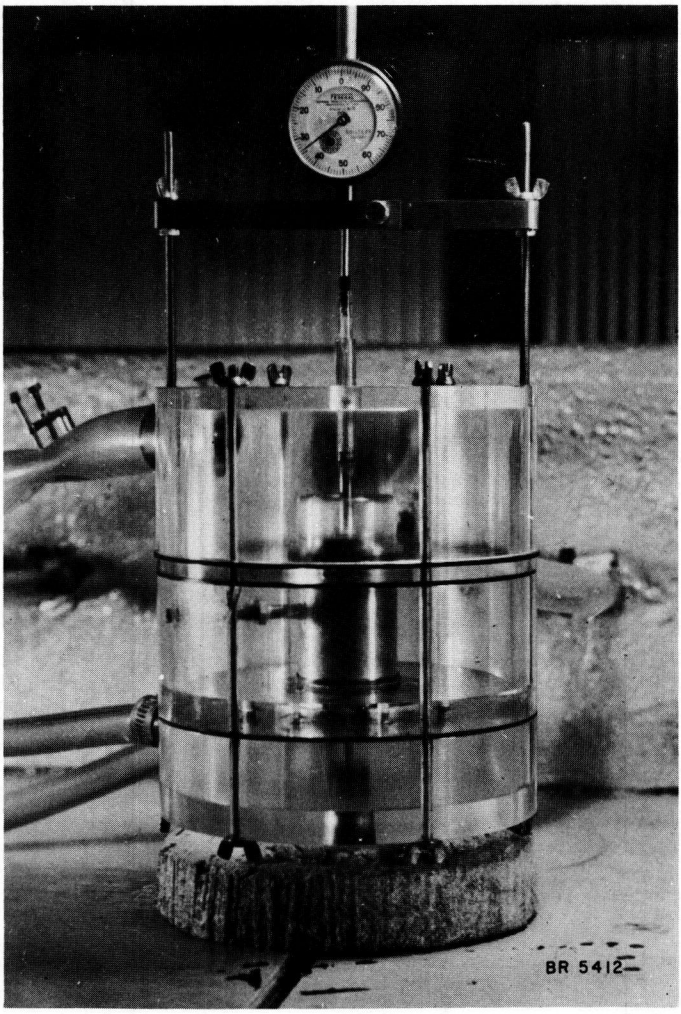

Figure 1. The frost cell in operation.

Leda clay was dried, crushed, then passed through a 100-mesh sieve and thoroughly mixed in an end-over-end shaker. This mix is designated as sample No. 4. Samples No. 1, 2, and 3 consisted of Leda clay and various proportions of Ottawa sand passing a 100-mesh sieve. Sample No. 6 was a mixture of Labrador silt and Leda clay. Samples No. 5 and 7 were composed solely of ground Ottawa sand; they differed in particle size only. Sample No. 5 was the portion passing the No. 325 sieve; No. 7 consisted of sand in the particle size range between the No. 200 and No. 325 sieves.

In all cases, the Ottawa sand was acid washed subsequent to grinding and finally washed with distilled water until the pH reaction of the filtrate was neutral. The hydrometer analyses for the soil samples are shown graphically in Fig. 3, with the exception of the two sand samples. Table 1 gives the Atterberg Limits for samples 1 to 4.

Specimen Preparation

The cylindrical specimens, $1\frac{5}{16}$ in. in diameter and approximately 3 in. long, were prepared directly in the frost cell in $\frac{1}{2}$-in. layers at the air-dry moisture content. Sample No. 4 was prepared at a density of 1.26 gr/cm^3 since this was the highest density

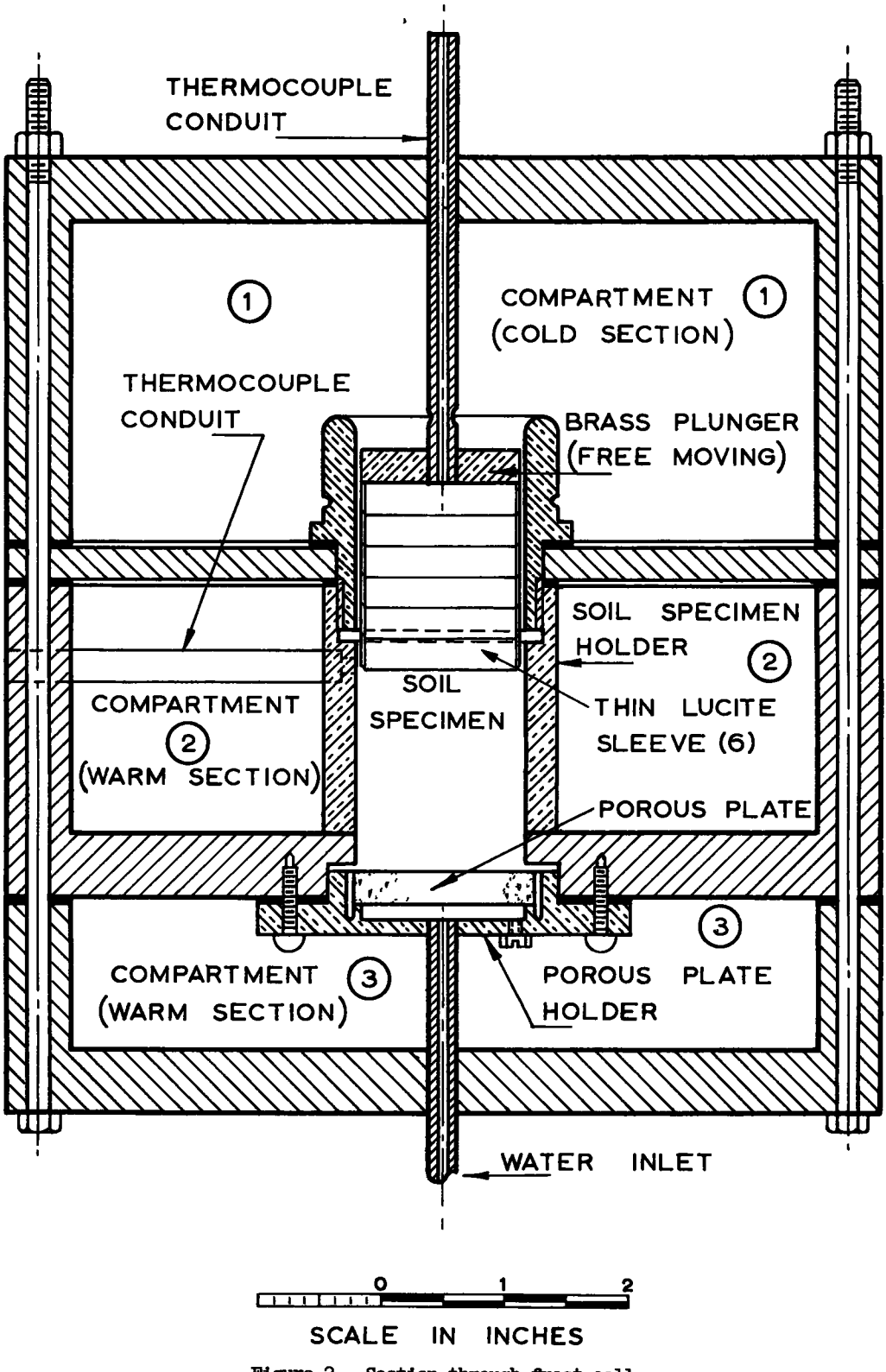

Figure 2. Section through frost cell.

TABLE 1

ATTERBERG LIMITS FOR THE FOUR FINE-GRAINED SOILS USED IN THE FREEZING EXPERIMENTS

Sample No.	Liquid Limit	Plastic Limit	Plasticity Index
1	23.7	16.1	7.6
2	33.2	20.7	12.3
3	39.0	23.8	15.2
4	54.2	31.8	22.4

TABLE 2

FINAL MOISTURE CONDITIONS OF THE UNFROZEN SOIL
(Temperature of 1.5 C on Warm Side and -6 C on Cold Side)

Sample No.	Percent Moisture Contents				pF[a]
	1	2	3	Ave.	
4	34.5	35.0	34.8	(34.8)	3.70
3	27.2	27.2	27.2	(27.2)	3.46
2	23.2	23.2	23.1	(23.2)	3.46
1	17.9	18.0	18.0	(18.0)	2.98
6[b]	27.8	28.0	28.2	(28.0)	2.60

[a] log moisture tension expressed in cm of water
[b] average of two experiments

TABLE 3

FINAL MOISTURE CONDITIONS OF THE UNFROZEN PORTION
(Temperature at Warm Side 1.5 C and -3 C on Cold Side)

Sample No.	Percent Moisture Content					pF
	1	2	3	4	Ave.	
4	34.6	34.6	34.6	34.4	(34.6)	3.70
6	26.2	24.9	24.6	25.6	(25.3)	2.66
5[a] sand pass 325	30.5	31.3	31.3	32.4	(31.3)	2.13
7 sand 200-325	31.4	30.9	29.6	30.4	(30.6)	1.5

[a] average of two experiments

TABLE 4

FINAL MOISTURE CONDITIONS OF THE UNFROZEN PORTION FOR SPECIMENS PREPARED OF TWO DIFFERENT SOILS

(Upper Half Containing Ice Lens Consisting of Sample No. 3 and Lower Half as Designated in the Table)

Sample No. (of lower half)	Percent Moisture Content (of lower half)				Percent Moisture Content Sample No. 3 (upper half)	pF
	1	2	3	Ave.		
6[a]	11.3	11.2	11.2	(11.2)	26.8	3.50
5[b] sand pass 325	4.0	4.4	4.3	(4.25)	27.6	3.44

[a] temperature of warm side 1.5 C, cold side -6 C
[b] temperature of warm side 1.5 C, cold side -3 C, and is the average of two experiments

obtainable in the air-dry state. Samples No. 5 and 7 were prepared at a density of 1.5 and 1.6 gr/cm^3 respectively, and all other samples at 1.4 gr/cm^3. No. 30 copper-constantan thermocouples were placed at ½-in. intervals in the bottom 2-in. portion and one was positioned at the top of the specimen. To avoid errors in temperature measurement due to heat conduction along the thermocouple wire, one complete turn equal to the circumference of the specimen was coiled at the level where the thermocouple was placed. Each thermocouple was positioned in the middle of the cylindrical specimen.

After preparation, the specimens were allowed to absorb water from a free water-table, level with the base of the specimen, until no further water was withdrawn from the reservoir.

The pF/Moisture-Content Relationship

The various mechanisms whereby water is held in the soil are still not known with certainty. There appears, however, to be general agreement that, at high moisture contents, moisture is held in the soil by surface tension, and that at low moisture contents the surface forces on the solids play a major role. Irrespective of the actual mechanism, many workers have shown that there is a continuous relationship between pF and moisture content from saturation to oven dryness.

The pF term introduced by Schofield (3), is the logarithm of the length of water column in cm required to give a certain moisture tension, i.e., pF=log h, where h is the water column length in cm. The pF/moisture-content relationship is dependent on the direction from which any equilibrium point is approached. As a result, for any porous material there is usually both a wetting and a drying curve for this relationship. Since the freezing of soil is a drying process, this so-called hysteresis phenomenon need not be further considered.

The pF/moisture-content curves for the soils used in these studies were determined by the porous plate (4) and pressure membrane (5) techniques. In the range pF=0 to

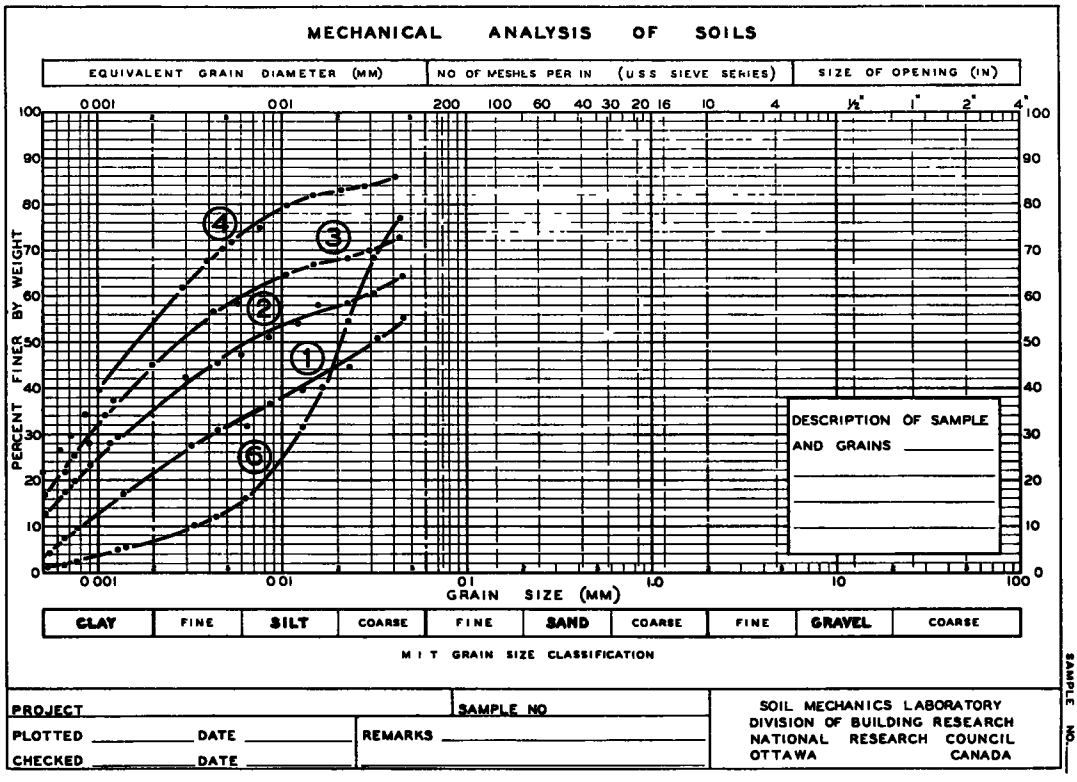

Figure 3.

pF=3, a previously saturated soil sample is placed on a porous ceramic plate across which a pressure difference is maintained. Provided a liquid contact exists between sample and porous plate, the sample will continue to release water until pressure equilibrium is established. The equilibrium moisture content is determined either by oven drying the sample or by measuring the moisture loss from the saturated condition. The limit of usefulness of a porous plate depends on the size of the largest pores. When air begins to pass through the plate, the pressure difference cannot be maintained and other techniques must be used.

For the range from pF=3 to pF=4, the porous plate is replaced by a porous membrane such as Visking sausage skin. In this way, sufficient points of equilibrium may be established to construct a continuous pF/moisture-content curve. The relationship between the largest pressure difference maintainable across a porous plate or membrane and the pore radius is given by the so-called height-of-capillary-rise equation:

$$h = \frac{2s}{rdg} \qquad (1)$$

where h = height of liquid column;
r = radius of curvature of liquid surface, also the radius of pore when maximum curvature is developed;
d = density of the water;
g = acceleration due to gravity; and
s = surface tension for air-water interface.

In the cgs system

$$\text{Schofield's } pF = \log h = \log\frac{(2s)}{(rdg)} \qquad (2)$$

The pF/moisture-content relationships for the soils used are shown in Fig. 4. To evaluate whether the relationship determined at 20 C could be used near the freezing point, some of the determinations were repeated at 1.5 C for three soils over the pF range 1.8 to 3.2. It can be seen that within the normal fluctuations caused by experimental error, the relationship is apparently similar at both temperatures. Hutcheon (6), after completing a literature review on the effect of temperature on moisture retention, has examined the applicability of the equations proposed by Edlefsen and Anderson (7) and Croney and Coleman (8). The equation proposed by the first-mentioned authors can be expressed in the form:

$$H_T = \frac{T_1T_2\ (\log H_2 - \log H_1)}{T\ (T_1 - T_2)} + \frac{(T_1 \log H_1 - T_2\ \log H_2)}{T_1 - T_2} \qquad (3)$$

where T, T_1 and T_2 = absolute temperatures; and
H, H_1 and H_2 = relative humidity expressed as a fraction and at the appropriate temperature.

When applied to absorption data for Sitka spruce, Hutcheon obtained good correlation between predicted and experimental values at relative humidities below 90 percent.

In the high humidity range corresponding to pF values less than 4.5, limited experimental data showing temperature dependence appear in the literature. The experimental results in Fig. 4 at two temperatures suggest that pF data in the high moisture-content region are applicable over a fairly wide temperature range. The effect of temperature on pF through surface tension was shown to be small by Croney and Coleman (8), in the following equation:

$$pF_1 - pF_2 = \log T_1 - \log T_2 + \log d_2 - \log d_1 \qquad (4)$$

where T_1 and T_2 = surface tension of air-water interface at two different temperatures;
d_1 and d_2 = density of water at two different temperatures. The equation predicts a change of approximately 0.10 units for a 10C change in temperature.

Sample Freezing Procedure

Upon completion of the water absorption process in the soil samples, the circulation

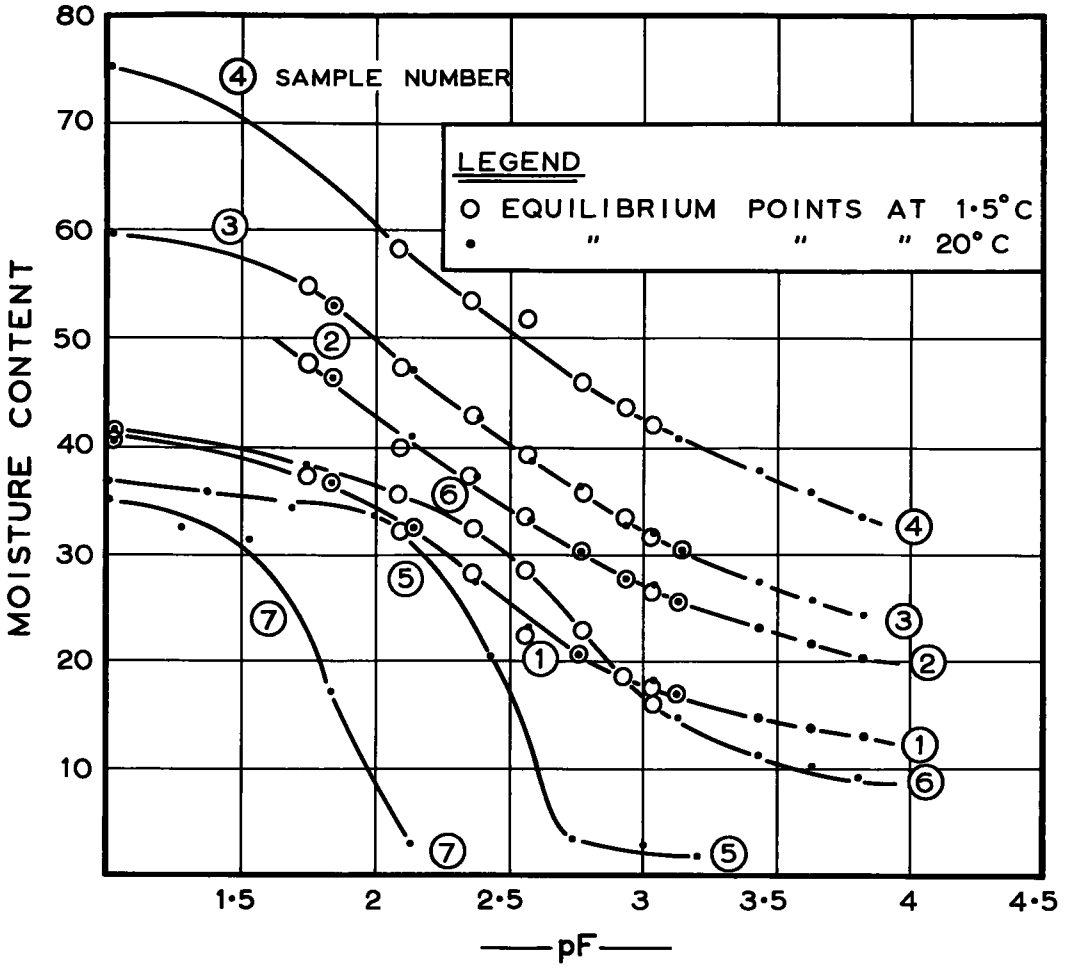

Figure 4. The pF/moisture-content relationship.

of the temperature conditioning fluid (1. 5 C) was started through compartments 2 and 3. When the specimen reached temperature equilibrium with the circulating fluid in compartments 2 and 3, circulation was started through compartment 1 using fluids from the second tank which were delivered to the compartment at either -3 or -6 C, depending on the particular experiment.

Crystallization was mechanically induced when the temperature at the top of the specimen indicated supercooling of approximately 2 C. An extensometer was mounted on the cell to measure the movement of the plunger which rested on the top of the specimen. The system was permitted to operate as an "open" system, with a free water-table at the bottom of the specimen, until the maximum heave rate under these conditions had been attained. During this period the rate of moisture flow into the specimen and the measurements of heave were obtained. After the establishment of the rate of maximum heave, the external source of water was removed. Further heaving occurred as a result of moisture loss from the unfrozen portion. The system now operated as a closed system.

When the extensometer readings indicated that heaving had almost ceased, i. e., that the heaving rate was approaching zero, the apparatus was dismantled and the unfrozen portion of the specimen was sectioned into ½-in. layers for determinations of moisture content. In soils where a high pF was induced a small residual amount of heaving was

still evident at the time of sampling. This was attributed partly to vapour flow. With the pF/moisture-content relationship known for each soil, the soil-moisture/tension induced by ice segregation could be obtained indirectly from the moisture content of the sample. The sampling procedure was performed as rapidly as possible to minimize redistribution of moisture. In the light-textured soils, a small amount of melting seemed to occur at the ice-water interface. This was not considered serious enough to invalidate the conclusions.

Experimental Results and Discussion

In all the experiments discussed in this paper, the temperature of the temperature-conditioning liquids was not altered after the experiment was started. The freezing plane was allowed to penetrate naturally into the specimen. At the conclusion of the experiments, the length of the unfrozen portion was approximately 1.75 in. when the temperature on the cold side was held at -6 C. With a cold side temperature of -3 C, the length of the unfrozen portion was about 2 in.

Although the frost cell was designed to give a constant temperature over the unfrozen portion, this objective was not completely achieved. Two typical temperature distributions are given in Fig. 5 for sample No. 6 at the two different cold-side temperatures. In general, the temperature distributions were the same for all samples. There were, however, minor differences due to swelling which displaced the thermocouples to some extent. The temperature distribution in the frozen layer was not measured since it was found that, as the thermocouple wires were frozen in, there was some interference with the heaving process. It can be seen that the largest temperature gradient in the unfroz-

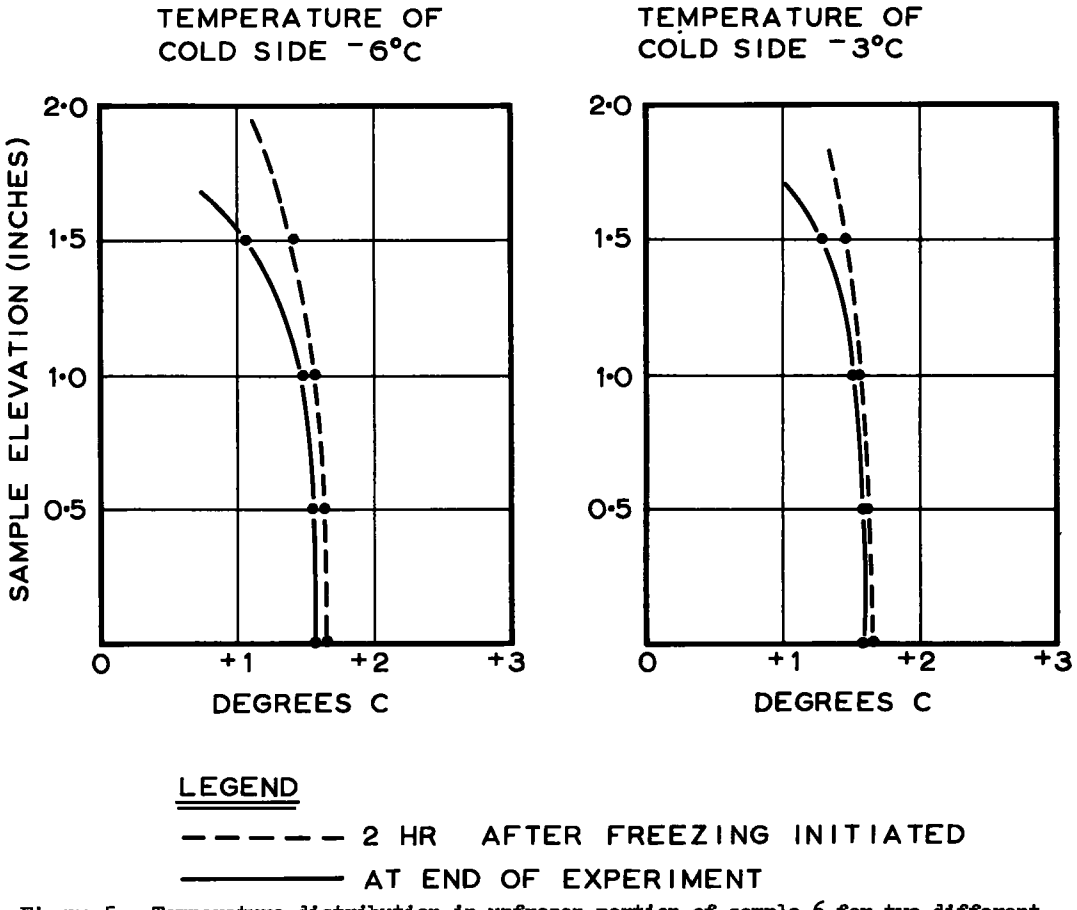

Figure 5. Temperature distribution in unfrozen portion of sample 6 for two different temperatures at the cold side.

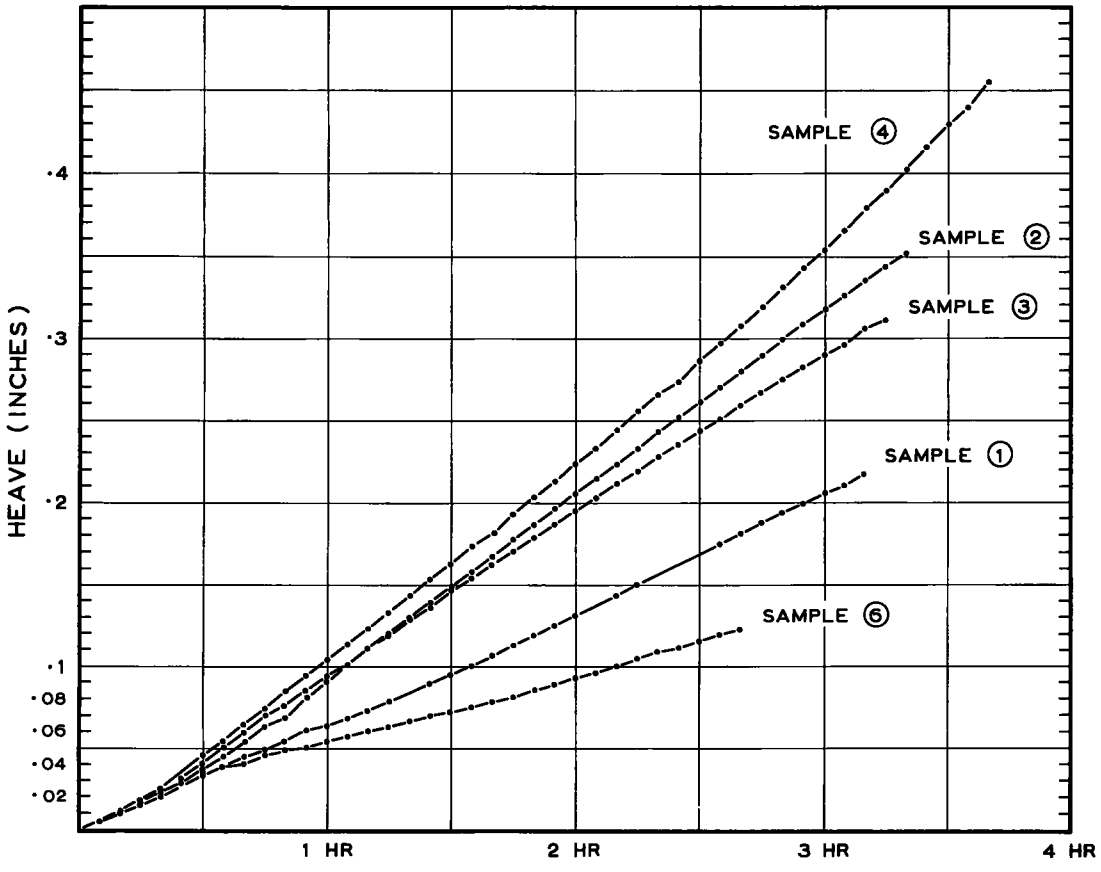

Figure 6. The amount of heave versus time with free water table at the base of the specimen (temp. of warm side 1.5 C, cold side -6 C).

en portion of the sample occurred immediately beneath the freezing zone. No influence of this temperature gradient upon moisture contents could be detected, i. e., the moisture contents were essentially the same in all sections of the unfrozen sample at sampling time.

Figure 6 shows the heave-time relationship, plotted at 5-min intervals, when the cold side was maintained at -6 C and with a free water-table at the base of the specimen. There appears to be a relationship to soil texture evident in the comparison of Fig. 3 with Fig. 6. The finer the texture of the sample, the greater is the rate of heave.

The open system part of the experiment was terminated when it became evident that the maximum rate of heave had been obtained. (In the case of sample No. 4, the maximum rate was probably not obtained before the external source of water was cut off, as indicated by the shape of the heave-time relationship.) The end of each curve marks the time when the external source of water was cut off; further heaving could occur only as a result of internal water loss. It was then possible to determine the moisture tension induced in the unfrozen portion of each soil due to a freezing plane.

Figure 7 shows the results of the heave measurements during the entire experimental period which were terminated when the heave rate approached zero. As already noted, a very small amount of heaving was still evident in the heavy-textured samples when the experiment was terminated; a contribution attributed, in part, to vapour flow. Figure 8 shows that the dominating characteristics of frost heaving are determined by the soil at the ice-water interface. These experiments were carried out in the same way as those summarized in Fig. 7. The lower curve shows the heave versus time relationship for sample No. 6. The results shown in the upper curve are for a specimen containing sam-

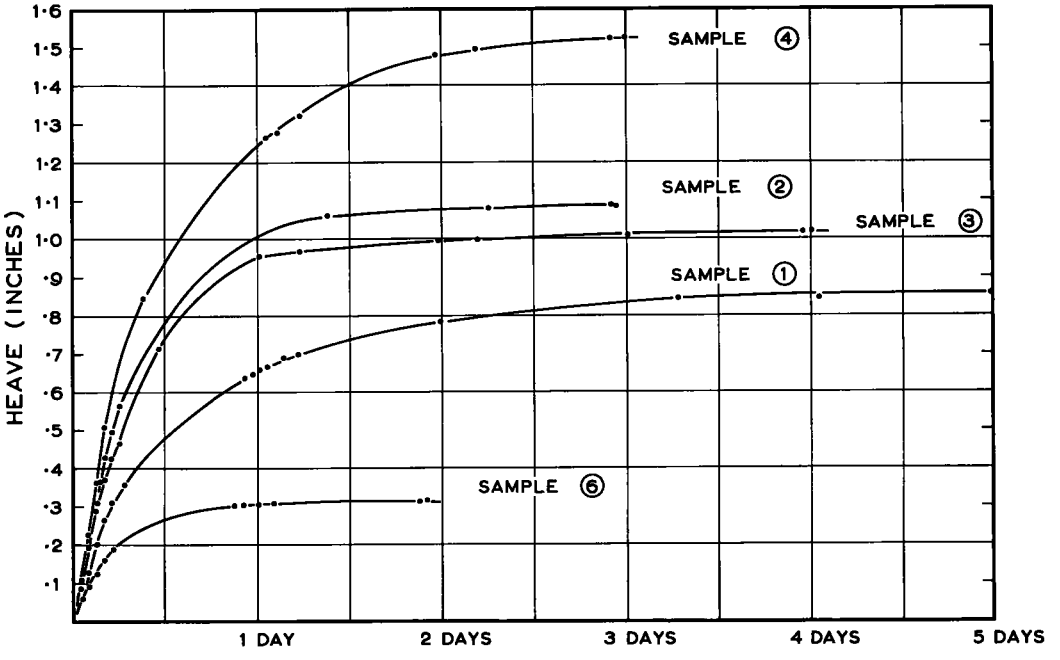

Figure 7. The amount of heave versus time for a number of different soils (temp. of warm side 1.5 C, cold side -6 C).

ple No. 6 in the lower half and sample No. 3 in the upper half. The freezing zone remained in the portion of the specimen containing sample No. 3, but when heaving approached zero, it had penetrated to within ½ in. of sample No. 6. The upper curve shows that the heaving characteristics were dominated by the soil at the ice-water interface (sample No. 3), and that sample No. 6 acted merely as a transmission zone for

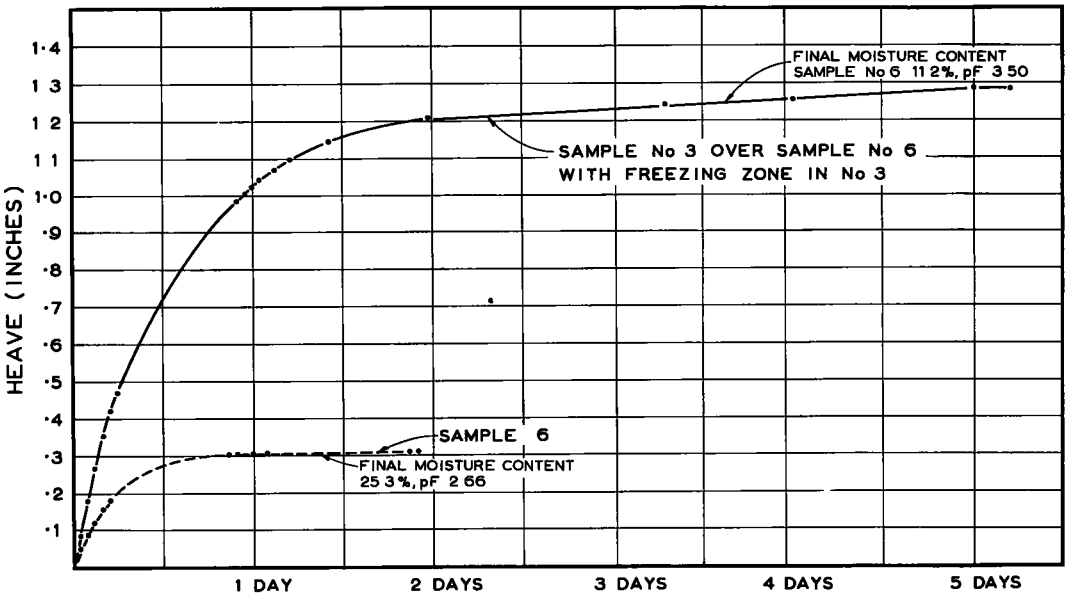

Figure 8. The amount of heave versus time showing the added heave from sample No. 6 when the freezing zone is located in a layer of finer textured soil (No.3).

moisture flow when it operated as an open system, and as a source of water supply in a closed system.

Similar experiments with other soils confirmed these conclusions. The coarsest sample used as a transmission zone was sample No. 5 (the portion of finely ground sand passing the No. 325 sieve). These experiments indicate the ability of coarser-

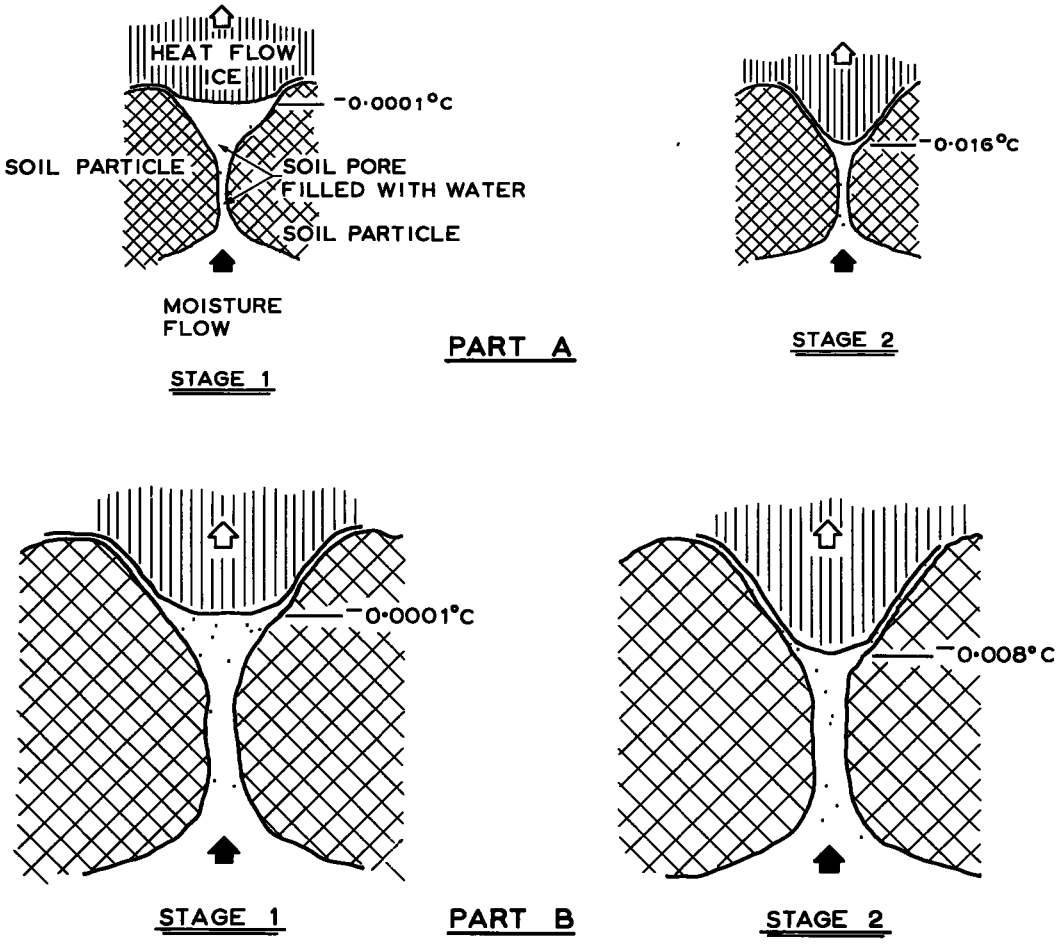

Figure 9. An enlarged schematic diagram of two different pore sizes showing stages in the movement of the ice/water interface with assumed freezing point depressions.

grained soils to act as effective transmission zones or as sources of water supply, if the frost line intercepts small layers or islands of heavier-textured materials.

Tables No. 2, 3, and 4 show the moisture contents and corresponding moisture tensions when heaving approached zero in a closed system. The numbers along the top of the table designate the position of the layers in the soil column, No. 1 being the bottom ½-in. layer, No. 2 the second ½-in. layer, etc. It should be noted that the final moisture content was essentially constant throughout the unfrozen portion of the specimen for any given soil. The moisture contents of the unfrozen portion, which are essentially the same in all layers, reflect the moisture tension induced by the freezing zone through the liquid phase. The last column gives the moisture tension in terms of Schofield's pF. This pF value was obtained from Fig. 4, which gives the pF/moisture-content relationship for each sample.

Table No. 3 gives similar data to that in Table No. 2, but for a temperature of -3 C on the cold side instead of -6 C. A comparison of the results for samples No. 4 and 6

in Tables 2 and 3 shows that the final tension in the soil moisture is not influenced by the temperature on the cold side.

In the case of the lower temperature, the frost line penetrated a little more than ¼ in. further. The transient soil moisture tensions however, appear to be dependent on rate of heat removal.

When the specimen was composed of layers of two different soil samples, the moisture tension induced was shown to depend on the soil type in which the freezing zone was located. These results are shown in Table No. 4. By referring the moisture contents in Table No. 3 to Fig. 4, it can be seen that the moisture content of sample No. 6 was drawn down to that corresponding to the pF of the soil above it which contained the freezing zone, in this case sample No. 3. A pF of approximately 2.6 was induced when the entire specimen consisted of sample No. 6. This sample has an average moisture content of 25.3 percent at this pF. With the freezing zone in sample No. 3 above it, the equilibrium moisture content was 11.2 percent, which corresponds closely to the pF induced in sample No. 3. Similarily for the sand, in sample No. 5 (passing No. 325) the moisture content was 31.3 percent (Table No. 3), but with the freezing zone in sample No. 3 (Table No. 4), its moisture content was reduced to 4.25 percent. According to the pF/moisture-content relationship for this sample, the moisture content should have been reduced to about 2 percent at a pF of 3.44. That this failed to occur may have been due to a number of causes, such as sample No. 3 shrinking away from the sand or that, at this very low moisture content, transmission of moisture was very low and the equilibrium conditions were not quite attained. Nevertheless, the amount of moisture released during frost action in closed systems appears dependent on the pF induced at the ice front and this, in turn, depends on soil type. The finer the texture of the soil, and consequently the smaller the pores, the greater the pF induced. The pF's induced when heaving approached zero ranged from 1.5 for a sand (sample No. 7) to 3.7 in Leda clay (sample No. 4). These tensions expressed in psi are 0.98 and 120 respectively.

In the light of these experimental results, attention is now invited to some of the significant features of a soil system which appear to be dominant in the development of soil moisture tensions during unidirectional freezing.

Suggested Mechanism in the Development of Tensions

It will be recalled that the free energy of a system always decreases in a spontaneous change. If the temperature is lowered in an ice-water system originally in equilibrium, the specific free energy of each phase at constant pressure will change with temperature according to the following equation: $df = -sdt$. The phase with the greatest specific entropy, s, will have the greatest free energy for a given decrease in temperature. The spontaneous change will be the conversion of water to ice which is made possible by the temperature drop.

The size of a stable spherical crystal of a solid in its own melt is known to be temperature dependent. The relationship is given by the following equation used recently by Sill and Skapski (9):

$$\Delta T = \frac{2T_m \sigma_{sl}}{r \rho_s Q_f} \qquad (5)$$

where r = radius of curvature of the crystal (critical size);

ρ_s = density of the solid;

σ_{sl} = interface tension between solid and liquid;

Q_f = heat of fusion;

T_m = the temperature of melting at zero curvature of the solid/liquid interface; and

ΔT = the depression in freezing point below T_m.

Application of this relationship to the unidirectional freezing of saturated salt-free soils in a closed system, shows that the temperature at which an ice-water interface can advance into a soil pore depends on the size of the pore, i.e.,

$$\Delta T \propto \frac{1}{r}$$

(where r is now considered to be radius of the soil pore). Thus it can be seen that the radius of the soil pore sets the size of the advancing tongues of ice. It is then clear that the advance of the ice-water interface will occur at a lower temperature in a soil containing mostly small pores than in a soil in which large pores predominate.

Winterkorn (10) has used the second law of thermodynamics to give a quantitative measure of the free energy or maximum amount of work available during frost action. More recently Jumikis (11) has compared these theoretical values with experimental results obtained under dynamic conditions. The law is used here to describe the amount of work solely as a result of the depressed freezing point. Under these circumstances, the amount of energy available is directly proportional to the freezing point depression and gives a method of evaluating ΔP_w, the induced soil moisture tension.

$$W_{max} = Q_f \frac{(T_2 - T_1)}{T_2} = \frac{Q \Delta T}{T_2} = V_w \Delta P_w \qquad (6)$$

where W_{max} = maximum work available or free energy;

Q_f = latent heat of fusion;

T_2 = the freezing point of free water and is equal to T_m in equation (4);

T_1 = the temperature at which freezing is occurring at the water-ice interface;

ΔT = freezing point depression;

V_w = specific volume of water; and

ΔP_w = change in soil moisture tension at equilibrium as a result of ΔT.

It has been assumed in Fig. 9 that a microscopic section of the soil-water-ice system can be represented schematically for purposes of clarity. These sketches are not to scale and are merely intended to help to illustrate the pertinent features under discussion. Stage 1 in both sketches shows that the water is freezing close to 0 C in the wide portion of the soil pore. In order for the ice to invade the narrow neck, a certain freezing point depression must take place, i.e., the 0 C isotherm must advance ahead of the freezing plane to fulfill the requirements of equation (4). In the case of the larger pore in Stage 2 of Fig. 9B, ΔT is much smaller at the soil-water interface. Ultimately, as the size of the pore considered is increased to the size that exists in coarse sand, the temperature of the freezing plane will be very close to 0 C and a correspondingly small tension would be induced in the soil moisture. In the period between Stages 1 and 2, a sufficient flow of water to the freezing zone may retard the advance of both the zero isotherm and the freezing plane. In this situation the rate of heat removal from the freezing plane will largely control the rate of heave; it is at this stage that ice lens growth takes place. When the flow of moisture is restricted, the temperature will drop at a given point in the soil, larger pores may be emptied through connecting channels, and the process will continue in the soil below.

A phenomenon which is also possible is that crystallization may occur in soil pores below the existing ice-water interface before the water freezes in the smallest pores. Many cases of unfrozen layers have been reported in the literature. The invasion of ice by way of large surrounding pores may also occur and the complete development of freezing point depression, demanded by the smaller pores, may be interrupted. These considerations generally appear to account for the high moisture tensions developed in fine-grained soils and the relatively small tensions in coarse-grained soils which were originally saturated identically and subjected to the same temperature conditions.

There are still many uncertainties that prevent the useful application of this concept. In equation (5), which relates the minimum radius of curvature of the solid-liquid inter-

face to freezing point depression, only approximate values for interface tension are available. It is indeed uncertain whether the equation can be rigidly applied to minute pores where the force fields occupy a considerable portion of the pore or when the soil moisture is under tension in unsaturated systems. This point is discussed in some detail by Gold (12). While it is generally true that the dimensions of the soil pores decrease with decreasing particle size no exact mathematical solution of pore size or pore size distribution is possible and, in the development of moisture tension, the existence of some large pores may tend to nullify the effect of the smaller pores.

Pore sizes in swelling soils will vary with changing moisture content. Since the freezing phenomenon is a drying process, the soil moisture tension induced in this way will tend to decrease pore size. The freezing point depression due to dissolved solids in the soil moisture is superimposed on the depression due to pore size. Since salts will tend to accumulate during the flow of moisture to the freezing front, a satisfactory allowance for this effect is problematic.

CONCLUSION

The experimental results herein presented show that: (a) for the materials at the densities used, the rate of moisture flow due to unidirectional freezing in an open system is greatest for the heaviest-textured soil and least for sand; this could occur only as a result of higher moisture tensions induced at the freezing zone; (b) the moisture tension developed in a closed system appears to be largely dependent on soil texture; the greater the proportion of fines, the higher the moisture tension, and thus, more moisture is made available for heaving; (c) at two different cold-side temperatures, the moisture tension of the unfrozen portion was the same but caused only a shifting of the freezing plane; and (d) in specimens prepared in layers from two different materials, the moisture tension in the unfrozen portion is dependent on the material in which the freezing zone is located.

Theoretical considerations show that moisture tensions can develop in soils during freezing as a result of freezing point depressions. The freezing point at the ice-water interface and its radius of curvature must decrease as smaller pores are invaded by ice. As a consequence, higher tensions are developed in soils with small pores than with large pores. This appears to be in agreement with the experimental results presented.

ACKNOWLEDGMENT

This paper is a contribution from the Division of Building Research, National Research Council of Canada and is published with the approval of the Director.

REFERENCES

1. E. Penner, "Soil Moisture Flow During Ice Segregation," Bulletin No. 135, Highway Research Board, 1956.

2. L. A. Richards and D. C. More, "Influence of Capillary Conduction and Depth of Wetting on Moisture Retention in Soil," Transactions, American Geophysical Union, Vol. 33, 1952, pp. 531-554.

3. R. K. Schofield, "The pF of the Water in Soil," Third International Congress on Soil Science, Vol. 2, 1935, pp. 37-48.

4. L. A. Richards and M. Fireman "Pressure-Plate Apparatus for Studying Moisture Sorption and Transmission by Soil," Soil Science, Vol. 56, 1943, pp. 395-404.

5. L. A. Richards, "Pressure Membrane Apparatus, Construction and Use," Agricultural Engineering, Vol. 28, 1947, pp. 451-454.

6. W. L. Hutcheon, "Moisture Flow Induced by Thermal Gradients within Unsaturated Soils," Ph. D. Thesis, University of Minnesota, 1955.

7. E. Edlefsen and A. B. C. Anderson, "Thermodynamics of Soil Moisture," Hilgardia, Vol. 15, 1943, pp. 31-298.

8. D. Croney and J. D. Coleman, "Soil Thermodynamics Applied to the Movement

of Moisture in Road Foundations," Proceedings, Seventh International Congress on Applied Mechanics, Vol. 3, 1948, pp. 163-177.

9. R. C. Sill and A. S. Skapski, "Method for the Determination of the Surface Tension of Solids from their Melting Points in Thin Wedges," Journal of Chemical Physics, Vol. 24, 1956, pp. 644-651.

10. H. F. Winterkorn, Discussion of "Suction Force in Soils upon Freezing," by A. R. Jumikis, Proceedings, American Society Civil Engineers, Vol. 81, 1955, Separate No. 656, pp. 6-9.

11. A. R. Jumikis, "The Soil Freezing Experiment," Bulletin No. 135. Highway Research Board, 1956.

12. L. W. Gold, "A Possible Force Mechanism Associated with the Freezing of Water in Porous Materials," presented at the 1957 annual meeting of the Highway Research Board.

A Possible Force Mechanism Associated with the Freezing of Water in Porous Materials

LORNE W. GOLD
Division of Building Research, National Research Council, Ottawa, Canada

The thermodynamic equilibrium conditions for a water-ice interface in a pore of a porous medium are derived. It is found that, taking the geometry and physical dimensions of the pore into consideration, a positive pressure must develop between the ice and the solid in order for equilibrium to be maintained when the temperature at the freezing plane is depressed. A simple model utilizing this mechanism exhibits the same properties as a frost-heaving soil. The influence of air in the pores is briefly discussed.

●WHEN WATER is present in porous materials and is allowed to freeze, a force may be developed which is not directly related to the expansion that occurs when water changes to ice. Although many observations have been made on this phenomenon, particularly in the field of soil mechanics, a satisfactory explanation of the origin of this force has not appeared. Experiments to date indicate how the magnitude of this force depends on certain physical characteristics of the system. The following are some of the facts observed during experiments that a theory on the origin of this force must explain:

1. During the freezing process, the freezing plane may remain stationary while the ice phase continues to grow. When this occurs, the frozen portion is displaced relative to the unfrozen and a layer of ice, often called an ice lens is formed. The displacement may be microscopic or it may amount to several inches. This displacement occurs upwards in soil and is called frost heaving. The occurrence of heaving implies that: (a) Water is drawn from the unfrozen portion to the freezing plane by a force occurring at the freezing plane and is thus under tension; (b) The force developed at the freezing plane is capable of exerting the pressure required to displace the frozen portion relative to the unfrozen; and (c) The pressure thus developed is transmitted from the ice phase to the unfrozen solid through a mobile layer which has at least quasi-liquid properties since the ice phase can continue to grow.
2. The magnitude of the force that can be developed during the heaving process depends on the size of the pores in the solid. Generally, for a granular material, the smaller the grains the larger the force (1).
3. The magnitude of the force developed at the freezing plane can be observed in two ways: (a) If the porous solid is confined and an unlimited supply of water is available, the magnitude of the force at the freezing plane is indicated by the amount of pressure which must be applied to prevent heaving; and (b) If the porous solid is unconfined, the magnitude of the force at the freezing plane is indicated by the tension that must be applied to the water to prevent heaving (2).

Under normal conditions, a porous body will contain both water and air. During freezing the solid-water-ice-air system undergoes changes in such a direction as to attempt to maintain thermodynamic equilibrium at the freezing plane. This paper develops the conditions for thermodynamic equilibrium between a water-ice interface in a small space. The influence of air in the system, with the resulting more complicated interface conditions at the freezing plane, is briefly discussed.

Description of the System

Figure 1 shows a hypothetical cross-section of the freezing plane in the pore space of a granular material. It will be assumed that the freezing plane occupies the x-y plane and heat conduction is in the z-direction. Since the system is dynamic a temperature gradient exists in the z-direction but it will be assumed that the temperature

difference between points A, B, and C is small compared to the depression of the equilibrium temperature of the freezing plane from O deg C. This would allow, to a first approximation at least, the application of thermodynamic principles to the establishment of steady state equilibrium conditions between A, B, and C.

It is assumed that a water film exists between the solid particle and the ice. Such a film on the surface of a solid has both liquid and solid attributes. A significant and sometimes very large pressure applied normal to the film is required to cause it to fail and, in this respect, its behaviour is solid-like. In the plane of the film there is a high degree of mobility and, in this respect, its behaviour is liquid-like. Such a film existing between the ice and solid would enable pressures to be transmitted from the ice to the solid and still allow water molecules to move from the pore space at A to the ice at C.

The water in the unfrozen portion is continuous as described in publications dealing with soil moisture, and is capable of being placed under tension. Let this tension be p_t. If the freezing plane is curved, pressures that owe their existence to this curvature are produced in the ice immediately adjacent to the curve surface. The magnitude of this pressure is given by:

$$p_s = C\left(\frac{1}{r_1} + \frac{1}{r_2}\right) \qquad (1)$$

in which C is a constant that depends on the interfacial energy between water and ice, and r_1 and r_2 are the principal radii of curvature of the surface (3). The sign of p_s depends on the curvature; it is positive on the concave side of the surface and negative on the convex. Thus at B, $p_s = p_{s1}$ is positive, whereas at C, $p_s = p'_{s1}$ is negative. As the ice at the interface at C grows, a pressure is developed and transmitted from the ice through the film to the solid. Let the value of this pressure be p'_{ot}. This pressure would tend to zero as B is approached.

Equilibrium Conditions[1]

The independent variables involved in this problem are pressure and temperature. Therefore, when discussing equilibrium, the appropriate thermodynamic function to use is the Gibb's thermodynamic potential:

$$g = u + pv - Ts$$

in which

g = thermodynamic potential in ergs per gm;
v = specific volume, in cu cm per gm;
p = pressure, in dynes per cm;
s = entropy in ergs per deg K per gm;
T = absolute temperature (deg K); and
u = internal energy in ergs per gm.

For equilibrium to exist between A, B, and C, the thermodynamic potential must be the same at these points. If a small change $dg = vdp - sdT$ occurs, then $dg_A = dg_B = dg_C$ when equilibrium is reestablished. In the following, changes in g are with respect to its value for T = 273.16 deg K and p = 1 atm.

First consider equilibrium conditions between A and B. If the temperature of the pore space drops by ΔT, the freezing plane will advance. As the freezing plane advances, the internal geometry of the solid requires that the surface take on a curvature as shown in Figure 1. If we assume that the water is under a tension, the change in pressure at A is equal to $dp_A = p_t$. The change in pressure at B at equilibrium is given by $p_{s1} + (p_t - p_{sw})$ where p_{sw} is the tension required in the water to establish

[1] The author wishes to draw attention to a very recent paper, "Resistance of Concrete to Frost at Early Ages," by T.C. Powers, presented at the RILEM Symposium on Winter Concreting, Copenhagen, February 1956, in which Mr. Powers applies the same thermodynamic principles to frost action in concrete.

naturally the same curvature in the water surface as in the ice.[2]

$$p_{sw} = - p_{si} \qquad (2)$$

If the ice and water are to be in equilibrium at the freezing plane after the temperature change ΔT then

$$v_w p_t - s_w \Delta T = v_i (2 p_{si} + p_t) - s_i \Delta T. \qquad (3)$$

Where the subscript w refers to values for water and i to values for ice. Thus

$$\Delta T = \frac{p_t (v_w - v_i) - 2 v_i p_{si}}{s_w - s_i} \qquad (4)$$

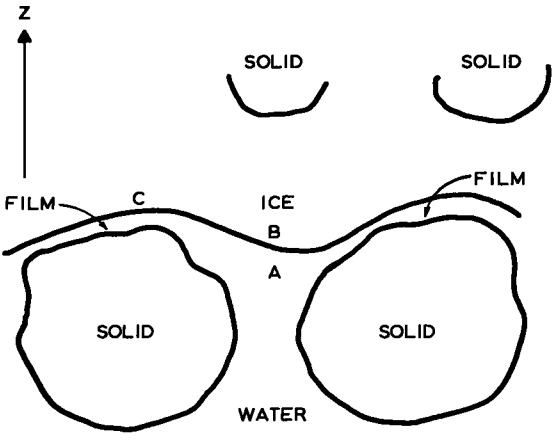

Figure 1. A hypothetical cross-section of the freezing plane in the pore space of a granular material.

In Eq. 3 $(v_w - v_i)$ and p_t are negative, $(s_w - s_i)$ is positive. Therefore, if the temperature is depressed below 273.17 deg K, a curvature must develop in the freezing plane to produce a positive p_{si} to reestablish equilibrium. From Eq. 1 and 4, it is seen that the greater the tension p_t, the larger is the curvature required to establish equilibrium between the ice and water for a given ΔT. The dimensions of the pores in the porous system impose a maximum value on the curvature of the interface. If the conditions are such that a surface with a larger curvature is required to establish equilibrium, the freezing plane would be able to advance to the next pore space. (In private correspondence the author has seen a discussion of this from the point of view of the kinetics of freezing prepared by Dr. B. Chalmers and his associates at Harvard University.)

The variables in Eq. 4 are potentially capable of changing in value as long as the heat flow from the freezing plane is greater than to it, i.e., ice is being formed at the freezing plane. When the condition is reached in which the heat flowing to the freezing plane exactly equals the heat flowing away, a value of ΔT, p_t and p_{si} will be associated with each pore, consistent with Eq. 4. The value of p_t will be the same for each pore.

If we let the pressure at B, which corresponds to the maximum curvature compatible

---

[2] The reasoning behind the expression for the change in pressure at B is as follows:

Consider the ice interface BC and the corresponding water interface being established in air. The pressure at B in the ice would therefore be $p_{si} = C_{ia}\left(\frac{1}{r_1} + \frac{1}{r_2}\right)$ and the pressure in the water would be $p_{sw} = -C_{wa}\left(\frac{1}{r_1} + \frac{1}{r_2}\right)$ where C_{ia} depends on the surface energy for an ice-air interface and C_{wa} on the surface energy for a water-air interface. Now, consider the ice surface replacing the air over the water surface as in Figure 1. C_{ia} and C_{wa} now become C_{wi} which depends on the surface energy between water and ice. If the surface film between the water and ice is to have the same curvature under the influence of pressure in the water only, then $p_{sw} = -C_{wi}\left(\frac{1}{r_1} + \frac{1}{r_2}\right) = -p_{si}$. Now the pressure at A in the water must be equal to the pressure of the rest of the water in the porous solid (assuming flow is negligible) and can be controlled independent of the surface curvature whereas p_{si} existing in the ice is completely determined by the curvature. If the pressure in the water at A is changed by $p = (p_t - p_{sw})$ and the curvature of the surface remains the same, an equal change in pressure must occur at B.

with the pore space, be p_{sim} and the tension in the water be p_t, then the freezing point depression required to freeze all the water in the pore is given by:

$$\Delta T_m = \frac{p_t (v_w - v_i) - 2 p_{sim} v_i}{s_w - s_i} \quad (5)$$

Thus the greater the tension p_t, the smaller is the freezing point depression ΔT_m required to freeze all the water in the pore.

In establishing the conditions for equilibrium between points A and C, it will be assumed that as long as the water in the pore space is not completely frozen, a water film exists between the ice and the solid. Figure 1 shows that a positive curvature developed in the ice at B results in a negative curvature at C. Let the pressure at C due to this curvature be p'_{si} as calculated from Eq. 1. In this case p'_{si} is essentially constant since the solid determines the values of r_1 and r_2. At C the pressure p'_{ot} also exists and is transmitted from the ice through the film to the solid. Thus the change in pressure at C is $dp_c = p'_{si} + p'_{ot}$ and in order to reestablish equilibrium between A, C, and B, $dg_A = dg_B = dg_C$, $v_w p_t - s_w \Delta T = v_i (2 p_{si} + p_t) - s_i \Delta T = v_i (p'_{si} + p'_{ot}) - s_i \Delta T$ (6)

Therefore,

$$p'_{ot} = 2 p_{si} + p_t - p'_{si} \quad (7)$$

p_t and p'_{si} are negative and p_{si} is positive. From Eq. 7 it is seen that depending on the values of p_{si}, p_t and p'_{si}, a positive pressure p'_{ot} is required to establish equilibrium for a temperature depression ΔT.[3] What Eq. 7 states is the obvious fact that at equilibrium the pressure in the ice at C must equal the pressure at B when ΔT at A equals ΔT at B.

To have a clear understanding of the conditions imposed by Eq. 7, consider the case where the tension in the water is zero ($p_t = 0$). If the temperature in the pore is depressed by ΔT, the thermodynamic potential in the water is increased by $dg_A = -s_w \Delta T$ and in the ice by $dg_C = dg_B = - s_i \Delta T$. But $dg_A > dg_B = dg_C$, therefore equilibrium will be upset and the ice phase will grow. To reestablish equilibrium, the pressure in the ice must be increased. This is accomplished at B by the positive curvature that develops in the freezing plane but at C this curvature is zero or negative, i.e., $dg_C < dg_B$. Water molecules will continue to migrate to C, therefore, until the build-up of ice at this point results in the development of the required positive pressure p'_o, the value of p'_{ot} for $p_t = 0$. At equilibrium, the value of p'_o can be obtained from the condition $dg_A = dg_B = dg_C$. $-s_w \Delta T = v_i (2 p_{si}) - s_i \Delta T = v_i (p'_{si} + p'_o) - s_i \Delta T$, therefore,

$$p'_o = 2 p_{si} - p'_{si} \quad (8)$$

When p_t does not equal zero, p'_{ot} as given by Eq. 7 is not due alone to the pressure developed by the formation of the ice lens at C and the subsequent heaving. If the tension in the water is not satisfied by the curvature developed at B, i.e., if the term $p_t - p_{sw}$ (see footnote 2) does not equal zero, then this unbalance will contribute to p'_{ot}. If $p_t - p_{sw}$ is negative there will be a net downward pull which will result in a positive pressure contribution to p'_{ot} at C. If $p'_{ot} = p'_o + p'_t$, where p'_t is the contribution due to the tension in the water and p'_o is the actual heaving pressure, then

$$p'_o + p'_t = 2 p_{si} - p'_{si} + p_t \quad (9)$$

Eqs. 4 and 9 give the conditions which must be satisfied at A, B, and C if equilibrium is to be established when the temperature of the pore is depressed by ΔT and the

---

[3] In establishing Eq. 6 and 7, a possible contribution to p'_{ot} due to the tension in the film between the ice and solid at C, not balancing the tension in the water surface at B has been neglected. This component would be very difficult to calculate since the film, which must be in equilibrium with all surrounding pores, does not have the same behaviour as a liquid with regard to applied pressure. It is possible that the film over the solid can alter its thickness and thus its energy and in this way always maintain equilibrium with the forces at the periphery. This would imply that p'_{si} would be altered accordingly.

water is under a tension p_t. If $p'_o = O$ (no overburden pressure) then

$$p'_t = 2\, p_{si} - p'_{si} + p_t \qquad (10)$$

Eqs. 4 and 10 give the conditions that must be satisfied to establish equilibrium by applying tension to the water only when the pore temperature is depressed by ΔT. A little thought soon indicates the difficulty of determining explicitly the value of p'_t, for it depends on the area over which the net downward pull of the water on the ice acts relative to the area over which p'_t acts.

Limitations Imposed on p_t

The increase of p_t in most problems encountered in practice is due to the drying action that results when water is drawn to the freezing plane. The distribution in pore and grain size would ensure a variation in the degree of advancement of the freezing plane through the various pores even if the temperature depression were the same in each. Initially the temperature depression may be very large so that the freezing plane could advance readily through all pores if conditions required it. As the freezing plane advances or the heat flow away from the freezing plane decreases, the temperature gradient at the freezing plane would decrease and a time would be reached when the freezing plane would be unable to advance through the smaller pores in pace with the larger. This would mean that the freezing plane would establish different stages of advancement that could exist for appreciable time (Figure 2). Such projections as A (Figure 2), would tend to act as anchors because if heaving occurs, solid particles B and C must also lift. Not onlv will p'_t be greatly increased but also the area containing A, B, and C will be unable to contribute its maximum force-developing potential to the heaving pressure.

As p_t becomes larger, the pores, depending on their size, begin to empty of water. This probably has a great influence on the rate at which equilibrium can be established. Considering these factors, it is expected that the rate of heaving and the maximum developable heav-pressure will drop off rapidly when p_t reaches a value large enough to initiate the emptying of the pores.

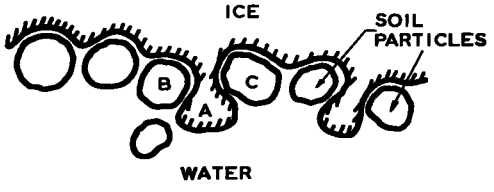

Figure 2. A hypothetical ice-water interface in a porous material.

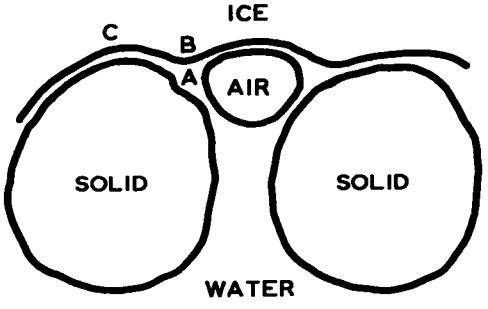

Figure 3. A hypothetical ice-air-water interface in a porous material.

Effect of Air

In the natural porous solid, air probably occupies a significant portion of a unit volume. Furthermore, as the water freezes, the air would be forced ahead of the freezing plane and, in time, much of the pore space at the ice-water interface would be occupied by air (Figure 3). If the air bubbles are treated on the same basis as the solid, (surface energy terms being those for water-air and ice-air interfaces), the preceding discussion concerning equilibrium would still apply to points A, B, and C (Figure 3).

The volume and pressure of the air in the bubble can change with time. The maximum pressure that could be developed in the air bubble would depend on the water tension p_t, the volume of air, and the minimum radius of curvature of the water-air interface compatible with the pore size. The air bubble would begin to contribute to the heaving pressure when its radius exceeded the minimum compatible with the pore for, if the air is to pass into the next pore, its pressure must increase until it over-

comes the capillary forces associated with the water in the constriction between the pores. The expansion that occurs when water changes to ice is a mechanism by which the pressure in the air bubble can be increased.

Under normal conditions it is possible that all the interfaces at the freezing plane are either air-ice or solid-film-ice. Since the interface energy associated with ice and water is probably much less than that associated with air and water (evidence to date indiciates that it is less by a factor of 10) the forces associated with a system containing air should be somewhat larger than with one not containing air.

Air bubbles and columns that occurred in an ice lens formed in a water-saturated clay-silt specimen, are shown in Figure 4 (magnified 16 times). Of particular interest is the shape of the bubbles and the fact that they occur in rows orientated in the direction of freezing, similar to those formed when water freezes in bulk. The air bubbles are not resolved to the naked eye but appear as striations in the ice. The occurrence of rows of bubbles with no solid particles in the immediate vicinity would indicate that certain sites must act as nucleating centers for air and, as the lens grows, parcels of air are removed from these collection centers.

DISCUSSION

In the preceding section, the conditions were derived which must be satisfied if ice and water are to be in equilibrium in a small space for a given temperature depression and water tension. In practice, only one of the variables involved, p_t, can be measured directly. To estimate the value of the remaining independent variables,

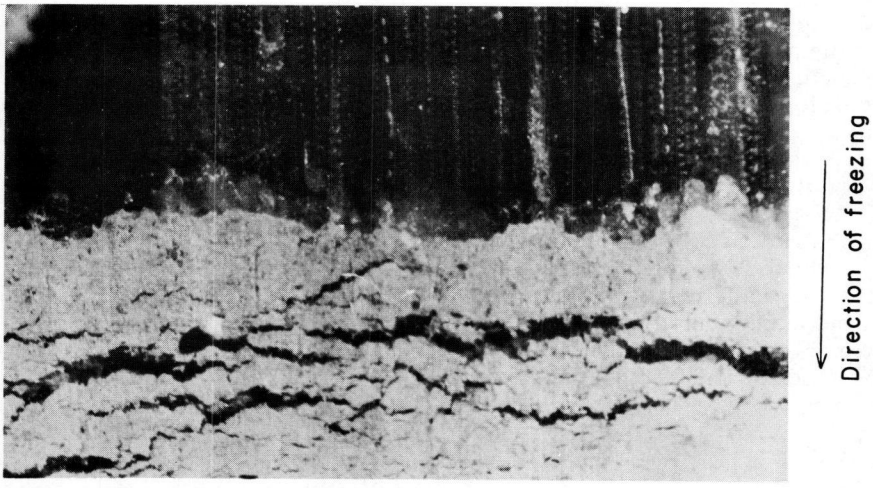

Figure 4. Air bubbles and columns photographed in an ice lens formed in a clay-silt soil (magnification 16 x).

assumptions must be made regarding the curvatures associated with the pore and solid, the energy of the ice-water interface, and the temperature depression at the freezing plane in each pore. The nature of these assumptions would ensuue that the final values arrived at would be no more than "educated guesses." The heaving pressure, which can be measuued in practice, is the sum of pressures in the ice integrated over their respective pore and solid areas. Thus it would appear impractical at this stage to bridge the gap between theory and observation, i.e., to attempt to calculate possible heaving pressures from theoretical considerations only.

Perhaps the greatest use of the preceding theoretical considerations is in gaining a better understanding of the mechanism of frost heaving, the factors involved, and their possible relationships to each other in a practical problem. For instance, consider the very simple system of spheres of radius r_1 (Figure 5). Let the minimum radius compatible with the pore space formed be r_2. The number of spheres per unit area, equal to the number of pores per unit area is proportional to $\frac{1}{r_1^2}$. From Eq. 1:

$$p_{sim} = \frac{2C}{r_2}$$

$$p'_{si} = -\frac{2C'}{r_1}$$

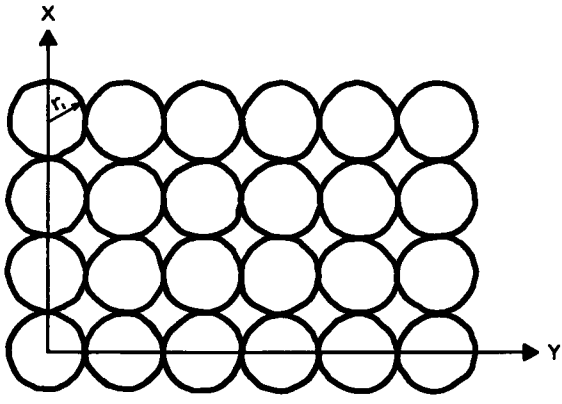

Figure 5. A hypothetical spherical particle arrangement for a porous material.

If we assume a constant temperature depression ΔT in each pore consistent with water tension p_t, then the contribution at equilibrium to the heaving pressure by the ice in the pore = $p_{si} + p_t$ and by the ice above the sphere = $2\,p_{si} + p_t - p'_{si}$. Total maximum heaving pressure P_o would be given approximately by an equation of the following form:

$$P_o \propto \frac{1}{r_1^2}\left\{(p_{si} + p_t)\,\gamma\,r_2^2 + (2\,p_{si} + p_t - p'_{si})\,\beta\,r_1^2\right\}$$

Therefore,

$$P_o \propto \left(\frac{2C}{r_2} + p_t\right)\left(\gamma\,\frac{r_2^2}{r_1^2} + \beta\right) + \left(\frac{2C}{r_2} + \frac{2C'}{r_1}\right)\beta \qquad (11)$$

γ and β constants.

From Eq. 11 derived on the basis of a very simple model, it is seen that the maximum possible equilibrium heaving pressure increases with decreasing particle and pore size. Eq. 11 also indicates that the heaving pressure required to establish equilibrium can be reduced to zero by a sufficiently large water tension. If $p_t = 0$, the heaving can be stopped by applying the pressure P_o. This system has the same behavior as is observed in practice. Eq. 11 also indicates that if there is a correlation between pore size and particle size, a factor obtained from the particle-size distribution curve, which is a measure of the term $\sum_r \frac{n_r}{r}$ where n_r is the number of particles per unit area of radius r, might be of value as a measure of susceptibility of a material to frost action.

Finally, the following points should be emphasized with regard to the presented theory. The source of the force potential, which results in frost heaving and the movement of water through the porous materials, is a temperature depression existing at the freezing plane. This temperature depression raises the thermodynamic potential of the water above that of the ice. If the temperature depression remains constant, the ice must raise its thermodynamic potential to be in equilibrium with the water. This can be done by increasing its internal pressure at the freezing plane. In the pore space, this increase in pressure can be established through the development of a positive curvature in the ice surface; this fact is implicit in the derivations of Eq. 4. If the curvature required for equilibrium is too great, the ice will propagate through the pore.

For equilibrium conditions over the remaining freezing surface, i.e., above the solid particles, it has been assumed for simplicity in this presentation that the particles be spheres. This assumption is not necessary for p'_i, the internal ice pressure due to the curvature at the solid-ice interface, can have any value including zero (a flat surface). Equilibrium conditions still require that a positive pressure be built up in the ice above the solid (the pressure at B, Figure 1, must be equal to the pressure at C), and this fact is obvious when p'_1 is made zero in Eq. 7. Therefore, any granular material has a potential for heaving, the first and most important requirement being that a temperature depression exist at the freezing plane. If the granular material is very fine, it will be more susceptible to frost heaving because the pore size requires that significant temperature depressions be established at the freezing plane before the ice will propagate through the pore. If the granular material is very coarse, the contribution to heaving from the pore space portion of the freezing plane will be very small. Also, since the ice readily propagates through the pore, by the time the termperature depression at the solid-film-ice interface is of a value to ensure an appreciable contribution to the heaving pressure, the particle will likely be "frozen

in" (Figure 2). If the extraction of heat is rapid enough or the boundary conditions are such that water can migrate to the solid-film-ice interface before the ice has propagated through the pore, then there is a possibility that heaving will occur even in a gravel.

As yet the boundary conditions which exist in a porous material, and to which any thermodynamic relation must be subject, are not adequately known. The theory indicates that the following three variables are involved:

1. The temperature depression at the freezing plane,
2. The pressure existing in the ice, and
3. The pressure existing in the water.

Further carefully planned experiments are required to bring out the relationships that actually exist between these three variables in any particular situation.

ACKNOWLEDGMENTS

The author wishes to acknowledge the valuable assistance given to him by various members of the Division of Building Research, National Research Council, in the preparation of this paper. He wishes especially to acknowledge the contributions of Messrs. E. Penner, P.J. Sereda, and Dr. J.M. Kuzmak, who through discussion, helped to bring the assembled ideas to maturity. This paper is a contribution from the Division of Building Research, National Research Council of Canada and is presented with the approval of the Director.

REFERENCES

1. Beskow, G., "Soil Freezing and Frost Heaving with Special Application to Roads and Railroads," Swedish Geol. Soc., Series C 375, 26th year book, No. 3 (1935). Translated by J.O. Osterbery, Tech. Inst. Northwestern Univ., Evanston Ill., Nov. 1947. (With a special supplement for the English Translation of progress from 1935 to 1946)

2. Penner, E., "Soil Moisture Tensions and Ice Segregation." Paper to be presented at the 36th Annual Meeting of the Highway Research Board, Washington, D.C., Jan. 7-11, 1957.

3. Glasstone, S., "Textbook of Physical Chemistry," Second Edition, Publisher, D. Van Norstrand Co. (1951).

Discussion

WARREN L. LAWTON, Technical Development Branch, Civil Aeronautics Administration, Indianapolis—The writer is of the opinion that the water causing frost heaving is being moved up under the ice by a positive pressure. There is no physical property that would produce a negative pressure in soil water greater than atmospheric pressure. The forces that affect the flow of water in soil are cohesion, adhesion, surface tension, and viscosity. It should be remembered that these fundamental properties can be varied by temperature, vapor pressure, interface conditions, salt content, and many other factors.

These forces are all present in soil masses in the field. As the soil mass goes through cycles of wetting and drying or freezing and thawing, each force produces its own phenomenon.

Cohesion tends to pull the water out of the voids and off of the soil particles and return the water to the water table. This force is limited to a negative value of 14.7 psi for water, a tensile strength for ice, and a positive value for vapor pressure.

Adhesion tends to hold the water to the particle of soil. Its value depends upon the molecules that compose both the surface and the inside of the soil particle. It also depends upon the distance between the water molecule and soil particle. The water affected by adhesion is drawn toward the soil particle and produces a positive pressure on the water between it and the soil particle.

Surface tension tends to move the water around until it is uniform over everything. It will produce a positive or negative force in the water depending upon the pore shape and vapor pressure.

Viscosity only affects the moving water and limits the quantity that can be moved per second.

Now let us consider the frost action. If water is removed from the surface of a soil particle, the water in its new state must have a greater cohesion than the adhesion of water to the soil particle, or it will return to the soil. This means that the cohesion of ice is greater than the adhesion of the water. Since the freezing occurs on one side of the particle before it does on the other side, the surface tension and thickness of the water film will be changed at this point. Both the surface tension and adhesion will tend to drive the water from the rest of the particle over this depleted area until equilibrium is again established. If the forces tending to move the water are greater than the weight of the ice, the ice is lifted. Then a new cycle starts and the ice crystal continues to grow.

Since there is a water interface between the water on this particle and surrounding particles, water is moved from all particles to replenish the water removed by freezing. The same surface tension and adhesion is the force that moves the water from one particle to another. The speed and quantity of water that moves depends upon the viscosity and capillary size. As long as the water is brought to the freezing plane, the ice crystal continues to grow. Should the water move too slowly or stop, the freezing plane will move deeper into the soil. In all of this, it is assumed that there is enough heat transfer to cause freezing.

Freezing temperatures can and often do exist below the point of frost heaving. If this water is moving and is not frozen under these conditions, something must reduce the freezing point of the water. There are two possible causes, dissolved salts and increased hydrostatic pressure. Since there is no evidence of salt crystals being formed, the reduced freezing point is caused by an increase in hydrostatic pressure. This pressure can only be produced by surface tension and adhesion. Cohesion produces a negative force which would elevate the freezing point of water.

LORNE W. GOLD, Closure—Mr. Lawton's discussion does bring up two points upon which I would like to comment although, generally, I would conclude that we do not differ very much in our mental picture of what is happening at the freezing plane.

Can water support a tension greater than 14.7 psi? You certainly cannot grasp water and place it in tension in a testing machine like you would a piece of steel, still, the energy of interaction between water molecules is of such an order that it requires a very large tension to pull them apart. When water exists in a fine pore system or on a surface, then the forces associated with the interaction energy of the molecules play a major role in determining the behavior of the water. In such a system, the intermolecular forces can become effective in a way they never could in larger hydraulic systems. It is possible for water to withstand considerable tensions under such conditions. On page 179 of Dorsey's book: "Properties of Ordinary Water Substance" reference is made to a number of papers describing experiments in which water was subject to tensions of over 10 atmospheres.

In referring to the depression of the freezing point of water Mr. Lawton states: "There are two possible causes; dissolved salts and increased hydrostatic pressure." I would like to point out that in deducing the change in freezing point with pressure, it is not necessary that the pressure be the same on both the liquid and the solid and this must be recognized in making calculations. For example, if water is under a positive pressure greater than atmospheric and ice forms from this water but is subject to atmospheric pressure, the freezing point of ice and water is actually greater than 32 deg F. Edlefsen and Andreson in their paper: "Thermodynamics of Soil Moisture," Hilgardia, Vol. 15, No. 2, February 1943, bring this point out quite clearly in Section 30.

Temperature Effects on Phase Composition and Strength of Partially-Frozen Soil

C. W. LOVELL, JR., Research Engineer
Purdue University, Lafayette, Indiana

The primary objective of this study was the determination of the relative amounts of frozen and unfrozen moisture in several fine-grained soils over a range of below freezing temperatures. A secondary goal was the definition of the importance of subzero temperature (and phase composition) on the strengths of the same test soils.

Three soils were utilized—a silt of glacial origin, a silty clay of the Wisconsin drift, and a clay derived in place from limestone. The soils were characterized in the usual manner, and in addition their specific heats and behaviors in a desorption process were defined.

The calorimetric method was used to determine the amount of ice in a molded specimen of known total moisture, density, and subzero temperature. The phase composition of the test soils was found to vary significantly between soils at a given temperature level, and to change significantly for a single soil with lowering of temperature. For example, comparing soils molded to standard Proctor peak conditions, the following approximate percentages of original moisture frozen obtained: at -3 C silt 73 percent, silty clay 42 percent, clay 16 percent; at -25 C, silt 83 percent, silty clay 62 percent, clay 50 percent.

Attempts to correlate the results of experimental desorption tests with the calorimetric data met with very limited quantitative success.

Unconfined compression tests were undertaken at controlled subzero temperatures with stress rates of loading of 160 or 200 psi per minute. Maximum compressive stress demonstrated a high temperature dependency for all test soils. For example, again comparing samples molded to standard Proctor peaks, the approximate ratio of compressive strength at -18 C to that at -5 C was more than 4 to 1 for the silty clay and almost 3 to 1 for the clay.

It was concluded that substantial proportions of the total moisture (defined by drying to constant weight at 105 C) of fine-grained soils may remain unfrozen at temperatures as cold as -25 C and that the changes in strength accompanying change in temperature within this range emphasize the practical significance of relative phase composition.

● THE FACT THAT soil moisture commonly remains unfrozen at temperature below 0 C is a widely recognized one. It is further conceded that there are important implications or consequences of this phenomenon. For example, the very process of ice segregation in freezing soils is dependent upon the feeding moisture in the smaller pores remaining unfrozen. Also, accurate estimates of depth of freeze or depth of thaw of soil require good knowledge of the temperature at which phase changes will take place in the soil water. Finally, in the perma-frost regions of the world the high capacities of frozen ground to support loads may be utilized more rationally if the phase composition of the ground at various subzero temperatures (-C) is reasonably defined.

The primary purpose of the research reported herein then was to determine the freezing behavior of certain fine-grained soils—specifically to ascertain the relationships between temperature, and percentages of soil moisture unfrozen (or frozen) at such temperature. A secondary purpose of the research was to relate the above data to some measure of soil strength—specifically, compressive strength.

The number of variables that can be involved in a study of this purpose are understandably quite large. Temperature was an obviously critical variable, and the effects of it were studied from values just below 0 C to nearly -25 C. Soil texture was a second obvious variable, and three fine-grained soils of significantly different characteristics

were chosen—a clayey silt, a silty clay, and a clay.

The factors of moisture content and density (or unit weight) are very important, but due to physical limitations neither was studied as a primary variable.

Direction, rate, and type of freezing are also obviously important. However, all test samples were given the same primary treatment of rather rapid cooling from all sides without access to additional water during the cooling process (closed—system freezing). This meant that the moisture was frozen substantially in place, and that the moisture content and distribution, and density of the test samples were "controlled" to the highest degree believed practicable.

Strength evaluation of partially-frozen samples was achieved by means of the most simple type of test, undrained cylindrical compression in an unconfined condition. Loading was achieved at controlled stress rates apparently most descriptive and desirable for partially-frozen soil, approximately 200 psi per minute.

SOIL MOISTURE

The total amount of soil moisture present in a given quantity of soil is ordinarily defined arbitrarily with references to a condition achieved by oven-drying to constant weight at 105 C. Even more important than the total amount of moisture present is the distribution of the moisture within the solid—voids system of the soil mass. Understandably, the definition of soil moisture distribution is a complex problem, and rather imperfectly answered by the present state of knowledge.

Classification

Soil moisture is ordinarily classified in an engineering sense on the basis of difficulty of removal from the soil mass by gravity drainage. On the most general scale, the breakdown is into "free" and "held" moisture. The free water may be removed from the soil by ordinary drains. The held water may not be removed directly by gravity because of the force magnitude by which it is held in soil pores or around the soil particles. These forces in the ultimate may be complex combinations of attractions that are intermolecular, electrical, magnetic and gravitational in nature.

A further subdivision on the basis of drainability may be envisioned as indicated in Figure 1.

A somewhat different approach to the classification of soil moisture may be made

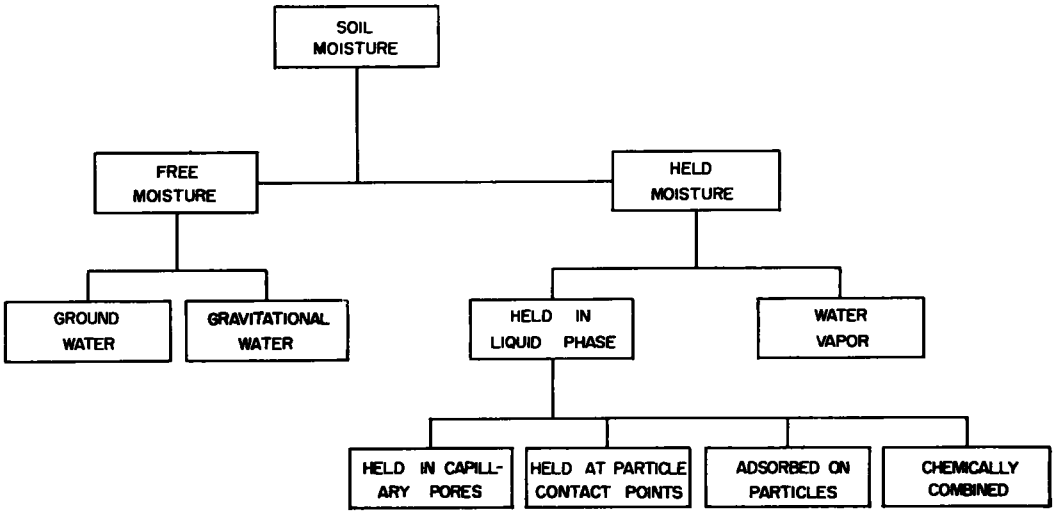

Figure 1. Engineering classification of soil moisture.

on the basis of relative position of the moisture within the soil pores, and on the relative magnitude of force holding the water within the system. For example, Michaels (1) suggests that four types of water may exist in a wet soil mass: pore water, solvation water, absorbed water and structural water.

Suction

Because of the attractive forces exerted by the soil on the held water, this water is considered to be in a state of negative pressure, tension, or suction. Thus in a relatively wet soil mass all air-water interfaces consist of menisci, and the relative curvature at each of these menisci is indicative of the pressure difference across the meniscus, the suction of the liquid phase, and the equilibrium vapor pressure of the gas phase.

The vapor pressure of the soil air may be related to the saturation vapor pressure at that temperature, and expressed as a relative or percentage humidity. Such pressure or relative humidity may be measured directly, or calculated from a knowledge of the magnitude of soil water suction with which it exists in equilibrium.

A number of approaches have been utilized to express the magnitude of soil water suction. However, the range of values of possible interest is so large that a logarithmic rather than arithmetic scale of reference is commonly employed. Schofield (2) introduced the pF scale to meet the need for a convenient logarithmic scale of measure. If the soil water suction is expressed in terms of the length in centimeters of an equivalent water column, the common logarithm of this length is the pF value.

The use of suction (pF) or of vapor pressure (or relative humidity) allows a more rational approach to the problems of moisture retention and moisture movement. For example, moisture may or may not move from a location of high moisture content to one of lower moisture content, but will always move (within the limits imposed by gravity) from, (a) low suction (pF) to high suction, or (b) high vapor pressure (or relative humidity) to low vapor pressure.

As a further example, soil water existing in equilibrium at a high suction value will

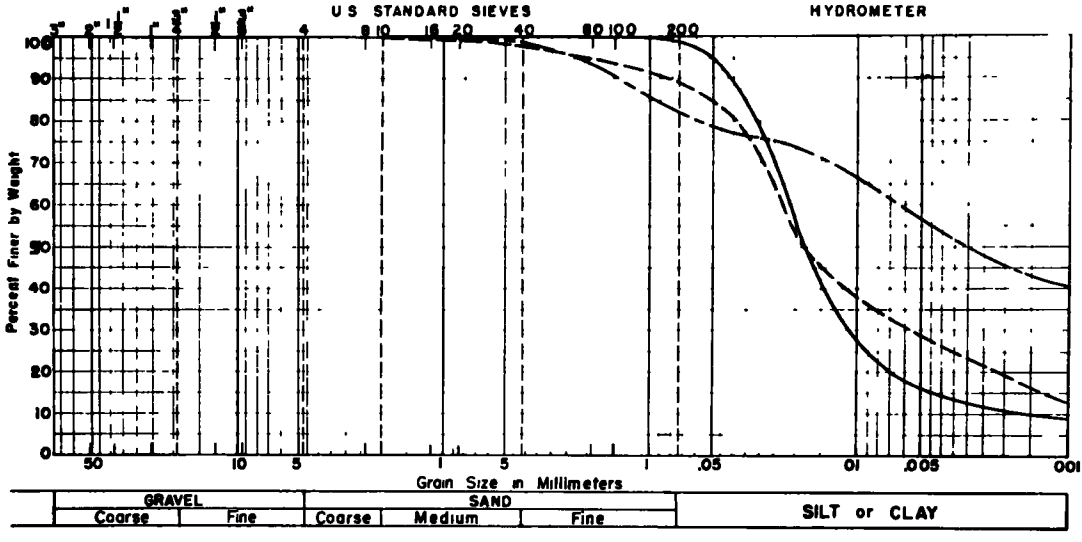

Remarks	SOIL	PERCENTAGE OF SIZES				
		SAND	SILT	CLAY (<.002mm)	<NO 200	<.002mm
	SILTY CLAY	106	678	216	894	530
	CLAYEY SILT	12	871	117	988	560
	CLAY	182	360	458	818	735

GRAIN SIZE DISTRIBUTION
——— CLAYEY SILT ——— CLAY
– – – – – SILTY CLAY

Figure 2.

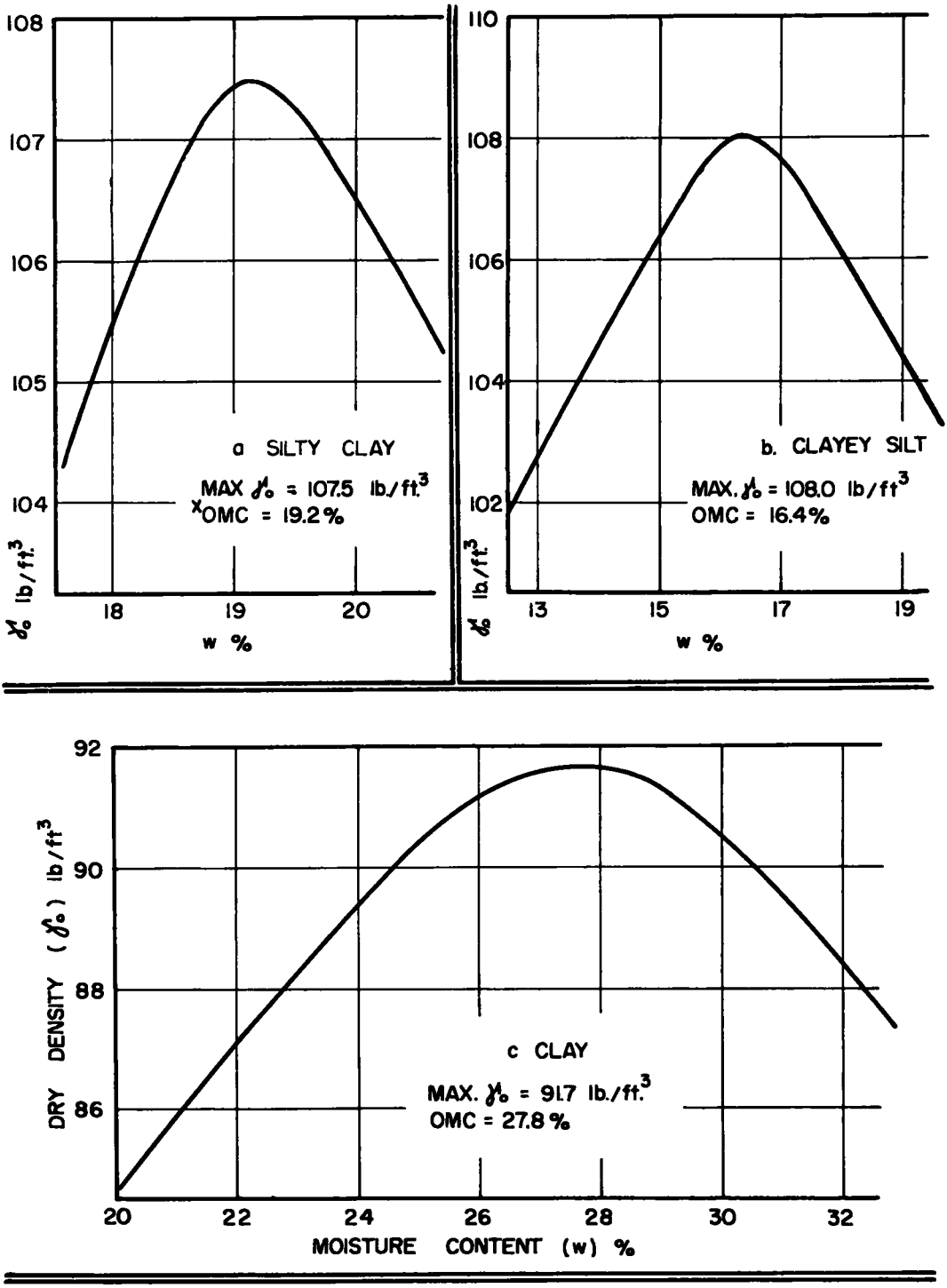

Figure 3. Moisture density relations at standard Proctor compactive effort.
*(OMC = optimum moisture content).

freeze much less readily with the lowering of temperature than would the same soil water under lower suction. Indeed, the suction value may be used to calculate theoretical freezing point depression, all soil water having the same theoretical depression at a given suction level. The quantities of unfrozen moisture in equilibrium at a given suction level and sub-zero temperature of course vary considerably from soil to soil.

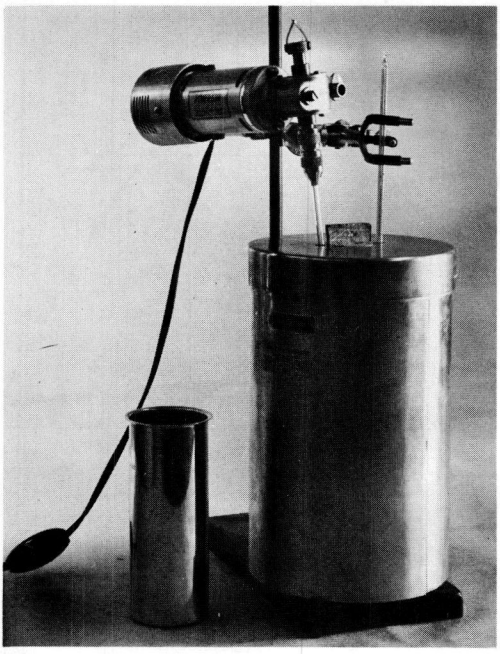

Figure 4. Calorimetric equipment.

Freezing of Soil Moisture

The lowered or depressed freezing point of the water in soil pores has been the object of much study. To briefly summarize, two general theories have been advanced to explain and describe this phenomenon:

1. Early investigations appear to have concentrated on the capacity of salt solutions to lower the freezing point. At high moisture contents the concentration of the salt solution in the soil water is relatively low, and the most free water in the system should freeze at only slightly depressed temperatures. However, as the moisture content is reduced, either as a result of desiccation by evaporation or by freezing process, the salt concentration of the re-

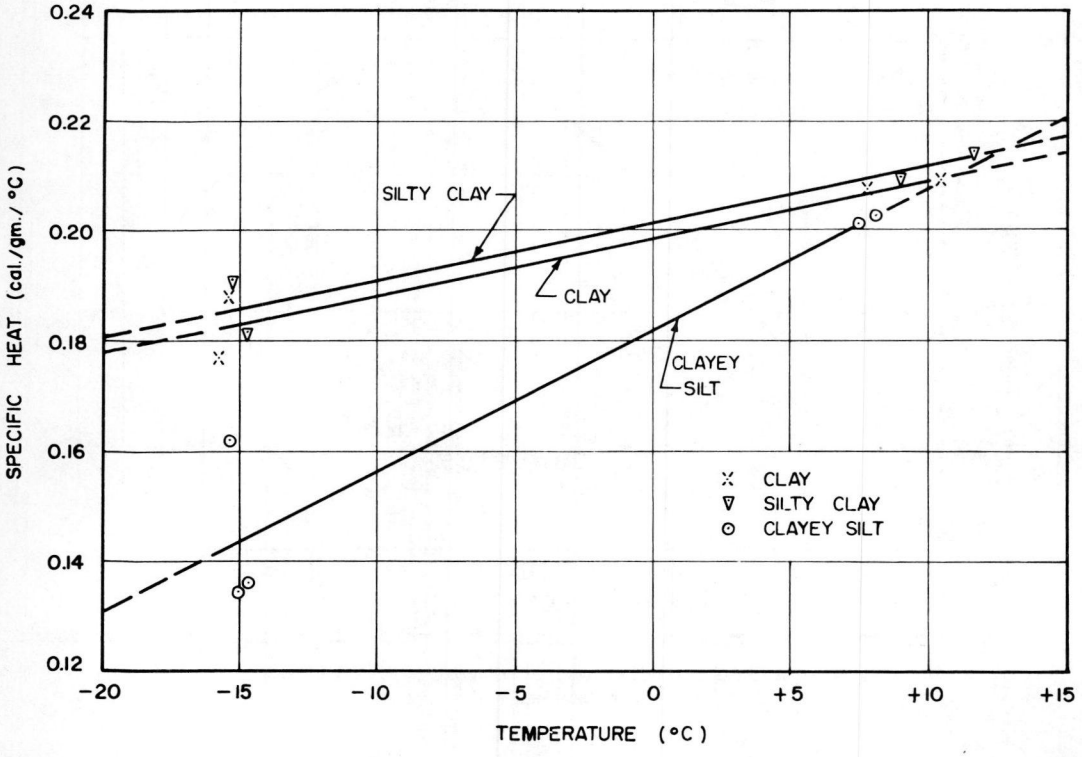

Figure 5. Variation of specific heat with temperature.

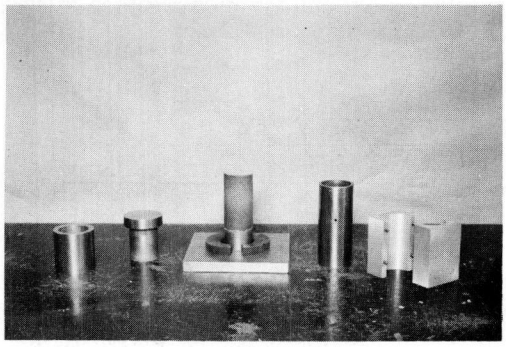

Figure 6. Molding cylinder and accessories.

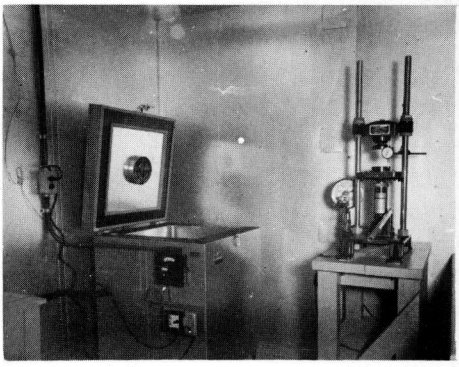

Figure 7. Controlled freezing cabinet (left). Hydraulic loading press (right).

maining liquid is increased, and progressively lower temperatures should be required to freeze this liquid. The contributions of Bouyoucos (3, 4, 5, 6, 7,) in development of this theory are prominent.

2. Later investigations have indicated that the dominant role of influence belongs not to the concentration of the salts, but to the relative magnitude of the negative pressure or suction forces with which the soil moisture is held within the soil system. The magnitude of these forces varies inversely and exponentially with the distance from the soil particle. Accordingly, the most free water in a wet soil mass exists under relatively small suction force, and freezes at only slightly depressed temperature. As such water is removed from the liquid phase by either evaporation or freezing, further freezing may occur only at significantly depressed freezing points because of the magnitude of the suction under which the solvation water and absorbed water exist (1, 8). Beskow (9) formulated such an hypothesis based upon the "adsorption power" of the soil particles.

Parker (10) compared the two causative effects and concluded that each contributed in about the following manner: (a) that the freezing point depression under very small suction was caused basically by the material in solution; (b) that the depression for water under intermediate suction was roughly additive of suction and solution effects; and (c) that the moisture at high suction had a depression controlled almost completely by the pressure. In addition, although the effect of the solution concentration increased with decreasing moisture content, at all but the very wet conditions of the soil the pressure or suction effect apparently had dominant influence in determining the soil water freezing point.

No formal hypothesis of freezing behavior was formulated as a result of the research reported herein. However, the belief that suction influence is dominant in all except the very wet soil conditions is shared by this writer.

DESCRIPTION OF TEST SOILS

Three soils were selected: (1) A red-colored clay derived from limestone; (2) a brown glacial silty clay, pedologically classified as Crosby, "B" horizon; and (3) a tan glacial clayey silt. The soils were selected partially on the basis of the difference in freezing behavior expected of them, and with the hope that these different behaviors would tend to "bracket" the fine-grained soil range. All soils are native to the state of Indiana.

Each soil was sampled in quantity, possessed, and subjected to the common simple characterization tests: Atterberg limits, grain size distribution, specific gravity, and Proctor compaction. Processing included disaggregation to pass the No. 4 sieve and air drying. Accordingly, the reported laboratory behavior of these soils is to some degree peculiar to this processed condition, and may differ significantly from the in-situ behavior.

Results of the Atterberg limits evaluation of plasticity, and the measurements of specific gravity of the soil solids are presented in Table 1.

TABLE 1

ATTERBERG LIMITS AND SPECIFIC GRAVITY

Soil	Liquid Limit	Plasticity Index	Sp. Gravity
Clayey Silt	26.8	5.3	2.75
Silty Clay	35.4	15.9	2.69
Clay	75.4	49.4	2.81

Grain size distributions are presented in Figure 2, where the textural scale shown is that of the Unified Soil Classification System (11). Also on this figure are tabulated percentages of the sand, clay and silt sizes (interposing a division between silt and clay sizes of 0.002 mm), as well as the amounts finer than the No. 200 sieve and 0.02 mm. The latter size is a familiar one in frost susceptibility ratings (12).

Moisture-density relations at the standard Proctor level of dynamic compactive effort are presented in Figure 3.

SPECIFIC HEAT DETERMINATIONS

Since a thermal approach to the problem of determination of relative phase composition (ice and water) of soils at subzero temperatures was adopted for this study, it was necessary to ascertain specific heat[1] values for the test soils.

As might be expected, specific heats of the various inorganic soil constituents are very similar, and have in many cases been approximated by a single average value such as 0.19 or 0.20[2] (13, 14, 15, 16). However, Kersten (17) measured a small but definite decrease in specific heat with temperature, and concluded that values of 0.15 to 0.17 were more reasonable for temperatures of soil freezing. These values are for the dry soil solids.

Apparatus and Procedure

The use of calorimetric equipment and the general method of mixtures for determination of specific heats of soils is reported in detail by Kersten (17, 18). The specific equipment utilized in this study is illustrated in Figure 4.

The calorimeter consists of an outer metal jacket within which a large Dewar vessel with silvered surfaces is mounted, an insulated cover with suitable openings for stirrer, thermometer and introduction of sample, and two aluminum cups of approximate 250 and 500-ml. capacity.

Stirring was accomplished with a glass rod powered by a variable-speed electric motor. The thermometers used had a range of -35 to +25 C, a least graduation of 0.1 C, and were checked for calibration at the ice point.

The procedure employed was somewhat different than that reported by Kersten. Rather than introducing the soil into the calorimetric liquid and observing the temperature change that resulted, the test run was started with the soil inside the calorimeter and in equilibrium with liquid partially filling the cup. To effect the temperature change, additional liquid of known temperature was added to the cup. This method appeared to minimize experimental difficulties, and did not require evaluation of the heat of wetting of the soil solids.

Heat exchange between the calorimeter cup contents and surroundings during test required the customary small correction on the plot of time vs. temperature to obtain the true temperature change. For these tests, the simple procedure of extending the

[1] Specific heat is defined as the quantity of heat required to change the temperature of a unit mass of a substance by one degree.

[2] Units are either cal./gm./C or Btu's/lb/F.

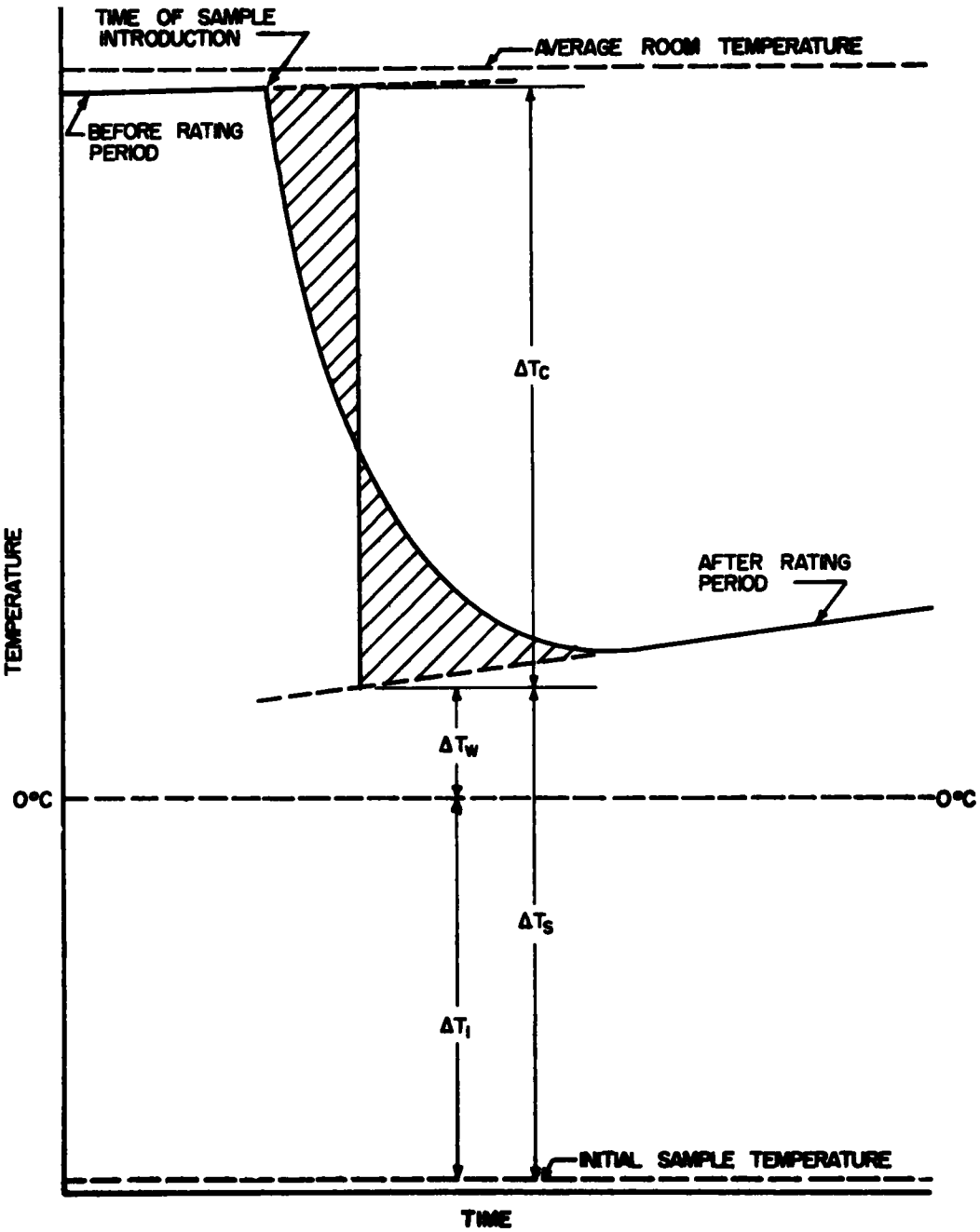

Figure 8. Schematic calorimeter curve.

linear "before" and "after" rating curves to the mid-point time of liquid introduction was used to define the true change.

Since heat gained by the calorimeter and its contents equalled heat lost by the liquid added:

$$C_S = \frac{W_{LA}\, C_{LA}\, \Delta T_{LA} - W_{LC}\, C_{LC}\, \Delta T_C - E \Delta T_C}{W_S\, \Delta T_C}$$

Where, C_S = specific heat of soil solids
W_{LC} = weight of liquid in calorimeter
W_{LA} = weight of liquid added to calorimeter
W_S = weight of soil solids
C_{LC} = specific heat of liquid in calorimeter
C_{LA} = specific heat of liquid added to calorimeter
ΔT_C = temperature change of calorimeter and contents
ΔT_{LA} = temperature change of liquid added to calorimeter
E = water equivalent of calorimeter

Results

Specific heats were determined at only two general temperature levels–10 C and -15 C. An interpolated plot of specific heat and temperature for all soils is presented as Figure 5.

Some temperature dependency of the specific heats is observed, and the absolute magnitudes of the specific heat values are in reasonable agreement with those previously reported. Additional experimental work would have undoubtedly allowed refinement of these results.

MOULDING AND FREEZING TEST SPECIMENS

Moulding

In preparation of test specimens it was considered quite important to exercise good control over the quantities of moisture content and density. Specifically, it was desired to: (a) achieve a given moisture-density combination to the greatest practical precision in a moulded sample; (b) achieve uniform moisture-density relations throughout the sample; and (c) reproduce a uniform moisture-density condition between a number of samples.

This is an old problem, yet one that has never been answered satisfactorily, to the knowledge of this writer. It is known that neither purely dynamic nor purely static type of compaction (as normally applied) achieves a uniform sample condition (19). Leonards (20) reports favorable results with the use of static compaction on both ends of a sample with large diameter-to-height ratio, with subsequent cutting and trimming of small specimens from the large compacted mass.

For a variety of reasons, it was decided to establish, by trial-and-error procedure, combined dynamic and static compaction techniques which would produce the desired levels of moisture content and density uniformly in individual cylindrical samples of size 1.4 (dia.) x 2.8 in. The usual moisture-density level for sample mounding was arbitrarily selected as that existing at the peak of the standard Proctor curve (Figure 3).

In such a trial-and-error approach to the attainment of a given moisture-density combination with a given soil and sample size, many details of procedure may be varied: distance of static displacement, top and bottom; timing of displacement, top and bottom; length of period static load applied; allowance for rebound; number of layers for dynamic compaction; weight of dynamic compaction hammer; height of hammer drop; number of hammer blows; etc. Nevertheless, compaction techniques were worked out for the standard Proctor optimum moisture content conditions for all test soils.

Molding proper was accomplished in stainless steel cylinders complete with collar, compaction head, and compaction base. These items are illustrated in Figure 6. All were machined to very close tolerances.

Samples were molded in small batches, and one sample from each batch was sliced into parts immediately after molding to ascertain that the desired moisture-density level and uniformity probably obtained in the other batch samples, which were used in

duplicate for phase relation or strength determinations. The results of this same physical slicing process of course constituted the original basis for selection of the appropriate compaction to be adopted for each desired soil-moisture-density combination. Such checks revealed that it was possible to control the molded moistures within one-half to one percentage points, and the dry densities within two to three lb per cu ft.

Thus, the molding procedures outlined above adequately served the purposes of

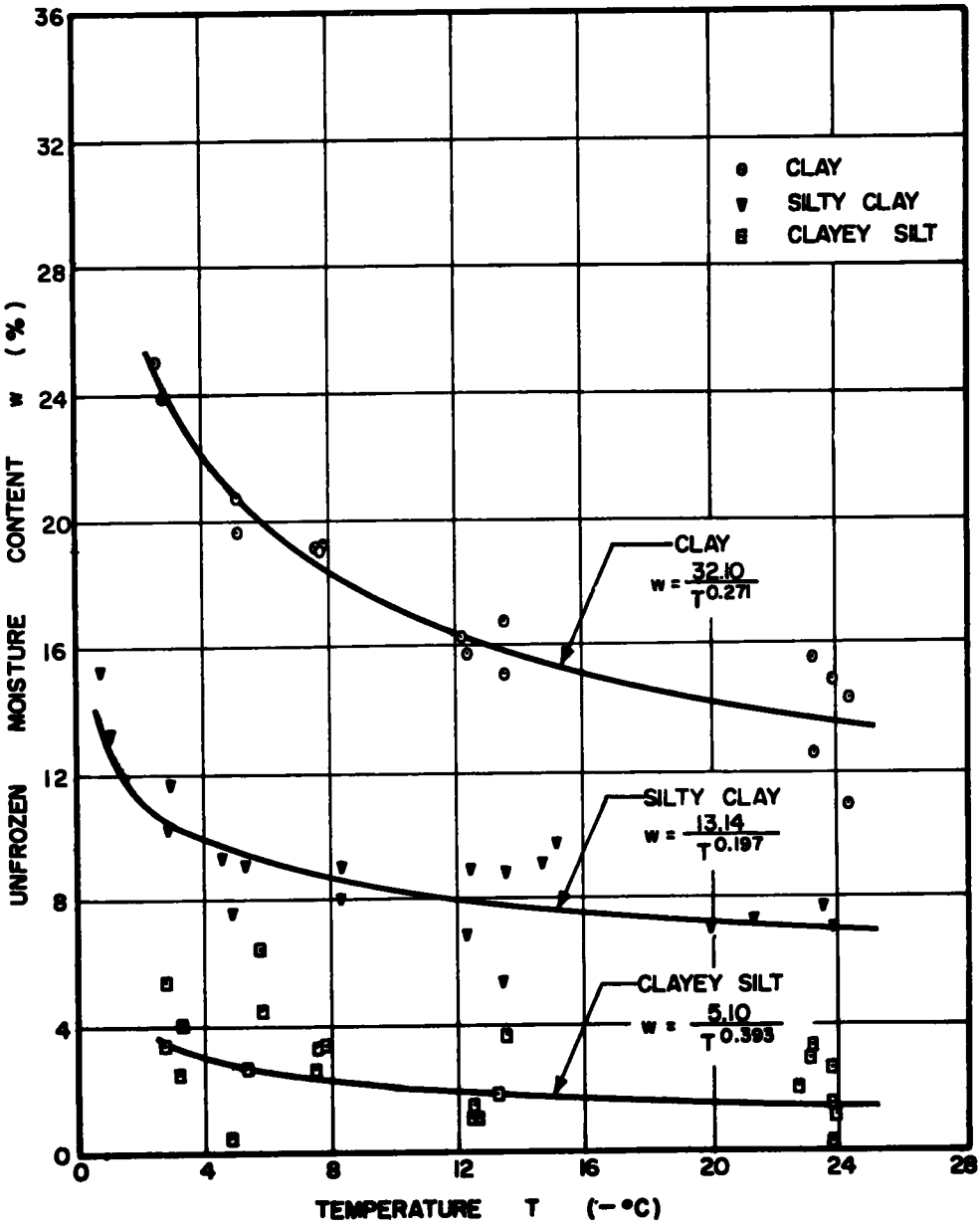

Figure 9. Unfrozen moisture content vs. temperature—all calorimetric points.

this study. However, the writer does not wish to particularly recommend them because of the great amount of care and effort involved in proper execution.

Freezing

Molded and extruded samples were brought to appropriate temperatures for phase relation or strength determinations within a freezer. In the early phases of the study an ordinary horizontal-type deep freeze was used for this purpose. Later, a special cabinet located within a walk-in cold room became available. This cabinet, shown in general view by Figure 7, has a range of ambient to -20 F, and a temperature controller with an on-off differential of 0.5 F. The cabinet also has forced circulation from a small fan in the lid.

Samples that were to be used for phase relation (calorimetric) tests had a 24-gage copper-constantan thermocouple inserted in their tops. The thermocouples not only provided good determination of initial temperature in the calorimetry, but also served as excellent "handles" for the partially-frozen samples.

The procedure for bringing soils to the appropriate subzero test temperature was to merely place them, exposed on all sides, within the freezer preset at this particular temperature. Samples remained in this position for a period sufficient to ensure equilibrium with the freezer ambient—some 18 to 24 hours. During this time the samples experienced some redistribution of moisture due to the established cooling gradients, and lost some moisture to the atmosphere of the freezer by process of limited evaporation and sublimation. Checks indicated that the magnitude of these chances was small. In any instance, the average moisture content of the sample used for either strength or calorimetric tests was determinate at the conclusion of such a test.

Since molded moisture contents were always measurably below saturation and conditions were not conducive to ice segregation, the samples did not exhibit significant volume increase on freezing.

DETERMINATIONS OF ICE IN PARTIALLY – FROZEN SOILS

The calorimetric technique has apparently had a little application to the specific problem of this study. Such technique has been used to determine the free water content of snow (21), and preliminary unpublished experiments on soils have been undertaken by the Arctic Construction and Frost Effects Laboratory[3], New England Division, Corps of Engineers.

Despite the limited knowledge available with regard to use of the calorimetric method for partially-frozen soils, it was decided to utilize this technique rather than the dilatometric (7, 22) or other method.

Briefly stated, the technique involves placing a sample of known subzero temperature, moisture content and density into a calorimetric cup of relatively warm liquid at known temperature. The heat required to melt the ice is indicated by the resultant temperature change within the calorimeter. By use of appropriate specific heats and the latent heat of phase change, it is possible to solve the thermal equation for the weight of ice present. An additional simple step permits calculation of the amount of unfrozen moisture at a given subzero temperature or of the percentage of total soil moisture that was frozen at this temperature.

Apparatus and Procedure

The calorimetric apparatus is described in the section "Specific Heat Determinations". The only alteration required for this test series was the substitution of a stainless steel stirrer for the glass one shown in Figure 4. The glass stirrer proved too fragile to withstand occasional contacts with the sample in the calorimeter cup.

The initial sample temperature (in the freezer) was obtained by means of a thermocouple embedded in the sample. A conventional potentiometric setup was utilized to obtain such readings.

[3] Information furnished by Mr. J. F. Haley, Assistant Chief of the Laboratory.

After the conventional "before" rating of the calorimeter and its liquid contents (water) had been established, and the temperature of the sample in the freezing cabinet determined, the sample was rapidly transferred, suspended by the thermocouple wire, from freezer to calorimeter. Then followed the usual procedure of stirring and observation of temperature change with time, until a final "after" rating period was defined.

Once within the calorimeter cup, the sample soon thawed, crumbled, and settled to the bottom. Stirring could not serve to keep any appreciable portion of the soil in suspension, but merely circulated the liquid within the cup and around the loose soil particles.

At the conclusion of the test the average moisture content and density of the tested sample could be determined by weight differences of the calorimeter cup contents, and checked against the nominal moulded values.

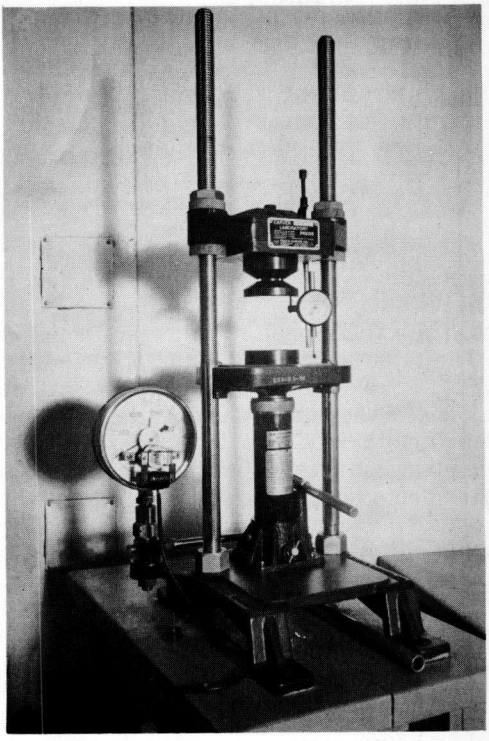

Figure 10. Details of hydraulic loading device.

Method of Calculation

The equality by means of which the amounts of ice present in the samples were determined is a simple thermal one which states that:

Heat lost by the calorimeter and its liquid contents = heat gained by the soil solids + heat gained by the unfrozen moisture in the sample + heat gained by the ice in the sample + heat of fusion of the ice + heat gained by the water derived from the melted ice.

Expressed symbolically, the equation reads,

$$E\Delta T_C + W_{WC}C_{WC}\Delta T_C = W_S C_S \Delta T_S + (W_W - W_I)\ C_{WU}\Delta T_I + W_I C_I \Delta T_I + W_I L_f + W_W C_W \Delta T_W$$

where E = water equivalent of calorimeter

W_{WC} = weight of original calorimeter water

W_S = weight of soil solids

W_W = weight of total soil moisture

W_I = weight of ice (frozen moisture)

$W_W - W_I$ = weight of unfrozen moisture

C_{WC} = specific heat of original calorimeter water

C_S = specific heat of soil solids

C_{WU} = specific heat of unfrozen (undercooled) water (below 0 C)

C_I = specific heat of ice

C_W = specific heat of water (above 0 C)

L_f = latent heat of fusion of ice (at 0 C)

ΔT_C = temperature change of calorimeter and contents

ΔT_S = temperature change of soil solids

ΔT_I = temperature change of ice and unfrozen (undercooled) moisture (below 0 C)

ΔT_W = temperature change of soil moisture (above 0 C)

A solution for W_I or $(W_W - W_I)$ is required.

Specific heats for normal water, undercooled water, and ice were taken from handbook tables (23, 24) for appropriate "average" or midpoint range temperature. Specific heat values for the soil solids were determined experimentally as previously described. The values used were, again, those at the midpoint soil temperature.

The latent heat of fusion of ice used in these calculations was that at 0 C. In other words, it was assumed that the ice was warmed to 0 C prior to melting. This may or may not be the actual occurrence. However, use of the assumption considerably simplifies the thermal equation and probably introduces only a very small error under the given test conditions[4]. Considering the over-all precision of the test series, further refinements here were not considered justified.

The temperature changes to be used in the calorimetric equation were determined from a plot of the time-temperature values. Such a plot is presented schematically in Figure 8. To compensate for the effect of heat losses to the surroundings, a somewhat more refined technique than that employed for the specific heat determinations was employed. The rating portions of the time-temperature plot were extended, and by trial and error with an ordinary polar planimeter the time value which defined equal areas on either side of the curve (shown as shaded portions of Figure 8) was defined. The temperature intercept between the extrapolated rating curves at this time was considered to be the temperature change that would have occurred in the calorimeter without any external thermal influence (25).

To ascertain the adequacy of the calorimetric technique, a substance of known thermal characteristics and phase composition - ice - was melted in the calorimeter. Two test runs for initial sample temperature of -6.4 and -6.3 C showed calculated percentages of moisture frozen of 99.3 and 99.7 percent, respectively (as compared to the actual 100 percent). This evidence supports the basic validity of the calorimetric technique.

Results

Test results are summarized in Table 2. The dry densities shown are the average values for the samples, and were obtained by the product of molded sample volume (V) and weight of solids (W_S) in the calorimeter cup. The original moisture content (w_1) is also an average value for the entire sample, and equals the quotient[5] of total weight of soil moisture (W_W)—frozen and unfrozen, at the time of introduction into the calorimeter cup—by W_S.

The fraction of soil moisture frozen is obtained by dividing the weight of ice (W_I) by W_W. The unfrozen moisture content (w) is the quotient of the weight of unfrozen moisture ($W_W - W_I$) by W_S.

Certain samples of each soil were molded to an average moisture-density combination different than that approximating standard Proctor optimum values. These samples appear in Table 2 under grouping 2. Average values and ranges[6] of values are shown for each grouping in the table.

The relation between subzero temperature (T) and unfrozen moisture content (w) may apparently be most closely approximated by a parabolic expression of the form $w = cT^m$, where c and m are constants. This relationship is linear on a log-log scale.

[4] The difference in specific heats of ice and undercooled water is approximately ½ calorie/gram/C, as contrasted to the latent heat effect of about 80 calories/gram.

[5] Multiplied by 100 to give moisture content as a percentage.

[6] Only a portion of the range indicated is unintentional variation.

TABLE 2

SUMMARY OF CALORIMETIC RESULTS

Soil and Group	Run No.	Original % (lb/ft^3)	Original w_1 (%)	Test Temperature (-C)	% Original Moisture Frozen	Unfrozen w % at Test Temperature
Silty Clay Group 1	51G	105.2	19.1	21 3	61.6	7.3
	52G	106.4	18.6	22.0	62.4	7 0
	69G	108.0	18.4	8.3	52.7	8.7
	70G	106.7	19.1	8.3	57.9	8.1
	71G	108.2	18.2	8.3	50.8	9.0
	79G	105.0	21.3	12.4	58.2	8.9
	80G	106.3	19.3	12.2	64 9	6.8
	83G	105.3	20.9	0.8	27.0	15.3
	84G	106.5	19 5	1.1	32.5	13.2
	103G	107.7	18.7	3.0	38 2	11.6
	104G	108.3	16.8	2.95	39 2	10.2
	109G	106.8	18.4	14.7	50.3	9.1
	110G	106 6	18.9	15.2	48.7	9.7
Average		106.7	19.0			
Range		105.0 to 108.3	16.8 to 21.3			
Silty Clay Group 2	112L	111.1	10.9	4.55	14.85	9.3
	119L	112.2	11.5	13.4	53.3	5.4
	120L	111.8	13.4	13.55	34.3	8.8
	123L	110.6	13.7	23 5	43.9	7.7
	124L	111.6	13.1	23.8	45.7	7.1
	131L	110.3	11.8	5.35	22.7	9.1
	132L	112.0	10.6	4.85	28.3	7.6
Average		111.4	12.1			
Range		110.3 to 112.2	10.6 to 13.7			
Clay Group 1	54G	90.8	27 8	23 9	48 1	14 9
	72G	91.4	28 0	7 8	32 2	19 0
	73G	91.7	27 4	7 8	30 0	19.2
	74G	91 9	27 7	7 65	31 1	19 1
	81G	90 1	29 2	12 3	44 4	16 2
	82G	90.7	28.4	12.15	44.8	15 7
	85G	89.8	29 1	2 5	13 8	25 1
	86G	90.7	28.0	2 8	24 8	23 9
	90G	91 0	28 1	23 25	44.4	15 6
	91G	91 4	27 5	23 3	54 1	12 6
	101G	90 7	28 6	5 1	27 7	20 7
	102G	91 4	27 7	5 2	29 3	19 6
Average		91 0	28.2			
Range		89 8 to 91.9	27.4 to 29 2			
Clay Group 2	115L	91.1	26.2	13.55	35.9	16.8
	116L	91.7	24.85	13.55	39.05	15.1
	125L	91.3	26.6	24 35	46.3	14.3
	126L	91.4	25 5	24.3	56.9	11.0
Average		91.4	25.8			
Range		91.1 to 91 7	24 85 to 26.6			
Clayey Silt Group 1	49G	108 8	16 0	22 65	86 9	2 0
	66G	107.8	16.2	7 7	79 3	3.4
	67G	107 6	15 9	7 5	79.2	3.3
	76G	107.1	15 9	3 25	74 8	4 0
	87G	107 6	17.1	23 05	82 0	3 1
	88G	106.8	17 0	23 1	80.6	3 3
	96G	107 5	16.8	3 1	85 4	2.5
	97G	108.0	16 4	2.8	67.3	5 4
	99G	107 5	16 4	5 8	72.7	4.5
	100G	107.2	16.5	5.65	61.4	6.4
Average		107.6	16.4			
Range		106.8 to 108.8	15.9 to 17.1			
Clayey Silt Group 2	77G	108.8	14.7	12.4	90.8	1.4
	68G	108.7	15.0	7.4	82 4	2.6
	75G	107.0	15.0	3.35	82.5	2.6
	78G	108.6	15.0	12.4	92.4	1 1
	114L	107.6	14.0	13.2	86.3	1.9
	117L	107.7	15.0	13.5	75.1	3.7
	118L	107.0	13.5	12.55	91.6	1.1
	121L	107.3	15.4	23.75	83.2	2.6
	122L	107.6	14.6	23.75	90.3	1.4
	127L	108.3	14.2	23.7	92.3	1.1
	128L	108.8	13.4	23.7	98.7	0.2
	129L	107.9	12.8	4.75	96.6	0.4
	130L	107.6	12.6	5.25	79.6	2.6
Average		107.9	14.25			
Range		107.0 to 108.8	12.6 to 15.4			

Figure 9 illustrates the sum total of experimental determinations. By the method of least squares (26) the equation of the straight line which best fitted the total data for each soil was determined. The scattering of points is considerable, particularly for the clayey silt. However, this figure does clearly illustrate that the curves follow the qualitative pattern that would have been predicted from a knowledge of the soil texture, plasticity index, or quantity of clay sizes—namely that with exposure to a given sub-freezing temperature the clay will contain more moisture in an unfrozen condition than the silty clay, which will in turn contain more than the clayey silt.

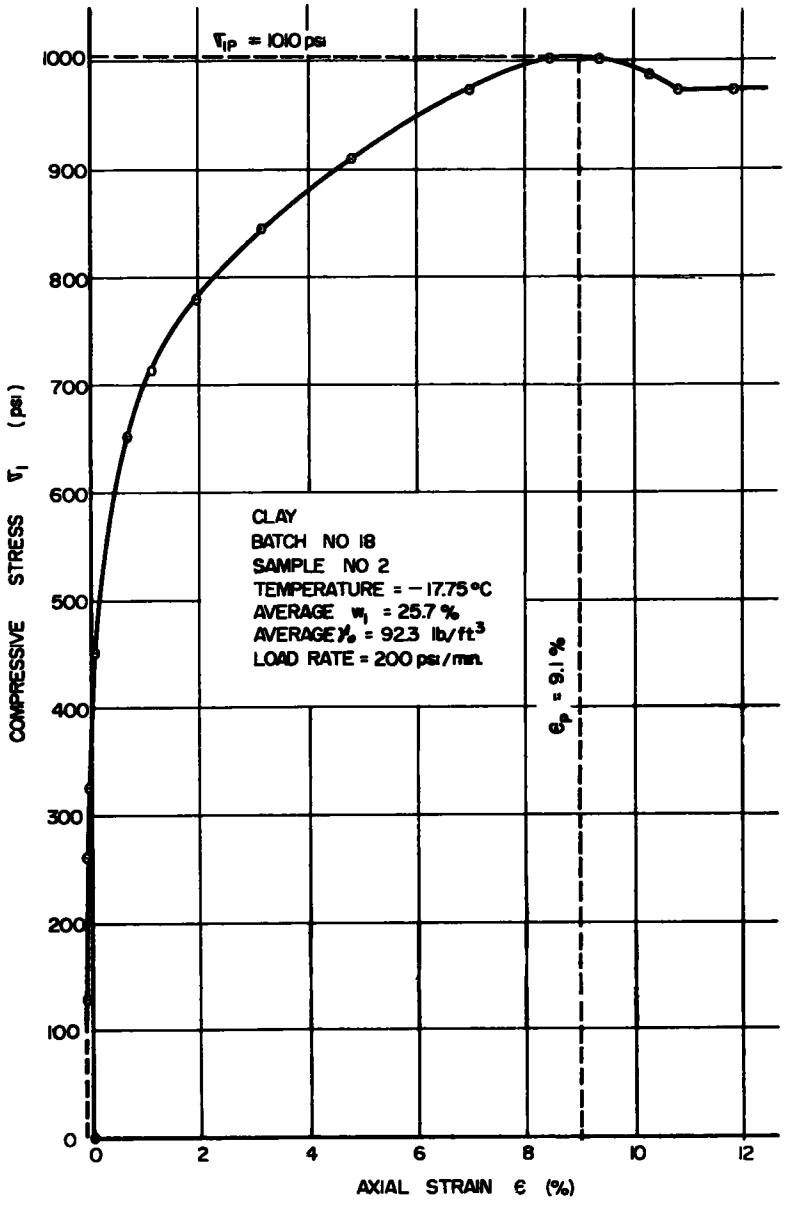

Figure 11. Sample stress-strain curve.

Other analyses were made breaking the data into groups as indicated in Table 2. A comparison of group 1 data, for which the average initial moisture contents and dry

densities are very closely those of the standard Proctor compaction peak, is made at selected temperatures in Table 3.

TABLE 3

COMPARATIVE PHASE COMPOSITION AT SELECTED TEMPERATURES

Soil	Unfrozen Moisture Content w (percent)			
	at -3 C	at -15 C	at -25 C	Ratio $\frac{-3\ C}{-25\ C}$
Clayey Silt	4.4	3.1	2.8	1.55
Silty Clay	11.05	8.0	7.2	1.53
Clay	23.6	15.8	13.9	1.70
	Percentage Moisture Frozen $(\frac{w_1-w}{w_1}100)$			
	at -3 C	at -15 C	at -25 C	Ratio $\frac{-25\ C}{-3\ C}$
Clayey Silt	73.4	81.0	82.9	1.13
Silty Clay	41.8	58.0	62.1	1.48
Clay	16.3	44.0	50.6	3.11

DETERMINATIONS OF PARTIALLY-FROZEN STRENGTHS

It was proposed to show by means of these tests the relative effect of the phase composition (ice and water) peculiar to a given soil and particular test condition on compressive strength. Commensurate with the purpose of the strength determinations, the test procedures used were selected for: (a) simplicity, and (b) adherence to generally accepted methods.

The type of strength test selected for this study was simple undrained unconfined cylindrical compression. Sample size was 1.4 in. (dia) x 2.8 in. The advantages of simplicity for this type of test are of course even stronger for partially-frozen materials.

Until very recently, the only source of data relative to strengths of partially-frozen soils was that described in the foreign literature. Summaries of this data appear in Muller (27), Herrin (28) and in particularly good detail in Corps of Engineers (29). The work of American investigators is now beginning to appear, for example, Kersten and Cox (30) and Corps of Engineers (29)[7].

Stress-controlled rates of loading are most common for partially-frozen soils (29), as contrasted to the strain rates popularly employed for unfrozen materials. In addition, partially frozen materials are usually loaded at what would constitute a very rapid rate for unfrozen soils. In this particular test series, samples were loaded at stress rates of either 162 or 200 psi per minute.

Apparatus and Procedure

Loading was accomplished at controlled temperatures by means of a standard laboratory model hydraulic press (Figures 7 and 10). Load was applied manually and read by calibrated load gages. The two gages used had load capacities of 2,500 and 5,000 lb, with respective least divisions of 25 and 50 lb.

Good loading-rate control was achieved by attaching a small synchronous motor (of the electric clock variety) to the maximum hand of the load gage. By means of interchangeable plastic gear combinations, various speeds of movement of the maximum hand could be achieved. This hand thus became a pacing hand for the manual operation of the hydraulic jack. Strain was recorded to 0.001 in. by means of an ordinary 1-in. capacity dial.

[7]Studies of strength properties of partially-frozen soils by the Arctic Construction and Frost Effects Laboratory, New England Division are continuing.

TABLE 4

SUMMARY OF PARTIALLY-FROZEN STRENGTH DATA

Soil and Group	Batch - Sample No.	Test Temp (-C)	Average w_1 (%)	Average γ_d (lb/ft^3)	Rate of Loading (psi/min)	ϵ_{1p} (%)	Max. Stress σ_{1p} (psi)
Silty Clay Group A	26-1	5.15	15.3	106.5	162	5 35	424
	26-2	5.1	16.4	106.5	162	4 6	443
	27-1	10 25	16.7	107.1	162	9.0	645
	27-2	10 3	16.9	107 1	162	7 7	796
	28-1	17 7	17 2	106 4	162	12.7	1700
	28-2	17 7	17.2	106.4	162	8 5	1655
Average			16 6	106.7			
Range			15 3 to 17 2	106.4 to 107.1			
Group B	23-1[1]	13.5	12.45	112.0	162	7 3	909
	23-5[1]	13 5	12 45	112.0	162	5 5	974
	25-1[1]	5.1	11 2	111.2	162	3 6	558
	25-5[2]	5 1	11.2	111.2	200	2.3	527
	24-1[3]	23 65	13.4	111.1	200	5 4	1728
Average			12.1	111.5			
Range			11.2 to 13 4	111 1 to 112.0			
Clayey Silt Group A	19-1	5 4	8.3	116.8	162	1.7	487
	19-2	5 4	8.1	116.8	162	1 95	491
	20-1	9 5	6.6	113.5	162	0.85	620
	20-2	9.45	7.6	113.5	162	1.6	715
	21-1	17.7	8.5	-	162	1 7	1210
	21-1	17.7	8.5	-	162	1 0	1185
Average			7.9	115.15			
Range			6 6 to 8.5	113 5 to 116.8			
Clayey Silt Group B	15-1[3]	13.0	14 25	107 4	162	4 2	1295
	15-5[3]	13 0	14.25	107 4	162	4 1	1300
	16-1[3]	23.75	15.0	107 4	162	2 1	1624
	16-5[3]	23.75	15.0	107 4	162	3 1	1624
	17-1[4]	23 7	13.8	108 6	200	8 0	2516
	17-5[4]	23.7	13 8	108 6	200	7.0	2390
	18-1[4]	5 0	12 7	107 8	200	4.45	747
	18-5[4]	5 0	12 7	107.8	200	4.4	682
Average			13 9	107 8			
Range			12.7 to 15.0	107.4 to 108 6			
Clay Group A	16-1[5]	5 15	25 2	91 7	162	8.5	367
	16-2[5]	5 3	25.5	91 7	162	14 2	390
	17-1[5]	10.3	24.9	92 7	162	10 1	590
	17-2[5]	10 35	24 95	992 7	162	7.8	568
	18-1[6]	17.7	26.2	92 3	200	10 6	1007
	18-2[6]	17 75	25.7	92 3	200	9 1	1010
Average			25.4	92 2			
Range			24.9 to 26.2	91 7 to 92 7			
Group B	14-1[5]	13.55	25 5	91 4	162	16 6	812
	14-5[5]	13 55	25 5	91 4	162	7 9	649
	15-5[6]	24.3	26 05	91.3	200	6.0	1250
Average			25 7	91 4			
Range			25.5 to 26.05	91 3 to 91.4			

[1] Group A1 Avg w_1 = 12 0 Avg γ_d = 111 7 Range of w_1 = 11.2 to 12.45 Range of γ_d = 111.2 to 112.0
[2] Group A2 Avg w_1 = 12 3 Avg γ_d = 111 15 Range of w_1 = 11.2 to 13.4 Range of γ_d = 111 1 to 111.2
[3] Group A1 Avg w_1 = 14 6 Avg γ_d = 107.4 Range of w_1 = 14.25 to 15.0 Range of γ_d = 107 4 to 107.4
[4] Group A2 Avg w_1 = 13 25 Avg γ_d = 108 2 Range of w_1 = 12.7 to 13.8 Range of γ_d = 107 6 to 108.6
[5] Group 1 Avg w_1 = 25.3 Avg γ_d = 91 9 Range of w_1 = 24.9 to 25.5 Range of γ_d = 91.4 to 92.7
[6] Group 2 Avg w_1 = 26 0 Avg γ_d = 92 0 Range of w_1 = 25 7 to 26 2 Range of γ_d = 91.3 to 92.3

Strength samples were exposed on all sides to the selected test temperature within the freezing cabinet for a period of 18 to 24 hours. The loading press was also located in the cold room, which had an ambient closely equal to that of the freezer. The sample temperature was considered to be the mean within the freezer, and the test was conducted in a manner to strictly minimize change of this sample temperature. For example, the sample was touched only by objects of essentially the same temperature.

The test was carried sufficiently far to define a peak compressive stress (σ_{1p}). As no corrected area formula was considered applicable, the molded or nominal sample area was used to convert load to stress. Figure 11 is a reasonably typical stress-strain plot[8].

RESULTS

All strength data are summarized in Table 4. The average moisture contents (w_1) listed include all moisture, unfrozen and frozen, in the sample at the time of test.

[8] The failure of the curve to pass through the origin was due to minor physical difficulty in correlating zero stress and zero strain.

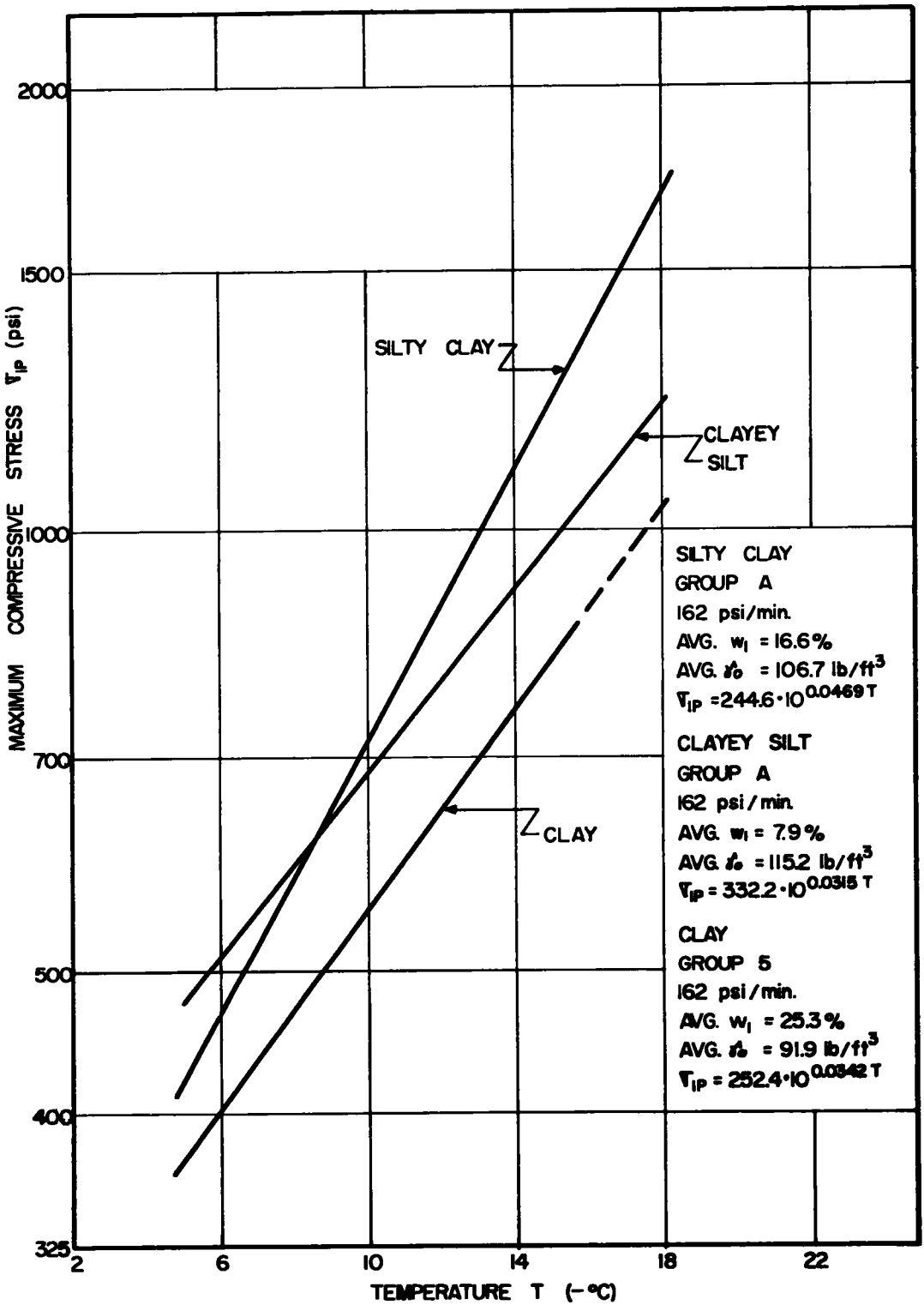

Figure 12. Variation of compressive strength with temperature—all test soils.

Average dry density values are those of "duplicate" check samples in the same soil batch. The primary breakdown of the data into groups A and B represents slight differences in the test procedures which apparently were of only minor influence and are not discussed herein. However, within these groupings significant variations occurred in (a) speed of loading and (b) magnitude of initial moisture-density, necessitating subgroupings for purposes of data analysis. These subgroupings are also indicated in Table 4. Within a given subgrouping, speed of loading is constant and the moisture-density combinations which existed at the time of testing show a rather small range of variation.

Most of the tested samples demonstrated definite failure surfaces with an average approximate angle of 60 deg with the major principal plane. A few samples bulged at top or bottom under load. With a few other samples the upper swiveled loading head tilted considerably before peak load was reached. These difficulties were encountered most frequently with the silty clay. In only one sample (clay) did failure appear to be definitely attributable to weakness along a compaction plane.

All tested samples were later broken apart and examined for evidence of macroscopic concentrations of ice. In only the clay samples at temperatures of -10 C or lower were ice crystals visible. In the case of all other samples, the only ready evidence that they were partially frozen was afforded by their coldness and by extreme hardness. Even very small fragments of the partially-frozen soils could not be crushed between the fingers, until heat from the hand effectively thawed them.

What is believed to be the most significant portion of the strength data is collected in Figure 12, which constitutes a graphical comparison of strengths between the three test soils. The comparison is most valid between the silty clay and clay, which at the time of compression tests existed at approximately standard Proctor optimum moisture content (ice and water) and maximum dry density.

The linear variations shown are the results of least squares analysis. Equations of these lines in the exponential form, $\sigma 1P = c \times 10^{mT}$, are presented on the figure[9]. As was the case with the phase composition equations, these equations are valid for subfreezing temperatures within the test range, and only for soils that have been exposed to sufficient undercooling to initiate freezing.

Since the strength tests were not rational, the strength values presented are intended for use only in a comparative or relative sense.

Large increases in strength with decrease in subzero temperature are shown by Figure 12. Comparisons at selected temperatures are tabled below.

TABLE 5

COMPARATIVE STRENGTHS AT SELECTED TEMPERATURES

Soil	Maximum Compressive Stress $\sigma 1P$ (psi)			
	at -5 C	at -12 C	at -18 C	Ratio $\frac{-18\ C}{-5\ C}$
Clayey Silt	477	794	1227	2.57
Silty Clay	420	894	1708	4.07
Clay	374	649	1042	2.79

The group 1 calorimetric data show that for the silty clay and clay soils at slightly higher but comparable moisture contents and at very nearly equal densities, the following percentages of moisture frozen obtained at the previously tabled temperature values:

[9] Where T is the numerical value of the subzero temperature, and c and m are evaluated contents.

TABLE 6

Soil	Percentage Moisture Frozen			
	at -5 C	at -12 C	at -18 C	Ratio $\frac{-18\ C}{-5\ C}$
Silty Clay	47.6	56.3	59.5	1.25
Clay	26.6	40.8	46.5	1.75

Strictly comparable data is not available for the clayey silt.

It is seen in comparing two temperature levels such as -5 C and -18 C, that the unconfined compressive strength increases exponentially with the relative percentage of moisture frozen. For the silty clay for example, the amount of moisture frozen at -18 C is only 1¼ times that frozen at -5 C, but the compressive strength at the colder temperature is over 4 times that at the warmer level.

Summary of Results and Conclusions

Determinations of Ice in Partially-Frozen Soils. In Table 2 are summarized the results of 59 separate calorimetric determinations of the phase compositions of the three test soils at temperatures from -0.8 C to -24.35 C. The variation of unfrozen moisture content (w) with subzero temperature (T) was found to assume the form $w = cT^m$, where c and m are constants.

The test soils were found to differ significantly from each other in phase composition at a given subzero temperature, and to change appreciably in individual phase composition with lowering of temperature. For example, comparing soils molded to standard Proctor peaks, the following approximate percentages of original moisture frozen obtained: at -3 C, clayey silt 73 percent, silty clay 42 percent, clay 16 percent; at -25 C, clayey silt 83 percent, silty clay 62 percent, clay 50 percent.

It was concluded that very substantial proportions of the total soil moisture of fine-grained materials (defined by drying to constant weight at 105 C) remains unfrozen at temperatures as cold as -25 C. Apparently the more clayey the soil, the greater the quantity of unfrozen moisture.

The calorimetric approach to the solution of phase composition of partially-frozen soils (as utilized in this study) required some simplifying assumptions, but was judged reasonably accurate and workable. Reproducibility of results for the clayey silt soil was poor.

Estimation of phase composition of partially-frozen soils from experimental sorption data for these soils was given detailed consideration. An attempted correlation of such data with "converted" calorimetric and cooling curve data met with little quantitative success, and is not reported in this paper.

Determination of Partially-Frozen Strengths. Unconfined compressive strengths of samples of known moisture, density and temperature were obtained by means of a hydraulic press located within a cold room. Tests were of the stress rate type, at speeds of 162 or 200 psi per minute.

Compressive strengths demonstrated a strong temperature dependency. For example, again considering soils molded at approximately standard Proctor peaks, the approximate ratio of compressive strength at -18 C to that at -5 C was 4.1 to 1 for the silty clay and 2.8 to 1 for the clay. The changes in phase composition, expressed as a ratio of percentage of original moisture frozen at -18 C to that at -5 C, were 1.25 to 1 for the silty clay and 1.75 to 1 for the clay.

It was concluded that the changes in phase composition of partially-frozen fine-grained soils which can take place at temperatures of natural occurrence apparently are responsible for large and important changes in unconfined compressive strength. The practical implications of the changes in strength coincident with change in subzero temperature are of considerable significance.

ACKNOWLEDGMENTS

This work was sponsored by the Snow, Ice and Permafrost Research Establishment (SIPRE), Corps of Engineers, Wilmette, Illinois, under the direction of James E. Gillis, Jr. W. K. Boyd, Chief, Frozen Ground Applied Research Branch, directed the work for SIPRE. The research was conducted within the laboratories of the Joint Highway Research Project, School of Civil Engineering, Purdue University, under the direction of Prof. K. B. Woods. Important contributions were made to this project by Dr. W. L. Dolch, Research Chemist, of the Purdue staff.

REFERENCES

1. Michaels, A. S. "Altering Soil-Water Relationships by Chemical Means." Proceedings of the Conference on Soil Stabilization. Massachusetts Institute of Technology, Cambridge, 1952. pp. 59-67.

2. Schofield, R. K. "The pF of the Water in Soil." Transactions, Third International Congress for Soil Science. Vol. 2. Oxford, England, 1935. pp. 37-48

3. Bouyoucos, G. J. An Investigation of Soil Temperature and Some of the Most Important Factors Influencing It. Experiment Station Technical Bulletin No. 17, Michigan Agricultural College, Lansing. 1913. pp. 168-180.

4. Bouyoucos, G. J. The Freezing Point Method as a New Means of Measuring the Concentration of the Soil Solution Directly in the Soil. Experiment Station Technical Bulletin No. 24, Michigan Agricultural College, Lansing. 1915. 44 pp.

5. Bouyoucos, G. J. "Degree of Temperature to Which Soils Can be Cooled Without Freezing." Journal of Agricultural Research. Vol. 20, No. 4, 1920. pp. 267-269.

6. Bouyoucos, G. J. "Movement of Soil Moisture from Small Capillaries to the Large Capillaries of the Soil upon Freezing." Journal of Agricultural Research. Vol. 24, No. 5, 1923. pp. 427-432.

7. Bouyoucos, G. J. "The Dilatometer Method as an Indirect Means of Determining the Permanent Wilting Point of Soil." Soil Science, Vol. 42, 1936. pp. 217-223.

8. Lambe, T. W. "The Structure of Inorganic Soil." Proceedings, American Society of Civil Engineers. Vol. 79, Separate No. 315. Oct. 1953. 49 pp.

9. Beskow, Gunnar. Soil Freezing and Frost Heaving with Special Application to Roads and Railroads. The Swedish Geological Society, Series C, No. 375, 26th Year Book No. 3 (With a special supplement for the English translation of progress from 1935 to 1946). Translated by J. O. Osterberg. Published by the Technological Institute, Northwestern University, Evanston, Illinois. 1947. pp. 14-21.

10. Parker, F. W. "The Effect of Finely Divided Material on the Freezing Points of Water, Benzene and Nitrobenzene." Journal of the American Chemical Society. Vol. 43, Part 1, 1921. pp. 1,011—1,018.

11. Corps of Engineers. The Unified Soil Classification System. Technical Memorandum No. 3-357. Vol. 1. Waterways Experiment Station, Vicksburg, Mississippi. Mar. 1953. 30 pp. Supp. tables and plates.

12. Corps of Engineers. "Airfield Pavement Design—Frost Conditions." Engineering Manual for Military Construction. Part 12, Chapt. 4, Oct. 1954. p. 2.

13. Kersten, M. S. "Thermal Properties of Soil." Frost Action in Soils, A Symposium. Highway Research Board Special Report No. 2, Washington, D. C. 1952. pp. 161-166.

14. Shannon, W. L. and Wells, W. A. "Test for Thermal Diffusivity of Granular Materials." Proceedings, American Society for Testing Materials. Vol. 47, 1947. pp. 1,044-1,055.

15. Corps of Engineers. Addendum No. 1, 1945-1947, to Report on Frost Investigation, 1944-1945. New England Division, Boston, Mass. 1949. 50 pp. Supp. plates.

16. Baver, L. D. Soil Physics. 2nd Ed. Wiley and Sons, New York. 1948. pp. 288-310.

17. Kersten, M. S. Thermal Properties of Soils. Bulletin No. 28, Engineering Experiment Station, University of Minnesota, Minneapolis. 1949. 225 pp.

18. Kersten, M. S. "Specific Heat Tests on Soils." Proceedings, Second Interna-

tional Conference on Soil Mechanics and Foundation Engineering. Vol. 3. Rotterdam, 1948. pp. 12-15.

19. Mayo, R. I. "Compression Tests on Stabilized Soil Mixtures." A Thesis submitted in partial fulfillment of the MS degree requirement, Purdue University, Lafayette, Ind. 1939.

20. Leonards, G. A "Shearing, Resistance of Partially Saturated Clays." A Thesis submitted in partial fulfillment of the PhD degree requirement, Purdue University, Lafayette, Ind. Feb. 1952.

21. Taylor, Andrew. Snow Compaction. SIPRE Report 13. Snow, Ice and Permafrost Research Establishment. Corps of Engineers, Willmette, Ill. Jan. 1953. p. 16.

22. Powers, T. C. and Brownyard, T. L. "Studies of the Physical Properties of Hardened Portland Cement Paste." Proceedings, American Concrete Institute. Vol. 43, 1947. pp. 934-969.

23. Hodgman, C. D. (editor). Handbook of Chemistry and Physics. 30th Ed. Chemical Rubber Publishing Co., Cleveland, Ohio. 1947.

24. Perry, J. H. (editor). Chemical Engineers' Handbook. 2nd Ed. McGraw-Hill, N. Y. 1941.

25. Eaton, V. E. et. al. "Specific Heat of a Solid." Selective Experiments in Physics. Central Scientific Co., Chicago. 1941. 4 pp.

26. Ostle, Bernard. Statistics in Research. The Iowa State College Press, Ames. 1954. pp. 119-126.

27. Muller, S. W. Permafrost or Permanently Frozen Ground and Related Engineering Problems. J. W. Edwards, Ann Arbor, Michigan. 1947. pp. 34-56.

28. Lovell, C. W. and Herrin, Moreland. Review of Certain Properties and Problems of Frozen Ground, Including Permafrost. SIPRE Report 9. Snow, Ice and Permafrost Research Establishment, Corps of Engineers, Wilmette, Illinois. Mar. 1953. pp. 89-98.

29. Corps of Engineers. Investigation of Description, Classification and Strength Properties of Frozen Solids. Report of Investigations for Fiscal Year 1951, with Appendix A. SIPRE Report 8. New England Division, Boston, Mass. 1951. 88 pp. Supp. Tables and plates.

30. Kersten, M. S. and Cox, A. E. "The Effect of Temperature on the Bearing Value of Frozen Soil." Load Carrying Capacity of Roads Affected by Frost Action. Bulletin No. 40, Highway Research Board, Washington, D. C. pp. 32-38.

Soil Moisture Transfer in the Vapor Phase Upon Freezing

ALFREDS R. JUMIKIS, Professor of Civil Engineering, Rutgers University, New Brunswick, N. J.

In this study the validity of the assumption serving as a basis for the soil freezing experiment is examined, namely, that the upward flow of soil moisture from ground water toward the freezing ice lenses takes place virtually unaccompanied by vapor diffusion.

Two cases were studied: (1) upward diffusion of vapor to air (voids in soil not filled with water), and (2) upward diffusion of vapor through water (soil voids filled with water).

The study reveals that upon freezing the amounts of soil moisture transferred in the vapor phase are small. Therefore the mechanism of vapor diffusion in the soil freezing experiment can be considered as being of little significance.

● UPON freezing of the soil moisture flowing upward from the ground water to the freezing ice lenses within a certain soil system a fundamental change in phase of state takes place, namely, water changes from liquid to ice.

Soil moisture in the form of vapor may also be present in that soil system. Upon freezing, aqueous vapor also undergoes a fundamental change in phase, namely, vapor moisture transforms into ice. It is obvious that in the process of changing the phase temperature is always one of the necessary factors.

In order that an upward flow of soil moisture may take place, there must be, besides temperature difference, a potential as well, viz., the presence of a pressure difference between the lower and upper parts of the system.

The potential or driving force to cause the process of an upward flow of the soil moisture may be a hydraulic one (or, more precisely, a hydrodynamic pressure), or it may be a vapor pressure gradient with a pressure drop from the lower part to the upper part of the system, that is, in the direction from the ground-water table towards the freezing ice lenses.

In order to study the physical process of the upward flow of soil moisture upon freezing, and particularly to learn what are the magnitudes of the pressure differences, viz., subpressures for various types of soil at various environmental conditions, and because all physical laws are derived from experiment, it is believed that soil freezing should be studied experimentally.

Assumption—In studying physical processes in a complex system such as the freezing process in soil, and because of lack of certain scientific information which would serve as a basis for such studies, it is necessary to make some assumptions at the outset in order to agree on certain facts.

In theorizing about the migration of the soil moisture and in planning a soil freezing experiment, one of the assumptions the author made is that the soil moisture transfer in the vapor phase (= vapor diffusion) upon freezing is negligible, and therefore it can be ignored (1, 2).

References to Other Authors—The aforementioned assumption was based on information given by several authors in their works. Thus, for example, the noted geologist Gunnar Beskow, a Swedish authority on soil freezing and frost heaving (3), reasoning from his research and many field and laboratory observations, believes that in many cases the transfer of soil moisture towards the cold front in the soil takes place by vapor diffusion, but that this is not always necessarily so, and that vapor diffusion is not a necessary step in the process of the upward migration of soil moisture towards the forming and downward-progressing ice lenses upon freezing.

A. W. Porter (4), a former professor of physics at the University of London, writes: "All surface-tensions with which we have to deal are in reality interfacial tensions, since a liquid is always in contact with its own vapor or the gas in which it is immersed.

The effect due to the gas is known, however, to be very small."

Another reference relative to this subject is found in the works of H. F. Winterkorn (5), who writes that the phenomenon of the soil moisture diffusion in the vapor phase, caused by vapor pressure differences, is of little practical importance.

The Problem—In order to learn the significance and the effect of vapor pressure and vapor diffusion in the soil freezing process, and in order to examine the validity of the assumption that the upward flow of soil moisture upon freezing is virtually unaccompanied by vapor diffusion, this assumption was studied theoretically, using assumed values for physical constants.

In this study only soil freezing with water supply solely from the ground water is considered because freezing under such conditions, subsequently followed by thawing, causes the greatest damage to highways.

Vapor Diffusion

Two Kinds of Soil Freezing—In thermal soil mechanics two principal types of soil freezing can be distinguished: (1) freezing with possible upward water supply from the ground-water table (real or perched) to the downward-freezing ice lenses, and (2) freezing when there is no ground water present, or when the ground water is too deep to affect the soil freezing, i. e., no water supply from ground water to the freezing ice lenses is available.

As previously explained, only the first case is examined here.

The soil voids proper may be considered as substantially a network of small, irregular cellular units or, for simplicity and convenience of explanation, as irregular capillary voids or tubes. The soil voids communicate with each other through narrow necks at the contact points of the soil particles (Figs. 1, 2 and 3).

The voids of a soil may be filled with water, gas (for example, air, moisture vapor, or gases dissolved in ground water), or both moisture and gas. Thus, the principal constituent parts of a soil are: the solid soil particles, or simply solids, the water and the gas. It is generally assumed that most of the volume of the voids of frost-susceptible soils such as silt, clayey silt and silty clay is derived from capillaries filled with soil moisture, assuming that ground water is present in the soil.

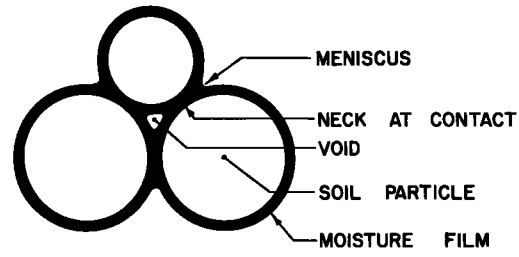

Figure 1. Narrow necks at the contact points of the soil particles.

If a certain volume of air, vapor or gas is entirely surrounded by water it is called a globule or bubble.

Thus soil can be considered as a porous medium, and thereby as a disperse system. As such, it can be considered as a carrier of soil moisture, aqueous vapor or gas. Vapor and gas are transferred through the voids of the soil, filled or not filled with moisture, by way of diffusion. Diffusion, in its turn, is effected by aqueous vapor pressure difference as a driving force.

Vapor Pressure—Diffusion of aqueous vapor in a soil system generally takes place when there exists a vapor pressure difference. Hence, vapor pressure difference can be considered, among other potentials which are available for the transference of moisture in soil, as one of the potentials or driving forces causing the soil moisture to move upward in the vapor phase, It is obvious that in a laterally insulated system consisting of a soil sample in the form of a vertical cylinder (where the moisture films are connected with the ground water table) and subjected to freezing from its top, the vapor pressure must be larger at the lower end of the system and smaller at the upper end (Fig. 4). This is because in wintertime, when temperatures of the air, viz., ground surface, are at or below freezing, the upper layers of the soil are cooler than the lower ones. Thus during a freezing season heat in soil is flowing upward.

Diffusion Caused by Several Factors—The upward diffusion of soil moisture in the vapor phase by vapor pressure can take place under the following conditions:

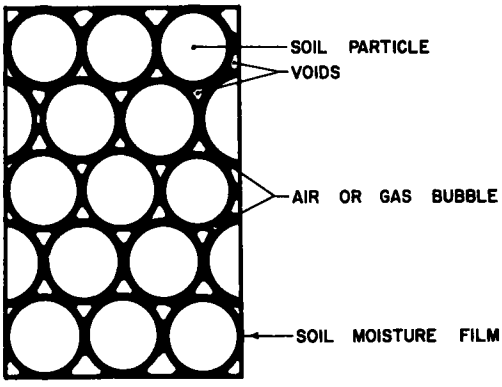

Figure 2. Idealized capillary network.

1. There might be a difference in temperature ($T_1 - T_2$) at the bottom and top of the freezing soil system, the bottom being at a higher temperature (viz., ground-water temperature, which, depending upon the depth below the ground surface, varies during a winter, according to the author's observation, from about 6 deg C to 10 deg C) than the top (freezing temperature at about 0 deg C as it would be during a freezing season). Such temperature differences cause a vapor pressure difference ($p_1 - p_2$) under the influence of which aqueous vapor diffusion in soil takes place. Thus, $p_1 - p_2 = f(T_1 - T_2)$.

2. There might be a vapor pressure difference in soil due to a difference or variation in capillary moisture surface tension, S, i.e., $p_1 - p_2 = f(S)$.

Upon the commencement and prevalence of such conditions the assumed continuous threads, paths or capillaries of soil moisture, particularly the weaker stressed part which is located farthest from the soil particles and may merge with that absorbed to

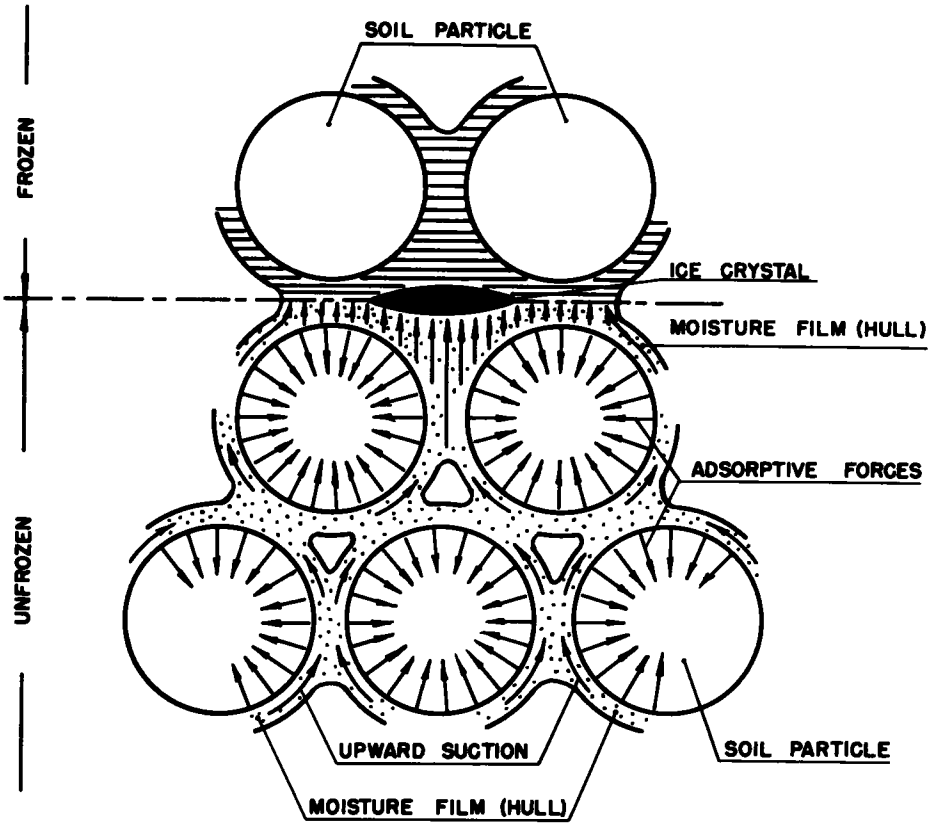

Figure 3. Sketch illustrating the concept of the upward flow of soil moisture toward an ice crystal.

the surface of an adjacent soil particle, can under certain circumstances be interrupted by the formation of vapor or gas bubbles. Thus, diffusion and condensation of soil moisture would take place within the freezing soil system.

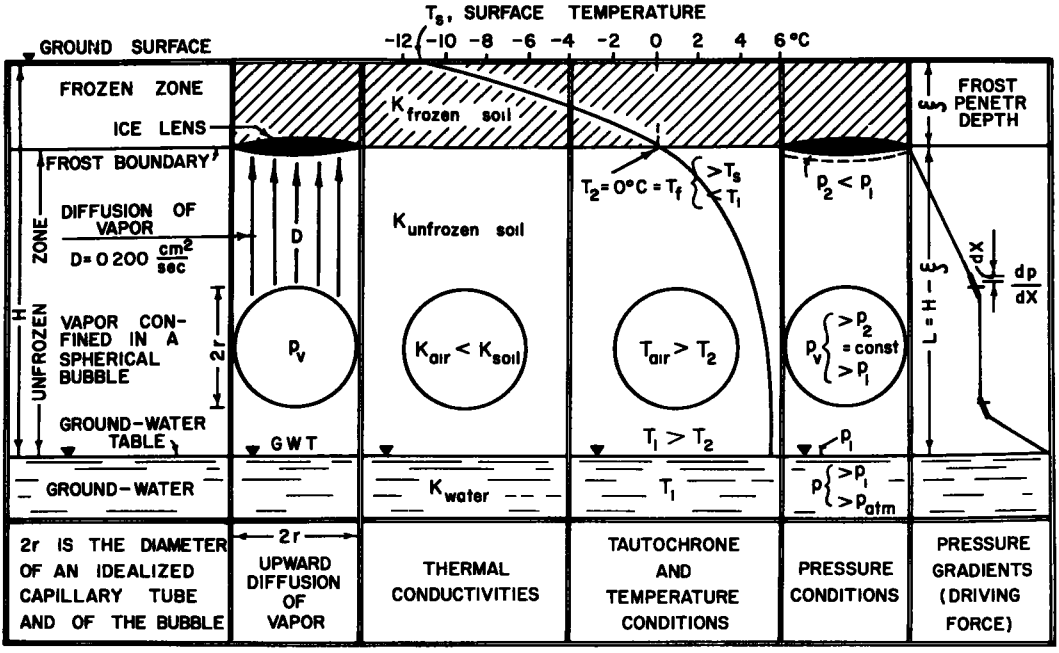

Figure 4. The freezing soil system-upward diffusion of vapors.

I. Diffusion as a Function of Temperature

Diffusion System—Assume that at the beginning of the freezing period and at the beginning of observation there is present in an idealized soil capillary, besides soil moisture, also some water vapor in the form of bubbles which are surrounded by water. Assuming also that those voids which are not occupied by water communicate with each other through the narrow necks at the contact points of the particles and that in these voids there is some vapor present, this case becomes essentially a problem of diffusion of one gas into another, or, in other words, diffusion of aqueous vapor to air (Fig. 4).

Temperature Conditions—Now, upon freezing, the soil gradually chills from the ground surface down (see tautochrone, Fig. 4). However, because the air in the bubble has a relatively smaller coefficient of thermal conductivity than the chilling soil (including air in the voids) above the bubble, there is established a relatively large temperature difference across the bubble between its temperature and that of the soil above the bubble. Because the temperature within the bubble is greater than that of the soil above it, the aqueous vapor within the bubble is also greater than that outside and above the bubble. Such a condition may cause more vaporization and consequently cause the aqueous vapor in the soil to flow upward. Thus, the aqueous vapor has a tendency to diffuse from places of higher pressure to places of lower pressure until a pressure equilibrium is achieved. Also when the moisture content of the soil is uniform throughout the system vapor diffuses with the temperature gradient, i. e., in the direction of heat flow. These conditions are illustrated schematically in Fig. 4.

Soil temperature measurements during the years 1949 to 1955 at Rutgers University show that the average soil temperature gradient during several winters in 34 types of New Jersey soils for depths from zero to about 30 inches below the ground surface vary from i_T = 0.038 to 0.078 deg C/cm, or approximately from i_T = 0.04 to 0.08 deg C/cm.

Because of the physical quantities involved, as well as for convenience, let us in

this study avail ourselves of the significance of the soil moisture diffusion in the vapor phase by vapor pressure as the driving force to the c. g. s. -system.

Thermal Properties—Assuming for air containing some aqueous vapor a coefficient of thermal conductivity of $K_{air} = (5.1) \cdot (10^{-5}) \left[\frac{cal}{cm \cdot sec \cdot {}^{o}C} \right]$, and one for a moist soil near freezing temperature of $K_{soil} = (252) \cdot (10^{-5}) \left[\frac{cal}{cm \cdot sec \cdot {}^{o}C} \right]$, their ratio

$$\frac{K_{air}}{K_{soil}} = \frac{(5.1) \cdot (10^{-5})}{(252) \cdot (10^{-5})} \approx \frac{1}{50},$$

shows that in this example the coefficient of thermal conductivity of air is approximately 50 times less than that of the soil.

Upon chilling the soil downward, such a ratio of thermal conductivities would give us a thermal gradient across the aid space or bubble of vapor or gas between 2 - 4 deg C/cm.

Vapor Pressures—It is known that the pressure of a saturated vapor is determined only by its temperature. Also the pressure is independent of its volume if the temperature is unchanged. Thus, the vapor determines its own volume for any given temperature. The saturation vapor pressure of an aqueous vapor is defined as the pressure at a given temperature when completely saturated.

Aqueous vapor can be admixed to the soil air or to the atmospheric air in a limited amount only. This is true because its partial pressure can never be greater than the saturation pressure at a given temperature. Therefore, it is satisfactory in this study to neglect the consideration of the degree of saturation and/or the relative humidity and to operate here merely with the saturation vapor pressure, which are the maximum pressures.

Table 1, Column 2, gives an idea of the magnitudes of the saturation vapor pressures p_{max} in mm of mercury at various temperatures and $p_o = 760$ mm Hg under standard pressure conditions. These p_{max} -values were taken from the International Critical Tables (6). Column 3 of Table 1 shows pressure differences of water vapor in mm Hg. Column 4 shows the weight of water in grams per cubic meter of saturated aqueous vapor (= absolute moisture) D_V, which is also known as the density or unit weight of vapor at a given temperature. Vapor densities D_V as in Column 4 were calculated by the combined Boyle's-Charles'-Gay Lussac's general gas law by means of the following equation (7):

$$D_V = (288.9) \cdot \left(\frac{p_{max}}{{}^{o}K} \right), \quad (1)$$

where $${}^{o}K = 273^{o}\ C + T^{o}\ C \quad (2)$$

is the absolute temperature of the vapor D_V. In Column 5 it is shown that the average aqueous vapor pressure differences for 1 deg C temperature difference within a temperature range from 0 deg C to 5 deg C is approximately 0.38 mm Hg.

Figure 5. Vapor pressure and density curves.

Aqueous vapor pressures p_{max} and vapor densities D_V as a function of temperature are also shown in Fig. 5. From this graph it can be seen that as the temperature of the soil moisture increases, the vapor expands and the pressure of the saturated vapor increases. Vice versa, when the vapor is cooled heat is abstracted from it and the vapor will contract.

Whenever the temperature of the soil moisture, viz., soil, is known the vapor pressure can be found from Fig. 5 or from Table 1.

TABLE 1

SATURATED AQUEOUS VAPOR PRESSURES

Soil Air Temperature °C	Saturated Aqueous Vapor Pressure		Vapor Density	Average Vapor Pressure Difference
	Pmax, in mm Hg	Differences, in mm Hg	D_V in g/m³	in mm Hg/° C
1	2	3	4	5
-5	3.163		3.353	
		0.247		
-4	3.410		3.615	
		0.263		
-3	3.673		3.893	
		0.283		
-2	3.956		4.193	
		0.302		
-1	4.258		4.513	
		0.321		
0	4.579		4.854	
		0.347		
1	4.926		5.222	
		0.368		0.380
2	5.294		5.612	
		0.391		
3	5.685		6.026	
		0.416		
4	6.101		6.467	
		0.442		
5	6.543		6.934	
		0.470		
6	7.013		7.434	

Pressure Differences—For temperatures of 2 deg C to 4 deg C (near freezing), as seen from Columns 3 and 5 of Table 1, the average difference in aqueous vapor pressure is about 0.38 mm Hg per degree centigrade. Thus, for temperatures from 2 deg C to 4 deg C per width x of the air space, that is, "thickness" of the bubble, the corresponding average vapor pressure differences can be calculated

as $2 \times 0.38 = 0.76$ mm Hg

and $4 \times 0.38 = 1.52$ mm Hg,

respectively. This corresponds to a variation in unit pressure gradient of 1.034 g/cm² and 2.06 g/cm², respectively, or, assuming that the unit weight of one cubic centimeter of water is one gram, the above pressures, expressed in terms of pressure heads of a column of water, are: dp = 1.034 cm and dp = 2.06 cm, respectively.

Diffusion Theory—The phenomenon of upward diffusion of soil vapor is analogous to diffusion of a gas through another gas. In this study the two gases are the aqueous vapor and air. Thus, our vapor diffusion problem in the soil freezing experiment can be treated by Fick's first law of diffusion (8). In this law it is assumed that the diffusion of matter is analogous to the heat transfer in the steady state through a slab according to Fourier's law, the difference being that the coefficient of gas (vapor) diffusion D takes the place of the coefficient K of the thermal conductivity.

Thus, according to Fick's law the quantity W of a gas or vapor in a translational perpendicular diffusion through a given cross-sectional area A of the diffusion capillary, in a short time interval dt, and at constant temperature, is proportional to this area, to the time and to the concentration gradient $\frac{dc}{dx}$. Generally,

$$W = -D \cdot A \cdot \frac{dc}{dx} \cdot dt \qquad (3)$$

where

W = quantity of a substance in grams diffused during time t through area A;

D = constant of proportionality, in cm²/sec;

A = cross-sectional area, in cm²;

c = the concentration of the diffusing substance given as amount of substance per cubic centimeter;

x = coordinate perpendicular to a reference plane, or distance in cm along the path of diffusion; and

$\frac{dc}{dx}$ = concentration gradient (Fig. 6).

The minus sign indicates that diffusion takes place from a region of higher concentration to one of lower concentration.

The term "concentration" is a very important concept for the understanding of the solution of a problem. This term means a quantity of matter, expressed in moles or grams contained in a unit of volume, for example, cubic centimeter, or liter, or cubic meter.

According to Jost (9), the unit chosen for the quantity of a substance in the definition of diffusion W given above is not specified, since the law of diffusion is independent of the special choice. Therefore, the following units, generally, can be chosen: mass (in grams or any other unit); number of molecules; cubic centimeters of gas at standard temperature and pressure conditions; or whatever unit may seem most convenient in the case under consideration.

The coefficient of proportionality, D, is termed the coefficient of diffusion for one

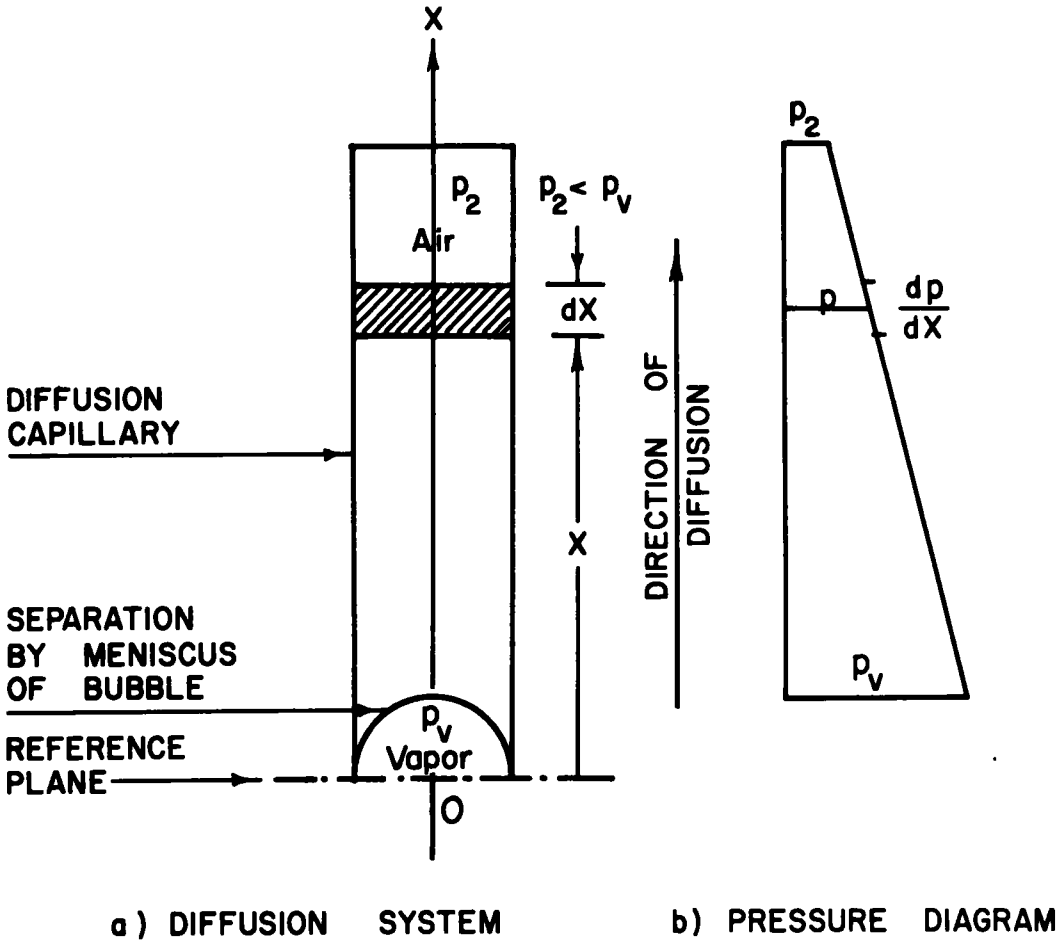

Figure 6. Vapor diffusion.

gas to another gas, in $\frac{cm^2}{sec}$. In this problem the two gases are vapor to air. Here, this coefficient represents a quantity of gas by weight diffusing one cm per second through an area of one square centimeter when the concentration gradient is a unity. At 0° C and 760 mm Hg pressure, the coefficient of vapor diffusion into air is

D = 0.203 as determined by H. Houdaille (10), and

D = 0.198 as determined by A. Winkelmann (11).

For this study it is satisfactory to assume a value for vapor to air diffusion of D = 0.20, which is an average of the two values just given.

Application of Diffusion Theory to Soil Mechanics, viz., Soil Freezing, Problem— In order to apply the diffusion theory to our soil system the molar concentration gradient dc/dx is replaced by the partial pressure gradient dp/dx. According to the general gas law (12),

$$p = c \cdot R \cdot T \left[\frac{g}{cm^2}\right] , \qquad (4)$$

where

R = gas constant in $\frac{cm}{K}$, and

T = absolute temperature in degrees Kelvin.

Expressing from Equation 4 the concentration c,

$$c = \frac{p}{R \cdot T} \left[\frac{g}{cm^3}\right] , \qquad (5)$$

and substituting it in Equation 3, obtain

$$W = -D \cdot A \cdot \frac{1}{R \cdot T} \cdot \frac{dp}{dx} \cdot t \left[g\right] . \qquad (6)$$

The minus sign now accounts for diffusion that takes place from higher values of pressure to lower ones. Because diffusion is a slow process, instead of dt, time t is used. The unit of time was chosen to be the day = 86,400 seconds. Equation 6 is now rewritten showing the proper units:

$$W\,(g) = -D \cdot (cm^2/sec) \cdot A \cdot (cm^2) \cdot \frac{1}{R \cdot (cm/K) \cdot T(K)} \cdot \frac{dp\ (g/cm^2)}{dx\ (cm)} \cdot t\ (sec), \qquad (7)$$

$$W\,(g) = -D \cdot A \cdot t(cm^3) \cdot \frac{1(g/cm^2)}{R(cm/K \cdot T(K)} \cdot \frac{dp \cdot (1)}{dx \cdot (1)} . \qquad (8)$$

From Equation 8 it can be noted that the expression

$$\frac{1}{RT} \frac{g}{cm^3} = \frac{p_v = 1 g/cm^2}{RT} \left(\frac{g}{cm^3}\right) \qquad (9)$$

represents the density of vapor, D_v, at pressure of $p_v = 1\ g/cm^2$. Therefore Equation 9 can be equated to Equation 1, and the latter substituted into Equation 8:

$$W = -D \cdot A \cdot t \frac{dp}{dx} \cdot D_v \cdot \qquad (10)$$

Amount of Vapor Diffused—Since 1 g/cm^2 of pressure corresponds to 0.735 mm Hg, the vapor density D_v is calculated as follows (at 0° C and 760 mm Hg):

$$D_v = (288.g) \cdot \frac{0.735}{273} = 0.755 \left[\ g/m^3\ \right] \qquad (11)$$

or

$$D_v = (0.755) \cdot 10^{-6} \left[\ g/cm^3\ \right] . \qquad (12)$$

Thus, the amount in grams of aqueous vapor, W, diffused through an area of A = 1 cm^2, during a day (t=86,400 sec.), under a driving force of $\frac{dp}{dx}$ = 1.034 $g/cm^2 \cdot cm$ at a vapor density of $D_v = 0.775 \cdot 10^{-6}$ g/cm^3 with a coefficient of diffusivity of D = 0.20, is

a) in the first case:

$$W = \left| -(0.20) \cdot (1) \cdot (86,400) \cdot (1.034) \cdot (0.775) \cdot (10^{-6}) \right| = 0.0138(g) \qquad (13)$$

b) in the second case:

$$W = \left| -(0.20) \cdot (1) \cdot (86,400) \cdot (2.06) \cdot (0.775) \cdot (10^{-6}) \right| = 0.0276(g) \quad (14)$$

These quantities correspond to a sheet of water of .14 mm per day and .28 mm per day, respectively, which quantities, indeed, seem to be of too little practical significance to take them into consideration in the soil freezing experiment.

II. Diffusion as a Function of Moisture Surface Tension

General Considerations—Diffusion of soil moisture in the vapor phase with vapor pressure as a driving force can take place owing to the difference in capillary moisture surface tension. In essence, this case presents a problem of upward diffusion of water vapor through water. Now, in order that such a diffusion may take place, there must prevail a certain relationship between the aqueous vapor pressure and the soil moisture tension. Further, consider that within a soil system containing in its voids some water, there are scattered many bubbles of gas (air, or vapor, or gas). According to the minimum principle in nature the surface of these small bubbles should tend to decrease. This tendency results in merging together of the small bubbles into a single bubble upon their direct contact with each other. The shape of the bubble then tends to approach a sphere which, according to geometry, has the least surface area as compared with the equivalent volume of the sum of the small bubbles.

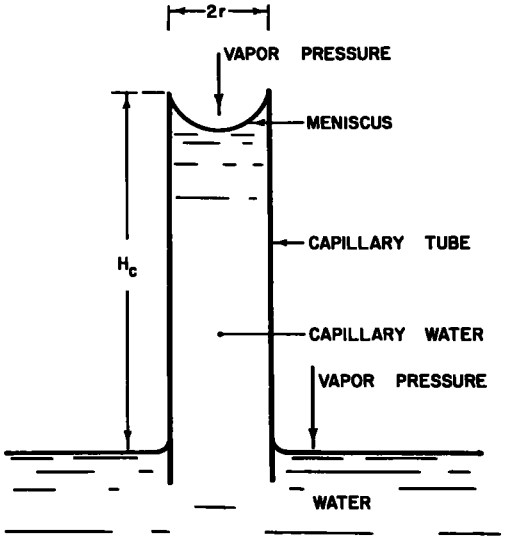

Figure 7. Water in contact with its own vapor.

If the small bubbles do not make contact, then it is possible that their merger into a single bubble would take place upon vaporization.

The following study is based on the general concepts of capillary theory. According to this theory the capillary water in a capillary tube is in contact (through its meniscus) with its own vapor (Fig. 7). It is then assumed that upon freezing there is enclosed vapor present between the upper meniscus and the lower 0^0 C-isothermal surface or bottom plane of the frozen soil (Fig. 8). This assumption, however, is a pretty weak point to defend; this is because upon the attachment of water molecules to the ice lens no meniscus or (vapor) space between the ice lens and the water in the capillary tube can be observed, unless incidentally there happens to be a larger air void in the soil directly underneath the ice lens. However, if we assume (a) that upon freezing the water is in contact with the solid ice, (b) that water is connected to the ice lenses directly without the vapor phase, and (c) that the removal of water molecules from the capillary water and their attachment to the growing ice crystal or lens would cause an effect equivalent to that which would occur if there were actually vapor pressure present, then this problem can be studied by means of the capillary theory.

Pressure, Surface Tension and Curvature of Meniscus—Suppose now that there is a spherical bubble of gas present in the soil water. Assume that the diameter of the bubble, viz. the capillary tube, is 2r. Also, assume that the bubble interrupts the continuity of the capillary water in the tube so that there is no water contact between the upper meniscus and the ground-water table (Fig. 9).

Theoretically the spherical shape of the bubble is possible because of the existence of an internal pressure p_V inside the bubble. This internal pressure, for example vapor pressure, acts on the inside surface of the sphere. Besides, the internal or vapor pressure, viz. gas pressure, must be greater than the external or outside pressure p_L.

Under these conditions, there exists inside the bubble a pressure difference or resulting (=excess) pressure, $p_v - p_L$, expressed in physical units of dynes per cm^2.

The total pressure tending to force the two hemispheres apart is

$$(p_v - p_L) \cdot \pi \cdot r^2 \quad \left[\text{dynes}\right], \qquad (15)$$

where r is the radius of the spherical bubble, viz. capillary tube. This total pressure is balanced by the surface tension of the hemispherical gas-moisture film which acts circumferentially around a circle through the largest diameter plane. The magnitude of this total surface tension force is

$$S_* \cdot 2\pi r \quad \left[\text{dynes}\right], \qquad (16)$$

where S_* is surface tension in dynes per cm.

At force equilibrium,

$$(p_v - p_L) \cdot \pi \cdot r^2 = 2 \cdot \pi \cdot r \cdot S_*. \qquad (17)$$

Then the difference in vapor pressure and water pressure is

$$p_v - p_L = \frac{2 \cdot S_*}{r} \quad \left[\frac{\text{dynes}}{\text{cm}^2}\right]. \qquad (18)$$

This equation represents Laplace's law, and establishes the relationship between the pressure on the liquid and its meniscus surface curvature. In Equation 18, $\frac{2 \cdot S_*}{r}$ is the excess pressure on one side of the film (directed from inside to outside of the spherical bubble) of constant surface tension. To increase the gas bubble in size or

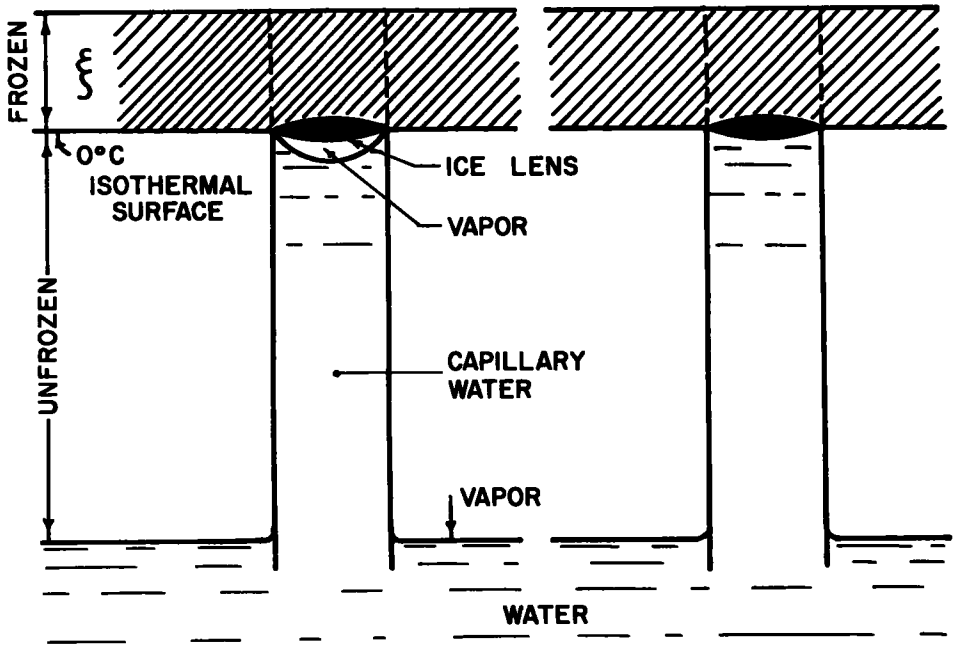

a) VAPOR BETWEEN ICE LENS AND CAPILLARY WATER.

b) CAPILLARY WATER IN DIRECT CONTACT WITH ICE LENS.

Figure 8. Ice-vapor and ice-water interfaces.

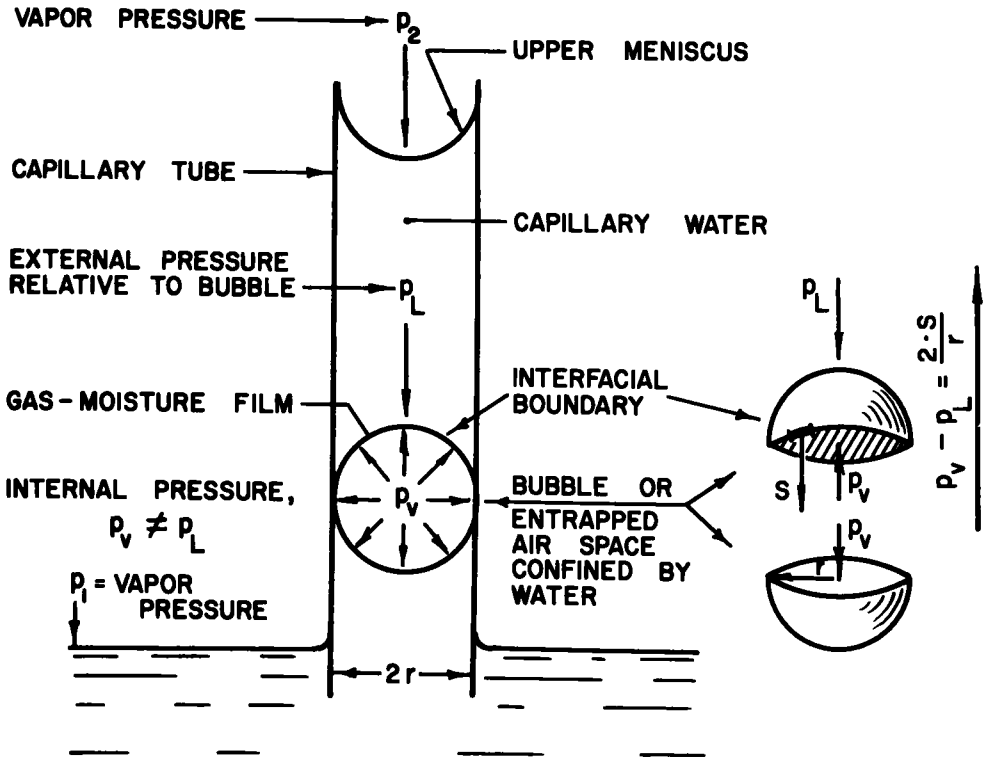

Figure 9. Bubble in capillary water.

to expand it within a void in the soil, an excess pressure increment is needed, so that

$$(p_V - p_L) > \left(\frac{2 \cdot S_*}{r}\right) \quad . \tag{19}$$

At this point, however, it is pertinent to remember that at the outset of this problem nothing was said as to the cause of the internal pressure p_V, viz. pressure difference $(p_V - p_L)$.

If we assume that the cause of the pressure is vapor, then the following general relationship (based on work consideration) between vapor pressures p_1 and p_2 and surface tension S (or radius of the curved surface of the meniscus) as given by Kelvin (13) is applicable:

$$R \cdot T \cdot \ln \frac{p_1}{p_2} = \frac{2 \cdot S}{\gamma_w \cdot r} \quad , \tag{20}$$

where

p_1 = vapor pressure over a plane reference surface of water, for example, ground-water table;

p_2 = vapor pressure over a concavely curved capillary meniscus surface;

R = gas constant, in cm/deg T,

T = absolute temperature in degrees Kelvin;

γ_w = unit weight of water, in grams per cubic centimeter, and

S = surface tension at temperature T, in grams per cm.

These conditions are illustrated in Figure 10.

Developing $\ln \frac{p_1}{p_2}$:

$$\ln \frac{p_1}{p_2} \quad \ln\left(1 - \frac{p_2 - p_1}{p_2}\right) \approx \frac{p_1}{p_2} - \quad (21)$$

(for small pressures),

obtain

$$p_1 - p_2 = \frac{2 \cdot S \cdot p_2}{\gamma_w \cdot r \cdot R \cdot T} \cdot \left[\frac{g}{cm^2}\right] \quad (22)$$

According to the general gas law, the expression

$$\frac{p_2}{R \cdot T} = D_v$$

represents the density or unit weight of vapor, D_v (14).

Thus, Equation 22 can be rewritten as

$$p_1 - p_2 = \frac{2 \cdot S}{\gamma_w} \cdot D_v \cdot \frac{1}{r} . \quad (23)$$

The interpretation of this equation is that the vapor pressure over a concave meniscus in a capillary tube is less than that over a plane surface by an amount of $2 \cdot S \cdot D_v / \gamma_w \cdot r$. The effect of surface tension on the vapor pressure is to vary the latter as the curvature $\frac{1}{r}$ of the capillary meniscus varies. However, because the variation in surface tension due to small soil temperature variations in winter below the frozen is small, the variation in pressure difference is also relatively small.

The pressure differences ($p_1 - p_2$) can now be calculated, provided that the quantities $2 \cdot S \cdot D_v / \gamma_w$ and $1/r$ are known. These quantities are obtained from the capillary theory.

Capillary Pressure—According to Laplace, the capillary pressure P_c, or the carrying capacity of the meniscus, is equal to the weight of the capillary water column (Fig. 11):

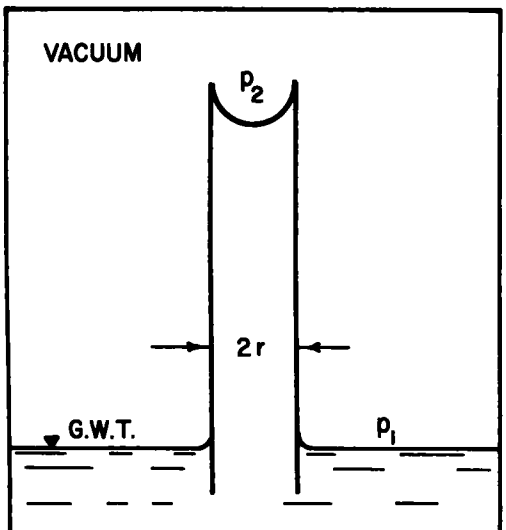

Figure 10. Kelvin's condition for relationship between vapor pressure and surface tension, viz. radius of curvature.

$$P_c = \gamma_w \cdot g \cdot H_c = \frac{2 \cdot S_*}{r} \left[\frac{dynes}{cm^2}\right], \quad (24)$$

where

γ_w = unit weight of water, in g/cm^3;

g = 981.4 cm/sec^2 = acceleration of gravity;

H_c = capillary height, in cm;

S_* = surface tension, in dynes/cm, and

r = radius of meniscus, in cm, which, when normally developed, equals the radius of the capillary tube.

It follows that

$$H_c = \frac{2 \cdot S_*}{\gamma_w \cdot g} \cdot \frac{1}{r} \left[cm\right], \quad (25)$$

or

$$H_c = \frac{2 \cdot S}{\gamma_w \cdot r} \left[cm\right], \quad (26)$$

where S is now in grams per centimeter, as one dyne equals $(1.0197) \cdot (10^{-3})$ grams. The term H_c is also called the capillary

suction height, or capillary coefficient.

Multiplying H_c by a unit area and by the unit weight of water $\gamma_w = 1\ g/cm^3$, one obtains H_c as a unit pressure in g/cm^2, which is also termed the capillary pressure.

Stress in Capillary Water—It is interesting to note that the capillary phenomenon presupposes a tensile resistance of the capillary water (observe in Fig. 12 that the capillary water column seems to be hanging with its full weight at the meniscus). Besides, physically, with the ascent of the vapor from the plane surface of water the vapor pressure decreases, i. e., vapor pressure decreases when rising from a lower to a higher level. Thus, for the conditions it can be said that the larger the negative capillary pressure or subpressure, the larger is the curvature of the capillary meniscus and the larger is the vapor pressure p_2 as compared with p_1.

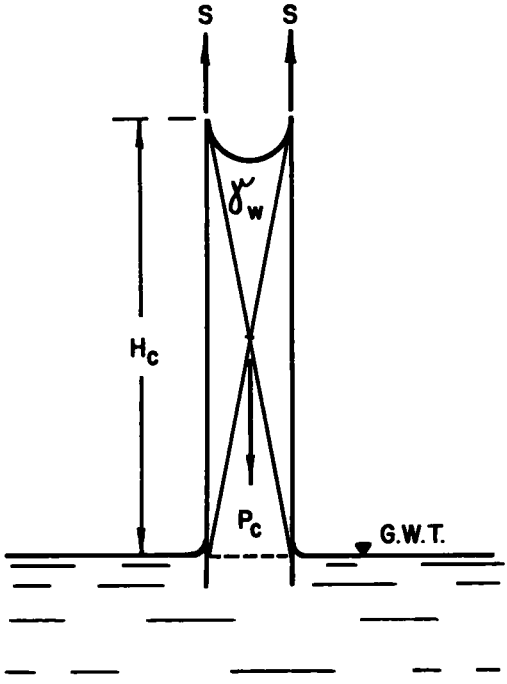

Figure 11. Illustrating weight of the capillary water columns.

Bubble in a Capillary Tube—Assuming that the continuity of the capillary water column in a capillary tube is interrupted by a confined air space or a large void in the form of an entrapped, spherical bubble (Fig. 9), it becomes apparent to the reader that in order that an upward diffusion of soil moisture in the vapor phase upon freezing may take place, there should exist a vapor pressure difference, viz. capillary pressure difference between the plane surface of reference or the ground-water table and the curved meniscus surface of the capillary water. Further, referring back to the study of vapor diffusion in air caused by temperature variations, it can also be inferred that in order to bring about some appreciable amount of vapor diffusion one would expect that the vapor pressure difference in the freezing soil system should be of a high order of magnitude.

Stresses in Capillary Water at the Position of the Bubble—The stress σ_{a-b} in the capillary water at the position a-b of the bubble is

$$\sigma_{a-b} = \gamma_w \cdot (H_c - h_c) \qquad \left[g/cm^2 \right] \tag{27}$$

The vapor pressure within the bubble is $p_v\ g/cm^2$ (Fig. 13).

At force static equilibrium in section a-b c-d of the capillary column the following equation applies:

$$p_1 - (H_c - h_c) \cdot \gamma_w = p_v - \frac{2 \cdot S}{r} \quad , \tag{28}$$

and the vapor pressure difference in such a case is

$$p_1 - p_v = (H_c - h_c) \cdot \gamma_w - \frac{2 \cdot S}{r} \tag{29}$$

Again, from this equation it can be seen that if the variation in surface tension S due to the soil temperature variations is small, the vapor pressure difference $(p_1 - p_v)$ is likewise small.

Vice versa, from Equation 29 it can also be seen that should large vapor pressure differences be needed, there should be concurrently also available large capillary pressure differences. These, of course, are not available in wintertime below the frozen soil layer because of the narrow temperature range above freezing (from about

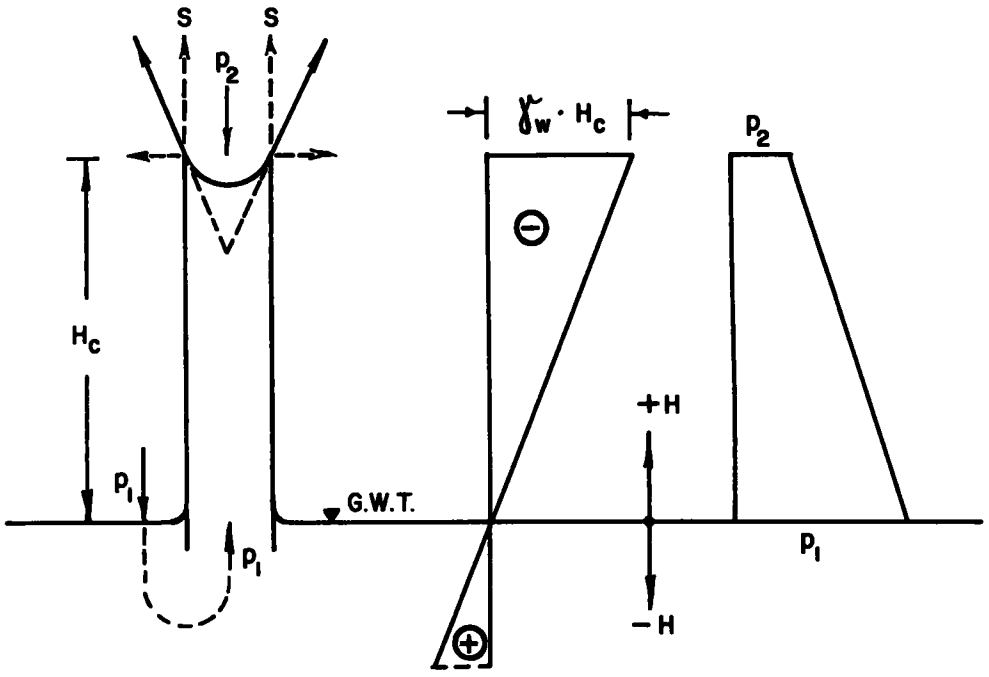

Figure 12. Tension in capillary water.

0 deg C to about 6 deg C to 8 deg C).

Capillary Constant—Referring now back to Equation 23, the quantity $2 \cdot S/\gamma_w$ is customarily termed the capillary constant, and is designated

$$\frac{2 \cdot S}{\gamma_w} = a^2 \qquad \left[cm^2 \right] \cdot \tag{30}$$

Thus, the capillary height H_c in Equation 26 can now be expressed as

$$H_c = a^2 \cdot \frac{1}{r} \qquad \left[cm \right] \tag{31}$$

and the vapor pressure difference based on work considerations as in Equation 23 now is

$$p_1 - p_2 = \frac{2 \cdot S}{\gamma_w} \cdot D_v \cdot \frac{1}{r} = a^2 \cdot D_v \cdot \frac{1}{r} \tag{32}$$

The capillary constants, a^2, are computed and compiled in Column 4, Table 2. The $(p_1 - p_2)$-values are computed as a function of r and are compiled in Column 6, Table 2. From Columns 2 and 4, it can be seen that as the temperature decreases the surface tension and the capillary constants increase. Also, it can be observed that within a temperature range from -5 deg C to +5 deg C the capillary constants vary very little. Therefore an average capillary constant, namely, $a^2 = 0.1545$ cm^2 at 0 deg C can be used in calculating the radius of the meniscus, viz. the radius of an ideal capillary tube (-size of uniform voids in a soil) for different capillary heights, H_c:

TABLE 2

CAPILLARY CONSTANTS AND $(p_1 - p_2)$-VALUES AT DIFFERENT TEMPERATURES

T°C	Surface Tension S g/cm	Water Density γ_w g/cm³	Capillary Constant $a^2 = \frac{2S}{\gamma_w}$ cm	Vapor Density D_v g/cm³	$p_1 - p_2 = a^2 . D_v . \frac{1}{r}$ g/cm²
1	2	3	4	5	6
-5	$*77.91 \cdot 10^{-3}$	0.9992	0.1562	$3.353 . 10^{-6}$	$0.522 \cdot 10^{-6} \cdot \frac{1}{r}$
-4	$77.76 \cdot 10^{-3}$	0.9994	0.1559	$3.615 . 10^{-6}$	$0.562 . 10^{-6} . \frac{1}{r}$
-3	$77.61 \cdot 10^{-3}$	0 9996	0.1556	$3.830 \cdot 10^{-6}$	$0.594 \cdot 10^{-6} \cdot \frac{1}{r}$
-2	$77.45 \cdot 10^{-3}$	0.9997	0.1552	$4.193 \cdot 10^{-6}$	$0.649 \cdot 10^{-6} \cdot \frac{1}{r}$
-1	$77.29 \cdot 10^{-3}$	0.9998	0.1549	$4.513 \cdot 10^{-6}$	$0.697 \cdot 10^{-6} \cdot \frac{1}{r}$
0	$77.13 \cdot 10^{-3}$	0.99986	0.1545^{+}	$4.854 \cdot 10^{-6}$	$0.748 \cdot 10^{-6} \cdot \frac{1}{r}$
1	$76.99 \cdot 10^{-3}$	0.99992	0.1543	$5.222 \cdot 10^{-6}$	$0.803 \cdot 10^{-6} \cdot \frac{1}{r}$
2	$76.83 \cdot 10^{-3}$	0.99996	0.1540	$5.612 \cdot 10^{-6}$	$0.864 \cdot 10^{-6} \cdot \frac{1}{r}$
3	$76.69 \cdot 10^{-3}$	0.99999	0.1536	$6.026 \cdot 10^{-6}$	$0.924 \cdot 10^{-6} \cdot \frac{1}{r}$
4	$76.54 \cdot 10^{-3}$	1.00000	0.1533	$6.467 \cdot 10^{-6}$	$0.989 \cdot 10^{-6} \cdot \frac{1}{r}$
5	$76.40 \cdot 10^{-3}$	0.99999	0.1530	$6.934 \cdot 10^{-6}$	$1.059 \cdot 10^{-6} \cdot \frac{1}{r}$
6	$76.25 \cdot 10^{-3}$	0.99996	0.1527	$7.434 \cdot 10^{-6}$	$1.133 \cdot 10^{-6} \cdot \frac{1}{r}$

+ Values calculated from International Critical Tables

* Average $a^2 = 0.1545$ at 0 deg C

$$r = \frac{a^2}{H_c} = \frac{0.1545}{H_c} \qquad \left[\text{cm} \right] . \tag{33}$$

The "r's" as seen in Table 3, are calculated for capillary pressure differences of H_c = 1 cm, 10 cm, 50 cm, 100 cm, 500 cm and 1,000 cm, respectively.

Pressure Differences—One observes from Table 3 that the vapor pressure differences for each particular capillary pressure difference H_c and at temperatures at or near freezing ($\approx$ 0 deg C) (a condition that pertains to soil freezing and in which we are particularly interested) are very small. In order to have vapor pressure differences of 1.035 g/cm² to 2.06 g/cm² (as we had in the case of vapor diffusion into air) to diffuse 0.0138 g and 0.0276 g per day, we ought to have at about 0 deg C a pressure difference about 1,000 times larger than those at H_c = 250 cm and H_c = 500 cm, respectively, that is to say, we must have a capillary pressure difference of 250,000 cm per cm and 500,000 cm per cm of the thickness, viz. width of the air space, respectively, or 250 m to 500 m per one millimeter, respectively, which would give us a 1.21 g/cm² and 2.42 g/cm² vapor pressure difference, respectively. The values of these would then be approximately equal to 1.035 g/cm² and 2.06 g/cm², respectively.

Diffusion as a Function of S—As the capillary pressure is equal to

$$P_c = \gamma_w \cdot H_c \qquad \left[\frac{g}{cm^2} \right] \tag{34}$$

TABLE 3

RADIUS OF MENISCI, r, IN CM
AS A FUNCTION OF VARIOUS CAPILLARY HEIGHTS
(in cm and inches)

H_c in	cm	1	10	50	100	500	1000
	inches	0.39	3.94	19.70	39.37	196.85	393.70
Radius r		0.1545	0.01545	0.0031	0.001545	0.00031	0.0001545
1		2	3	4	5	6	7
T deg C		*DIFFERENCE IN VAPOR PRESSURE, $p_1 - p_2 = f(S)$, in $\frac{g}{cm^2}$ FOR VARIOUS RADII AND AT DIFFERENT TEMPERATURES					
-5		3.37	33.7	168	337	1685	3370
-4		3.63	36.3	181	363	1815	3630
-3		3.84	38.4	192	384	1920	3840
-2		4.20	42.0	210	420	2100	4200
-1		4.51	45.1	225	451	2255	4510
0		4.84	48.4	242	484	2420	4840
1		5.19	51.9	259	519	2595	5190
2		5.57	55.7	278	557	2785	5570
3		5.98	59.8	299	598	2990	5980
4		6.40	64.0	320	640	3200	6400
5		6.85	68.5	342	685	3425	6850
6		7.46	74.6	373	746	3730	7460

*The $(p_1 - p_2)$ in this table consist of the true $(p_1 - p_2)$-values multiplied by 10^6. To obtain the real $(p_1 - p_2)$-values, multiply the figures in this table by 10^{-6}. For example, $p_1 - p_2 = 6.40 \times 10^{-6} = 0.00000640$ at T = 4 deg C for H_c = 1 cm.

For H_c = 250 cm, $p_1 - p_2 = 1210 \cdot 10^{-6}$ g/cm^2 = 0.00121 g/cm^2.

which at equilibrium is in balance with the difference in vapor pressure $(p_1 - p_2)$ g/cm^2, then, substituting into the diffusion Equation 6 the vapor pressure symbol dp by its equivalent capillary pressure, $H_c \cdot \gamma_w$, obtain the amount of moisture in grams per 86,400 seconds (=24 hours) transferred in the vapor phase:

$$W = -D \cdot A \cdot t \cdot \frac{1}{R \cdot T} \cdot \frac{\gamma_w \cdot H_c}{x} \qquad (6)$$

$$= D \cdot A \cdot t \cdot D_v \cdot \frac{H_c}{x} \qquad \left[g \right], \qquad (35)$$

or

$$W = \left| - (1) \cdot (1) \cdot (86,400) \cdot (0.755) \cdot (10^{-6}) \cdot \frac{H_c}{100 \cdot x} \right|$$

$$= (0.0006696) \cdot \frac{H_c}{x} \qquad \left[g \right] \cdot \qquad (36)$$

Here H_c is now expressed in meters, and x is the width of the air space, which is the diameter of the spherical bubble (=2 · r), in cm.

The small amount of soil moisture diffused in the vapor phase as a function of surface tension is to be interpreted as follows: in order to diffuse 6.7 g/cm of soil moisture during one day, theoretically 1,000 m of capillary pressure would be needed. However, such an immense capillary pressure is practically very rarely available under normal conditions. On the other hand, if the length of the freezing season is to be of 100 days duration, and the capillary pressure H_c = 1 m = 3.28 feet, then the moisture transferred during this time would be 0.067 grams. One sees that the diffused quanti-

ties of soil moisture, considering surface tensions, are really very insignificant. Therefore, it seems that this kind of mechanism for the upward supply of soil moisture toward the freezing ice lenses can be ignored.

Effect of Capillary Radius on Vapor Diffusion—Expressing $\frac{2 \cdot S}{r}$ from Equation 29 obtain

$$\frac{2 \cdot S}{r} = p_v - p_1 + (H_c - h_c)\,\gamma_w \tag{37}$$

It can be observed that the smaller h_c is, the larger is $\frac{2 \cdot S}{r}$, and the smaller is r, in turn. When h_c becomes zero, r is at its minimum.

For these conditions Equation 37 can be rewritten as follows:

$$\frac{2 \cdot S}{r_{min}} = H_c \cdot \gamma_w + p_v - p_1 \tag{38}$$

But

$$H_c \cdot \gamma_w = \frac{2 \cdot S}{r_2} \tag{39}$$

where r_2 is the upper meniscus in the tube, causing the capillary column, the height

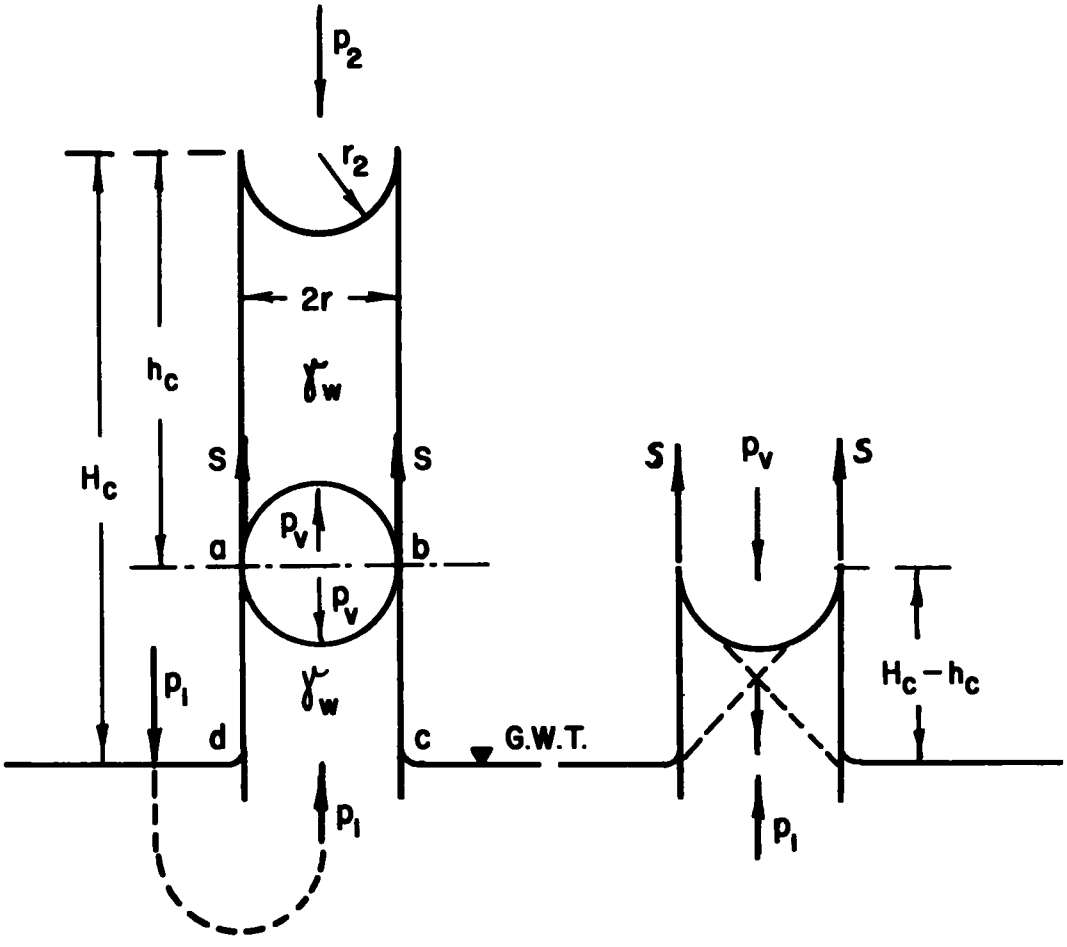

Figure 13. Stresses in capillary water at the position of the bubble.

of which is H_c, to rise. Note that $r_2 \neq r$ (see Fig. 14). Hence Equation 38 can be rewritten as

$$\frac{2 \cdot S}{r_{min}} = \frac{2 \cdot S}{r_2} + p_v - p_1 \quad . \tag{40}$$

From here one sees that

$$\frac{2 \cdot S}{r_{min}} < \frac{2 \cdot S}{r_2} \quad , \tag{41}$$

and therefore

$$r_{min} > r_2 \tag{42}$$

From Equations 40 and 42 we deduce that no matter what the position of the bubble, its radius r_{min} will always be larger than the radius r_2 of the capillary. This requires revision of Figure 9 as now shown in Figure 14.

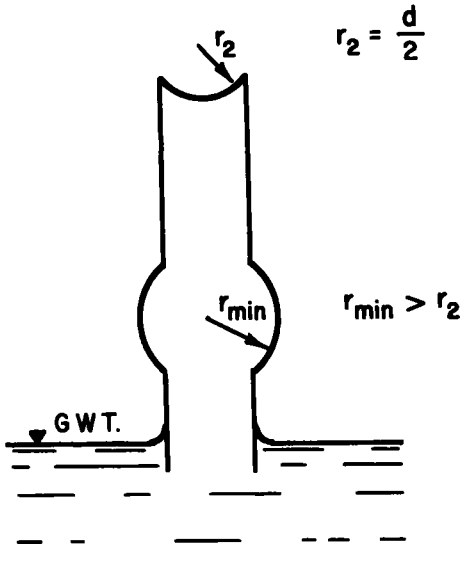

Figure 14. Revision of Figure 9.

Besides, physically r_2 cannot be less than the radius $\frac{d}{2}$ of the capillary tube. These considerations lead to the deduction that formation of aqueous vapor and/or gas in soil is more likely to take place in coarse voids than in fine ones, for example such silty sands, silt, silty clay, clayey silt or clay.

Evaluation of Study

Comparison of Calculated Values with Possible Field Conditions—Variation in soil temperature may cause soil moisture vapor in soil voids to vary in density and pressure. However, as seen from Table 1, as well as from observations, soil temperature below the frozen layer does not vary appreciably. Consequently, vapor pressures during the freezing season are not of great magnitude, nor do they vary appreciably. Vapor diffusion is probably more pronounced in spring and fall, when temperatures change more rapidly.

The intensity of vapor exchange in soil depends upon the texture of the soil. In soils with large sizes of voids (= function of coarse soil particles and loose packing) vapor exchange would take place more intensively than in a soil, the void sizes of which are of very fine dimensions.

Because the most troublesome soils relative to upward migration of soil moisture upon freezing are the fine silty sands, the silts in particular, and the silty clays, all of which can be broadly classified as fine soils, it can be deduced that soil moisture transport in the vapor phase in such soils would be of lesser quantity than in coarse-grained soils.

The amount of soil moisture transferred in the vapor phase upon freezing is indeed very small as compared with the high moisture contents in the frozen soil where groundwater supply for the formation of ice lenses is available. The calculated values here can be taken as the maximum ones. Actually they would be even less if we consider the following.

Upon freezing the downward-progressing freezing surface of the frozen soil is at a

temperature of about 0 deg C = 32 deg F. During a cold snap the temperature at the 0 deg C-isothermal surface of the frozen soil layer drops somewhat below 0 deg C. Under these conditions more ice lenses are formed.

Upon formation of ice latent heat is set free and the temperature at the downward-progressing freezing isothermal surface returns to 0 deg C. Thus during a cold snap the freezing process is a slow one and the increase in frost penetration with depth is relatively small. From what has been said above it can be reasoned that during the seasons of freezing and thawing, temperature variations on the soil or road surface have, practically speaking, little influence on the soil temperature conditions below the 0 deg C-line, which in turn explains the small order of magnitude of the soil moisture diffused in the vapor phase.

Comments—Owing to the small amount of vapor transferred, it seems that for simplicity the factor vapor diffusion within the freezing soil system can be disregarded. Because of some unavoidable uncertainties contained in the fundamental assumptions of the theories as well as in the assumed numerical values for the various coefficients, it seems that in this instance simplicity is of much greater importance than accuracy at the start of our studies of the complex soil-freezing problem. In a simplified theory it is easier to evaluate the practical consequences of various deviations from the assumptions, and then this would permit introducing improvements as our knowledge increases.

CONCLUSIONS

This study considers two cases of soil moisture diffusion in the vapor phase, namely

1. (a) diffusion of vapor to air as a function of temperature differences, i.e., the driving force or vapor pressure difference is a function of temperature variation, $p_1 - p_2 = f(T_1 - T_2)$,
   (b) diffusion across an air space (bubble) in soil water as a function of capillary moisture surface tension, i.e., $p_1 - p_2 = f(S')$.
2. The study brings out the relatively small order of magnitude of the pressure differences when operating with such assumed values, which from experience indicates that they are optimum, reflecting pretty nearly the actual or real conditions.
3. The amounts of soil moisture transferred upward in the vapor phase toward the freezing ice lenses upon freezing can in both cases be considered as very insignificant. Therefore upward vapor transfer in soil upon freezing can be considered as an ineffective mechanism of moisture transport.
4. Moisture diffusion in the vapor phase in soil would take place in soil with larger void sizes rather than with fine void sizes.
5. This study reveals that the assumption made to serve as a basis for the soil freezing experiment, namely, that the upward flow of soil moisture from ground water toward the freezing ice lenses in a frost-susceptible soil takes place virtually unaccompanied by vapor diffusion, can be considered as justified.
6. Other possible transport mechanisms for the upward flow of soil moisture upon freezing should be investigated.

ACKNOWLEDGMENT

This report concerns a phase of the project "Upward Migration of Soil Moisture under Freezing Conditions," NSF Grant 1968. The author wishes to express his appreciation to the National Science Foundation for supporting this research.

REFERENCES

1. A.R. Jumikis, "The Frost Penetration Problem in Highway Engineering," Rutgers University Press, New Brunswick, New Jersey, 1955, p. 111.
2. A.R. Jumikis, "The Soil Freezing Experiment," Paper, presented before the 35th Annual Meeting of the Highway Research Board, Washington, D. C., January, 1956, p. 12.
3. G. Beskow, "Tjälbildningen och Tjälliftningen, Statens Vaginstitut," Stockholm, 1935, p. 9.

4. A.W. Porter, "Surface Tension," Encyclopedia Britannica, Vol. 21, Enclyclopedia Britannica, Inc., Chicago, 1952, p. 597.
5. H. F. Winterkorn, "Appendix C, Earth Environment, ERDL Project Contract No. DA-44-009 Eng. 1773," November 28, 1953, Department of Engineering Research, The Pennsylvania College, College Park, Pennsylvania, p. 185.
6. "International Critical Tables of Numerical Data, Physics, Chemistry and Technology, for the National Research Council of the U.S.A.," McGraw-Hill Book Co., New York, 1928, Vol. III, p. 211.
7. O. Maas and E.W.R. Steacie, "An Introduction to the Principles of Physical Chemistry," John Wiley and Sons, New York, 1931, page 11-20.
8. S. Glasstone, Textbook of Physical Chemistry, 2nd Edition, D. Van Nostrand Company, Inc., New York, 1946, p. 1257.
9. W. Jost, "Diffusion in Solids, Liquids and Gases," Academic Press, Inc., Publishers, New York, 1952, p. 1.
10. G.W.C. Kaye and T.H. Laby, "Tables of Physical and Chemical Constants," Longmans, Green and Co., London, 10th Ed., 1948, p. 47.
11. F.E. Fowle, "Smithsonian Physical Tables," 7th Ed., The Smithsonian Institution, City of Washington, 1920, p. 167.
12. F.H. Macdougal, "Thermodynamics and Chemistry," John Wiley and Sons, Inc., New York, 1926, p. 13.
13. S. Brunauer, "The Absorption of Gases and Vapors," Princeton University Press, Princeton, New Jersey, 1943, p. 120.
14. J.K. Vennard, "Elementary Fluid Mechanics," John Wiley and Sons, New York, 1950, p. 6.

The Effect of Freezing on a Capillary Meniscus

ALFREDS R. JUMIKIS, Professor of Civil Engineering, Rutgers University

● THE PURPOSE OF this article is to describe the effect of freezing on a capillary meniscus as observed in experiments performed at the Soil Mechanics Laboratory, Rutgers University, in pursuing the project "Upward Migration of Soil Moisture under Freezing Conditions," sponsored by the National Science Foundation. Experiments show that upon freezing the capillary meniscus disappears, and the water comes in direct contact with the downward-freezing ice lenses, thus furnishing the evidence for what was hitherto an assumption. This assumption forms a basis on which the project mentioned above partially rests.

Introductory Notes

In designing a soil freezing experiment and the necessary equipment for studying the upward transport of soil moisture upon freezing, it is necessary to make certain assumptions upon which to base the study. Among several assumptions the following one is made:

A growing ice lens is in direct contact with a thin hull or film of soil moisture similar to the adsorbed layers which form on many other solids that are in contact with water, permitting it to move up and supply the necessary moisture for the growth of the ice lenses. The moisture films, in turn, are in direct contact with the ground-water table (1). The question has often arisen as to what is the nature of the driving force for the upward flow of soil moisture upon freezing: is it the open, curved capillary meniscus, concave to its vapor, or is it something else?

The following has been indicated as the objection against the capillary theory: Under actual conditions, one has to assume that if on freezing the frost reaches the capillary meniscus, the lower boundary of the downward-growing frozen layer of soil (= ice lens) is in direct contact with the upper boundary surface (= menisci) of the capillary soil moisture. On the other hand, it is understood that the capillary forces are present only at the time when there are open or free-surface menisci present which form a moisture-air boundary. In other words, at the air-capillary water interface (= meniscus) the capillary water should be in contact with its own vapor. With regard to these two points, it is, therefore, difficult to imagine how a surface of free menisci at the lower ice boundary can exist, and at the same time capillary subpressure for the upward transport of soil moisture upon freezing develop. This inconsistency has been pointed out already by Taber (2, 3, 4).

Purpose of Experiment

From physics, it is known that under non-freezing conditions capillary water in an idealized, vertical capillary tube is in contact with its own vapor. The water and vapor are separated by a concave interface or meniscus relative to vapor. These conditions are illustrated in Figure 1.

However, very little is known as to what happens to the meniscus when frost penetrates the ground downwards, reaches the meniscus and passes by it. In other words, it is interesting to know, as illustrated in Figure 2 (a), whether the concavely curved meniscus under freezing conditions still exists, which would mean that between the downward-freezing ice layer or lens and the water in the capillary there is a space, probably occupied by aqueous vapor, or, as was assumed for the basis of study and as is illustrated in Figure 2 (b), the water is in direct contact with the downward-freezing ice lenses.

In order to learn what happens to a capillary meniscus or water-vapor interface upon freezing and to examine and verify the validity of the assumption that the soil moisture films are in direct contact with the freezing ice lenses, appropriate laboratory experiments were improvised.

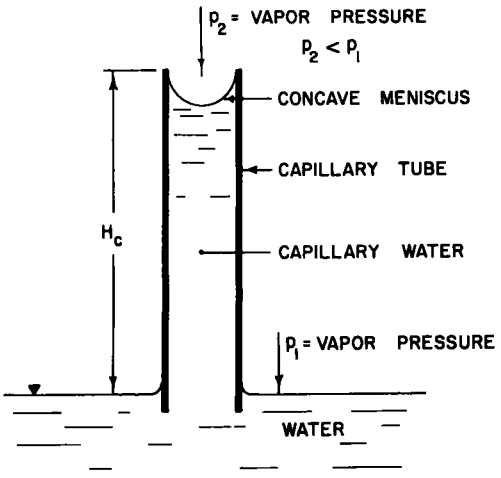

Figure 1. Water-vapor interface.

Method of Experiments

The method which has been used in these improvised experiments consists of freezing distilled water in a verticle capillary tube and observing by means of optical magnification the changes in shape a capillary meniscus undergoes under freezing conditions, and fixing the changes photographically (5).

Apparatus

The principle of the apparatus used in these experiments is shown in Figure 3. A capillary tube of pyrex glass of 1 mm I.D. was immersed in distilled water. The capillary height was observed to be H_c = 11.0 mm. The meniscus was kept at the upper end of the tube, upon which a container of dry ice was placed. This situation approximately corresponds to conditions in the field, the walls of the tube and the bottom of the container simulating the frozen mineral particles of the soil.

The dry ice had to be kept in a container because when a fragment of dry ice was placed directly at the upper end of the tube, the developing gas forced the meniscus vigorously down, and such a condition simply does not duplicate the phenomenon in the field. The use of ordinary ice was too time-consuming. The temperatures of the water and the environment of the upper end of the tube were measured by means of thermistors and a Wheatstone bridge. The changes in the meniscus upon freezing were observed by means of a 35 mm reflex camera with a lens attachment which magnified the object to be observed about twice. Also, by means of this camera photos of the menisci were taken.

As can be understood from this description, the apparatus seems to be relatively simple. However, the preparation of the meniscus specimen and the work of experimentation and observation are very tedious, cumbersome, time-consuming, and require much patience.

Observations

The experiments on the effect of freezing on a capillary meniscus permitted very

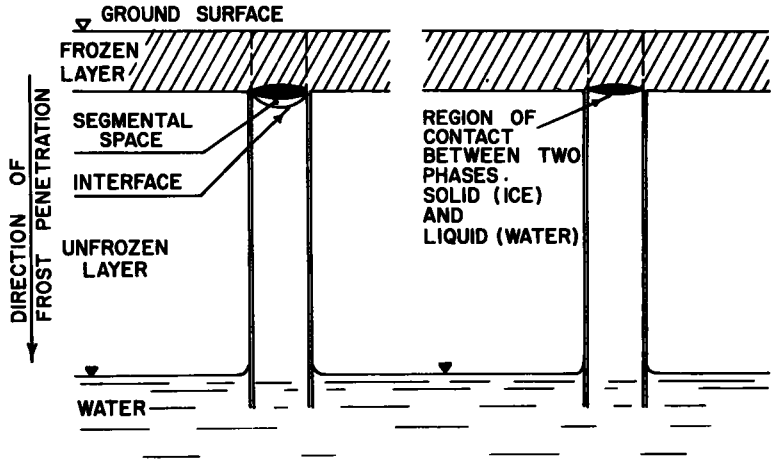

Figure 2. Ice-vapor and ice-water interfaces.

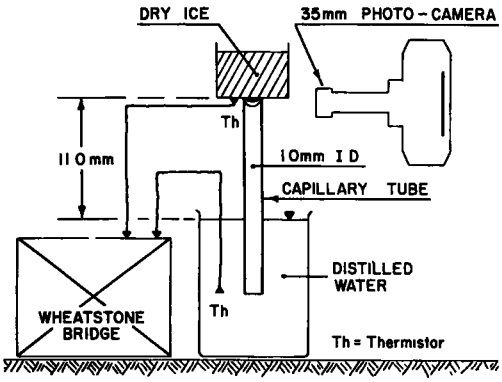

Figure 3. Apparatus.

clear observation of the following phenomena: After commencement of freezing of the meniscus in the direction of the inner part of the tube by placing the ice container, the outside bottom of which was covered with a thin sheet of clean ice, in contact with the upper end of the vertical glass tube, the meniscus flattens out, becomes shallower, narrower, decreases concentrically in size toward the center of the tube, and finally disappears entirely. Thus a direct contact between the ice and water is established as shown in Figure 2 (b), and the water is no longer in contact with its own vapor.

The stages of disappearance of the meniscus upon freezing are illustrated in Figure 4. This phenomenon takes place in one gradual, smooth, continuous process, and within a time of approximately 20 to 30 seconds, depending on the environmental temperature conditions around the meniscus. Also, the time depends upon whether the outside bottom of the ice container, which is covered with thin, clean ice, is covered with snow or not. In observing the disappearance of the meniscus one gets the impression that there exists some kind of a central, effective force lifting the meniscus and the water underneath the meniscus up and attaching the water flush to the ice lenses of the cold outside bottom of the ice container. Thus, the meniscus is no longer present, nor is there a segmental space between the ice container and the water in the tube (Fig. 5). Upon the lifting up of the water and attachment of the latter to the ice-covered bottom of the ice container no interruption of the water column in the tube was observed. This indicates that the amount of water which upon freezing is lifted up and attached to the freezing ice lenses is replenished in the glass tube or capillary from the beaker, viz., ground water. Continuing freezing, the water in the tube freezes, appearing opaque in color. The ice freezes and expands downward, i.e., in the direction of the least resistance. No heave could develop because of the weight of the ice container. To prevent supercooling the water the capillary was occasionally tapped (this simulated vibrations induced on roads by traffic). However, the disappearance of the meniscus upon freezing also took place without tapping the tube and without any noticeable difference in time as compared with tapping.

Discussion of Observations

The observations made in these experiments seem to indicate that whatever amount of moisture in the form of vapor there might have been on the concavely curved meniscus at the moment of commencement of freezing, all that moisture was frozen to form a direct contact between the capillary water and ice lenses. The swift lifting up of the meniscus and its direct attachment to freezing ice indicates that the vapor pressure over the curved meniscus (or water-vapor interface) is neutralized and the meniscus destroyed. Thus, upon freezing, the solid phase (= ice) replaces the vapor phase, and, as there is no meniscus nor any segmental space above the meniscus present, there is also no vapor pressure present, i.e., $p_2 = 0$. Hence, after the replacement of the vapor phase by ice, it seems practically that the capillary presupposition that capillary water is in contact with its own

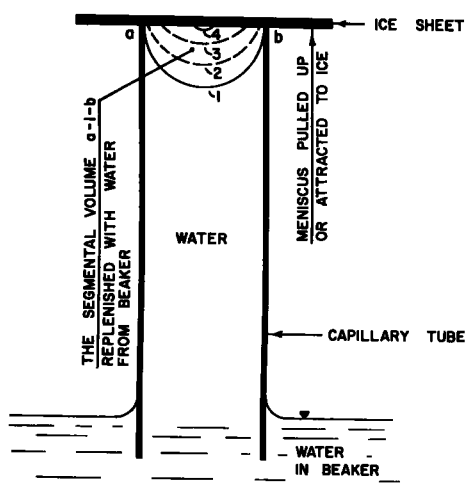

Figure 4. Stages of disappearance of meniscus upon freezing.

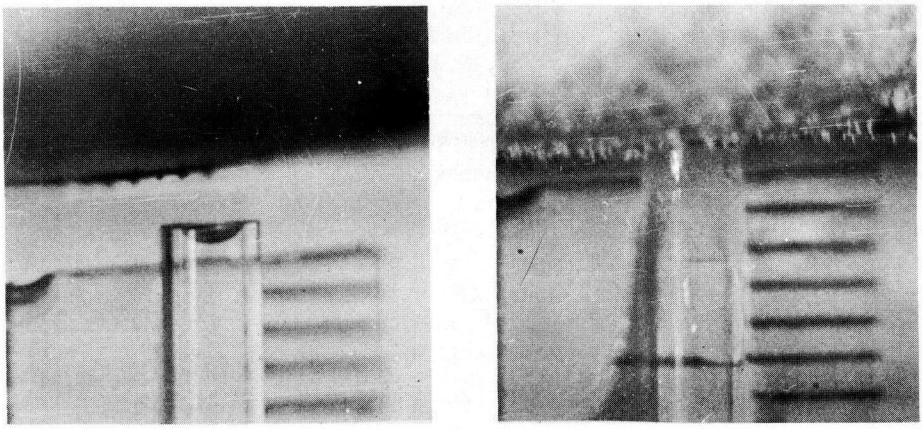

Figure 5. Action of freezing on a meniscus, showing (a) meniscus upon commencement of freezing and (b) water in direct contact with ice lenses.

vapor (which is true under non-freezing conditions) no longer holds. We must, therefore, assume (after freezing causes the transition from the vapor phase to ice) that for freezing conditions there exists a different concept of the mechanism of the driving force for the upward supply of soil moisture from the ground water to the downward-freezing ice lenses.

That water from a water reservoir (ground water), located at some distance below the downward-freezing soil layer, is being sucked up or, better said, moved upward is evidenced experimentally in a soil freezing experiment by the loss of water from a burette to the soil under controlled conditions and by the increase in the amount of water in the experimental freezing soil sample over the original moisture content present when the soil sample was prepared for the freezing experiment.

CONCLUSIONS

Although the freezing process by means of dry ice is an accelerated one, it is believed that it reflects pretty truthfully the stages of disappearance of the menisci.

The observations made in these experiments are valuable because they (a) throw light on what really happens to the meniscus in the region of contact between the water-vapor interface upon freezing; and (b) verify the soundness of the theoretical assumption made which, among other assumptions, forms the basis for the theoretical-experimental research on the upward migration of soil moisture upon freezing; (c) in particular, the results of these simple experiments establish the fact that upon freezing the upward-transported soil moisture is in direct contact with the downward-freezing ice lenses.

The research work on the upward migration of soil moisture upon freezing is being continued.

ACKNOWLEDGMENT

The effect of freezing on a capillary meniscus as reported in this article constitutes a phase within the scope of the research project "Upward Migration of Soil Moisture under Freezing Conditions" sponsored by the National Science Foundation.

Joseph D. Sage, Research Assistant in Civil Engineering, Rutgers University, performed with great patience the experiments relative to changes of menisci upon freezing.

REFERENCES

1. A. R. Jumikis, "The Soil Freezing Experiment," presented before the Highway Research Board at its 35th Annual Meeting, January, 1956, Washington, D. C.

2. S. Taber, "Frost Heaving," Journal of Geology, July-August, 1929, Vol. 37, No. 4, University of Chicago Press.

3. S. Taber, "The Mechanics of Frost Heaving," Journal of Geology, May-June,

1930, Vol. 38, No. 4, University of Chicago Press.

4. A.R. Jumikis, The Frost Penetration Problem in Highway Engineering, Rutgers University Press, 1955, New Brunswick, N.J.

5. J.D. Sage and A.R. Jumikis, Project NSFG 1968, Upward Migration of Soil Moisture under Freezing Conditions, "Investigations on the Effects of Freezing Temperatures on the Capillary Menisci of Water in Glass Tubes," Progress Report No. 4, June, 1956, Rutgers University, New Brunswick, N.J.

DISCUSSION

WILLIAM S. HOUSEL, Professor of Civil Engineering, University of Michigan, Ann Arbor, Mich., and Research Consultant, Michigan State Highway Department — This paper brings up the most intriguing subject of a mechanism for describing capillary phenomena and the forces which may be involved in the formation of a capillary meniscus. The growth of frost plates and the forces involved in the flow of capillary moisture to the freezing surface, which are discussed by Penner (1) and Gold (2) may be explained in several ways, depending largely on a matter of viewpoint or perhaps a matter of definition. On the other hand, this may be referring to the matter under discussion too casually, as the description of any physical phenomenon in anything but the most realistic terms may lead away from the truth. A theory has been most aptly defined as a logical description of the results of observation; so, after all, the validity of any theory will ultimately depend on the terms which have been used to describe the phenomenon under consideration, and whether these terms represent fact or fiction. The ingenious experiments conducted by Professor Jumikis may prove to be a valuable contribution in that they serve to demonstrate more clearly the real mechanism involved in capillarity.

For almost twenty years the writer has been trying without too much success to call attention to the misconceptions in the traditional concepts of capillarity (3, 4) and the confusion they have caused in soil mechanics. A substitute mechanism has been suggested which avoids the inconsistencies involved in surface tension as the basic concept. The suggested substitute postulates a fixed volume of water proportional to the maximum area under the meniscus, with the supporting reaction supplied by the internal pressure in the liquid. The necessary pressure differential to sustain a column of water in a capillary tube, or to cause capillary movement of moisture, originates in the molecular attraction of the solid surface. The forces involved are transmitted by the combined interaction of molecular attraction and repulsion in the liquid, and their action does not require a gas-liquid interface, vapor pressure, or other attributes peculiar to the capillary meniscus. The capillary potential of any combination of solid and liquid may be measured as an integrated boundary effect and expressed quantitatively as a fixed volume or weight of liquid per unit length of wetted perimeter. The dimensional properties of the capillary channels can then be conveniently evaluated in terms of their perimeter-area ratio (5, 6).

The explanation of the behavior of the capillary column in terms of surface tension and the capillary meniscus with the differential vapor pressure seems strained and unrealistic when it is considered that the analogy of surface tension cannot be stretched to imply that the water-gas interface or boundary of the meniscus is a tensile membrane attached to the freezing surface. Actually, physical chemists declare that there is no structural continuity in this surface and the molecules in the interface are free to migrate in and out of the surface even though they are acted upon by molecular forces of attraction as well as forces of repulsion. Although Professor Jumikis indicates some of the inconsistencies which have been generally recognized, he seems to have difficulty in freeing himself from the assumptions of surface tension outlined in his introductory statement. At one point he states: "It is understood that the capillary forces are present only at the time when there are open or free-surface menisci present which form a moisture-air boundary." Later he speaks of the lifting up of the meniscus and its direct attachment to the freezing ice, following which the meniscus is destroyed and water from some distance below is sucked up to maintain the continuity of the capillary column of water. He then states that, "We must, therefore, assume . . . that for

freezing conditions there exists a different concept of the mechanism of the driving force for the upward supply of soil moisture from the ground water to the downward-freezing ice lenses."

This statement appears to be as far as the author was prepared to venture in departing from the traditional description of capillary flow in terms of surface tension. He has suggested no basic mechanism to take its place, although he recognizes the need for one. In the writer's attempt to explain these phenomena, the effort has been made to think in terms of both molecular attraction and repulsion as forces acting on the molecules. In so doing, it frequently seems to be more realistic to explain capillary movement of moisture in terms of pressure differentials as a push rather than a pull. Formulating a mechanism to explain frost plate formation provides an excellent example to illustrate the use of internal pressure rather than the mythical surface tension as the driving force.

Molecular repulsion is associated with the kinetic energy of the molecules, the forces which cause them to push about generating internal pressure in the liquid. At the beginning of the author's experiment, when the temperature begins to decrease, the kinetic energy of the molecules in the vicinity of the freezing zone is correspondingly decreased. The result is to create a pressure differential with respect to the main body of water which increases the capillary height and moves the column of water toward the ice lens. When molecules reach the freezing surface, the attractive forces exerted by the solid ice neutralize correspondingly greater amounts of molecular repulsion. This decreases the mobility of the molecules and causes a sharp drop in the kinetic energy of the molecules and the pressure which they exert in the liquid phase. This pressure drop causes a more marked pressure differential within the liquid and the water column is drawn quickly into contact with the freezing surface. It may be pertinent to note that this pressure differential remains long after the meniscus has disappeared and the water column continues to feed the growing ice plate. At no time in such a sequence of events is there any necessity for surface tension, the fictitious membrane which it implies, adsorbed layers of the wall of the capillary to serve as channels for the water to flow to the ice lens, or a pressure differential across the gas-liquid interface which inconveniently disappears as the experiment concludes.

REFERENCES

1. Penner, Edward, "Soil Moisture Tensions and Ice Segregation." Paper presented at 36th Annual Meeting, Highway Research Board, Washington, D. C. (Jan. 1957).

2. Gold, Lorne W., "A Possible Force Mechanism Associated with the Freezing of Water in Porous Materials." Paper presented at 36th Annual Meeting, Highway Research Board, Washington, D. C. (Jan. 1957).

3. Housel, W. S., "The Shearing Resistance of Soil, Its Measurement and Practical Significance." Proc. A. S. T. M., Vol. 39 (1939).

4. Housel, W. S., "Applied Soil Mechanics, Part I, Soil as an Engineering Material." Edwards Brothers, Ann Arbor, Mich. First Edition (1948).

5. Housel, W. S., "Misconceptions in the Use of Surface Tension Capillarity." Proc. Highway Research Board, Vol. 30, p. 465 (1950).

6. Housel, W. S., "Applied Soil Mechanics, Part I, Soil as an Engineering Material." Edwards Brothers, Ann Arbor, Mich. (1956).

ALFREDS R. JUMIKIS, Closure — Professor Housel's comment that the validity of any theory will untimately depend on the terms which are used to describe the phenomenon under consideration is quite pertinent. In this connection it suggests that in the progress in frost action research in soils sometimes several terms are used to designate one and the same thing; for example, driving force, driving pressure, pressure deficiency, subpressure, suction force, moisture tension, and other concepts. It seems that a point has been reached where revisions and definitions of the various concepts are in order. The discusser's comments strengthen this point indirectly.

In his third paragraph Professor Housel cites the sentence: ". . . It is understood that the capillary forces are present only at the time when there are open or free-

surface menisci present which form a moisture-air boundary" as a source of argument, without apparently fully appreciating the spirit of the corresponding part of the original text. At the end of the pertinent paragraph of the original article it is mentioned that a certain inconsistency has been pointed out already by Taber. The logical content of the matter is that in the original article, before describing observations from experiments there were presented at the beginning some concepts from the capillary theory under nonfreezing conditions in an open capillary tube (not voids nor capillaries in soil).

The object of the author's article is solely to report on the experiments; not to suggest any new basic mechanism to take the place of the capillary, or any other theory. In this respect, the title of the article seems to be satisfactorily limiting through inclusion of the words "Capillary Meniscus."

However, the following point of Professor Housel's discussion is in agreement with the author's view; namely, that "when the temperature begins to decrease, the kinetic energy of the molecules in the vicinity of the freezing zone is correspondingly decreased. The result is to create a pressure differential with respect to the main body of water toward the ice lens."

Because the ice lenses are coated with a film of water, under certain packing conditions of soil the ice lenses are connected, via the moisture films, with the ground water.

Study of Subsurface Temperature in Six Soils During the Winter of 1953 - 1954

HERBERT L. LOBDELL, Soils Engineer, Greer Engineering Associates,[1]
KENNETH A. TURNER, JR., Assistant Research Specialist in Instrumentation, and
ALFREDS R. JUMIKIS, Professor of Civil Engineering, Rutgers University

During the winter of 1953-54 subsurface temperature measurements were performed on six New Jersey soils. The studies revealed that:

1. Granular, non-plastic soils are better conductors of heat (and cold) than fine-grained soils and react to air temperature changes more quickly. Of the six soils studied, a clean sand (MRB A-3), was the best conductor and an MRB A-7-6 soil was the poorest conductor. Therefore, frost enters and goes out of granular soils more rapidly than in the case of fine-grained soils, causing more frequent freeze and complete thaw cycles.
2. A concrete slab is a better conductor of heat than soil of the same thickness. Therefore, freezing and complete thaw cycles occur more often below a concrete slab or pavement than in the adjacent shoulder.
3. A combination of a concrete slab over a granular soil is one that reacts most quickly to cold and warm spells. A shoulder of fine-grained soil shows little reaction to cold and warm spells (except at the surface) and reflects the over-all intensity of cold of the winter.
4. The freezing line generally penetrates to a greater depth in granular soils than in fine-grained soils.
5. There is a lag between the minimum air temperature of winter and the maximum penetration of the 32 degree line. In the cases studied the lag was one day, except for some of the shoulders of fine-grained soils, where the lag was several days.
6. Maximum heaving does not necessarily occur at the time of the maximum depth of the 32 degree line.
7. Most thawing in soil occurs from the top downward during thaw periods; however, some thawing takes place from the bottom.
8. Temperature studies indicate the necessity of measuring and knowing the surface temperature of the slab or ground surface.

● DURING the winter of 1953-54 subsurface temperature measurements were performed on six New Jersey Soils which were also being used for the purpose of frost heave and bearing-power loss studies. These soils had been compacted in 9 ft square pits and were topped by 4 ft square by 6 in. thick concrete slabs. Soil temperatures were measured at two inch intervals of depth under the centers of the slabs and in the adjoining shoulders.

INSTRUMENTATION

Thermistors

In order to measure subsurface soil temperatures some type of remote reading device was desirable. Type 17-A thermistors, obtained from the Western Electric Co., were selected. This type of thermistor is composed of an alloy of nickel oxide and manganese oxide. The material has a high negative temperature coefficient of electrical resistance. For example, as the temperature of a 17-A thermistor drops from 35 F to 25 F its electrical resistance increases from 3,150 to 4,250 ohms.

A 17-A Thermistor consists of a 3/16 in. diameter by a 1/32 in. thick disc having short wire leads soldered to each face. These leads were soldered to 20-strand plastic-covered wire used to conduct the thermistor circuits to the soil surface. The ther-

[1] Formerly Research Assistant in Civil Engineering, Rutgers University.

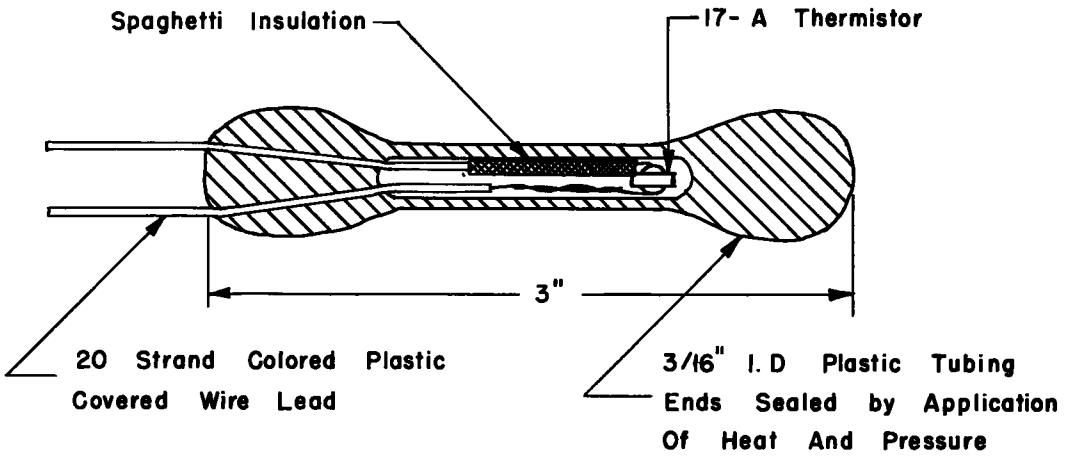

Figure 1. Section through a sealed thermistor unit.

mistors and underground connections were sealed within short lengths of plastic tubing (Figure 1). The thermistors were arranged in groups, spaced at proper intervals, and the wires cabled together.

Calibration

Figure 2 shows the standard temperature-resistance curve for 17-A thermistors. Manufacturing control of the thermistor material is such that all thermistors will have characteristics within ± 10 percent of the standard curve.

The thermistors were immersed, one group at a time, in an insulated tank of cir-

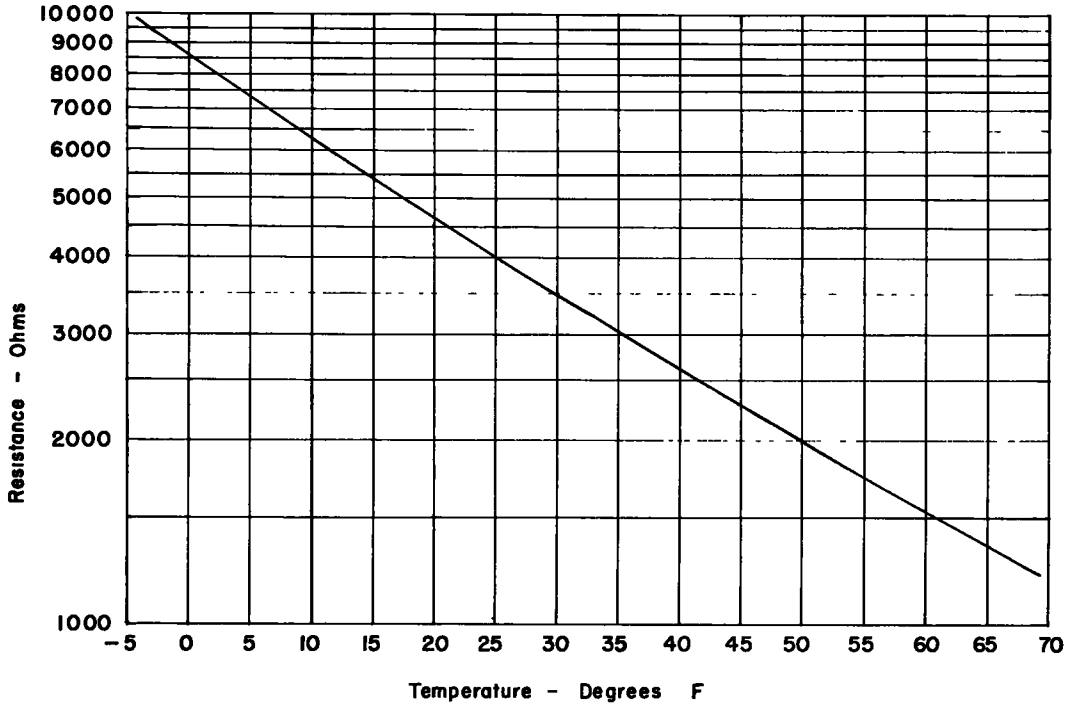

Figure 2. Standard temperature-resistance curve for 17-A thermistor.

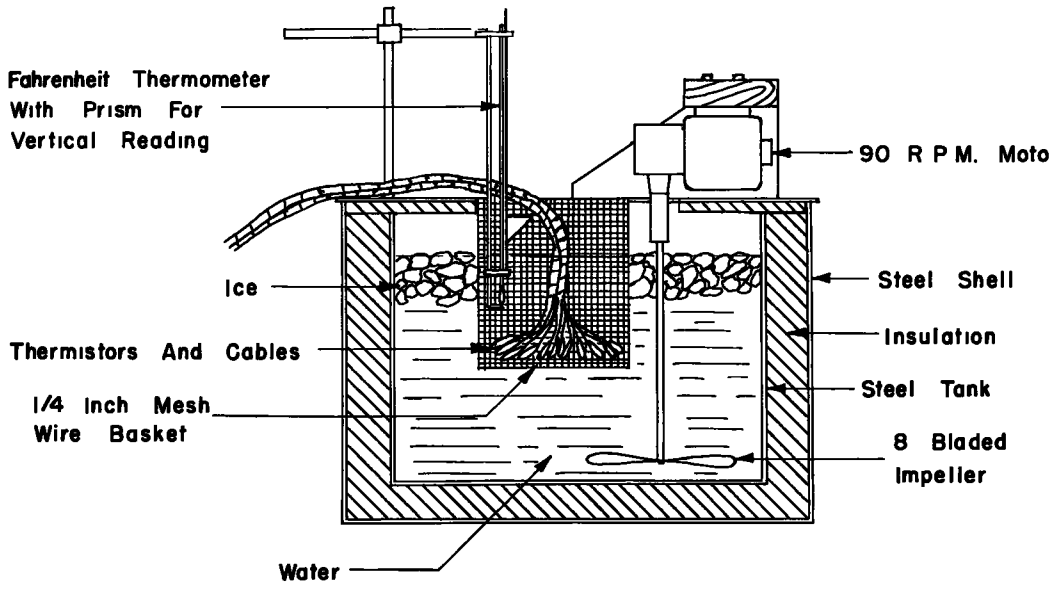

Figure 3. Thermistor calibration tank.

culating ice water at a temperature of 32 F (Figure 3). The resistance of each thermistor was then measured with a Wheatstone Bridge. A coefficient was determined for each thermistor by dividing the standard resistance at 32 F by the measured resistance.

Field Installation

The thermistor groups were installed at proper depths in 8 in. diameter auger holes at the center of the slab location and in the shoulder of each of the selected soils. The concrete slabs were then poured. A section of a completed installation is shown in Figure 4.

From the junction box at each installation underground multi-wire cables carried the thermistor circuits to an instrument shack. The cable resistance was measured and found to be negligible. Rotary selector switches, mounted conveniently on an instrument panel, were used to connect each thermistor individually to a Wheatstone

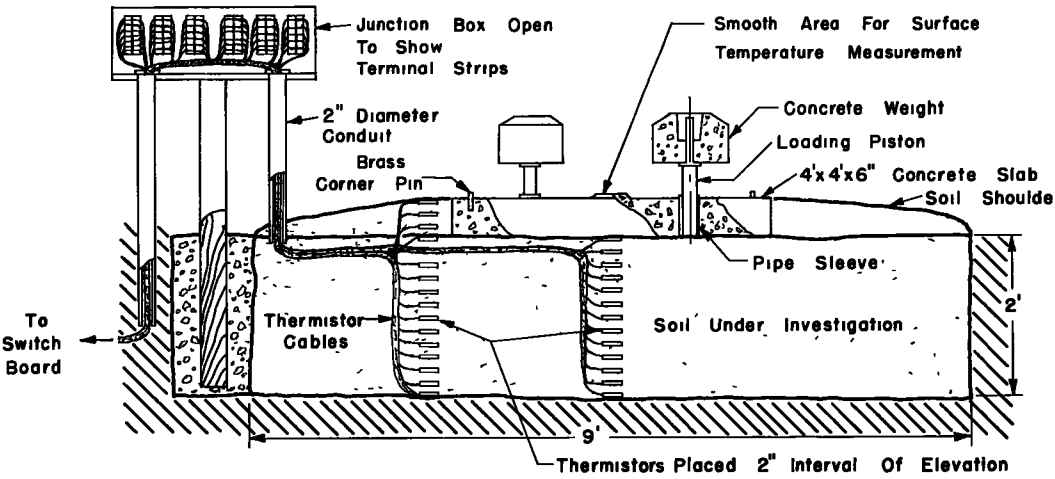

Figure 4. Field Installation.

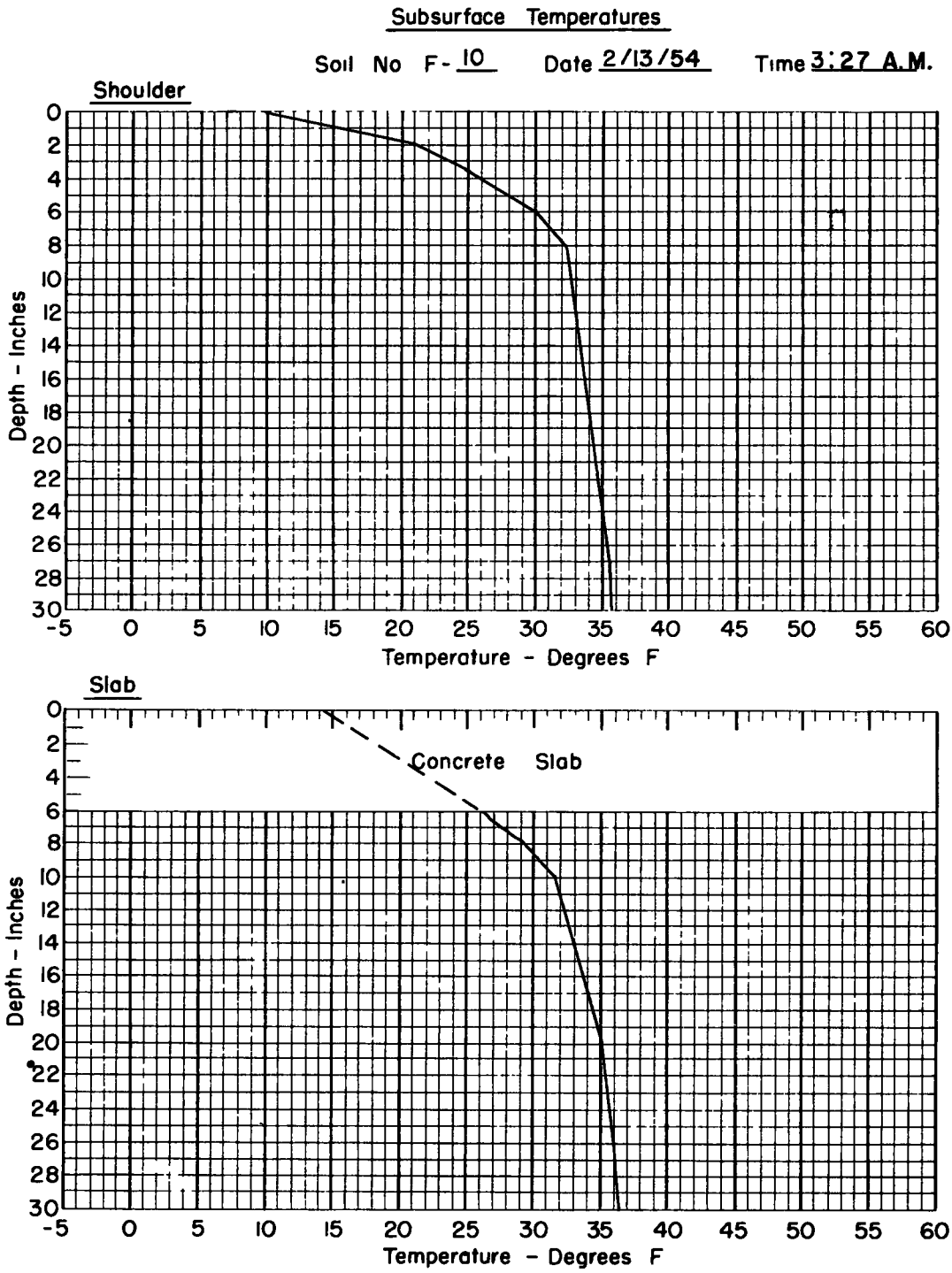

Figure 5. Subsurface temperature curves.

Bridge. When measuring thermistor resistance an optical galvanometer was used with the Wheatstone Bridge for ease in balancing.

Temperature Determination

From the standard temperature-resistance curve a table was prepared showing resistance ranges in ohms for each tenth of a deg F increment. The measured thermistor resistances were recorded on prepared data sheets. Standard resistances were determined by multiplying each measured resistance by the respective thermistor coefficient. Each thermistor temperature was then obtained from the table.

Slab surface temperatures were measured with a mercury thermometer. The thermometer was inserted in a small metal can filled with mercury and insulated against air temperature on the sides and top. The assembly was placed on prepared smooth areas at the center of each slab and left until the mercury attained the same temperature as the slab surface.

Temperatures of each soil were plotted as shown in Figure 5.

Air temperature measurements were made at a central location. Maximum-minimum thermometers were mounted on a post at elevations of 1 ft and 6 ft above the soil surface. The existing air temperatures were recorded at the time thermistor readings were made. Daily maximum and minimum temperatures were also recorded. A recording thermograph was mounted on the post at a 3 ft elevation. This instrument produced a continuous air temperature record.

SUBSURFACE TEMPERATURE STUDIES

General Notes

This study is based on subsurface thermistor readings in six soil installations in which readings were taken daily during the winter between December 31, 1953 and February 26, 1954, and between March 1 and March 9, 1954. Readings were taken four or more times a day during the periods January 12 to 14 and January 22 to February 17, 1954.

The six soils studied vary in type, ranging from a gravelly sand to a silty clay. The six soils with the Highway Research Board Classification and Atterberg limits for each are listed in Table 1.

TABLE 1

Soil Installation	HRB Classification	Liquid Limit	Plasticity Index	Fall 1953 Dry Density Lbs. Per Cu. Ft.
F-10	A-1-b	Non-Liquid	Non-Plastic	116
F-17	A-3	Non-Liquid	Non-Plastic	105
F-5	A-5	41	7	94
F-13	A-2-4	32	9	106
F-15	A-7-6	41	15	80
F-24	A-4	31	9	98

Figure 6 shows the grain size distribution curves for these six soils.

Graphs were plotted during periods of frequent thermistor readings of:

1. Temperature at 2 in. intervals of depth against time (temperature oscillation graphs), and
2. Isotherms against time, in which air and subsurface isotherms for 4 F intervals were plotted.

TOPICS COVERED IN STUDY

1. Time of minimum air temperature, maximum penetration of 32 deg line, and maximum slab heave.
2. Freeze and complete thaw periods between December 31, 1953 and February 17, 1954.
3. Trend of 32 deg line during cold spells.
4. Observations from temperature oscillation graphs.

Time of Minimum Air Temperature, Maximum Penetration of 32 deg Line and Maximum Slab Heave

Notes: All depths in this report are referred to slab or shoulder surfaces. Maximum heave in this report is defined as the maximum elevation to which a slab heaved about an original elevation which was assumed to be at zero at the start of the winter.

The minimum air temperatures of the winter were recorded four days apart, on January 14 and January 18. The minimum air temperatures at the 1 ft elevations were -5.5 deg and -11.0 F on January 14, and -6.0 F and -10.4 F on January 18.

The maximum penetrations of the 32 deg line and the date on which they occurred for each installation are listed in Table 2. There is also listed the heave of each slab at that time.

In all cases except the shoulders of F-13, F-15 and F-24, there was a one-day lag between the time of the low air temperature of January 18 and the time of the maximum depth of the 32 deg line. The date of the maximum depth of the 32 deg line for the shoulders mentioned (F-13, F-15, F-24), it was noted, was much later, which indicates a slower reaction to air temperature.

There was a snow cover of a few inches on the shoulders on January 19 and 20 remaining from the snow storm of January 11. The snow had been removed from the slabs so as to simulate highway conditions. It was difficult to evaluate the insulating effect of the snow cover because the maximum depth of the 32 deg line occurred at this time (January 19, 20) in three of the shoulders (F-10, F-17, F-5) and at a later time in the other shoulders (F-13, F-24, F-15). The snow cover probably was not deep enough to act as an effective insulator at this time.

The maximum heaves recorded for the slabs during the winter and the dates at which they occurred are listed in Table 3. The depth of the 32 deg line at these dates is also listed. Graphs showing slab movement throughout the winter are shown in Figure 7.

It was noted there was an interval of many days (6 to 14 days) between the date of

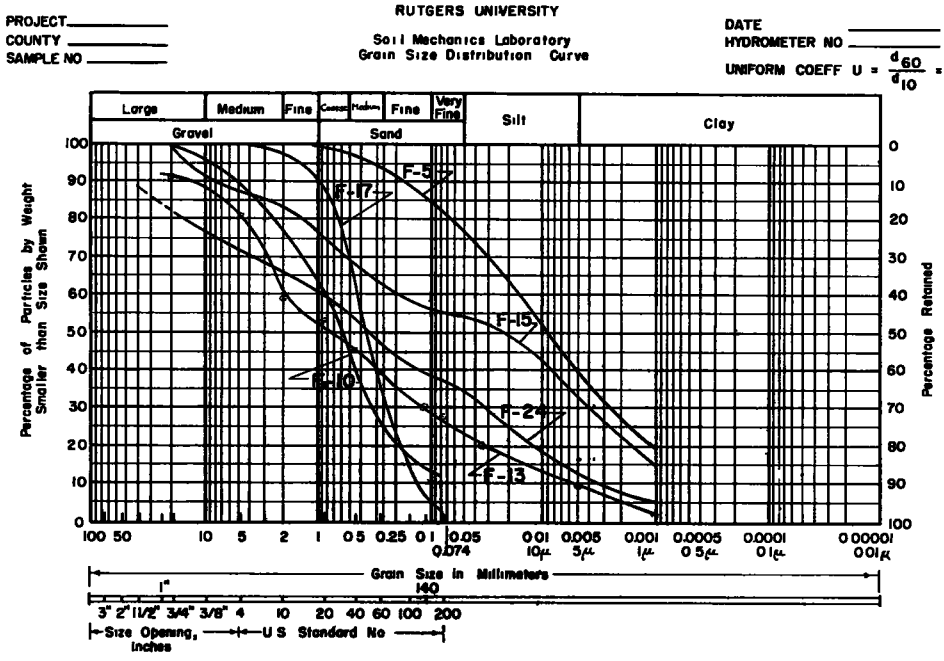

Figure 6. Grain size distribution curves of soils used for subsurface temperature measurements.

TABLE 2

Installation	Max. Depth of 32 deg Line	Date	Slab Heave
F-10 Slab	17.8 in.	Jan. 19	0.013 ft
F-10 Shoulder	15.8 in.	Jan. 19	
F-17 Slab	16.8 in.	Jan. 19	
F-17 Shoulder	10.0 in.	Jan. 19	0.012 ft
F-5 Slab	15.5 in.	Jan. 19	0.023 ft
F-5 Shoulder	12.1 in.	Jan. 19, 20	
F-13 Slab	14.5 in.	Jan. 19	0.020 ft
F-13 Shoulder	11.0 in.	Feb. 2	
F-15 Slab	13.8 in.	Jan. 19	0.036 ft
F-15 Shoulder	13.5 in.	Jan. 24	
F-24 Slab	12.0 in.	Jan. 19	0.064 ft
F-24 Shoulder	9.5 in.	Feb. 1, Feb. 14	

maximum penetration of the 32 deg line and the date of maximum heaving. Also, the depth of the 32 deg line at the time of maximum heaving was less than the maximum had been.

Increased moisture content in the soil installations is believed to be the reason that maximum heaving occurred at a later time than when the depth of the 32 deg line was a maximum. Examination of the weather records indicates that this is probably true because prior to January 19 (the date of maximum depth of the 32 deg line) little moisture could have entered the ground as a result of precipitation. Very little precipitation

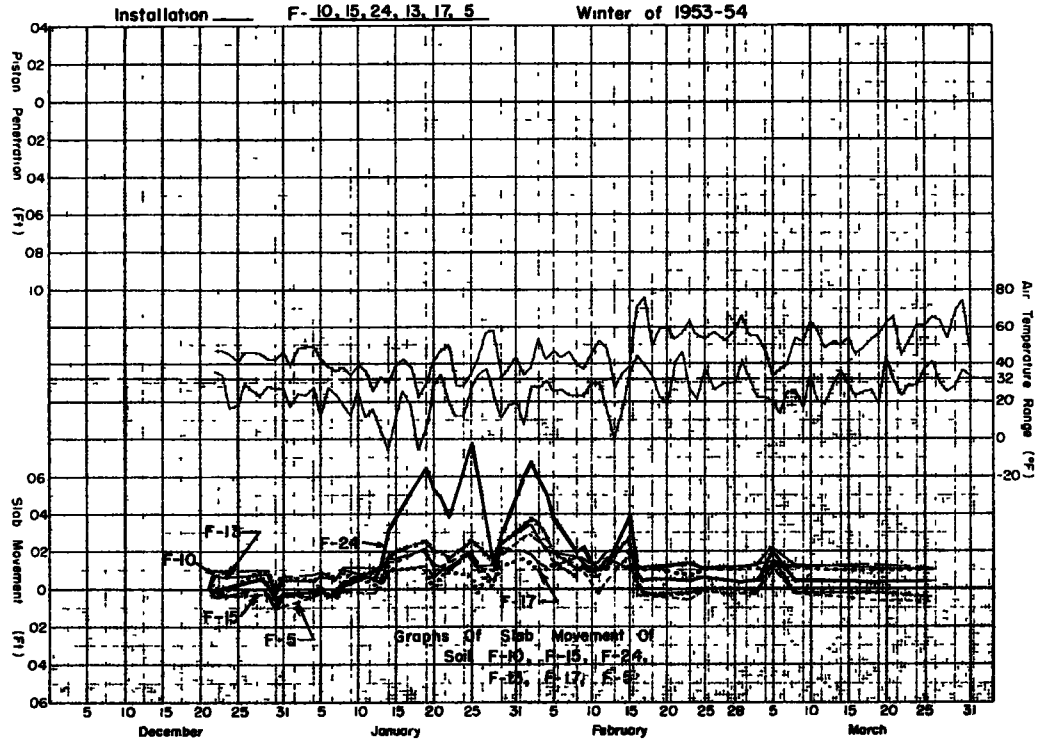

Figure 7.

occurred prior to January19 except the snow storm of January 11, and that remained largely unmelted. After January 19 (between January 20 and January 22) the snow melted and thus increased the moisture content of the soil installations. Because moisture is essential for the growth of ice lenses which cause heaving, it seems reasonable to assume that an increase in moisture content would result in an increase in heaving.

The maximum heave of F-24 Slab of 0.076 ft, incidentally, was the greatest heave measured of all thirty soil installations on which level readings were taken during the winter.

TABLE 3

Installation	Max. Heave	Date	Depth of 32 deg Line
F-10 Slab	0.023 in.	Jan. 29	10.0 in.
F-17 Slab	0.016 in.	Feb. 1	9.5 in.
F-5 Slab	0.032 in.	Feb. 2	12.0 in.
F-13 Slab	0.034 in.	Feb. 2	9.0 in.
F-15 Slab	0.047 in.	Feb. 2	10.5 in.
F-24 Slab	0.076 in.	Jan. 25	11.0 in.

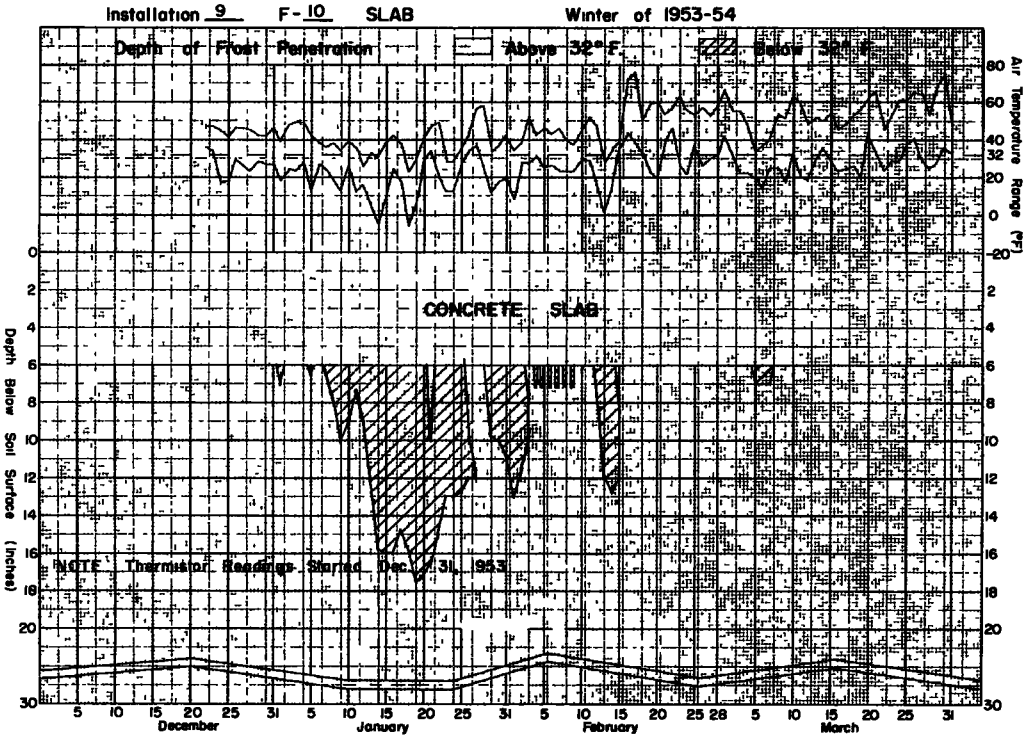

Figure 8.

Freeze and Complete Thaw Periods Between December 31, 1953 and February 15, 1954

December 31, 1953 was the date of the first thermistor readings and February 15, 1954 was the beginning of a general thaw period that caused all frost to come out of the ground. By complete thaw period, it is meant that the 32 deg line was completely above the ground.

The installations and a brief account of the freeze and complete thaw periods for each during this period, are as follows:

F-10 Slab—The 32 deg line entered the ground steadily on January 7 and remained in until February 3 except for one brief thaw. Between February 3 and February 12, the 32 deg line entered the ground only at night.

F-10 Shoulder—There were two brief complete thaws during the period.

F-17 Slab—The 32 deg line entered ground steadily on January 7 and remained in until February 3 except for one brief thaw. Between February 5 and February 9, the 32 deg line entered the ground only at night.

F-17 Shoulder—There were four complete thaws between December 31 and February 4. The 32 deg line entered the ground only at night between February 4 and February 11.

F-5 Slab—The 32 deg line entered the ground steadily on January 7 and remained in until the end of the period except for one brief thaw.

F-5 Shoulder—The 32 deg line remained below ground during the entire period.

F-13 Slab—The 32 deg line entered the ground steadily January 7, and except for one complete thaw remained in until February 6. Between February 6 and February 11, the 32 deg line entered the ground only at night.

F-13 Shoulder—The 32 deg line remained below ground during the entire period.

F-15 Slab—The 32 deg line penetrated the ground steadily on January 8 and remained in until the end of the period except for two complete thaws.

F-15 Shoulder—The 32 deg line remained below ground during the entire period.

F-24 Slab—The 32 deg line entered the ground steadily on January 8 and remained in until the end of the period except for one brief thaw.

F-24 Shoulder—The 32 deg line remained below ground during the entire period except for one brief thaw.

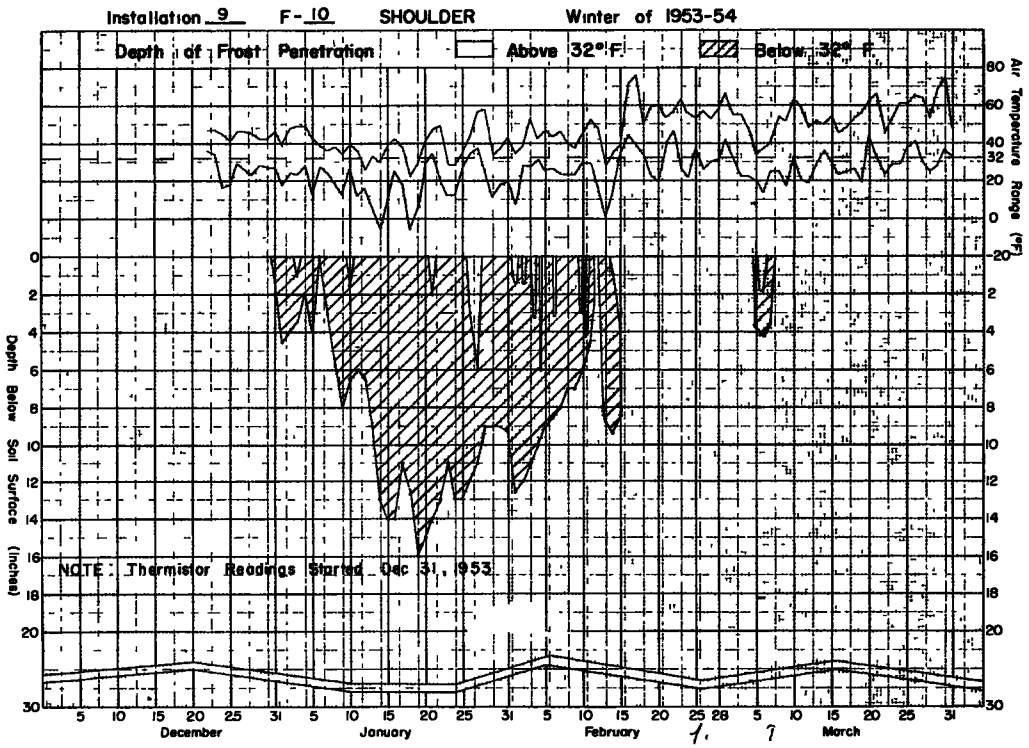

Figure 9.

Figures 8 through 19 are frost penetration curves for the winter based on daily morning readings which also illustrate the freeze and complete thaw periods.

A study of the freeze and complete thaw periods indicates that the slabs of F-17, F-10

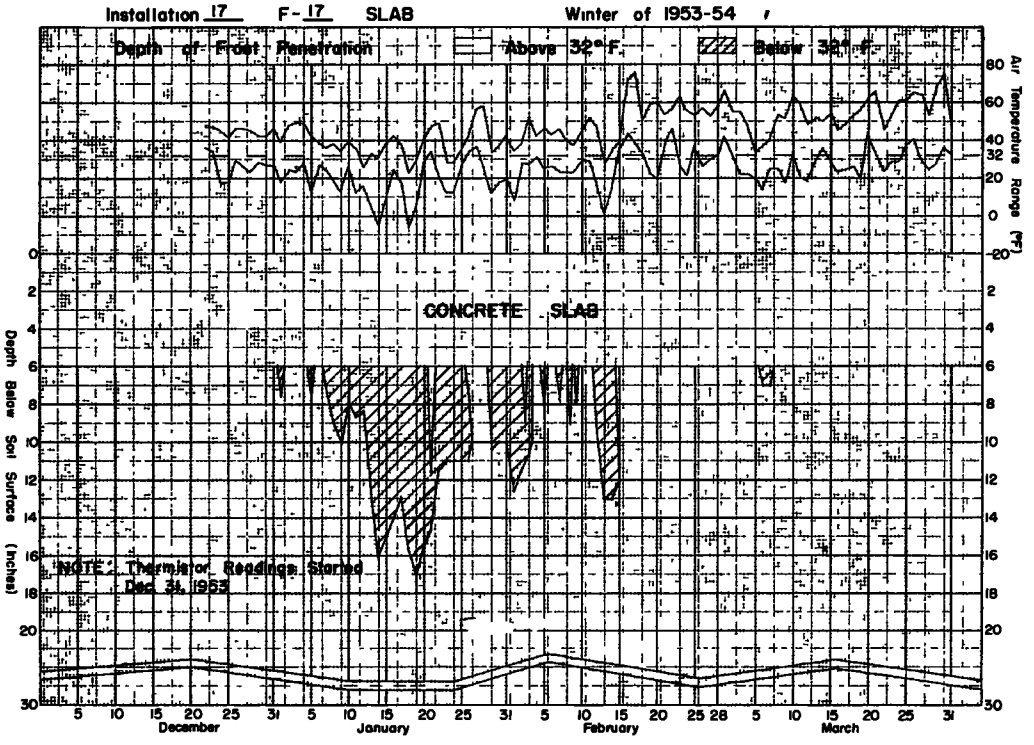

Figure 10.

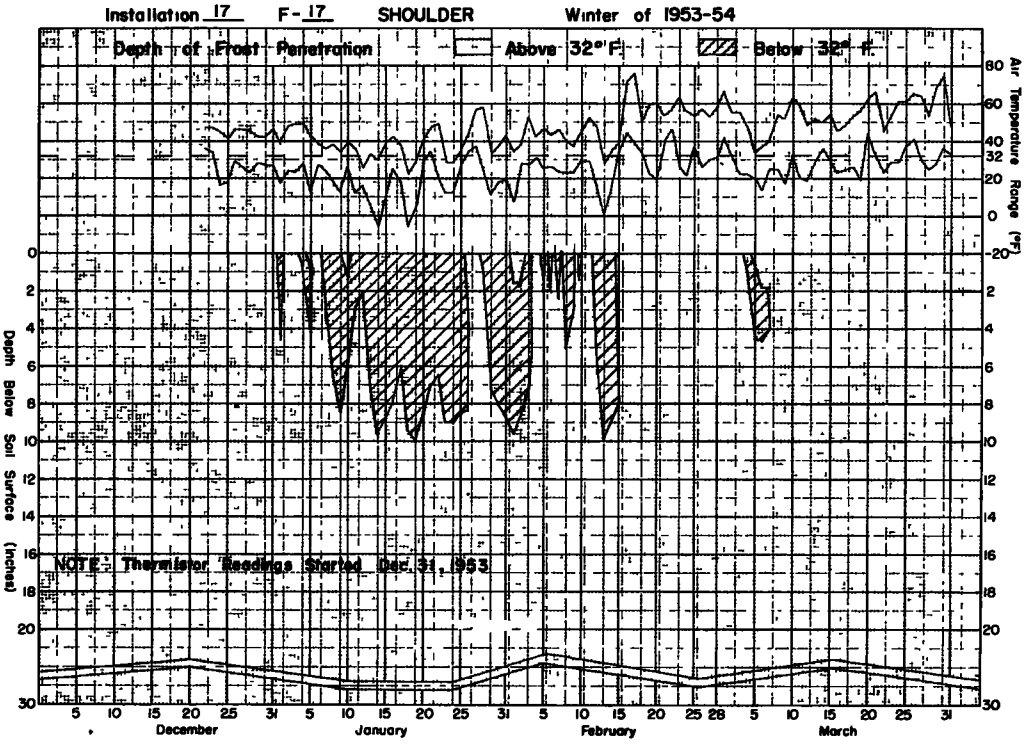

Figure 11.

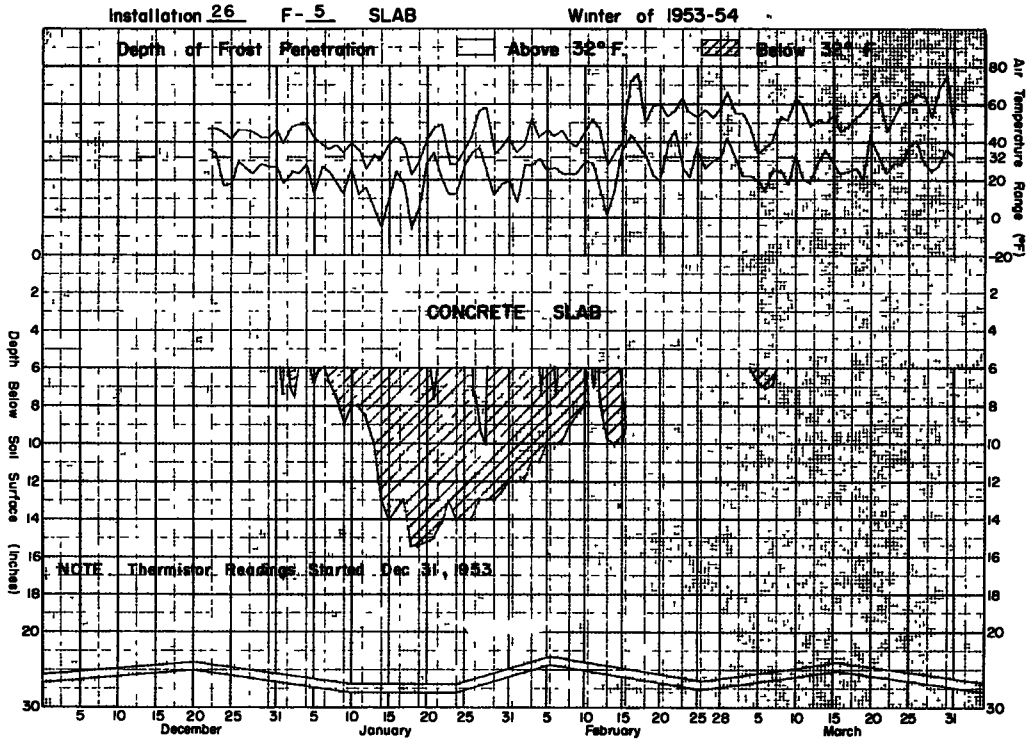

Figure 12.

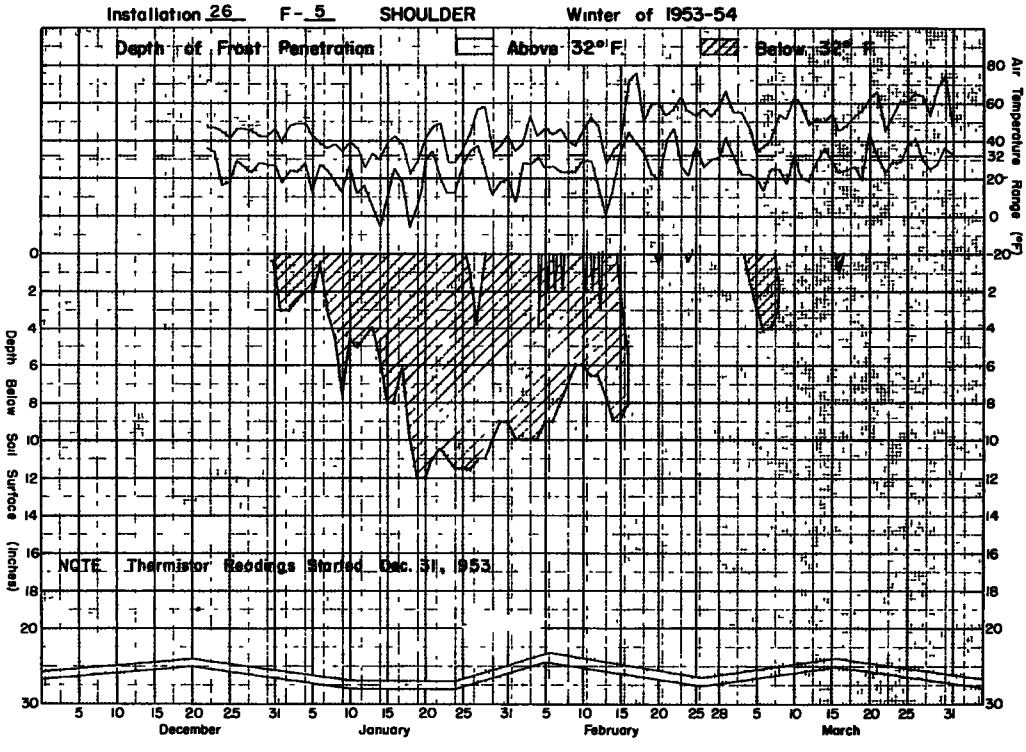

Figure 13.

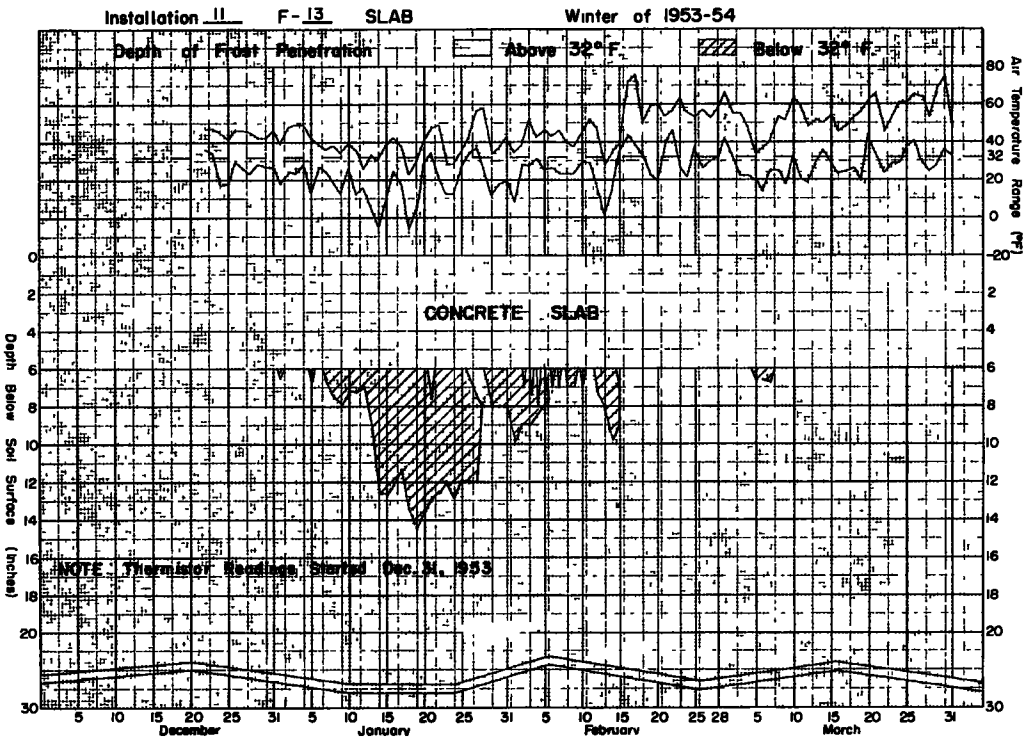

Figure 14.

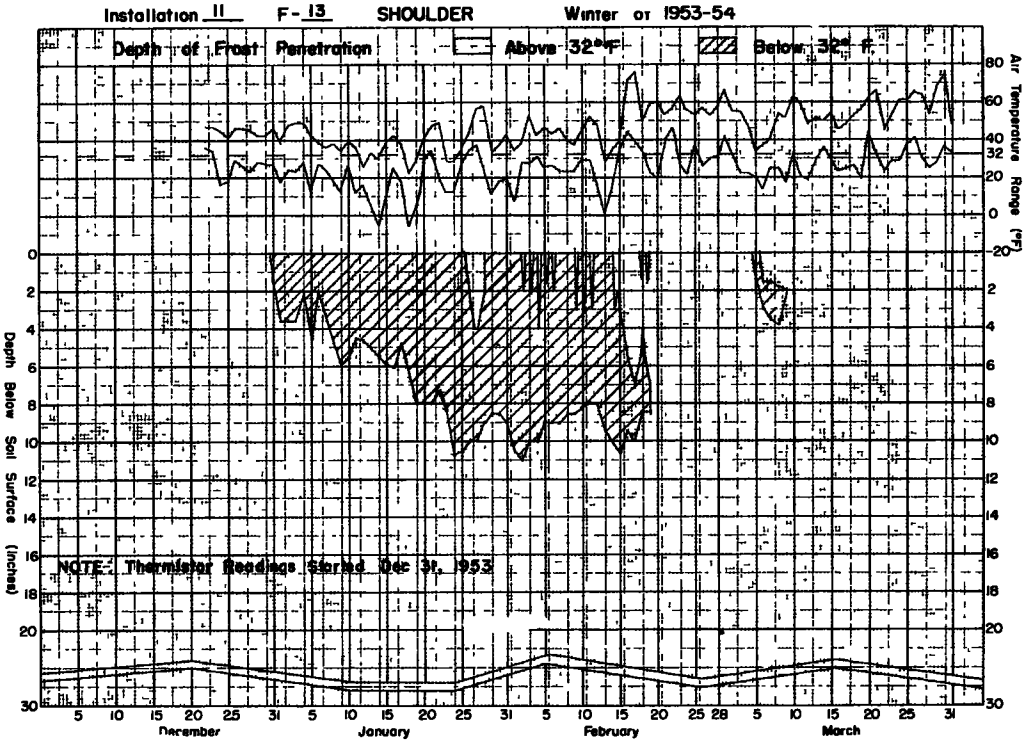

Figure 15.

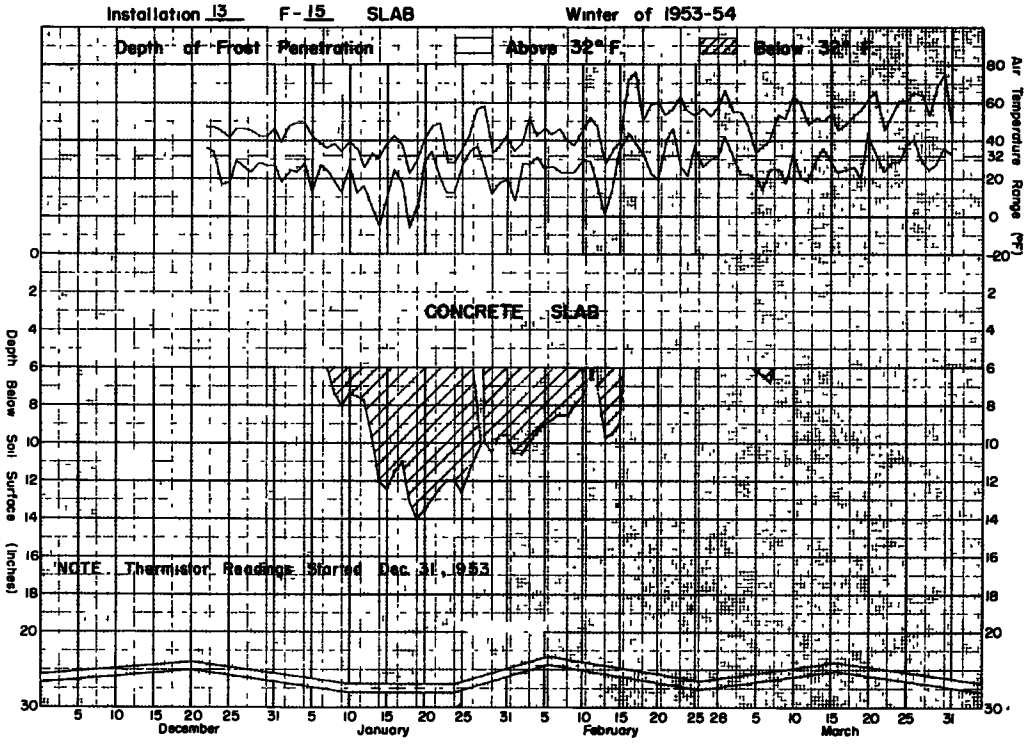

Figure 16.

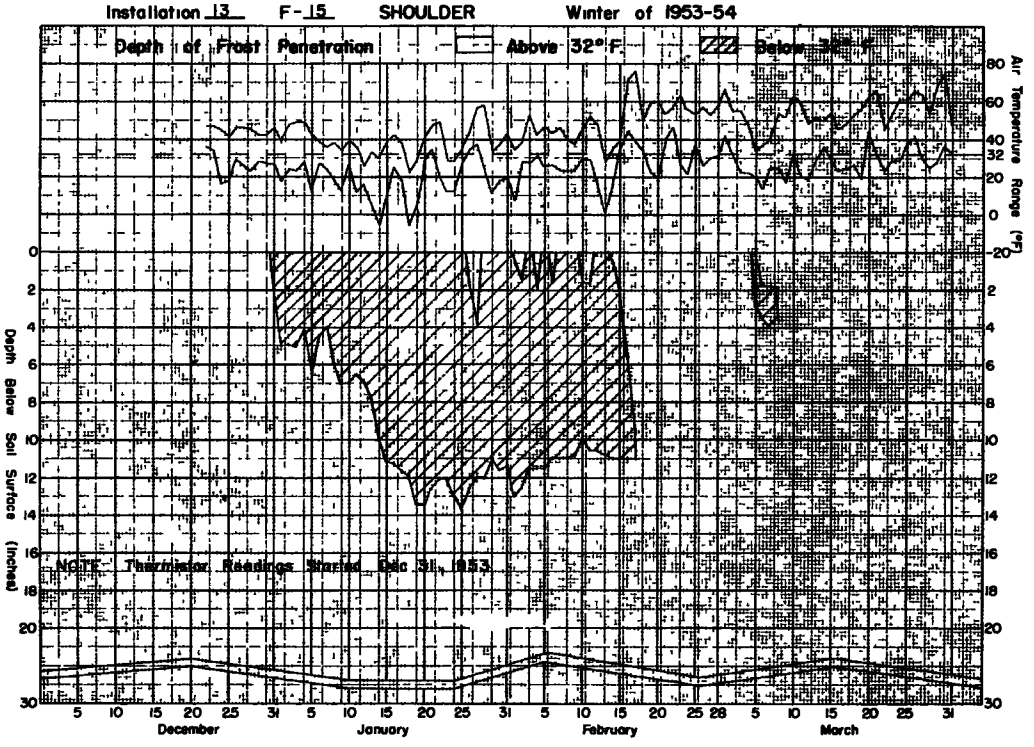

Figure 17.

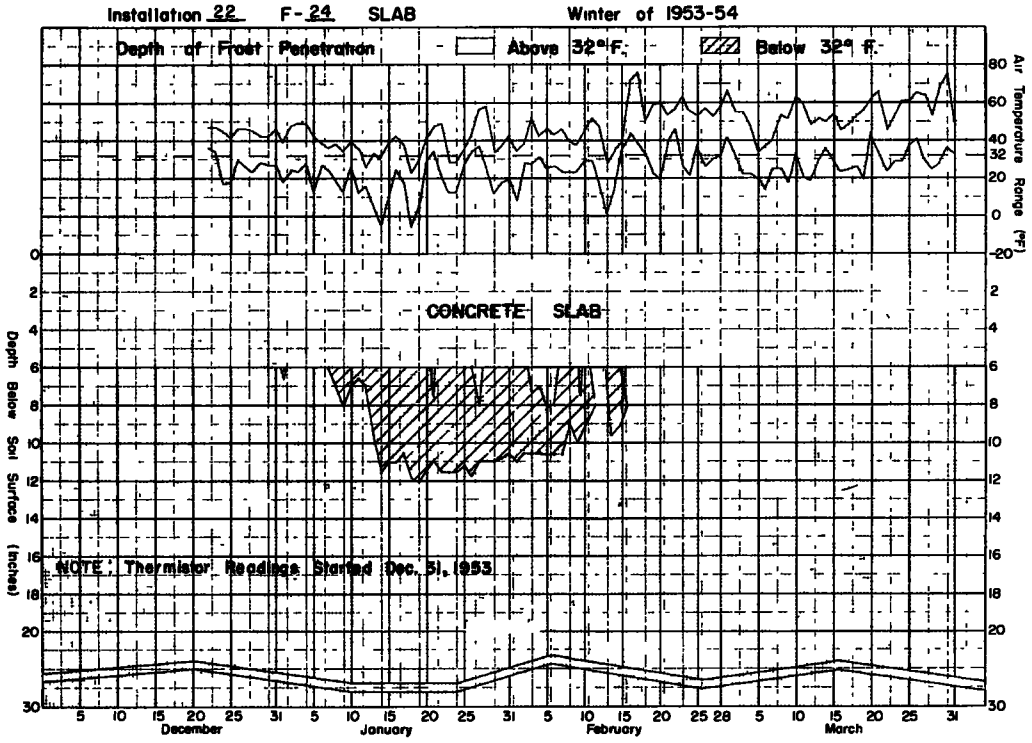

Figure 18.

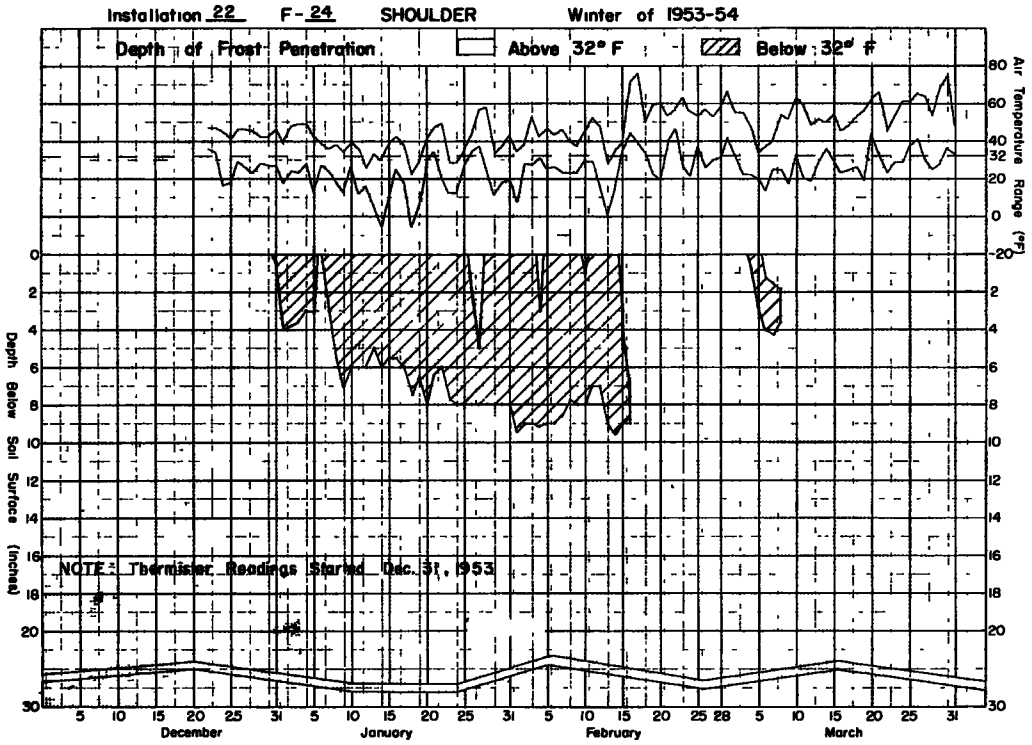

Figure 19.

and F-13 showed similar characteristics in that thawing occurred frequently in the latter part of the period while at the same time the slabs of F-15, F-5 and F-24 maintained below-freezing temperatures. In the shoulders, F-17 showed a rapid reaction to air temperatures, resulting in frequent freeze and complete thaw cycles. The other five shoulders showed a much greater capacity for retaining below-freezing temperatures, particularly F-13, F-5 and F-15, which maintained below-freezing temperatures throughout the entire period of December 31 to February 15.

In the early part of the period (December 31 to January 7) the frost did not penetrate the ground beneath the slabs steadily, while at the same time the shoulders were frozen to a depth of 3 to 5 in. Apparently the 32 deg line was at some level in the slab but not deep enough to penetrate steadily into the ground beneath it.

Trend of 32 deg Line During Cold Spells

Between December 31, 1953 and February 15, 1954, there were five cold spells (periods when air temperatures were below freezing for most of the time) and frequent thermistor readings were taken in all but the January 18-19 cold spell. The cold spells during which frequent readings were taken with the depth of the 32 deg at the start and at the end of the cold spells for each installation are listed in Tables 4, 5, 6 and 7.

TABLE 4

JANUARY 12 TO JANUARY 14 COLD SPELL

Installation	Depth of 32 deg Line, Inches		Change, Inches
	Start	End	
F-10 Slab	9.0	15.9	-6.9
F-10 Shoulder	6.8	13.5	-6.7
F-17 Slab	8.5	15.0	-6.5
F-17 Shoulder	2.0	9.5	-7.5
F-5 Slab	9.0	13.5	-4.5
F-5 Shoulder	4.5	6.5	-2.0
F-13 Slab	7.0	12.8	-5.8
F-13 Shoulder	4.5	5.5	-1.0
F-15 Slab	7.5	12.5	-5.0
F-15 Shoulder	7.0	10.5	-3.5
F-24 Slab	7.0	11.5	-4.5
F-24 Shoulder	5.5	5.5	0.0

It can be noted that there was a greater penetration of the 32 deg line in the granular soils F-10 and F-17 than in the other installations. In F-10 and F-17 the penetration in shoulders and slabs were about the same while in the other finer-grained soils, penetration was greater beneath the slabs.

The 32 deg line depth during the cold spell shown in Table 5 also reflects somewhat the effects of the cold spell on January 18-19, which was a colder period. The rise in F-10 is probably due to a comparative warming after the January 18-19 cold spell. The lowering of the 32 deg line in the shoulders of the other installations indicates a greater lag behind the same spell. At the same time there was practically no change in the slabs of these other installations.

Table 6 shows that all shoulders but F-17 were frozen at the start of the period, which again illustrates the inability of F-17 to retain below freezing temperatures. In contrast, it is seen that both shoulders and slabs of F-5 and F-24 remained frozen throughout.

Table 7 highlights characteristics in the installations that were observed earlier, which are (a) greater changes occur beneath the slabs than in the shoulders; (b) the granular soils F-17 and F-10 react much more quickly to air temperature changes

TABLE 5

JANUARY 22 TO JANUARY 24 COLD SPELL

Installation	Depth of 32 deg Line, Inches		Change, Inches
	Start	End	
F-10 Slab	15.0	13.0	+2.0
F-10 Shoulder	13.5	13.0	+0.5
F-17 Slab	11.5	11.5	0.0
F-17 Shoulder	6.5	9.0	-4.0
F-5 Slab	14.0	14.0	0.0
F-5 Shoulder	10.0	11.9	-1.9
F-13 Slab	12.5	12.5	0.0
F-13 Shoulder	7.0	11.0	-4.0
F-15 Slab	12.5	12.0	+0.5
F-15 Shoulder	11.5	13.5	-2.0
F-24 Slab	11.4	11.5	-0.1
F-24 Shoulder	6.0	8.0	-2.0

than the other four soils (it can be seen that the shoulders of F-5, F-13, F-15 and F-24 retained below-freezing temperatures throughout the period); (c) the 32 deg line penetrates deeper in the F-17 and F-10 than in the other soils.

The 32 deg line entered the soil of installations F-17 and F-10 very quickly with the beginning of the cold spell and also came out quickly with the beginning of the warm spell.

The soil below the slabs of F-24, F-15, F-5 and F-13 was not frozen at the start of the period but the shoulders were frozen to a depth of 6.5 to 11 inches. The 32 deg line reached about the same depth beneath the slabs as in the shoulders of these four installations (F-24, F-15, F-5 and F-13) during the cold spell but came out much more quickly with the warm spell. The shoulders of these four installations did not thaw out completely until one to three days after the soil beneath the slabs thawed out. It

TABLE 6

JANUARY 28 TO FEBRUARY 1 COLD SPELL

Installation	Depth of 32 deg Line, Inches		Change, Inches
	Start	End	
F-10 Slab	0	13.0	-13.0
F-10 Shoulder	10.5	13.0	- 2.5
F-17 Slab	0	12.5	-12.5
F-17 Shoulder	0	9.5	- 9.5
F-5 Slab	13.0	13.0	0.0
F-5 Shoulder	10.5	10.0	+ 0.5
F-13 Slab	0	10.0	-10.0
F-13 Shoulder	9.0	10.5	- 1.5
F-15 Slab	0	10.5	-10.5
F-15 Shoulder	12.0	13.0	- 1.0
F-24 Slab	11.0	10.8	+ 0.2
F-24 Shoulder	8.0	9.5	- 1.5

TABLE 7

FEBRUARY 11 TO FEBRUARY 14 COLD SPELL

Installation	Depth of 32 deg Line, Inches		Change, Inches
	Start	End	
F-10 Slab	0	12.7	-12.7
F-10 Shoulder	0	9.5	- 9.5
F-17 Slab	0	13.0	-13.0
F-17 Shoulder	0	9.0	- 9.0
F-5 Slab	0	10.0	-10.0
F-5 Shoulder	6.5	10.0	- 3.5
F-13 Slab	0	9.0	- 9.0
F-13 Shoulder	8	10.5	- 2.5
F-15 Slab	0	9.5	- 9.5
F-15 Shoulder	11.0	11.0	0.0
F-24 Slab	0	9.5	- 9.5
F-24 Shoulder	7.0	9.5	- 2.5

can be seen a thin lens of soil remained frozen in F-13 shoulder about two days after the other shoulders were completely thawed.

It was noted that with this sudden thaw period, most thawing of the soils was from the top downward.

Observations from Temperature Oscillation Graphs

The soils F-17 and F-10 showed a marked difference from the other soils throughout the winter because they reacted to air temperature changes much more quickly. Lower temperatures also penetrated deeper in these two soils, causing a smaller temperature gradient with depth. Of the two, F-17 reacted more rapidly than F-10 to air temperature changes.

In comparing the finer-grained soils F-5, F-24, F-13 and F-15, it was found that lower temperatures penetrated deeper in F-5 and F-24 than in F-13 and F-15, with a corresponding lower temperature gradient with depth. Of all six soils studied, F-15 showed the least reaction to air temperature changes.

There was a period in February during which the daily variation in temperature was quite uniform. There was a daily variation in temperature in F-17 to a depth of about 18 in. to 22 in. and in F-10 to a depth of about 10 in. to 18 in. and that there was a lag of about 4 to 6 hours behind the air temperature. In the other four soils there was little or no change in temperatures except to 8 in. or 10 in. below the surface, and here the change was generally slight.

A study of the temperatures at the bottom of the installation (30 in. below the surface) during the winter indicated that there was a slight but general lowering of temperatures in F-5, F-24, F-13 and F-15 with only a faint reflection of cold spells. At the same time and at the same depth in F-17 and F-10, there were definite rises and falls with warm and cold spells.

SUMMARY

The granular, non-plastic soils, F-17 and F-10, reacted to air temperature changes much more quickly than the finer-grained soils, F-5, F-13, F-15 and F-24, and therefore are better conductors of heat and cold. The frost entered into and went out of these granular soils more quickly than the finer-grained soils because of their greater conductivity.

The granular soils, F-17 and F-10, in general reacted in a similar manner during the winter. Of the two soils, F-17 was a better conductor and showed the least capa-

city for retaining low temperatures.

The finer-grained soils, F-5, F-13, F-15 and F-24, as a group, reacted similarly and it was difficult to find consistent differences as to frost penetration, temperature gradient with depth, and freeze and thaw periods. However of these four soils, F-15 (HRB Classification A-7-6) appeared to react the most slowly to air temperature changes and can be considered to be the poorest conductor (or best insulator). The dry density of F-15 in the fall of 1953 was 80 lb per cu ft, which was considerably lower than the other soils.

The 32 deg line generally penetrated to a greater depth in the granular soils (F-17, F-10) than in the finer-grained soils (F-5, F-13, F-24, F-15) during cold spells. The greatest penetration of the 32 deg line during the winter occurred below the slabs of F-17 and F-10.

Freeze and complete thaw cycles occurred more often below the slabs than in the adjacent shoulders. Therefore it can be said that the concrete slabs are better conductors of heat and cold than soil of the same thickness.

The shoulders of the finer-grained soils (F-5, F-13, F-24, F-15) showed little reaction to cold and warm spells (except at the surface) during the period studied, but instead tended to reflect the overall cold weather of the period itself. The shoulders of F-5, F-13 and F-15 retained 32 deg or below temperatures throughout the period.

There was a lag between the second minimum air temperature period of the winter and the time of the maximum penetration of the 32 deg line. The lag was one day for all but for the shoulders of F-13, F-15 and F-24, for which the lag was 6 to 14 days.

Maximum heaving did not occur at the same time as the maximum depth of the 32 deg line. In the cases studied, the maximum heave occurred many days (6 to 14 days) after the maximum depth of the 32 deg line and was attributed to an increase in the moisture content of the soils. Also, the depth of the 32 deg line at the time of maximum heaving was less than its maximum depth had been.

During the thaw periods, most of the thawing in the soils occurred from the top downward.

CONCLUSIONS

1. Granular, non-plastic soils are better conductors of heat and cold than fine-grained soils and react to air temperature changes more quickly. Of the six soils studied, F-17, a clean sand (HRB Classification A-3), was the best conductor and F-15 (HRB Classification A-7-6) was the poorest conductor. Therefore frost enters and goes out of granular soils more rapidly than fine-grained soils, causing more frequent freeze and complete thaw cycles.
2. A concrete slab is a better conductor of heat and cold than soil of the same thickness. Therefore freezing and complete thaw cycles occur more often below a concrete slab or pavement than in the adjacent shoulder.
3. A combination of a concrete slab over a granular soil is one that reacts most quickly to cold and warm spells. A shoulder of fine-grained soil shows little reaction to cold and warm spells (except at the surface) and reflects the over-all intensity of cold of the winter.
4. The freezing line generally penetrates to a greater depth in granular soils than in fine-grained soils.
5. There is a lag between the minimum air temperature of winter and the maximum penetration of the 32 deg line. (In the cases studied the lag was one day except for some of the shoulders of fine-grained soils, where the lag was several days.)
6. Maximum heaving does not necessarily occur at the time of the maximum depth of the 32 deg line.
7. Most thawing in soils occurs from the top downward during thaw periods.

ACKNOWLEDGMENT

The authors wish to express their appreciation to the New Jersey State Highway Department for having initiated the project which provided the material for this report, to the Joint Highway Research Committee and in particular to Chairman Allen

E. Ely for their interest and advice, and to E. C. Easton, Dean of the College of Engineering, Rutgers University, for his support of a project of such potential value to the state as a whole.

DISCUSSION

MILES S. KERSTEN, Professor, University of Minnesota—Temperature data beneath a simulated roadway surface such as presented in this paper are useful for checking methods which have been developed for calculating depths of freeze from air temperatures and certain soil data. (1) The New Jersey measurements could be of particular value since they are for a variety of soil textures and would help in depicting the effect of such a variable. They are also for a location where the magnitude of the cold, as measured by degree-days of freeze, is sufficient to cause some freezing of subgrades, but of a much lesser magnitude than is typical for Minnesota and other more northern states where some previous measurements have been made.

One very important item of needed information to calculate or estimate frost depths from air temperature data is the moisture content of the soil. No mention seems to have been made of this in the report. If it can be furnished it would be useful. One would suspect that the two sandier soils, F-10 and F-17, had much lower moisture contents than the other four soils. This would have a great influence on the rate of freezing and depth of freeze.

I believe care should be exercised in some of the terms which are used in problems of frost penetration. For example, conclusion (1) reads in part "Granular, non-plastic soils are better conductors of heat and cold than fine-grained soils—." Referring to the words "better conductors", this property is usually indicated by a coefficient of thermal conductivity, k, measured in such units as Btu per deg F per in. temperature gradient per square foot of area per hour. According to measurements made at the University of Minnesota (2) a sandy soil at a dry density of 116 lb per cu ft and at a moisture content of 5 percent would have a k of about 10 (units as above) in a frozen condition. A soil such as the F-5 silty soil in the New Jersey tests with a dry density of 94 lb per cu ft, if it existed at a moisture content of 22 percent, would have a k of 12. Even though the conductivity of the sand is less than that of the silt, the frost penetration for a given magnitude of "cold" could be much greater in the sandy soil than in the silt soil; this would be due to the much greater quantity of water in the silt which must be frozen, and the consequent greater quantity of heat represented by the latent heat of fusion which must be conducted out of the soil. With numerical values as indicated above, calculations of frost penetration in the sandy soil, without any pavement surfacing, would give depths about 1.7 times as great as calculated frost depths for the silt. Hence, it may not be entirely proper to designate soils in which frost penetrates rapidly or to great depths "good conductors."

A similar reasoning could be applied to conclusion (2) which states that a concrete slab is a better conductor than soil of the same thickness. Most concrete has a thermal conductivity, k, of about 10 to 12 Btu per deg F per in. per sq ft per hour. Frozen soils with relatively high moisture contents might have k-values appreciably greater than this. Even so, the frost might penetrate a few inches below a concrete pavement 6 in. which, resulting in a total depth of say 8 or 9 in. while it was penetrating only 4 or 5 in. into the soil in the shoulder alongside the slab. Again this would be due to the appreciable magnitude of the latent heat of fusion of the soil in the shoulder, whereas the concrete might contain only a small, almost negligible amount of moisture which would give it a small volumetric latent heat of fusion.

The conclusion that the freezing line penetrates to a greater depth in granular soils than in fine-grained soils is in agreement with measurements made in Minnesota.

REFERENCES

1. Carlson, Harry and Kersten, Miles, "Calculation of Freezing and Thawing Under Pavements." Highway Research Board Bulletin No. 71, 1953.

2. Kersten, Miles S., "The Thermal Conductivity of Soils." Highway Research Board Proceedings Vol. 28, 1948.

A. R. Jumikis, Closure—Mr. Kersten's remarks concerning the lack of mention of soil moisture content in this report are pertinent. Moisture content in soil has a great influence on the rate of freezing and depth of frost penetration.

Although moisture contents of these six soils in question were determined in the fall prior to the freezing season of 1953-4, and then again in the following spring after the frost went out of the ground, the soil moisture content data were not reported in this article. There were no moisture gages installed in the soil during the winter of 1953-4. Hence the variation in thermal properties of the soils because of the moisture changes during the freezing season could not be ascertained.

Being aware of the importance of and necessity for information on soil moisture contents during a freezing season, the authors installed soil moisture gages the following winter (1954-5) and included data on soil moisture contents obtained during the 1954-5 freezing season in a subsequent report*, actually being published prior to the discussion of the present article (concerning 1953-4). Illustrations on frost penetration depths and soil moisture contents and their variations are shown on pp. 97-108 of the previously mentioned report.

Mr. Kersten is quite right in saying that the property of heat conductivity of soil (referring to the expression "better conductors") can be characterized by a coefficient of thermal conductivity; for example, in Btu per foot per hour per degree F or calories per centimeter per second per degree C. With such data on hand, the soil thermal properties are readily characterized quantitatively. However, if such data are not on hand and one has to say something about the soil, the performance and the end results of the performance of the soil, as in this case, when subjected to freezing, can also be described qualitatively, especially when comparing the performance of several different soils among themselves, and particularly when heat transfer measurements and calculations are not and/or could not be done.

Under the circumstances, therefore, it is quite proper to compare the performance of several soils among themselves because all of the six soils were subjected to the same climatic and geographic environment (in one and the same frost yard and same position of the ground-water table) at the same time and during the same length of time. Thus, naturally, because of the varying properties among the soil types under consideration (their magnitudes are masked out, but they are there) one soil is obviously a "better conductor" of heat than another when compared for various climatic and geographic environmental conditions; then, of course, it is very difficult to say which soil is a "better conductor".

The author agrees that numerical heat conduction values of soils for varying moisture contents, even for one and the same type of soil, are very desirable factors in thermal soil mechanics. Much effort is still to be devoted to obtain such data for various types of soils, at various densities, moisture contents, and temperatures. Such data facilitate thermal calculations in highway and earthwork technology.

The same can be said about "good conductors" of concrete pavement slabs. The authors' conclusions were based on careful observations and considerations.

Mr. Kersten has studied frost penetration problems in Minnesota soils and it is gratifying to learn that temperature measurements made by the Joint Highway Research Project at Rutgers beneath a simulated roadway surface are useful in highway technology, and that some observations regarding frost penetration depths in granular soils made in New Jersey are in agreement with measurements made in Minnesota.

---

* Turner, K. A. Jr., and Jumikis, A. R.
"Subsurface Temperatures and Moisture Contents in Six New Jersey Soils, 1954-5."
HRB Bulletin 135, p. 77 (1956).

Theoretical and Practical Aspects of the Thermal Conductivity of Soils and Similar Granular Systems

MARTINUS VAN ROOYEN, Research Assistant, and
HANS F. WINTERKORN, Professor of Civil Engineering,
Department of Civil Engineering, Princeton University

The thermal conductivity of soils and allied phenomena play a major role in several engineering fields. A few examples are the frost problem in highway engineering, the dissipation of the Joule heat from buried electric cables, and the thermal exchange in heat pump systems.

It is not too difficult to measure actual heat conductivities of particular soils at specific moisture, density, and structural conditions. However, the values obtained can be used for purposes of prediction with regard to the normal weather – and seasonally conditioned changes in soil properties only by means of adequate hypotheses and theories. The more closely the theoretical concepts depict the actual mechanisms of heat transmission in soils, the fewer heat conductivity measurements must be made and the more useful to the engineer are those that are made.

Soils normally consist of solid, liquid and gaseous phases, and the mechanism of heat transmission differs for these different states. Therefore, the paper discusses thermal transmission in solid, liquid and gaseous phases before treating the more complex soil systems. The various theoretical and empirical equations available for the simple and complex systems are analyzed and results obtained with them are compared with actual experimental data.

The inadequacy of the present theories concerning thermal conductivity in soils is pointed out and ways toward correcting some of the deficiencies are indicated.

●SOILS ARE composed of solid, liquid and gaseous matter. In an undisturbed condition the solid particles and the liquid and gaseous phases in a grown soil are arranged in a definite structure or fabric, while in a completely disturbed condition distribution of particles and phases is random. The actual condition of most soils that are of interest to the engineer lies between these two extremes.

The thermal conductivity of a soil depends on the thermal conductivities of its solid, liquid and gaseous components, their volume proportions and their arrangement or structure. The structure itself is influenced by the size, shape and gradation of the components. Generally, solids conduct heat better than liquids, and liquids better than gases. It is important, therefore, whether in a soil structure the well conducting solid particles are in intimate contact with each other or whether and to what extent they are separated from each other by intervening liquid and gaseous phases.

In dispersed systems that are constituted of solid, liquid and gaseous phases, the transition from one phase to another is usually not abrupt. Rather, a transition zone is formed. This is especially important for the solid-liquid interfaces, in our case: the interface between soil particles and surrounding water films. The thickness and structure of this interaction zone are functions of the polar character of both, the solid surface and the surrounding liquid, and also of the temperature. This temperature dependence is the main cause for the transport of liquid in porous hydrophilic systems subjected to temperature gradients. In addition, diffusion and distillation may occur through the gaseous phase from locations of higher to those of lower temperatures. Hence, application of a thermal gradient to moist soils causes not only a heat transfer

through the different phases but also a mass transfer of the liquid in either or both, film and gaseous phases. Partial or complete removal of the liquid by these processes at a particular location in a soil lowers the thermal conductivity and also the heat capacity per unit volume of the soil at this location.

Considering the great complexity of heat transfer in natural soils one could be tempted to despair of the possibility of any significant practical results to be gotten from fundamental theoretical considerations. A theory covering all phenomena involved would be too cumbersome to handle, while one simple enough to be handled mathematically could not be expressive of the events actually taking place in a soil subjected to a temperature gradient. Such reasoning misses the most important point. It is better to have partial knowledge than none at all, as long as one realizes that it is partial. Also, all theory, even the best founded and simplest, proceeds by successive approximation, by starting with a simple picture and refining it when and as needed, employing physical parameters whenever it is easier to measure than to calculate them from basic assumptions. Even if we should never be able to do without actual determination of certain physical parameters, such as measured thermal resistivities, the mental discipline acquired and the creative imagination developed in pushing the theory as far as possible may pay a thousandfold by indicating ways and means to achieve desired practical ends. These ends are not only to predict thermal resistivities of soils from their composition and constitution, but also, and more importantly, to develop economical methods for maintaining the thermal behavior of soils at a level that is optimal for the intended purpose.

For the reasons given, the present report on the theory of heat transmission in soils and similar porous systems has been prepared. The treatment proceeds from the simpler to the more difficult aspects of the general problem.

THE NATURE OF HEAT

Heat is a form of energy. As in the case of other forms of energy a definite amount of heat can be expressed as the product of a capacity factor and an intensity factor. The former is the heat capacity, the latter the absolute temperature. The heat capacity per gram of a material is called its specific heat, that for the atomic weight in grams of an element is the atomic heat, and that for a gram mol of a compound is the mol heat. The total heat content U of a system possessing the heat capacity C and being at an absolute temperature T is expressed by

$$U = \int_0^T C\,dT$$

C itself is a function of the temperature.

The concept of heat as a form of motion of the ultimate particulate components of matter dates back to the ancients. Scientific proof of the essential validity of this concept was furnished by Rumford (Phil. Trans. 1798) and Davy (1799). This, however, was just a beginning. Only after Laplace, Dalton, Gay-Lussac, Dulong and many others had made their important contributions to the knowledge of the properties of gases, was it possible for Joule, Waterstone, Krönig and Clausius to found the kinetic theory of heat which was brought to maturity by Maxwell and Boltzmann.

The basic assumptions of this theory are amazingly simple. The experimentally found relationships between temperature, pressure and volume of normal gases led to the concept of the "ideal gas." The properties of the ideal gas are approached by many actual gases at normal temperature. The corresponding relationships can be expressed by the equation:

$PV = nRT$, in which

P = pressure
V = volume
n = number of moles of gas
T = absolute temperature
R = gas constant.

Both sides of the equation have the dimensions of energy or work, while R has the dimension of a specific heat or heat divided by temperature.

Numerical values for the specific heats and the mole heats of gases depend on whether they are determined at constant volume or at constant pressure. If determined at constant pressure, the volume will be increased and work will be done against the outside pressure. This work uses up heat energy. The difference between the mole heat at constant pressure C_p and that at constant volume C_v equals R = 1.985 calories. The ratio C_p/C_v for mono-atomic gases is 5/3 or 1.667; the more complex the gas molecules become, the larger becomes C_v and the smaller becomes C_p/C_v. Also, the heat capacities of mono-atomic gases are relatively independent of temperature. These gases have mole heats approximating $\frac{3R}{2}$ or 3 calories while gases having molecules composed of two and more atoms have temperature coefficients that increase with increasing complexity of the molecules. Between 0 deg and 1,000 deg C, the mol heats of N_2, O_2, CO and HCl increase from about 5 calories to 6.2, while those of H_2O, CO_2 and SO_2 start with about 6.7 and almost double in the given temperature range. From this type of evidence the theory concludes as follows:

The mole heat at constant volume, i.e., the amount of heat required to raise the temperature of one mole by one degree absolute, depends upon the number of different mechanical movements the individual molecules can make, or on the number of motion mechanisms in which they can invest energy. For each type of movement the energy $\frac{R}{2}$ is assigned per mole. Thus a mono-atomic gas, the atoms of which have no other possibilities than moving in the 3 dimensions of space, has a mole heat of $3\frac{R}{2}$ or about 3 calories. Diatomic molecules add to these 3 possible translatory movements rotations around two axes which results in mole heats of $5\frac{R}{2}$, while molecules with even more atoms have possible rotations about 3 axes with resulting mole heats of $6\frac{R}{2}$ or about 6 calories. This assignment of $\frac{R}{2}$ for each possible type of mechanical movement is called the equipartition theorem. In addition to the described types of movement there is the possibility especially at elevated temperatures for the various atoms in di- tri- and polyatomic molecules to oscillate with respect to each other. This again increases the mol heats.

The amazing thing about the kinetic gas theory is not that it has its definite limitations but rather how much can be done with a few simple assumptions, based, of course, on experimental results, and their logical mathematical development. The mechanical heat theory holds well for ideal gases and dilute solutions, but it becomes increasingly and often forbiddingly complex in the case of solids and liquids. Aside, however, from the unwielding complexity for many material systems, the purely mechanistic heat theory has its definite theoretical limitations. These become apparent when the thermal kinetic movements have grown sufficiently intensive to affect the electric constituents of the atoms and molecules in a way to result in electromagnetic phenomena and in the emission of electro-magnetic waves. Heat as a form of energy is, of course, also subject to Planck's quantum theory.

The modern theory of the specific heat of gases which takes the electromagnetic phenomena into account is largely due to Albert Einstein while that for the specific heat of solids has been developed mainly by Debye. The greatest difficulties to theoretical treatment are still offered by the liquids.

So far, main consideration has been given to the capacity factor of heat energy while the intensity factor, temperature, has been neglected. According to the kinetic theory of gases the absolute temperature is directly proportional to the kinetic translatory

energy present in the gaseous system under consideration. It is also a measure of the intensity of the total molecular movement in a gas. According to the kinetic theory of the specific heat the total translatory energy of one mole of a gas at an absolute temperature T equals $\frac{3R}{2}$ T. Recalling the ideal gas law PV = RT and the fact that PV also derives from the translational kinetic energy of a mol of gas at temperature T, one wonders why the proportionality constant on the right side of the equation is R and not $\frac{3R}{2}$. This can be explained in the following manner:

The pressure on the walls of a gas container is assumed to be the result of perfectly elastic recoil of the molecules hitting the walls at a particular moment. The molecules fly off the wall with the same speeds they had before the collision; that means they still possess their previous kinetic energies although the direction of movement has been reversed. However, there was an exchange of momentum with the wall which has received twice the momentum of the colliding particles. The pressure is, therefore, a function of twice the kinetic energy of the hitting particles or for one mol equal to f(3RT). Assuming that only one-third of the molecules in a mol hit the walls of the containing vessels at a particular moment the function becomes f(RT) or, as Boltzmann has shown in an exact presentation, the proportionality constant becomes equal to R. This is in agreement with the experimentally found gas law. According to the latter there exists no energy at absolute zero (T = 0); this means that all motion has stopped at this point.

In his derivation of the law of heat radiation from ideal black bodies Max Planck assumed that the walls of the hollow sphere representing the ideal black body consisted of oscillators. In order to accommodate the available experimental data Planck postulated that the oscillators involved could not take up energy continuously in arbitrary small increments but only in fixed units, called quanta. The magnitude of the quantum of energy ϵ depends on the oscillator frequency υ according to

$$\epsilon = h\upsilon \tag{2}$$

where h = Planck's constant (dimensions = Energy x time).

The average energy $\bar{\epsilon}$ of an oscillator is derived to be:

$$\bar{\epsilon} = \frac{h\upsilon}{e^{\frac{h\upsilon}{kT}} - 1} + \tfrac{1}{2} h\upsilon \tag{3}$$

where
e = the base of natural logarithms
k = the Boltzmann constant = $\frac{R}{N}$
R = universal gas constant
N = Avogadro's number
T = absolute temperature

This equation shows that even at the absolute zero temperature (T = 0) the oscillator possesses a residual energy of

$$\bar{\epsilon}_0 = \tfrac{1}{2} h\upsilon \tag{4}$$

Equation (3) yields the classical value of $\bar{\epsilon}$ = kT when $h\upsilon$ becomes much smaller than kT. At the present time, the quantum theory is accepted not only for radiant energy but also for all other forms of energy.

HEAT TRANSMISSION

The second law of thermodynamics is concerned with the degeneration of energy and the increase of the entropy. In accordance with this law, energy tends to go from a higher to a lower level of intensity. In the case of heat energy, this means that heat will flow from locations of higher to those of lower temperature. To achieve this end,

heat, as any other energy, will employ all ways and means at its disposition, though to different extent at different energy levels and depending on the composition and structure of the systems involved. Normally, there are available for heat transfer the following mechanism: radiation, conduction and convection.

Radiation

In heat emission by radiation the absolute temperature of the radiating body is the most important single factor. Radiation is the transportation of heat through empty spaces or transparent media. Total radiation follows the relation found by Stefan and Boltzmann for radiation of a perfectly black surface, viz:

$$q = \sigma A T^4$$

where
- q = time rate of energy flow
- A = the area through which the energy flows
- T = absolute temperature
- σ = a natural constant known as the constant of black body radiation.

For imperfect black bodies σ is replaced by another factor. The commonly used value for σ in the above equation is 4.96×10^{-8} in the c.g.s. system (43).

Conduction

Generally, heat conduction means the exchange of heat between continuous bodies or parts of a body. According to the kinetic theory, heat conduction is due to elastic impacts of molecules in gases, to longitudinal oscillations in solids which do not conduct electricity and oscillations plus movement of electrons in metals. The basic law for heat conduction in one dimension, also called Fourier's equation, is given by:

$$q = k \frac{A}{L} \Delta T,$$

where

q = energy flowing through area A per unit time when a temperature drop ΔT exists over a length L

k = coefficient of thermal conductivity, also called internal heat conductivity or just thermal conductivity.

Convection

Heat convection is the transportation and exchange of heat by mixing or interflow of multimolecular masses of liquids and gases that are at different temperatures. It is controlled by the laws of fluid dynamics as well as by those of heat conduction.

Newton in 1701 recommended the equation

$$q = h A \Delta T$$

to describe the transfer of heat q per unit time between a surface and a contacting fluid for a contact area A and a temperature difference ΔT; h is called the surface coefficient, film coefficient or coefficient of heat transfer. However, this equation is not exact and is more a definition of h than a law (43).

HEAT TRANSFER

Heat is propagated through space or different media in various manners depending on the type, composition and structure of the propagating substance.

(a) Heat transfer through a vacuum: the only way that heat can be propagated through a vacuum is by radiation. Radiation of heat being the same as light radiation, follows the laws of optics, both with regard to its geometry and dynamics, in addition to the previously mentioned energy radiation laws.

(b) Heat transfer through gases: the heat may be transported by radiation (if the gas is colorless), convection or conduction.

(c) Heat transfer through liquids: as in the case of gases, heat may be transferred by radiation (transparent liquid), convection and conduction.

(d) Heat transfer through solids: in dense transparent solids, radiation may contribute to the heat transfer. But, the most important mechanism at low temperatures is heat conduction. In porous or granular solids convection of gases or liquids in the pores contribute to the heat transfer. At very high temperatures, there will be internal heat propagation by means of radiation from pore wall to pore wall, which increases the apparent heat conductivity.

HEAT CONDUCTION IN HOMOGENEOUS SUBSTANCES

Conduction in Gases

According to the kinetic theory, the pressure of a gas is due to the force of the impacts of the gas molecules on the container wall. The temperature is proportional to the average translational kinetic energy of the molecules. The kinetic energy and its various manifestations such as pressure, temperature, specific heat, compressibility and others, will therefore be the dominating factors with respect to mass and heat transfer in gases.

The ideal gas is pictured as consisting of molecules, whose volume is no small as to be negligible in comparison with the total volume occupied by the gas. The molecules are conceived as elastic spheres with no attraction or repulsion forces between them. The ideal gas law and the corresponding thermodynamical treatments can be applied to this situation. If the actual volumes of the molecules and the interaction between them cannot be neglected changes in the ideal gas laws become necessary. The modifications by Van der Waals, Berthelot, Kammerlingh-Onnes and Beatie and Bridgeman are especially valuable.

It has been found that the coefficients of viscosity μ, thermal conductivity k, and diffusion D are proportional to one another. Within the normal range of pressures viscosity, thermal conductivity and diffusion are independent of the pressure. This is in agreement with the kinetic gas theory.

Consider two layers of gas molecules a distance δ apart where δ is the mean free path of a molecule. If the velocity gradient in the gas is given by $\frac{du}{dx}$, one layer of molecules will be moving relative to the other layer with a velocity $\delta \frac{du}{dx}$. Because of the thermal motion of the molecules in both layers, some molecules will be passing from the faster moving layer to the slower one, and vice versa. The molecules in the faster moving layer have a higher kinetic energy and those that pass over to the slower layer will transmit their excess energy to the new companion molecules of the slower layer, thereby increasing the kinetic energy of the slower layer. The reverse will happen when molecules from the slower layer pass over to the faster moving layer. The slow molecules increase their kinetic energy while the average kinetic energy of the faster layer is decreased. The over-all effect is a tendency to equalize the velocities of the two layers; the resulting physical phenomenon is that of viscosity.

A molecule of mass m in traveling from a faster layer to a slower layer will transport the momentum $m\delta \frac{du}{dx}$. If there are n molecules per cc and their average speed is $\bar{c}$, the total momentum transported per second is $\frac{1}{3} nm\bar{c}\delta \frac{du}{dx}$. Newton's law of viscous flow gives:

$$\text{Momentum change} = \text{Frictional force} = \mu \frac{du}{dx}$$

$$\mu \frac{du}{dx} = \frac{1}{3} nm\bar{c}\delta \frac{du}{dx}$$

$$\mu = \frac{1}{3} nm\bar{c}\delta$$

$$\mu = \frac{1}{3} \rho \bar{c}\delta$$

where

$$\rho = nm, \text{ the density of gas.}$$

The factor ⅓ derives from the assumption that about one-third of the molecules is moving from one layer to the other. The value of ⅓ (0.35 according to Boltzmann) is too low and a value of ⅔ should be used.

When the value of δ, the mean free path, is substituted in the equation the coefficient of viscosity becomes:

$$\mu = \frac{m\bar{c}}{3\sqrt{2}\,\sigma^2\,\pi}$$

where σ is the molecular diameter.

The last equation is independent of the pressure. This situation is only true for perfect gases. In the case of imperfect gases the equation fails and the viscosity increases with the density of the gas.

Because the temperature T is proportional to the kinetic energy and, therefore, to the square of the average speed ($\bar{c}^2$) of the molecules, it follows from the last equation that the viscosity μ increases linearly with $\sqrt{T}$. However, real molecules are not solid hard spheres but must be regarded as surrounded by force fields. The higher the speed of the molecules (higher temperatures), the further they penetrate the force fields of the molecules which they encounter. A correction for the effective cross-section has been applied by Sutherland (93) which has the following form:

$$\sigma^2 = \sigma_\infty^2 \left(1 + \frac{C}{T}\right)$$

where σ_∞ and C are constants, σ_∞ is the value of σ as T approaches ∞, or the diameter of the hard core of the molecules, C the Sutherland constant, and T the absolute temperature. Numerical values for the dynamic viscosity of a few gases are given in Table 1. Bromley and Wilke (11) showed how the viscosities of various gases may be

TABLE 1

NUMERICAL VALUES OF THE DYNAMIC VISCOSITY OF SOME CASES AT ATMOSPHERIC OR LOWER PRESSURES

Gas	Chemical Formula	Dynamic Viscosity in Poise x 10^{-6}					
		-200°C	-100 °C	0 °C	100 °C	200 °C	300 °C
Hydrogen	H_2	33	61	85	103	120	138
Nitrogen	N_2		114	165	208	246	
Air	-		120	171	218	259	296
Oxygen	O_2		132.5	193	247	295	
Carbon Dioxide	CO_2			139	188		

computed at various temperatures making use of tables of collision integrals published by Hirchfelder, Bird and Spotz (41). These collision integrals are based on an improved kinetic theory developed by Chapman and Cowling (16). An assumption is made for the energy of interaction potential between molecules, and it is possible to calculate accurately the viscosity for non-polar smooth spherical molecules.

The effect of pressure and temperature on the viscosities of gases has been investigated by Uyehara and Watson (96) on the basis of the law of corresponding states. They presented values of reduced viscosity against reduced temperatures for constant reduced pressure lines. Grunberg and Nissan (39) assumed that in a highly compressed fluid transfer of momentum may occur by two mechanisms, a translational type as in gases and a "vibrational" type as in liquids. The viscosity is correlated with reduced temperature and reduced density. It is claimed that the accuracy is in the order of 10 percent and that the method is applicable to highly compressed gases and to liquids

near the critical point. Comings and Egly (18) described a graphical method based also on the concept of corresponding states, to determine the viscosity of pure gases and of vapors at high pressure from known critical temperature and pressure data and viscosity values at atmospheric pressure. Othmer and Josefowitz (69) showed that at constant temperature the viscosity of a gas plotted against the kinetmatic pressure and divided by the density gives straight lines on an arithmetic plot.

Viscous flow involves the transfer of momentum across a momentum gradient, thermal conductivity the transfer of kinetic energy across a kinetic energy gradient and diffusion the transportation of mass across a concentration gradient. The concept employed for explaining viscous behavior of gases can also be applied to their thermal conductivities. The picture is that of molecules with higher kinetic energies moving to regions of lower kinetic energy (and vice versa) and exchanging energy by collisions. The basic relationship between the coefficient of thermal conductivity k and that of the viscosity μ is given by:

$$k = \epsilon\, c_v\, \mu,$$

in which:

ϵ = factor with values between 2.5 and 1.0
c_v = specific heat of the gas at constant volume

According to the equipartition theorem the same fraction of the specific heat is contributed by each degree of freedom. The respective theoretical mol heats are:

For monatomic gases	$C_V = \frac{3}{2} R$
Diatomic gases	$C_V = \frac{5}{2} R$
Tri- and more- atomic gases	$C_V = \frac{6}{2} R,$

R being the universal gas constant. The factor ϵ may be considered as a measure of the effectiveness with which a molecule carries and disposes of its energy load by collision. According to Eucken (29) molecules possessing higher energies transfer energy faster than molecules possessing smaller energies. It has also been considered whether energies of rotation and oscillation will be reduced on impact in the same proportion as the translational energies. Chapman (15) calculated a value of $\epsilon = 2.5$ for monatomic, spherical molecules with no central forces between them. For molecules possessing more than one atom, Eucken (27) obtained the following equation by considering energies of rotation and oscillation independent of the energy of translation.

$$\epsilon = \frac{4.47}{c_v} + 1$$

Incorporating the expressions for the viscosity and the Sutherland formula it follows (43) that:

$$k = \epsilon C_v \frac{B\sqrt{T}}{1 + \frac{C}{T}};$$

or:

$$k = \frac{BF(1 + GT)\sqrt{T}}{1 + \frac{C}{T}}$$

since within practical ranges:

$$\epsilon\, c_v = F(1 + GT).$$

With appropriate values for B, F, G, C, this equation gives thermal conductivity coefficients with an accuracy of 0 to 6 percent in the range - 180 deg C to 200 deg C.Table 2 gives some measured thermal conductivities of the most common gases.

It was pointed out previously that diffusion, viscous flow and heat flow of gases follow the same mechanism according to the kinetic theory. The previous considerations were for conditions of pure gases. It is obviously desirable to be able to predict

physical properties such as diffusion constants, coefficient of viscosity and thermal conductivity for gas mixture when the composition and properties of the pure substances are known. For the diffusion coefficient D'_A of gas A with respect to a mix-

TABLE 2

THERMAL CONDUCTIVITY OF SOME GASES

Gas	Molecular Weight		Thermal Conductivity in $\frac{\text{watt}}{(\text{sq cm})(^\circ\text{C per cm})} \times 10^{-4}$				
			-200°C	-100°C	0°C	100°C	200°C
Hydrogen	H_2	2	5.0	11.6	17.1	21.4	-
Nitrogen	N_2	28	.71	1.62	2.44	3.03	
Air	-	29	-	1.62	2.44	3.08	
Oxygen	O_2	32	.62	1.62	2.44	3.13	
Carbon Dioxide	CO_2	44			1.40	2.09	2.68

ture of gases, Wilke (99) derived an expression based on theories of Maxwell and Stefan. The expression is:

$$D'_A = \frac{1 - y_A}{\frac{y_B}{D_{AB}} + \frac{y_C}{D_{AC}} + \frac{y_D}{D_{AD}} + - -}$$

where y_A, y_B, - - - are the mole fractions of components A, B, C - - in the mixture and D_{AB}, D_{AC} - - - are the diffusion coefficient of component A with respect to the pure components in the mixture. This relationship was verified experimentally by Fairbanks and Wilke (33).

For the viscosity of a mixture of two gases Sutherland (92) and later Thiesen (95) proposed the formula for μ the viscosity of the mixture

$$\mu_n = \frac{\mu_1}{1 + \frac{x_2}{x_1} A} + \frac{\mu_2}{1 + \frac{x_1}{x_2} B}$$

where μ_1, μ_2 are the viscosities of the pure components of the mixture and x_1 and x_2 their respective mole fractions.
A and B are dimensionless constants.

A simplification as shown by Schudel (82) results in

$$\frac{A \rho_1}{\mu_1} = \frac{B \rho_2}{\mu_2} = C$$

where ρ_1 and ρ_2 are the respective densities of the two components in the mixture, and
C = Constant.

Buddenberg and Wilke (13) developed empirically the constant C in the formula of Schudel. Their expression is:

$$\mu_n = \frac{\mu_1}{1 + \frac{x_2}{x_1} \frac{1 \cdot 385\ \mu_1}{D_{12}\ \rho_1}} + \frac{\mu_2}{1 + \frac{x_1}{x_2} \frac{1 \cdot 385\ \mu_2}{D_{12}\ \rho_2}}$$

D_{12} being the diffusion coefficient of gas 1 with respect to gas 2.
This equation was generalized to include multicomponent systems, resulting in:

$$\mu_m = \sum_{i=1}^{n} \frac{\mu_1}{1 + \frac{1 \cdot 385\,\mu_i}{x_i \rho_1} \sum_{\substack{j=1 \\ j \neq i}}^{n} \frac{x_j}{D_{ij}}}$$

In a later article Bromley and Wilke (11) gave this expression as:

$$\mu_n = \sum_{i=1}^{n} \frac{\mu_i}{1 + \frac{1}{x_1} \sum_{\substack{j=1 \\ j \neq 1}}^{n} x_j \phi_{ij}}$$

where

$$\phi_{ij} = \frac{\left[1 + \left(\frac{\mu_1}{\mu_j}\right)^{1/2} \left(\frac{M_j}{M_1}\right)^{1/4}\right]^2}{\frac{4}{\sqrt{2}} \left[1 + \frac{M_1}{M_j}\right]^{1/2}}$$

M_i, M_j being the molecular weights of components 1 and j respectively.
This treatment resulted from an extension by Wilke (100) of the treatment presented by Buddenberg and Wilke.

Analogous to the expressions for the viscosity and diffusion coefficients of gas mixtures as given by the Sutherland expression, Wassiljewa (98) proposed an equation for the thermal conductivity of a mixture of gases given by

$$k_m = \frac{k_1}{1 + A_{12} \frac{x_2}{x_1}} + \frac{k_2}{1 + A_{21} \frac{x_1}{x_2}}$$

where k represents the heat conductivity with subscripts to indicate the components.
x_1 and x_2 are the mole fractions of components 1 and 2 respectively.
A_{12} and A_{21} are dimensionless constants.

In a paper on the thermal conductivity of gas mixtures, Lindsay and Bromley (54) developed the following general equation from simple kinetic theory and using Sutherland's model:

$$k_m = \sum_{1=1}^{n} \frac{k_1}{1 + \frac{1}{x_1} \sum_{\substack{j=1 \\ j \neq 1}}^{n} A_{ij} x_j}$$

and

$$A_{ij} = \frac{1}{4}\left\{ 1 + \left[\frac{\mu_i}{\mu_j} \left(\frac{M_j}{M_i}\right)^{3/4} \frac{\left(1 + \frac{S_i}{T}\right)}{\left(1 + \frac{S_j}{T}\right)} \right]^{1/2} \right\}^2 \frac{\left(1 + \frac{S_{ij}}{T}\right)}{\left(1 + \frac{S_1}{T}\right)} \quad ;$$

S_i and S_j are the Sutherland constants for the gases i and j respectively and S_{ij} is taken as the geometric mean of the two Sutherland constants

$$S_{ij} = \sqrt{S_i\ S_j} \quad ;$$

M_i and M_j are the molecular weights.

This equation was verified for a two-component gas mixture and is claimed to be accurate within an average deviation of 1.9 percent. An approximate value for the Sutherland constant was taken as $S = 1.5\ T_B$ where T_B is the boiling point at 1 atmosphere pressure. For gases where molecules have a strong dipole:

$$S_{ij} = 0.733\sqrt{S_i\ S_j} \quad .$$

Comprehensive reviews of literature on the molecular transport properties of fluids have been compiled by Johnson (46) during the past few years. Improvement of variable significance may be found in the literature listed. These reviews treat the viscosity, diffusion, thermal conduction and thermal diffusivity properties of gases and liquids.

Conduction in Liquids

In ideal gases the dispersive forces prevail and any interaction between individual molecules is negligible. The total energy of a gas is the sum of the kinetic energies of all the molecules. In liquids, the attraction forces between the molecules are sufficiently strong to lead to a condensed system but not strong enough to prevent considerable translation and rotation of the individual molecules. Liquids fall thus between gases which, at high temperatures at least, are characterized by complete disorder or randomness of the molecules, and crystals that hold atoms and molecules in nature's most orderly arrangement.

As a combination of the first and second law of thermodynamics we have the equation:

$$\left(\frac{\partial E}{\partial V}\right)_T = T\left(\frac{\partial P}{\partial T}\right)_V - P$$

where $\left(\frac{\partial E}{\partial V}\right)_T$ = change in internal energy E with volume change ∂V at constant temperature T;

$\left(\frac{\partial P}{\partial T}\right)_V$ = change of pressure ∂P with change in temperature at constant volume V.

In words the equation means:

Internal pressure = thermal pressure - external pressure.

The thermal pressure is a measure of the tendency of a substance to expand as the result of the thermal kinetic motion of its molecules. For an ideal gas:

$$\left(\frac{\partial E}{\partial V}\right)_T = 0,$$

which means that there is no intermolecular attraction. For a typical liquid the internal pressure is of the order of magnitude of 3,000 atmospheres; for water the internal pressure is about 20,000 atmospheres according to J.H. Hildebrand (40).

Another picture of the relation between vapors and liquids is that vapors may be considered as void space in which a few molecules are moving at random, while in the liquid state a number of holes are moving at random through the fluid substances. Increase in temperature of a liquid increases the concentration of molecules in its vapor and also the concentration of holes in the liquid. At the critical point the vapor density is the same as the liquid density. This behavior, pointed out by Cailletet and Mathias (1886) is called the law of rectilinear diameters.

The kinetic-molecular mechanisms of viscosity are different for gases and liquids. The viscosity of a gas increases with temperature and is practically independent of pressure. In the case of a liquid, the viscosity increases with increasing pressure and decreases exponentially with increasing temperature. The viscosity coefficient μ of a liquid is given by DeGusman (21) as:

$$\mu = Ae^{\frac{\Delta E\,(vis)}{RT}} \quad , \text{ where}$$

ΔE (vis) is a measure of the energy barrier to be overcome before viscous flow occurs or according to Eyring (38) the energy required to make holes of molecular size into which the moving molecules can slip.

This equation was developed from the Arrhenius equation for chemical reaction rates (1):

$$\ln k = \ln A - \frac{E}{RT}$$

or

in which

$$k = Ae^{-\frac{E}{RT}}$$

k is the reaction rate

A and E are constants, E being called the heat of activation.

The equation of Arrhenius has become generally accepted as the expression of the temperature dependence of the specific rates of reaction. The form of equation also proved to be valid in expressing physical phenomena which require time for their occurrence and take place with a unique velocity under definite conditions. This was shown by Glasstone, Laidler and Eyring (38) for processes such as viscosity, diffusion, dipole orientation in an electric field, electrolytic conductance and electrode phenomena.

From the free energy of activation $\Delta F^{\neq}$, Powell, Roseveare and Eyring (75) gave an expression for the fluidity

$$\phi \left(\phi = \frac{1}{\mu}\right), \text{ viz.:}$$

$$\phi = \frac{V}{Nh} e^{-\frac{\Delta F^{\neq}}{RT}}$$

where:

V = molal volume

N = Avogadro's number

h = Planck's constant

As shown by these authors, there exists a close correlation between $\Delta F^{\neq}$ the free energy of activation for viscous flow and ΔE_{vap} the energy change of vaporization. From this was derived the equation:

$$\mu = \frac{Nh}{V} e^{\frac{\Delta E_{vap}}{2 \cdot 45\, RT}}$$

For many liquids the ratio $\frac{\Delta F^{\neq}}{\Delta E_{vap}}$ lies between ⅓ to ¼; but for liquid metals the range is from ⅛ to 1/20. This leads to the conclusion that the units of flow in liquid metals are ions that are surrounded by an electron gas. At vaporization, the whole metal atom has to be expelled leaving a hole of corresponding size. The success of this theory to explain viscosity can be seen in the way it takes into account the effect of compositions. The corresponding equation for solutions is:

$$\mu = \frac{Nh}{V} e^{\frac{(N_1 \Delta F_1^{\neq} + N_2 \Delta F_2^{\neq} - \frac{\Delta F^E}{2.45}}{RT}}$$

This reduces to the best known empirical mixture law for not too imperfect solutions:

$$\log \mu = n_1 \log \mu_1 + N_2 \log \mu_2, \text{ in which}$$

N_1 and N_2 are mole fractions of substance 1 and 2 respectively.

ΔF^E is the free energy change of mixing (in excess of ideal). Similar molecular models are used for treating diffusion coefficients and ionic conductances.

From the Clausius Clapeyron equation

$$\frac{d \ln P}{dT} = \frac{L}{RT^2}$$

and the deGuzman treatment of fluidity ϕ, we obtain

$$\frac{d \ln \phi}{dT} = \frac{E}{RT^2} \qquad \text{in which}$$

P is the vapor pressure, T the absolute temperature, L the latent heat of vaporization, R the universal gas constant and E the activation energy for viscous flow; Othmer and Conwell (68) correlated viscosity, vapor pressure and latent heats of liquids. Their equation for viscosity μ is given as:

$$\log \mu = -\left(\frac{E}{L}\right) \log P^1 + C$$

where C is a constant. The authors maintain that the use of critical constants gives even better plots. Another attempt to relate viscosity and vapor pressure in a two-constant equation was made by Mitra and Chakravarty (62, 63). A simple two-constant equation of Mukherjee (65) combines the logarithms of viscosity, temperature and vapor pressure based on the assumption of free volume in liquids. Molecular refraction was used by Lagemann (52) to construct a nomograph for the determination of liquid viscosities. In a flow constant equation by Baum (7) the logarithm of viscosity is given as a function of absolute temperature. This expresses the fact that vapor pressure and viscosity of ten times plot as straight lines on log-log paper.

Cornelissen and Waterman (19) presented the following equation for the kinematic viscosity:

$$\nu = e^{\left(B + \frac{A}{T^X}\right)}$$ to correlate the variation of the kinematic viscosity ν with the absolute temperature T; the other symbols represent constants.

While heat conduction in liquids is just as in gases due to movement of atoms and molecules, its mechanism is quite different from that in gases. The most promising theory assumes that heat is transferred by longitudinal vibrations, similar to the propagation of sound in a medium.

Bridgman (10) derived an equation for the thermal conductivity of a liquid on the above assumption. If R is the universal gas constant and N Avogadro's number, then $\frac{3}{2} \frac{R}{N} \Delta T$ is the kinetic energy taken up by an atom of a monoatomic substance upon increase in temperature by ΔT. The energy increase per atom or molecule in

the solid state when heated by 1^0C will be $3\frac{R}{N} \times 1^0$, one-half of which is kinetic, the other half potential energy. Because the specific heat c_v does not change much in the transition from the solid to the liquid state, the expression for C_v previously derived for the solid state and the equipartition between potential and kinetic energy may be considered true for liquids also.

For a temperature gradient $\frac{dT}{dx}$ in a liquid with a molecular energy of $3\frac{R}{N}T$, the difference of energy between adjacent molecules in the direction of the temperature gradient is $3\frac{R}{N} \cdot \frac{dT}{dx} \cdot D$, where D is the mean distance of the centers of neighboring molecules when a simple cubical array is assumed. The difference in energy is assumed to be handed down a row of molecules with the velocity of sound v. The total energy passing a fixed point of any row of molecules per unit time is:

$$\frac{3R}{N} \cdot \frac{dT}{dx} D \cdot \frac{v}{D}$$

Dividing this expression by the cross-section D^2, we obtain a total energy transfer per unit cross-section of:

$$\frac{3R}{N} \cdot \frac{dT}{dx} D^{-2} v$$

By definition the transfer per unit cross-section equals $k\frac{dT}{dx}$, k being the coefficient of thermal conductivity. Combining the last two expressions, we obtain:

$$k = \frac{3R}{N} v D^{-2}$$

This equation, despite its simplicity, renders data that are in good agreement with actual measurements, although considerable discrepancies are found for several liquids. A good agreement exists for the experimentally determined and the calculated thermal conductivity of water which is 2½ to 5 times that of organic liquids. Bridgman reasoned that this high conductivity of water is due to its low compressibility. The formula gives the right sign for the temperature coefficient of thermal conductivity at atmospheric pressure, both for organic liquids and for water. Table 3 shows the agreement between the measured conductivities of some liquids and the values calculated by means of the formulas of Bridgman and Kardos. Kardos (48) considered each molecule as a unit possessing a certain energy with the drop in energy ΔQ and in temperature dt restricted to the distances between molecules. For a cubical array the distance between the surfaces of adjacent molecules is taken as L. By multiplying by $\frac{L}{D}$, the energy gradient is reduced to that of a quasi-homogeneous body. If, as before, the heat is assumed to be transmitted with sound velocity v, the heat flow per unit cross-section is:

$$q = -Lv\left(\frac{1}{D^3} \cdot \frac{dQ}{dt} \frac{L}{D}\right)\left(\frac{dt}{dx}\right)_L$$

From the basic equation of heat flow:

$$q = -k\left(\frac{dt}{dx}\right)_D = -k\frac{L}{D}\left(\frac{dt}{dx}\right)_L$$

The subscripts D and L denote over which range the derivatives are taken. For a cubical packing we obtain:

$$\frac{1}{D^3} \cdot \frac{dQ}{dt} = \rho c_p$$

TABLE 3

COEFFICIENTS OF THERMAL CONDUCTIVITY OF LIQUIDS FROM EXPERIMENT AND CALCULATION ACCORDING TO THE EQUATIONS OF BRIDGMAN AND KARDOS, AT 30 °C

Liquid		v cm/sec x 10^{-3}	D cm x 10^{-9}	k, watt/(sq cm) (°C per cm) x 10^{-3} Bridgman	Kardos	Exper.
Water	H_2O	145[a] 150[c]	31.0[a] 31.0[c]	6.21[a] 6.41[c]	5.96[c]	6.10[c]
Methyl alcohol	CH_4O	112[a] 113[c]	40.2[a] 40.8[c]	2.84[a] 2.79[c]	2.02[c]	2.11[c]
Ethyl alcohol	C_2H_6O	104[a] 114[c]	45.9[a] 46.0[c]	2.04[a] 2.22[c]	1.98[c]	1.82[c]
Isoamyl alcohol	$C_5H_{12}O$	124[c]	56.5[c]	1.60[c]	2.21[c]	1.48[c]
Glycerine	$C_3H_8O_3$	191[a]	49.5[a]	3.20[a]	5.75[c]	2.81[c]
Carbon bisulfide	CS_2	96[a] 106[b] 118[c]	46.0[a] 46.6[c]	1.87[a] 2.06[b] 2.23[c]	1.47[c]	1.59[c]
Acetone	C_3H_6O	108[a] 114[c]	49.5[a] 50.0[c]	1.81[a] 1.88[c]	1.82[c]	1.79[c]
Ether	$C_4H_{10}O$	92[a] 92[c]	55.0[a] 55.9[c]	1.25[a] 1.21[c]	1.40[c]	1.37[c]
Ethyl bromide	C_2H_5Br	90[c]	50.2[c]	1.48[c]	1.13[c]	1.20[c]
Ethyl iodide	C_2H_5I	78[c]	51.2[c]	1.23[c]	1.03[c]	1.11[c]

[a]Data for calculating coefficients were taken from (a) Chemical Engineer's Handbook. John H. Perry, McGraw-Hill, 1934; (b) Handbook of Chemistry and Physics. Chemical Rubber Publishing Co., 1946.

[b]Values of speed of sound v taken from Smithsonian Physical Tables.

[c]Other values taken from Heat Transfer (43).

where ρ is the density of the liquid and c_p the specific heat of the liquid at constant pressure. The equation for the coefficient of heat conductivity k is then:

$$k = \rho c_p v L$$

Kardoes gives a value of $L = 9.5\ (10)^{-9}$ cm considering the theory of van der Waal's forces, molecular weights, density and compressibility. However, the calculation of L must be considered to be only semi-empirical. For some liquids the Kardos equation gives better values than that of Bridgman, but falls down in the case of glycerine.

The model for the conduction of sound or heat according to Powell, Roseveare and Euring (75) follows that of Kardos. It assumes the signal to be transmitted between molecules by the speed of sound, and across the molecules almost immediately:

$$\frac{U\ (\text{liquid})}{U\ (\text{gas})} = \left(\frac{V}{V_f}\right)^{1/3},$$

where

V = molecular volume

V_f = molecular free volume (or volume between molecules)

U (liquid), U (gas) are velocity of sound in liquid or in gas respectively.

From the equation for the heat conductivity of gases (25) as interpreted by the authors:

$$K(\text{gas}) = \tfrac{1}{3}\left[\tfrac{1}{4}\left(\frac{C_p}{C_v} - 5\right)\right]\frac{N}{V}\,\bar{U}\,L\,C_v\,,$$

where

C_p and C_v = the specific heat at constant pressure and volume respectively for one molecule

$\bar{U}$ = average kinetic theory velocity

L = mean free path

$\frac{N}{V}$ = number of molecules per cc,

one obtains by multiplying the average velocity $\bar{U}$ by $\left(\frac{V}{V_f}\right)^{1/3}$,

replacing the L by $\left(\frac{V}{N}\right)^{1/3}$ and taking a value of 3k (k is the Boltzman constant) for C_v:

$$k\ (\text{liquid}) = 0.931\left(\frac{C_v}{C_p}\right)^{1/2} 3k\left(\frac{N}{V}\right)^{2/3} U\ .$$

This equation has the same form as that of Bridgman.

In an attempt to explain the abnormally high thermal conductivities of glycols and alcohols with respect to other "normal" liquids, Palmer (70) took into account the effect of the hydrogen bonding in these liquids. The "normal" liquids were classified as those which can be fitted with empirical equations. It is assumed that heat may be transported by two types of mechanisms – the transfer by collision between molecules and for hydroxyl groups by making and breaking of hydrogen bonds. More hydrogen bonds are broken where the heat intensity is higher, thereby absorbing heat, and more formed where the temperature is lower, thus releasing heat – a concept similar to that of von Grotthus for the electrical conductance of hydrogen ions in water. Further assumptions are that the effects of the two mechanisms are additive and that the normal entropy of vaporization (Trouton's constant) divided by the experimental value provides the parameter expressing the effect of hydrogen bonding.

A rather simple empirical equation by Weber:

$$k = 0.0043\ \rho\ C_p\left(\frac{\rho}{M}\right)^{1/3}$$

in which

k = thermal conductivity

ρ = density

C_p = the specific heat, and

M = molecular weight,

was shown by Smith (85) to check experimental values to within an average error of 14.8 percent. By modifying this equation as discussed above, Palmer was able to reduce the average error to 8.8 percent. His equation is given as:

$$k = 0.0947\ \frac{\rho C_p}{\frac{L_v}{T}}\left(\frac{\rho}{M}\right)^{1/3}$$

where

L_V = latent heat of vaporization and

T = absolute temperature;

Trouton's constant - an average for all liquids - was assumed to be equal to 21.

Various authors have attempted to correlate the thermal conductivity of liquids with other measurable properties. Sakiadis and Coates (80) proposed a revised correlation based on Kardos which fits the observed values better. They also based a correlation on the theorem of corresponding states from which the thermal conductivity of liquids may be calculated. Johnson and Huang (46, 45) presented charts for calculating thermal conductivities from viscosity and specific heat data. Riedel (46, 79) correlated thermal conductivity with compressibility and surface tension from consideration of corresponding states.

In addition to the above more-or-less theoretical approaches, other investigators have attempted to derive pure empirical formulas. Smith (85) presented two empirical equations with one and five constants respectively. This is to a certain extent an adaption of the equation by Weber. Bates (5, 4, 3) from determination of the thermal conductivity of water-glycerol, water-methyl alcohol and water-ethyl alcohol mixtures presented tables, graphs and empirical equations for the calculation of the thermal conductivity of the above mentioned mixtures. Bates (6) also determined experimentally the coefficient of thermal conductivity for nine liquid silicones. He also derived an empirical equation relating the thermal conductivity of a series of polymers with viscosity and temperature.

Conduction in Solids

The ideal solid is the crystal. Between the solid and liquid state there exists a variety of intermediate forms represented by rubbers, resins, glasses, liquid crystals, fibers and protoplasm. Understanding of the thermal conductivity in solids presupposes an understanding of crystal structures.

Crystal Structure. The first law of crystallography specifies that the corresponding interfacial angles (in different crystals) are constant and in no way dependent on the development of the respective faces. In 1784 the Abbé René Just Haüy proposed that the regular external form of a crystal results from an internal regularity in the arrangement of the primary building stones. This concept was later verified by the work of Max von Laue with x-ray diffraction.

The faces of crystals and the planes within crystals can be specified by a set of three non-coplanar axes. It has been found that there always exists a set of axes on which the reciprocal intercepts of crystal faces are small, whole numbers. These

TABLE 4

THE SEVEN CRYSTAL SYSTEMS

System	Axes	Angles	
Cubic	a = b = c	$\alpha = \beta = \gamma = 90^0$	Rock salt
Tetragonal	a = b; c	$\alpha = \beta = \gamma = 90^0$	White tin
Orthorhombic	a; b; c	$\alpha = \beta = \gamma = 90^0$	Rhombis sulfur
Monoclinic	a; b; c	$\alpha = \beta = 90^0$ $\gamma \neq 90^0$	Monoclinic sulfur
Rhombohedral	a = b = c	$\alpha = \beta = \gamma \neq 90^0$	Calcite
Hexagonal	a = b; c	$\alpha = \beta = 90^0$ $\gamma = 120^0$	Graphite
Triclinic	a; b; c	$\alpha \neq \beta \neq \gamma \neq 90^0$	Potassium dichromate

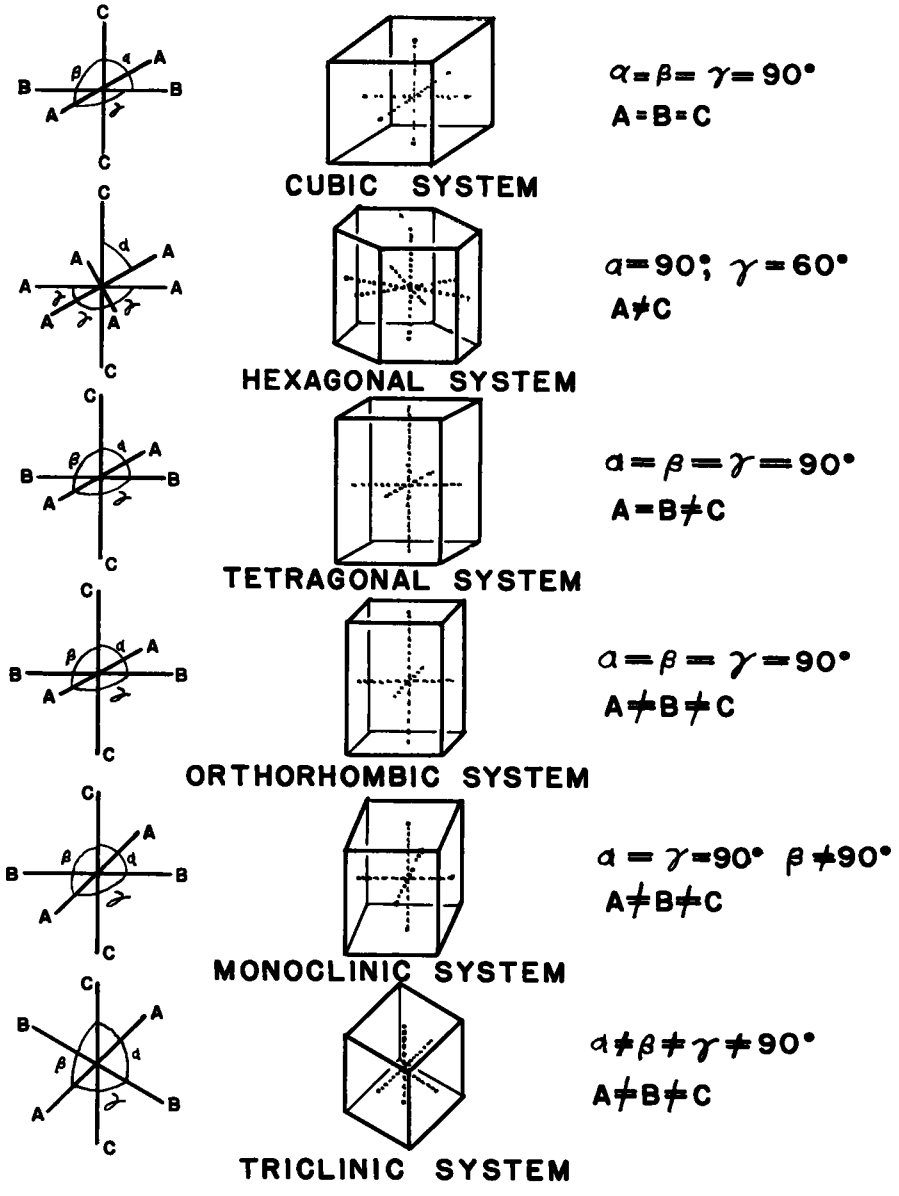

Figure 1. The six crystal systems.

reciprocal intercepts or Miller indices are used to define the crystal faces.

According to the set of axes used to define the crystal faces, the crystals may be divided into seven systems. If a, b and c represent the three non-coplanar axes making angles of α, β, and γ, respectively, with each other, the seven systems can be represented (64) as given in Table 4 or Figure 1.

The atoms in a crystal are orderly arranged in small groups or unit cells in such a way that the whole crystal may be built out of these small cells. If we take a corresponding point in each of these cells, we will end up with a regular array of points in space which is called a lattice or a space lattice. The lattice points can be connected by a regular network of lines in various ways. Thereby the lattice is broken up into the unit cells. A. Bravais (1848) showed that all possible space lattices can be organized into 14 classes (see Fig. 2).

By means of x-rays which are diffracted by the atoms in the crystal, the regular arrangement of the primary building stones was confirmed. The outstanding pioneering work in this connection was performed by Max von Laue (1912) and by W. H. Bragg

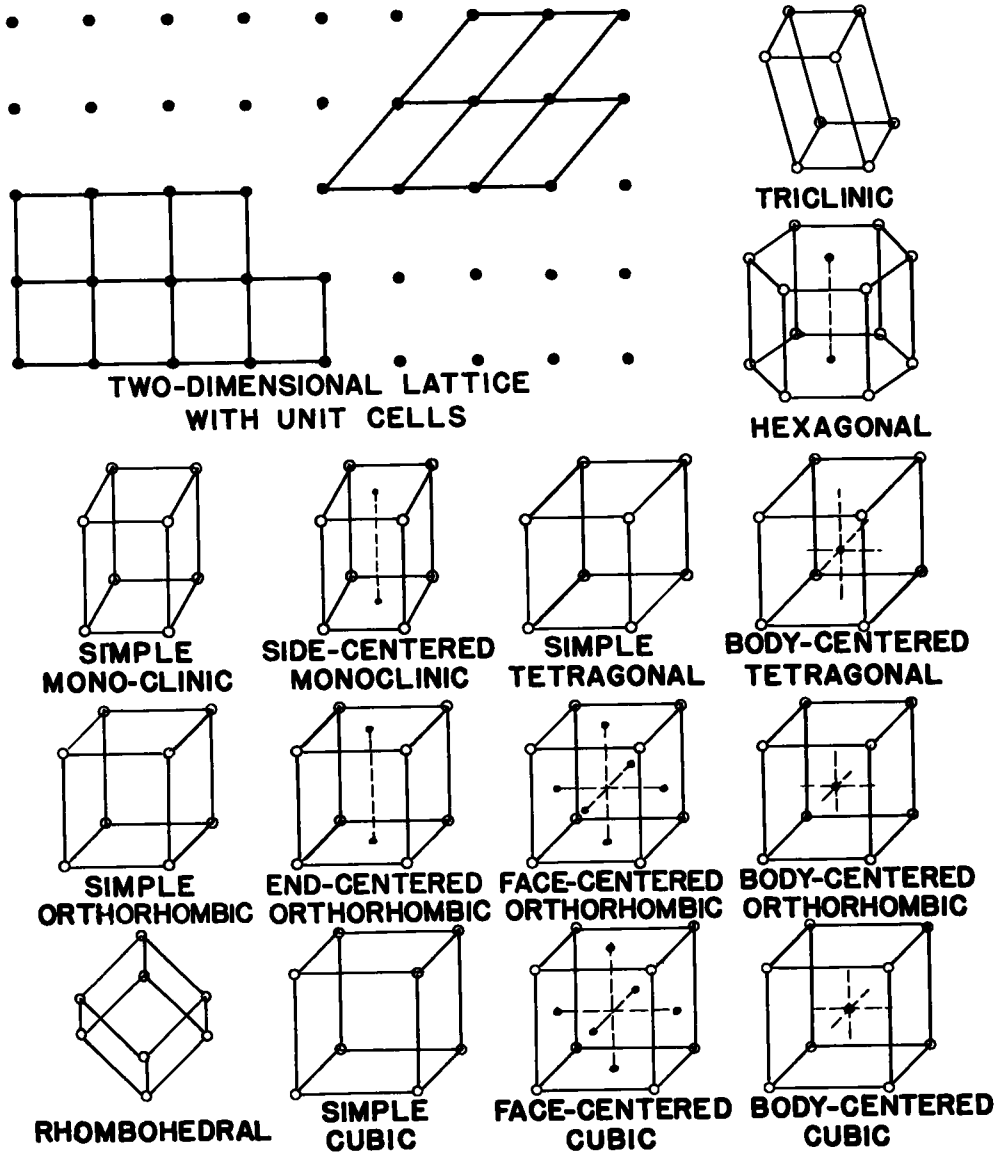

Figure 2. The fourteen Bravais crystal lattices.

and W. L. Bragg (9). Instead of using a single crystal with a definite orientation, P. Debye and P. Scherrer found that a mass of finely divided crystals with random orientations may be used.

Symmetry is described in terms of symmetry operations; application of such symmetry operations to one or more crystal faces reproduces the geometric form of the crystal. The symmetry of a crystal is evident not only in the face development but in all other physical properties such as electrical and thermal conductivity, density,

piezoelectric phenomena, and refractive index. The symmetry operations, rotation, reflexion, translation and their combinations follow from certain elements of symmetry such as rotation axes, mirror planes and centers of inversion. The total number of possible combinations of the symmetry elements found in crystals is 32. Hence, there exist 32 point-groups defining the 32 crystal classes. There are only seven crystal systems but each system contains several classes representing different degrees of symmetry.

The packing of the primary building stones is of the greatest importance in determining the crystal structure of a substance. Once the spatial requirements of the packing have been satisfied, the effect of cohesive forces or bonding must also be considered. There are two theoretical treatments with respect to bonding (64).

The crystal structure is pictured as a regular arrangement of atoms, each with electrons used to form bonds with surrounding atoms. The bonds may be:

(1) The Van der Waals-London bonds. These bonds are the result of second order forces between neutral atoms or molecules that are due to the polarization of one atom or molecule by the fluctuation of the charge distribution in a second, and vice versa.

(2) The ionic bonds. This is the type of bond that exists in the NcCl molecule. The ionic bond is spherically symmetric with no preferred direction. An ion will be surrounded by as many oppositely charged ions as is geometrically possible, provided that over-all electrical neutrality is satisfied.

(3) The covalent bonds. These bonds result from the sharing of electrons between atoms. They extend in three dimensions and may lead to a variety of crystal structures depending on the constituent atoms. The diamond crystal is an example of this type of bond.

(4) Intermediate type bonds. Bonds of this type arise from resonance between covalent and ionic bonds. Examples are the structures of the silver halides.

(5) The hydrogen bond. This type of bond is important in many crystal structures. Examples are certain inorganic and organic acids, salt hydrates and ice.

(6) The metallic bond. This is closely related to the covalent bond. There are more orbitals available for bond formation than electrons to fill them. The covalent bonds thus oscillate among the available positions. Another picture of the metallic structure is that of a lattice of separate metal ions surrounded by an electron gas. A ready flow of electrons will take place when an electric field is applied.

The band model theory assumes an arrangement of nuclei at their appropriate spacings. The total number of available electrons is poured into the resultant force field. The electrons will arrange themselves in bands of energy around the nuclei; each atomic orbital contributing one level to a band. In partially filled upper bands, the electrons may readily move from one level to an unfilled level within the band, giving rise to current flow when an electric field is applied. If the outermost bands of the nuclei overlap, the electrons can flow freely through the whole structure. For nuclei arranged at the points of a perfectly periodic lattice, there will be no resistance to the flow of an electric current. The perfect periodicity is disturbed by thermal vibrations of the lattice nuclei and also by introducing foreign atoms in the structure (alloys). This is the picture for conductors of electricity or metals.

Insulators have completely filled lower bands with a wide energy gap between the outermost filled band and the lowest empty band. Semiconductors have, in addition to the normal bands, also narrow impurity bands which are either unfilled levels closely above a filled band or filled levels below an empty band. The extra levels are a result of foreign atoms or departure from the ideal stoichiometric composition.

Conduction in Crystals. According to the Nernst theorem, the specific heats of elements and compounds becomes zero at or close to the absolute zero temperature. For solid elements, the atomic heats increase slowly from zero temperature to a temperature of 10 or 15 deg k, hence more rapidly; subsequently, they pass through a turning point and finally tend to reach asymptomatically an end value of 6 - 6.4 cal

according to the rule of Dulong and Petit. This rule, however, is only approximate. The atomic heat of cobalt reaches a value of 12 calories at 1,000 deg C while those of elements possessing atomic weights of less than 30 show slower increase with temperature. Immediately above the absolute zero point, the atomic heats are proportional to the third power of the temperature. The mole heats of compounds can be calculated approximately from the atomic heats of the components in accordance with Kopp's rule. The specific-, atom-, and mole-heats are important with respect to thermal diffusivity or thermometric conduction in addition to their theoretical

TABLE 5

VARIATION OF THERMAL CONDUCTIVITIES OF CRYSTALS
with Absolute Temperature k in watt/square cm °C per cm

Crystal	°K Temperature	k	Crystal	°K Temperature	k
Quartz	373	0.0902	Rock salt NaCl	373	0.0485
parallel to axis	273	0.1360		273	0.0698
	195	0.1960		195	0.1043
	88	0.4660		83	0.2666
	83	0.490	Potassium Chloride	373	0.0492
Perpendicular	373	0.0559	KCl	273	0.0698
to axis	273	0.0726		195	0.1041
	195	0.1010		83	0.2103
	83	0.246		23.1	0.478
	21	2.51		22	0.510
Calcite perpendicular to axis	374	0.0357		21	0.572
$CaCO_3$	273	0.0430	Corundum	273	0.104
	195	0.0577	Al_2O_3	373	0.0865
	83	0.1586		473	0.0692
Mullite	273	0.059		673	0.0588
$3\,Al_2O_3 \cdot 2SiO_2$	373	0.052		873	0.0519
	673	0.0346		1,073	0.0466
	1,073	0.0294		1,273	0.0415

From Eucken (30) Eucken (28) Jakob (43)

importance.

According to the trend of the specific heat near the absolute zero temperature, atoms and molecules have very little thermal motion at very low temperatures. It is logical to expect that the coefficient of thermal conductivity also becomes zero at the absolute zero temperature. Theoretical treatment of heat transfer is based on the assumption that the flow of energy between neighboring locations is proportional to the gradient of the internal energy. The heat flow through a unit area in the x-direction can be written as (43):

$$q = -B\frac{du}{dx} = -B\frac{du}{dT} \cdot \frac{dT}{dx} = -B\,c_v\frac{dT}{dx}$$

where

u = internal energy

c_v = specific heat at constant volume

B = constant

By definition:

$$q = - k \cdot \frac{dT}{dx}$$

It follows, therefore, that $\frac{C_v}{k}$ should be a constant. This is very roughly the case for quartz glass but not for quartz crystals.

Another mechanism must, therefore, exist which opposes that of the specific heat and which prevails at low temperatures. Eucken (30) found that the thermal conductivity of crystals decreased with increase in temperature at a rate almost inversely proportional to the absolute temperature (see Table 5).

According to Debye (20) the heat transfer in solids from hot to cold regions is by means of thermo-elastic waves. Bragg visualized the crystalline structure as atoms linked together by springs. Vibrations caused by heat displace the atoms from their normal position and thereby propagate the heat energy. The waves are of two kinds, namely, compressional and distortional, propagated with different velocities. Many simultaneous wave trains exist which are unharmonic and, therefore, give rise to disturbances which greatly increase with temperature. The most important of the disturbances is the heat motion of the crystal lattice itself; this may control the dependence of heat conduction upon temperature. The disturbances cause a scattering of the waves analogous to that of light in an opaque medium. The mean free path λ_s is defined as that distance in which the energy waves have been scattered in a ratio $\frac{1}{e}$ where e is the base of the natural logarithms. Debye derived the following equation for the thermal conductivity: $k = \frac{1}{4} \lambda_s W_s \rho_s c_v$, where W_s is the average propagation of the elastic waves, defined by:

$$W_s = \sqrt{\frac{M}{\rho_s}}$$

$$M = \frac{\Delta p}{\frac{\Delta V}{V}} = \text{bulk modulus}$$

ρ_s = density, and

c_v = specific heat of solid.

The evaluation of λ_s, the distance of comparatively free passage of the thermal waves, is rather difficult. Debye obtained λ_s numerically by expressing the mutual influence of the waves by the coefficients of thermal expansion and of mechanical compressibility. He showed that λ_s is almost proportional to $\frac{1}{T}$ from the fact that the thermal oscillations and, therefore, the wave disturbances decrease with decreasing temperature.

Meissner (60) pictured the crystal as a chain of many slightly damped oscillators, turned to the same frequency and coupled very loosely. These chain links have to be incited one after another and, because of the great number of elementary oscillators, it follows that they must be very loosely coupled and very slightly damped. These waves can exist only in crystals.

Experiments by de Haas and Biermasz (22) on quartz crystals, extending down to 2.77 deg K showed that the thermal conductivity of quartz reaches a maximum at about 10 deg K. The trend in the conductivity curve is towards zero at the absolute zero point. From measurements on KCl rods of different cross-sections and from different samples, de Haas and Biermasz (23, 22) concluded that the dimensions of the rods have an influence on the specific thermal resistance of a crystal. For thinner rods the resistance was more than for the thicker ones. The same was found in the case of quartz crystals. Table 6 and Figure 3, taken from de Haas and Biermasz's papers illustrate their conclusions. A discussion by Makinson (56) of the factors

determining the conductivity of real crystals may be used to explain the deviations from the theory of Debye. He considers that the scattering of the thermal waves is also produced by irregularities of atomic dimensions as would be caused by impurities and by large-scale interruptions of the lattice such as grain boundaries. A free path is defined for each of these sources of scattering. At high temperatures, the effective wave-lengths of the thermal waves are so short that the various lattice impurities have almost no influence upon the scattering, which is primarily due to lattice motion. The conductivity will then be approximately inversely proportional to the absolute temperature.

With decrease in temperature the effective wave-lengths increase, the effect of the lattice motion diminishes and conduction is limited first by small-scale irregularities and at very low temperatures by the size of the crystal itself. Figure 4, taken from Makinson's paper illustrates these points.

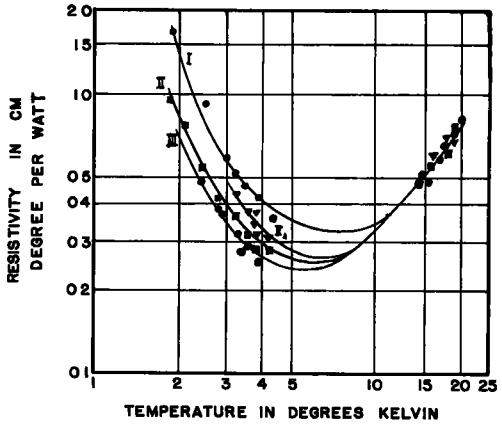

Figure 3. Thermal resistivity at low temperature (after de Haas and Biermasz).

At very low temperatures, the conductivity is limited by reflection of the thermal waves at the boundaries of the crystal grains. The smaller the grains, the higher is the temperature at which this condition becomes important. Scattering by irregularities or impurities of atomic dimensions reduces the conductivity below the value determined by lattice motion alone. The whole picture is still rather qualitative since it is not possible to fix precise temperatures and proportions of the curve for actual crystals. Furthermore, De Haas and Biermasz (23) have indicated that for a perfect crystal such as diamond the conductivity starts decreasing at a higher temperature than would have been believed from Makinson's concept. Measurements by Eucken (28) show results similar to those of De Haas and Biermasz; the conductivity of diamond is relatively temperature-independent or at least much less temperature conditioned than that of some other pure crystals. In Table 7 the average of three determinations by Eucken (28), De Haas and Biermasz (23) is presented; as a matter of interest, conductivity values for an Acheson graphite are also included (43).

Conduction in Metals. As in non-metallic crystalline substances, the thermal conductivity of metals increases with decreasing temperature (see Table 8).

At low temperatures, Eucken's equation can be applied:

$$\frac{k}{k_0} = \frac{T_0}{T}$$

where the subscript o relates to 0°C. By differentiation one obtains:

$$\frac{dk}{dT} = -\frac{k_0 T_0}{T^2}$$

At high temperatures, impurities in the metals may cause k to pass through a

TABLE 6

DE HAAS AND BIERMASZ' DATA SHOWING THE INFLUENCE OF THE ROD DIMENSIONS ON RESISTIVITY

w in deg C cm/watt

KCl rods, square with side length d								Quartz SiO_2 perpendicular to axis			
d = 0.763 cm		d = 0.511 cm		d = 0.383 cm		d = 0.252 cm		Diameter 0.454 cm		Diameter 0.216 cm	
T(°k)	w	T(°k)	w	T(°k)	w	T(°k)	w	T(°k)	w	T(°k)	w
19.27	0.721	19.83	0.758	19.25	0.778	19.24	0.730	19.81	0.266	20.12	0.270
18.59	0.693	17.29	0.637	17.99	0.668	17.93	0.674	17.75	0.213	18.80	0.236
16.95	0.611	16.38	0.596	17.05	0.647	16.41	0.590	16.75	0.182	17.17	0.196
15.12	0.493	14.73	0.498	15.77	0.570	14.83	0.507	15.99	0.164	15.82	0.167
3.90	0.262	4.12	0.280	4.18	0.290	4.28	0.360	15.40	0.146	15.11	0.151
3.66	0.290	3.86	0.285	3.88	0.31	3.91	0.419	4.10	0.331	4.62	0.435
3.51	0.286	3.50	0.311	3.75	0.36	3.55	0.472	3.83	0.386	3.81	0.66
3.31	0.322	3.17	0.352	3.69	0.34	3.32	0.527	3.47	0.439	3.45	0.82
2.94	0.379	2.83	0.411	3.52	0.36	3.02	0.620	3.13	0.551	3.10	1.06
2.90	0.388	2.46	0.537	3.30	0.44	2.49	0.921	2.68	0.745	2.73	1.37
2.47	0.495	1.87	0.973			1.92	1.67	2.32	1.066	2.37	2.09
										2.20	2.56
										1.80	4.54
										1.67	5.85

TABLE 7

THE THERMAL CONDUCTIVITY k OF DIAMOND AND ACHESON GRAPHITE

Diamond				Graphite	
De Haas and Biermasz		Eucken		Jacob (43)	
Temp °K	k watt/cm°C	Temp (°K)	k watt/cm°C	Temp °K	k watt/cm°C
89.4	14.3	345	1.53	123	1.78
20.6	8.3	273	1.51	273	1.75
18.8	7.5	196	1.55	423	1.70
17.0	5.89	88	1.27	573	1.54
15.8	5.14	21	0.92	773	1.26
14.9	4.45	These values obviously		973	0.93
14.0	3.33	are too low as indicated			
12.8	3.18	by the investigator.			
11.5	2.86				
4.21	0.222				
3.59	0.154				
2.99	0.126				

minimum with increasing temperature. With some non-metallic solid bodies such as carborundum bricks, a maximum has been observed for the k-values as a function of temperature. Both kinds of behavior can be derived from the equation

$$k = \frac{1}{aT + b + \frac{c}{T}} .$$

The constants a, b and c of the equation depend on the mixture of crystals and amorphous constituents and on the absolute values of their conductivities. These

constants may be found from measurements of k at three different temperatures. Impurities of metals must be considered as disturbances of the lattice structure.

Metallic single crystals have much higher conductivities than ordinary crystalline metals and a much steeper increase of k with decreasing temperature. A sudden drop occurs when the metal is melting, a behavior which corresponds with that of melting non-metallic crystalline substances.

There exists a simple relation between the thermal and electrical conductivity of most pure metals. It is expressed in the Wiedemann-Franz-Lorenz equation:

$$L = \frac{k}{k_e T} = \text{constant}$$

where

k = thermal conductivity
k_e = electrical conductivity
T = absolute temperature
L = so-called Lorenz number

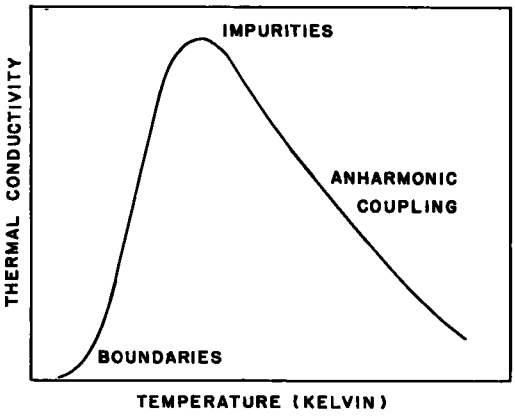

Figure 4. Variation of conductivity with temperature in dielectric crystals (after Makinson).

Drude (26) assumed that both the thermal and electrical conductances in metals are due to free electrons inside the metal which behave like gas molecules and move freely across the lattice of ions that form the skeleton of a metal. He derived an equation for the thermal conductivity of this electron gas analogous to that of a real gas. An expression for the electrical conductivity is known from the ordinary theory of electrons. The comparison leads to:

$$L = \frac{k}{k_e T} = 3\frac{(\bar{k})^2}{(\epsilon)} = \text{constant}$$

where

$\bar{k}$ = Boltzmann constant = $\frac{R}{N}$

ϵ = elementary charge of an electron

TABLE 8

THERMAL CONDUCTIVITY OF METALS
in watt/cm^2 ^{0}C per cm

Metal	Copper	Tin	Zinc	Nickel	Iron	Aluminum	Lead
Impurities	0.1	.03	0.2	0.1	0.1		.002
Temperature percent							
-200	5.36	0.845	1.21	1.16	1.002	2.60	0.444
-100	4.06	0.737	1.16		0.753	2.34	0.386
0	3.89	0.670	1.123	0.838	0.719	2.25	0.373
100	3.80	0.633	1.09	0.822	0.684	2.25	0.348
200	3.72	0.600	1.055	0.735	0.615	2.25	0.338
400	3.65	0.330[a]	0.934	0.588	0.485	2.25	0.15[a]
600	3.54		0.58[a]	0.648	0.398		0.14[a]

[a]Molten

Refinement of the theory leads to a factor 3.3 instead of 3.

The deviations of L for pure metals are not great but for alloys they are. The deviations are explained by the fact that in addition to the proper metallic thermal conductivity which may be proportional to the electrical conductivity, a non-metallic thermal conductivity of the lattice must also be considered, such as in electrical non-conductors. Its influence will be the greater, the smaller is the electrical conductivity of the material. Thus, for poor electrical conductors L should be very large. For

TABLE 9

LORENZ NUMBER L FOR SOME METALS AND ALLOYS
(taken from Jakob (43))

Metal	in 10^{-9} volt^2/C^2	Alloy	in 10^{-9} volt^2/C^2
Al	22.3	92% Al + 8% Cu	16.5
Cu	22.3	77% Mg + 20% Cu + 3% Si	19.0
Ni	23.3	82% Cu + 18% Zn	26.5
Zn	24.1	Steel with 1% C	27.7
Pb	24.7	86% Al + 14% Mg	28.3
Pt	25.1	88% Mg + 12% Al	35.8
Solid Hg	28.0	70% Cu + 30% Mn	44.0

Note: C is degree Centigrade or Kelvin

TABLE 10

RELATIVE VALUES OF a, b AND c FOR VARIOUS MINERALS
(from Thelen)

Isometric	All minerals	c 1.00	a 1.00	b 1.00	D
Tetragonal	Rutile	0.79	1.00	1.00	
	Zircon	0.90	1.00	1.00	
	Scapolite	0.85	1.00	1.00	
	Vesuvanite	0.95	1.00	1.00	
Hexagonal	Quartz	0.76	1.00	1.00	
	Specularite	1.10	1.00	1.00	
	Dolomite	1.05	1.00	1.00	
	Apatite	0.96	1.00	1.00	
	Tourmaline	1.15	1.00	1.00	
	Calcite	0.91	1.00	1.00	
Orthorhombic	Borite	1.00	1.06	1.03	
	Anhydrite	1.00	0.971	0.943	
	Staurolite	1.00	0.97	0.901	
Monoclinic	Tremolite	1.00	0.60	0.75	-5^0
	Hornblende	1.00	0.71	0.80	
	Epidote	1.00	0.93	1.09	-14.5^0
	Gypsum	1.00	0.80	0.65	$+17^0$

L-values of some pure metals and alloys see Table 9.

The influence of temperature upon L is not great. Between 0^0 and 900^0C, increments of 15, 12 and 26 percent have been observed with Swedish iron. The electrical superconductivity of metals at low temperatures has no thermal analogy.

Influence of Crystal Structure on Conductivity. The theories of the mechanism of heat transfer through solids presented this far, are applicable only to isotropic crystals or crystals in the regular (cubical) system. As was mentioned previously the thermal conductivity and other physical properties of the crystals vary along dissimilar crystal axes.

The anisotropism of crystals with respect to thermal conductivity was first extensively investigated by de Senarmont (24). His experimentations included quartz and a great number of other minerals. The wax-figure technique used by him was originated by Ingen-Houtz (42). Thin slices of crystal are covered with wax and perforated by a hole; through the latter a heated silver tube is passed. When the wire or tube is heated, the wax melts away from the hole at a rate proportional to the thermometric conductivity a of the crystal in the direction under consideration:

$$a = \frac{k}{\rho c_p}$$

where

k = thermal conductivity coefficient

ρ = density of the crystal

c_p = specific heat of the crystal

De Senarmont found spherical heat conductivity wax figures for the isometric system. For the tetragonal and hexagonal systems oblate or prolate ellipsoids of revolution (the c-axis being axis of revolution) were obtained. The orthorhombic, monoclinic and triclinic systems gave triaxial ellipsoids in all cases. In the orthorhombic system the three axes were parallel to the crystallographic axes. In the monoclinic system one axis was parallel to the orthodiagonal and in the triclinic no axis corresponded to any of the crystallographic axes.

If we designate the lengths of the axes of the isothermal ellipsoids by a, b and c (being in the same direction as the crystallographic axes in the orthorhombic system) we have:

$$a^2 = a_{11} = \frac{k_{11}}{c_p}; \quad b^2 = a_{22} = \frac{k_{22}}{c_p}; \quad c^2 = a_{33} = \frac{k_{33}}{c_p}$$

The ratios of a, b and c for minerals in the different systems are given in Table 10 taken from Thelen (94).

In the monoclinic system c signifies the length of the ellipsoidal axis paralled to the axis of elasticity which lies nearest to the crystallographic c-axis. The column headed D gives the position of the ellipsoidal c-axis with respect to the crystallographic c-axis. For a positive value of D the axis lies in the obtuse angle between the c-axis and the a-axis or clinodiagonal. The numbers show the magnitude of deviation from the c-axis. The third column indicates values parallel to the crystallographic b-axis. The second column indicates values along a line perpendicular to b; and the direction of c is indicated in the first column.

The equation for heat conduction in one direction was given as:

$$Q_x = -k\frac{dt}{dx}$$

where Q_x is called the "heat flux," "density of heat," or "intensity of the heat current."

The general equation for heat flow in a crystal (83) (91) (97) (44) is derived later on. For homogeneous isotropic bodies the direction of the heat flow is perpendicular to the isothermal planes in the body. In a nonisotropic crystal, the direction of the heat flux coincides with n, the normal to the isothermal planes, only when n is an axis of symmetry of the crystal.

When temperature differences exist from point to point in the crystal we may choose X, Y, Z as fixed rectangular coordinates with Q_X, Q_y, Q_Z and dt/dx, dt/dy, dt/dz the components of heat flux and temperature differences, respectively, in the chosen directions. The components of the heat flow will depend not only on the temperature differences in their respective directions but also on the temperature differences in the other two directions. From this the "fundamental law" of heat flow is derived.

$$-Q_X = k_{11}\frac{\partial t}{\partial x} + k_{12}\frac{\partial t}{\partial y} + k_{13}\frac{\partial t}{\partial z}$$

$$-Q_y = k_{21}\frac{\partial t}{\partial x} + k_{22}\frac{\partial t}{\partial y} + k_{23}\frac{\partial t}{\partial z}$$

$$-Q_Z = k_{31}\frac{\partial t}{\partial x} + k_{32}\frac{\partial t}{\partial y} + k_{33}\frac{\partial t}{\partial z}$$

The nine constants k_{11} to k_{33} are called the internal heat conductivities. They depend on the nature of the substance and the orientation of the coordinates. With increasing symmetry of a crystal the number of constants required for complete description of the thermal flux decreases, becoming one in the cubic system. The number of parameters required for the different crystal systems is shown in the following:

(1) All crystals in the cubical system:

$$a = b = c, \quad \alpha = \beta = \gamma = 90^0$$

$$-Q_X = k\frac{\partial t}{\partial x}; \quad -Q_y = k\frac{\partial t}{\partial y}; \quad -Q_Z = k\frac{\partial t}{\partial z}$$

(2) Anisotropic crystals with one isotropic axis and two-valued symmetry axes perpendicular to it.

$$a = b, \quad c, \quad \alpha = \beta = \gamma = 90^0$$

$$-Q_X = k_{11}\frac{\partial t}{\partial x}; \quad -Q_y = k_{11}\frac{\partial t}{\partial y}; \quad -Q_Z = k_{33}\frac{\partial t}{\partial z}$$

(3) Anisotropic crystals with one isotropic axis but no other symmetry axis.

$$a = b, \quad c, \quad \alpha = \beta = 90^0 \quad \gamma = 120^0$$

$$-Q_X = k_{11}\frac{\partial t}{\partial x} + k_{12}\frac{\partial t}{\partial y}; \quad -Q_y = k_{12}\frac{\partial t}{\partial x} + k_{11}\frac{\partial t}{\partial y}$$

$$-Q_Z = k_{33}\frac{\partial t}{\partial z}$$

(4) All rhombic crystals. They have the coordinates in the direction of the crystallographic axes.

$$a, \quad b, \quad c, \quad \alpha = \beta = \gamma = 90^0$$

$$-Q_X = k_{11}\frac{\partial t}{\partial x}; \quad -Q_y = k_{22}\frac{\partial t}{\partial y}; \quad -Q_Z = k_{33}\frac{\partial t}{\partial z}$$

(5) All monoclinic crystals. When the Y-axis coincides with the b-crystallographic symmetry axis.

$$a, \quad b, \quad c, \quad \alpha = \beta = 90^0; \quad \gamma \quad 90^0$$

$$-Q_X = k_{11}\frac{\partial t}{\partial x} + k_{13}\frac{\partial t}{\partial z}; \quad -Q_y = k_{22}\frac{\partial t}{\partial y}$$

$$-Q_Z = k_{31}\frac{\partial t}{\partial x} + k_{33}\frac{\partial t}{\partial z}$$

(6) All triclinic crystals.

$$a,\ b,\ c,\ \alpha \neq \beta \neq \gamma \neq 90^0$$

The general equation applies in this case.

If a heat source exists in a homogeneous crystal of infinite extent, the general equation will be applicable. Stokes (91) indicated that the stream lines for classes 3, 5 and 6 will not proceed in straight lines but in spatial spirals. Voigt (97) found from experiments on two apatites and dolomites that the differences $k_{23} - k_{32}$, $k_{13} - k_{31}$, $k_{12} - k_{21}$ are almost zero or so small that their real value cannot be determined accurately.

As shown previously: $Q_n = k_n \frac{\partial t}{\partial n}$. In this equation k_n changes with the direction n as the reciprocal square of the radius vector of a fixed ellipsoid. If $k_{23} = k_{32}$, $k_{13} = k_{31}$, $k_{12} = k_{21}$, the equation of the ellipsoid will be:

$$k_{11}x^2 + k_{22}y^2 + k_{33}z^2 + 2k_{23}yz + 2k_{31}zx + 2k_{12}xy = 1.$$

If the coordinates x, y, z are the main axes of this ellipsoid, then the equation becomes:

$$k_{11}x^2 + k_{22}y^2 + k_{33}z^2 = 1\ ;$$

and if the general equation is determined for the same coordinates, then:

$$-Q_x = k_{11}\frac{\partial t}{\partial x}\ ;\ Q_y = k_{22}\ \frac{\partial t}{\partial y}\ ;\ -Q_z = k_{33}\frac{\partial t}{\partial z}\ .$$

In the cubical system an infinite number of coordinate orientations exists which is independent of temperature. The heat conductivity is then expressed by one value of k.

For crystals in the hexagonal, rhombohedric and tetragonal systems the position of the main axes is fixed. This orientation is not temperature dependent. The heat conductivity is characterized by two values k_{11} and k_{33}. The axes coincide with the crystallographic axes.

The main axes in the rhombic system are also fixed and temperature independent; k_{11}, k_{22} and k_{33} express the main heat conductivities. The main axes correspond with the three crystallographic axes.

In the monoclinic system only one main conductivity axis is independent of the temperature – this axis corresponds to the crystallographic b-axis. The other two axes are temperature dependent and their direction must be given by the angle which they make with the crystallographic c-axis. In addition, the heat conductivity values are given by k_{11}, k_{22}, k_{33} (the main heat conductivities).

The three main conductivity axes in the triclinic system are all temperature dependent. The heat conductivity is characterized by k_{11}, k_{22}, k_{33} and the positions of the three axes by their relation to the three crystallographic axes.

The equation for the isothermal ellipsoid in a crystal is given by (44):

$$\frac{x^2}{k_{11}} + \frac{y^2}{k_{22}} + \frac{z^2}{k_{33}} = 1,$$

where the axes of the ellipsoid will be $\sqrt{k_{11}}$, $\sqrt{k_{22}}$, and $\sqrt{k_{33}}$, respectively. The isothermal ellipsoid is not to be confused with the heat conductivity ellipsoid as given previously.

If we consider the heat energy in an element (dx, dy, dz) of the material during the time element $d\tau$, the requirements for equilibrium are:

Total heat entering the element + Heat energy developed in the element	=	Total heat leaving the element + Heat energy stored in the element

This consideration leads to the equation:

$$\rho c_p \frac{\partial t}{\partial \tau} = \left(k_{11} \frac{\partial^2 t}{\partial x^2} + k_{22} \frac{\partial^2 t}{\partial y^2} + k_{33} \frac{\partial^2 t}{\partial z}\right) + q'$$

in which:

ρ = density

c_p = specific heat at constant pressure

q' = heat developed per unit volume and in unit time.

The thermal conductivities k_{11}, k_{22} and k_{33} are considered to be independent of temperature. If they are temperature dependent the equation becomes:

$$\rho c_p \frac{\partial t}{\partial \tau} = \frac{\partial}{\partial x} \left(k_{11} \frac{\partial t}{\partial x}\right) + \frac{\partial}{\partial y} \left(k_{22} \frac{\partial t}{\partial y}\right) + \frac{\partial}{\partial z} \left(k_{33} \frac{\partial t}{\partial z}\right) + q'$$

For the steady state with no heat evolution in the body and heat conductivities constant we obtain:

$$k_{11} \frac{\partial^2 t}{\partial x^2} + k_{22} \frac{\partial^2 t}{\partial y^2} + k_{33} \frac{\partial^2 t}{\partial z^2} = 0.$$

The mathematical treatment does not include the nature and extent of the influence various factors have on the absolute value of the thermal conductivity. Birch and Clarke (8) concluded that at relatively high temperatures a more correct statement of the experimental data is that the thermal resistivity tends to increase linearly with temperature and not directly proportional as was approximated by Eucken (30). From experiments on quartz crystals Birch and Clarke found that the conductivity does not decrease as rapidly as the theory would predict; indicating the possibility of some factor not included in the theory of Makinson. On some feldspar aggregates the conductivity increased with temperature – a phenomenon which is attributed to some crystalline imperfection and not completely to aggregation as was suggested by Eucken and Kuhn (32).

It is accepted that very fine imperfections may exist in crystals but the extent, degree of regularity and amount of disorientation in supposedly perfect crystals are not yet completely evaluated. It has been proposed that the mentioned factors are dependent upon the conditions of crystal growth and the mechanical and thermal history of the crystals. Evidence of the dependence of the conductivity even to high temperatures upon the fine-structure was presented by Powell and Griffiths (76). They found the thermal resistance of certain micas across the basal planes to decrease when the planes were pressed together as shown in Table 11. Wood (102) discovered, by means of x-rays, that the irreversible decrease of conductivity when mica is heated over 200 deg C (see Fig. 5) was due to the breaking up of the original mica structure into a group of small regions which were tilted from their original positions. Birch and Clarke obtained values of the conductivity of rocksalt at temperatures where impurities and imperfections should have very little effect. The resistivity was very closely a linear function of the temperature but the absolute values were much lower than those reported by Eucken and Kuhn from tests on crystals grown artificially from melts and solutions. Birch and Clarke concluded that the effect of fine-structure must persist to higher temperatures than was supposed previously.

Wooster (103) attempted to correlated the anisotropies in the thermal conductivity of crystals with their structure. For this purpose the crystals were divided into three groups:

(a) Crystals having bonds of about the same strength in the different directions. He assumes that the three principal conductivities k_1, k_2, k_3 are given by $\sum S \cos^2 \theta_1$, $\sum S \cos^2 \theta_2$ and $\sum S \cos^2 \theta_3$ respectively. The summation is taken over all the bonds in the unit cell; S is the number of equivalent bonds which makes angles θ_1, θ_2 and θ_3 with the principal axes.

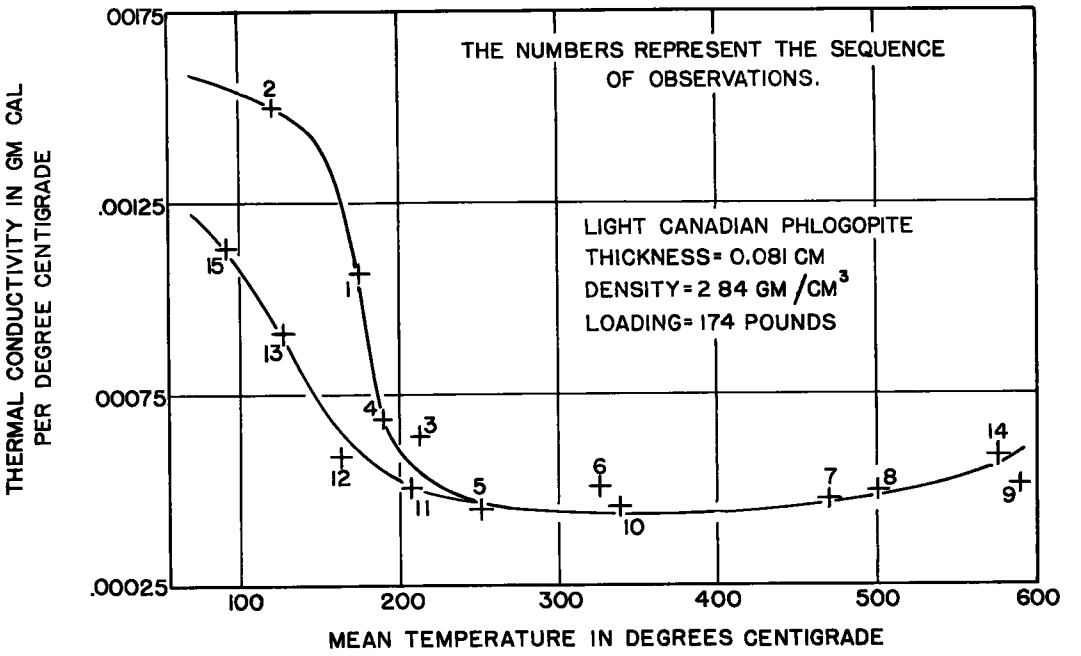

Figure 5. Temperature effect on a light Canadian phlogopite.

(b) Crystals having layered lattice structures; the conductivity in the plane of the layer is greater than that perpendicular to it.

(c) Crystals of the chain lattice type: the conductivity along the chains is greater than that perpendicular to it. The theory of Wooster was applied only to the first group but not to the second and third groups due to the inadequacy of the experimental data.

Thermal conductivity increases when magnesium (in dolomite) is substituted for calcium (limestone), which is explained according to the Debye theory as due to increase in density and sound velocity. The dense ultrabasic minerals having high elastic constants and high sound velocities give high conductivities as compared with the feldspars. Quartz, however, has a higher heat conductivity than either the ultrabasic silicates or the feldspars despite its lower density. To what extent this is due to the greater perfection of the quartz crystals is not known.

With increase in temperature the anisotropism in crystals with respect to thermal conductivity decreases as shown in Figure 6 taken from Birch and Clarke.

HEAT CONDUCTION IN HETEROGENEOUS SUBSTANCES

Conduction in Aggregates

The primary factors in the thermal conductivity of homogeneous aggregates are the conductivity of the single crystals and the thermal contact between them. However, to determine the average conductivity of a specimen containing a large number of crystals oriented at random it would be impracticable to attempt any rigorous computation. An average value for random orientation is obtained by averaging the conductivity value over-all direction for a single crystal. When the conductivity of a crystal does not vary greatly in different directions, then the average conductivity will not be very much different from the reciprocal of the average resistivity; for anisotropic crystals, however, they cannot be equal.

It was pointed out previously that the conductivity k_n in the direction n changes with the direction like the reciprocal square of the radius vector of a fixed ellipsoid. If for crystals having a principal axis the equation of the ellipsoid is expressed in

polar coordinates, then the thermal conductivity k_n is given according to Voigt (97) by:

$$k_n = k_{\perp} \sin^2 \beta + k_{||} \cos^2 \beta$$

where β is the angle between the principal axis and the given direction, $k_{\perp}$ and $k_{||}$ the thermal conductivities perpendicular and parallel, respectively to the principal axis.

By taking the averages of $\sin^2 \beta$ and $\cos^2 \beta$ over all directions an average value of k is obtained.

$$(\sin^2 \beta)\ \text{av.} = \frac{2}{3} \text{ and } (\cos^2 \beta)\ \text{av.} = \frac{1}{3}\ ;\ k_n = \frac{2}{3} k_{\perp} + \frac{1}{3} k_{||}\ .$$

The equation gives the conductivity of a single layer of crystals oriented at random,

TABLE 11

EFFECT OF PRESSURE ON THE THERMAL CONDUCTIVITY OF A MADAGASCAN DARK AMBER PHLOGOPITE
(after Powell and Griffith)

Pressure lb/sq in.	Thickness cm	Density gm/cm^3	Conductivity watt/cm^2 °C per cm 100°C	300°C	500°C
23	0.109	2.80	0.0046	0.0021	0.0021
48			0.00586	0.00252	0.00252
176	0.105	2.90	0.0067	0.00335	0.00377
330			0.00755	0.0046	0.00503

TABLE 12

MEAN CONDUCTIVITY OF QUARTZ AND CALCITE CRYSTALS
(in watt/sq cm °C per cm)

Temp., °C	Calcite				Quartz			
	$k_{\perp}$	$k_{||}$	k_{mean} $\sqrt[3]{k_{\perp}^2 k_{||}}$	k_{mean} $\frac{1}{3}(k_{||}+2k_{\perp})$	$k_{\perp}$	$k_{||}$	k_{mean} $\sqrt[3]{k_{\perp}^2 k_{||}}$	k_{mean} $\frac{1}{3}(k_{||}+2k_{\perp})$
-190	0.1845	0.3070	0.2182	0.2253	0.2455	0.490	0.309	0.327
0	0.0348	0.401	0.0365	0.0366	0.0684	0.1142	0.0811	0.0833
50	0.0301	0.0340	0.0313	0.0314	0.0565	0.0940	0.0670	0.0690
100	0.0272	0.0300	0.0281	0.0281	0.0495	0.0796	0.0580	0.0595
200	0.0238	0.0256	0.0244	0.0244	0.0407	0.0632	0.0471	0.0482

with heat flow perpendicular to the plane. On substituting the resistivity values for the various conductivities in the equation, the mean resistivity of a crystal can be calculated. The reciprocal of this mean resistivity is the conductivity of a filament of randomly oriented crystals placed on top of each other with the heat flowing along the filament. An aggregate may be considered to be composed of a great number of filaments or layers. Neither of these treatments is correct; for nearly isotropic minerals their results will approach each other but they will differ considerably in heterogeneous aggregates of minerals of greatly differing conductivities. The method is considered

chiefly because of its simplicity. Eucken and Kuhn (32) used the formula

$$k_{mean} = 3\sqrt{k_{\perp}^{2}\, k_{||}}$$

to calculate the mean conductivity k_{mean} of calcite. It may not be applicable to other minerals.

From measurements on natural crystals, crystals grown from melts and solutions, and on aggregates either natural or artificially pressed from crystals powders, Eucken and Kuhn attempted to determine the effect of the grain size on the thermal conductivity. They found that the experimental data obeyed approximately the following empirical equation:

$$k = \frac{k_0}{nB + 1}$$

in which

k = conductivity of the crystalline material

k_0 = conductivity of the compact crystal

n = number of grains per cm, and

$$B = \frac{T_S}{T_0} = \frac{\text{Temperature difference between adjacent grain surfaces}}{\text{Temperature decrease per cm length}}$$

It was indicated that the quality $\frac{BC_V}{k_0}$ is approximately temperature independent.

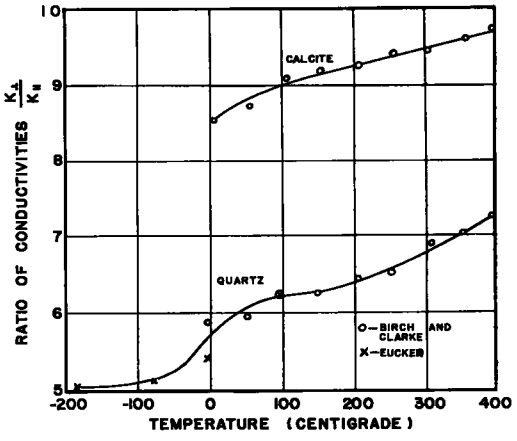

Figure 6. Variation with temperature of the ratio of conductivities perpendicular and parallel to the optic axis in quartz and calcite.

The formula does not apply for aggregates consisting of particles of one component crystallizing in the regular system.

According to data obtained by Birch and Clarke from tests on a marble, the value of B, the constant in Eucken and Kuhn's formula, varies proportionally with the size of the crystals. These authors (8) suggested that the reduced conductivity in the aggregates is due to spaces of relatively low conductivity between some crystals. Sample calculations are shown in Tables 12 and 13.

TABLE 13

VALUES OF B ACCORDING TO EUCKEN AND KUHN'S FORMULA

Temp.	k ideal	Marble						Limestone					
°C	Calcite	k	n	B	k	n	B	k	n	B	k	n	B
-190	0.218	0.0423	138	0.030	0.0563	103	0.028	Birch and Clarke's					
0	0.0478	0.0351	138	0.0026	0.0373	103	0.0027						
0	0.0366	Eucken and Kuhn's Data						0.0305	30	0.0067	0.0302	5,000	4×10^{-5}
50	0.0314							0.0268	30	0.0057	0.0257	5,000	4.4×10^{-5}
100	0.0281							0.0244	30	0.0050	0.0232	5,000	4.2×10^{-5}
200	0.0244							0.0214	30	0.0047	0.0200	5,000	4.4×10^{-5}

Mixed Aggregates

The shortcomings of the theory regarding the thermal conductivity of pure crystals, even in the regular system, point out the difficulties to be overcome in the development of a theory for the thermal conductivity of aggregates consisting of more than one component.

Mixed aggregates still exhibit a negative temperature coefficient like the crystals of which they are composed. However as Eucken and Kuhn (32) have pointed out, mixed crystalline aggregates cause a marked decrease in the absolute value of the thermal conductivity and in the negative temperature coefficient of the constituents crystals. From mixed crystals of KCl with various percentages of KBr, they determined the deviation of the measured values from the calculated ones using the mixing formula:

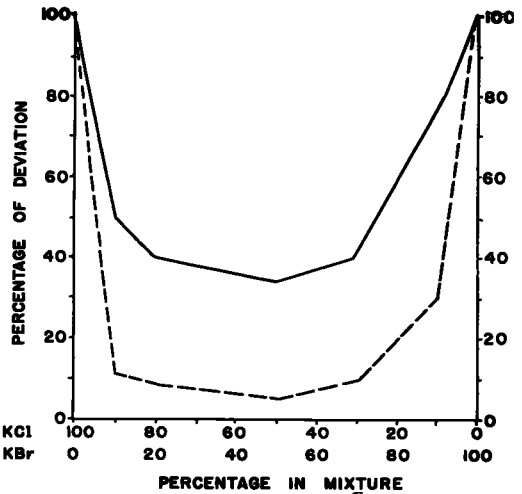

Figure 7. The deviation of the measured values from that calculated according to formula (after Eucken and Kuhn).

$$k_{mix} = \frac{n_{KCl} \cdot k_{KCl} + n_{KBr}\, k_{KBr}}{n_{KCl} + n_{KBr}}$$

where n represents the proportion of the respective component present in the mixture. The correlation between calculated and measured values is represented in Figure 7.

The authors maintain that Mathiesen's law for expressing the effect of impurities on the electrical conductivity may also be used to indicate the effect of impurities on the thermal conductivity, viz:

$$w_u = w_v + \Delta$$

where

w_u = thermal resistivity of an impure aggregate

w_v = thermal resistivity of a pure crystal = $\frac{1}{K}$

Δ = "Increment" resistance which should be independent of temperature.

Birch and Clarke used the concept that the heat flows through piles in the aggregate; no heat was supposed to flow across the side walls of the piles. The piles were considered to be one crystal thick and to contain the constituents in the same proportion in which they occur in the whole mass, in random distribution and in orientation. When the thickness of the sample was too small with respect to the crystal size, the "series" treatment became inappropriate and a "parallel" consideration was employed.

Although the heat flow is much more complicated than the previous two treatments suggest, the "series" concept was found to agree with experimental data within 5 percent, except where the crystal thickness was small with respect to the crystal size. In that case the parallel treatment gave correct values. The authors concluded that the grain size should not be important unless an appreciable proportion of the resistance occurs at the intercrystalline contacts. This resistance is low for relatively fresh igneous rocks. They ascribed the permanent decrease in conductivity of the rocks when heated over 300 deg C in part to loss of moisture and development of imperfections.

De Vries (25) expressed the thermal conductivity of a granular material as a function of the thermal conductivities and the volume fractions of its constituents by making use of the analogy between heat conductivity, electric conductivity, dielectric constant, magnetic permeability and diffusion coefficient. Because of mathematical difficulties only an approximate solution can be given. Different authors used different approximations to find a solution for the case of a composite material consisting of a continuous medium in which particles of spherical or ellipsoidal shape are distributed at random. All these theories were developed mainly in analogy with the theory of the dielectric constant. This means that the phenomena specifically associated with heat conduction are not taken into account.

Before the various theories studied by De Vries are discussed in detail, it might be advantageous to consider some other effects.

In the calculation of the thermal conductivity of mixed crystals either the method

used by Birch and Clarke can be followed or the theory of Maxwell-Burger-Eucken. Table 14 gives the conductivities of mixed crystals as determined by Eucken and Kuhn from pressed crystal pastes. The value of the conductivities of the pure crystals were also obtained from Eucken and Kuhn's data. The values were calculated for 0 deg C.

Table 15 gives examples taken from the investigations of Birch and Clarke. The rocks tested were considered to consist of major constituents such as quartz ($k_{av.}$ = .069),

TABLE 14

THERMAL CONDUCTIVITIES OF MIXED CRYSTALS
in watt/sq cm °C per cm

Composition by Volume, Percent			Shape of Particle	Measured Conductivity	Calc. Conduct.	
					Birch and Clarke	Burger and Eucken
Kcl	KBr	NaCl				
100	--	--	--	0.0900	--	--
--	100	--	--	0.0365	--	--
--	--	100	--	0.088	--	--
8.7	91.3	--	Spherical	0.0290	0.0385	0.0397
22.3	77.7	--	Spherical	0.0196	0.0420	0.0452
46.4	53.6	--	Spherical	0.0237	0.0504	0.0562
72	28.0	--	Spherical	0.0336	0.0636	0.0704
88.6	11.4	--	Spherical	0.0484	0.0770	0.0815
58		42	Spherical	0.0694	0.0891	0.0892

plagioclase feldspar ($k_{av.}$ = .019), olivine ($k_{av.}$ = .044), pyroxene ($k_{av.}$ = .0415) and orthoclase feldspar (k = .0193). The minor constituents were grouped with some of the major components, e.g.: hornblende and magnetite with olivine or pyroxene; sericite with feldspar; microperthite assumed to have a k value of 0.020; biotite assumed to have the same conductivity as pyroxene. The thermal conductivities were calculated for 50 deg C.

HEAT CONDUCTION IN GLASSES

It was observed that the thermal conductivity of quartz glass with the same chemical composition as that of a quartz crystal decreases with decrease in temperature. As was previously indicated $\frac{c_v}{k}$ is approximately constant for quartz glass where c_v = specific heat and k = thermal conductivity of the glass. Eucken (31) approximated the thermal conductivity of glass by the formula:

$$\frac{1}{k_g} = C + \frac{D}{T}$$

in which:

k_g = thermal conductivity of the glass

T = absolute temperature

C and D are constants

TABLE 15

THERMAL CONDUCTIVITIES OF CERTAIN ROCKS
in watt/ sq cm °C per cm

Rock	Composition[a]		Particle Size, mm	Measured Conduct.	Calc. Conductivity[a]	
	Mineral	Percent			Birch and Clarke	Eucken and Burger
Barre granite	Quartz Albite Orthoclase Biotite	26 37 25 12	1.2 x 0.8 medium 1.5 x 1 spheres	0.0264	0.0268	0.0309 (0.0280)
Quartz monzonite	Quartz Orthoclase $Ab_{72}An_{28}$ Biotite Hornblende	34 27 33 5 1	1 x 0.8 1.0 dia. medium spheres	0.0294	0.0264	0.0320 (0.0296)
Tonalite	Quartz $Ab_{55}An_{45}$ Biotite Hornblende	28 50 15 7	1 x 0.8 medium 1.2 x 0.9	0.0260	0.0268	0.0326 (0.0291)
Wisconsin gabbro	$Ab_{40}An_{60}$ Pyroxene Olivine	73 15 12	medium spheres spheres	0.0197	0.0209	0.0223
Rockport granite	Quartz Microperthite Amphibole	30 64 6	1.5 x 1 medium spheres	0.0340	0.0268 (0.0348)	0.0299 (0.0334)

[a] Biotite grouped with feldspar instead of with pyroxene, gives the values in parentheses in the last column. Both calculated values for Rockport granite are far off. Following the suggestion by Birch and Clarke that a parallel treatment would be more appropriate in this case, the value in parentheses in the fifth column was obtained. The value in parentheses in the last column was obtained by considering the quartz as the continuous medium and the other components as dispersed in it.

TABLE 16

THERMAL CONDUCTIVITY OF SOME GLASSES
in watt/sq cm °C per cm

Glass	Temperature °C						
	-200	-100	0	100	200	300	400
Quartz Glass	0.00612	0.0110	0.0136	0.0148	0.0158	0.0170	0.0185
Pyrex Glass			0.0120	0.0132	0.0144	0.0155	0.0166
Heavy Optical Flint	0.00303	0.0058	0.0071	0.0075			
Obsidianite			0.0135	0.0146	0.0157	0.0157	0.0179
Soiled Quartz Glass	0.00467	0.00900	0.01122	0.0125	0.0131		0.0150

From the concept of glasses being liquids with high viscosities, it was proposed that the Bridgman formula, developed for liquids, be used for calculating the thermal conductivity of glasses. Some basic differences exist, however, as was pointed out by Birch and Clarke (8): The molecular weight of glass is not exactly defined and two types of waves exist in glasses instead of the one compressional wave in liquids.

If the formula is used to determine the average distance between the heat propagating units from known conductivity values, it is found that the distance comes out to be in the order of the distance between nearest silica atoms in silica glass (3.3 Å). For this (8) a mean velocity $V = \frac{1}{3}(V_l + 2V_t)$ was used in the equation:

$$k = \frac{3\bar{k}V}{\delta^2}$$

TABLE 17

CONDUCTIVITY, k, OF SOME FIREBRICKS
in watt/sq cm °C per cm (from Ref 17)

Brick								
Type	Constituents, Percent					Density, lb/cu ft	Temp., °C	k
	MgO	Fe_2O_3	CaO	SiO_2	Al_2O_3			
Magnesite	86.8	6.3	3	2.6	--	158	204	0.0381
							650	0.0277
							1,200	0.0190
Alumina	--	--	--	--	82	170	500	0.0223
							800	0.0211
							1,100	0.0208
	--	--	--	--	41	115	500	0.0104
							800	0.0107
							1,100	0.0109
Silica	--	--	--	93	--	105	500	0.0132
							800	0.0147
							1,100	0.0161
	--	--	--	96	--	110	500	0.0147
							800	0.0163
							1,100	0.0177
Silicon carbide	--	--	--	--	--	129	600	0.1852
							800	0.1592
							1,000	0.1385
							1,200	0.1212
							1,400	0.109

where V_l and V_t are the velocities of the longitudinal (compressional) and distortional waves, respectively, $\hat{k}$ is the Boltzmann constant and δ is the distance between the nearest silicon atoms in silica glass.

The Debye formula gives greater distances for the mean free path (8.5 Å for silica glass, 4.9 Å for diabase glass). This indicates an atom-to-atom heat exchange. The thermal waves are scattered in such short distances by the random assembly of the atoms that the wave concept becomes irrelevant. For the same reason, small amounts of impurities probably have little influence. Table 16 gives a few values for the thermal conductivities of glasses.

CONDUCTION IN CRYSTALLINE-AMORPHOUS MATERIAL

Eucken (30) found from measurements on materials such as paraffin and ebonite that the thermal conductivity of these partly crystalline, partly amorphous materials is little temperature dependent. Jakob (43) discussed the variations encountered in the thermal conductivities of various sorts of magnesite bricks of about the same density and of moderately varying content in magnesium oxide (86 to 92 percent). He concluded that, in cases where small values of conductivity with positive temperature coefficients were observed, the bricks contained predominantly glassy substances. Where the conductivity was large and had a negative temperature coefficient, the materials consisted mainly of crystalline components. Analogous results were found by Birch and Clarke (8) on some feldspar aggregates.

Eucken (31) proposed the following approximate equations:

$$\text{for uniform crystals:} \quad \frac{1}{k_{cu}} = AT$$

$$\text{for mixed crystals:} \quad \frac{1}{k_{cm}} = AT + B$$

$$\text{for glasses:} \quad \frac{1}{k_g} = C + \frac{D}{T}$$

in which k_c and k_g are the thermal conductivities of the crystals and glasses and A, B, C and D are constants. Assuming (43) that the material is an aggregate of heat resistors of crystalline and amorphous types connected in series, the following expression is obtained:

$$k = \frac{1}{aT + b + \frac{C}{T}} \quad ,$$

a, b, and c being constants.

The equation gives an increase of k with increasing temperature if T is small and a decrease of k with increasing temperature if T is high. This results from the three equations of Eucken. It will be noticed, too, that the form of the equation is related to the curve by Makinson.

The burning of a refractory material influences k considerably because of the chemical and crystallographic changes as well as the changes in density due to sintering. Sintering or cementation also reduce the surface area per unit volume thereby improving the interfacial conductivity. In fire bricks the chemical composition has an influence on the conductivity. Table 17 shows the influence of predominance of MgO, Al_2O_3 and SiO_2 on the thermal conductivity of fire bricks.

CONDUCTION IN GRANULAR MATERIALS

Granular materials are defined as systems composed of a solid phase or phases within a liquid or gaseous environment. In such systems, the surfaces between the

phases are of more importance than in the case of pure solid aggregates.

Fine Powders

From considerations of the kinetic theory of gases, Kundt and Warburg (51) pointed out that for a gas flowing along a wall a discontinuity of velocity occurs. They also did experiments to verify their conclusion. Smoluchowski (89) applied this concept to thermal conduction and found, also from experiment, that a corresponding temperature discontinuity exists. The temperature discontinuity θ if replaced by an assumed continuous change of gas temperature dT leads to the equation (43):

$$k\frac{dT}{dn} = h\theta \qquad \text{or} \qquad \theta = \xi\frac{dT}{dn}$$

in which

k = thermal conductivity of the gas

n = distance in direction normal to the wall

h = coefficient of heat transfer between wall and medium, and

$\xi = \frac{k}{h}$ is a coefficient of discontinuity

An analogous ξ for the discontinuity θ in the velocity v of a gas flowing along a wall is given as:

$$\theta = \xi\frac{dv}{dn} .$$

The quantity ξ measured in centimeters is dependent on the type of gas and the character of the wall. The coefficient of discontinuity is of the same order of magnitude as the free path of the molecules and proportional to the free path; it is, therefore, also inversely proportional to the absolute pressure of the gas.

From measurements by Smoluchowski (90), Gehrcke (34) and Lasareff (53),

$$\xi = A \times (10^{-6})\frac{760}{p} ,$$

where

p = gas pressure in millimeters of mercury, and

ξ is measured in centimeters.

For air: $A = 13.4$ to 19.6

For CO_2: $A = 8.0$ to 12.7

For hydrogen: $A = 105$ to 145

The rate of heat conduction for two parallel walls at distance L and temperature difference ΔT will be

$$q = k\frac{A}{L}\Delta T .$$

When a perfectly conducting plate of thickness s is inserted, the total width of gas layer will be $(L - s)$ but the effective length will be $(L - 2 + 2\xi)$. For n plates we obtain:

$$q = k\frac{A}{(L - ns + 2n\xi)}T .$$

With decrease in pressure 2ξ will increase and will eventually become greater than s. The use of fine powders and reduction of pressure can lead to lower conductivity values than possessed by air.

While it is still widely believed that the lowest value of the thermal conductivity under atmospheric pressure is that of stationary air, it was shown by Kistler and Caldwell (50) on silica aerogel, by Johnstone, Jacobson and Prechshot (47) on zinc

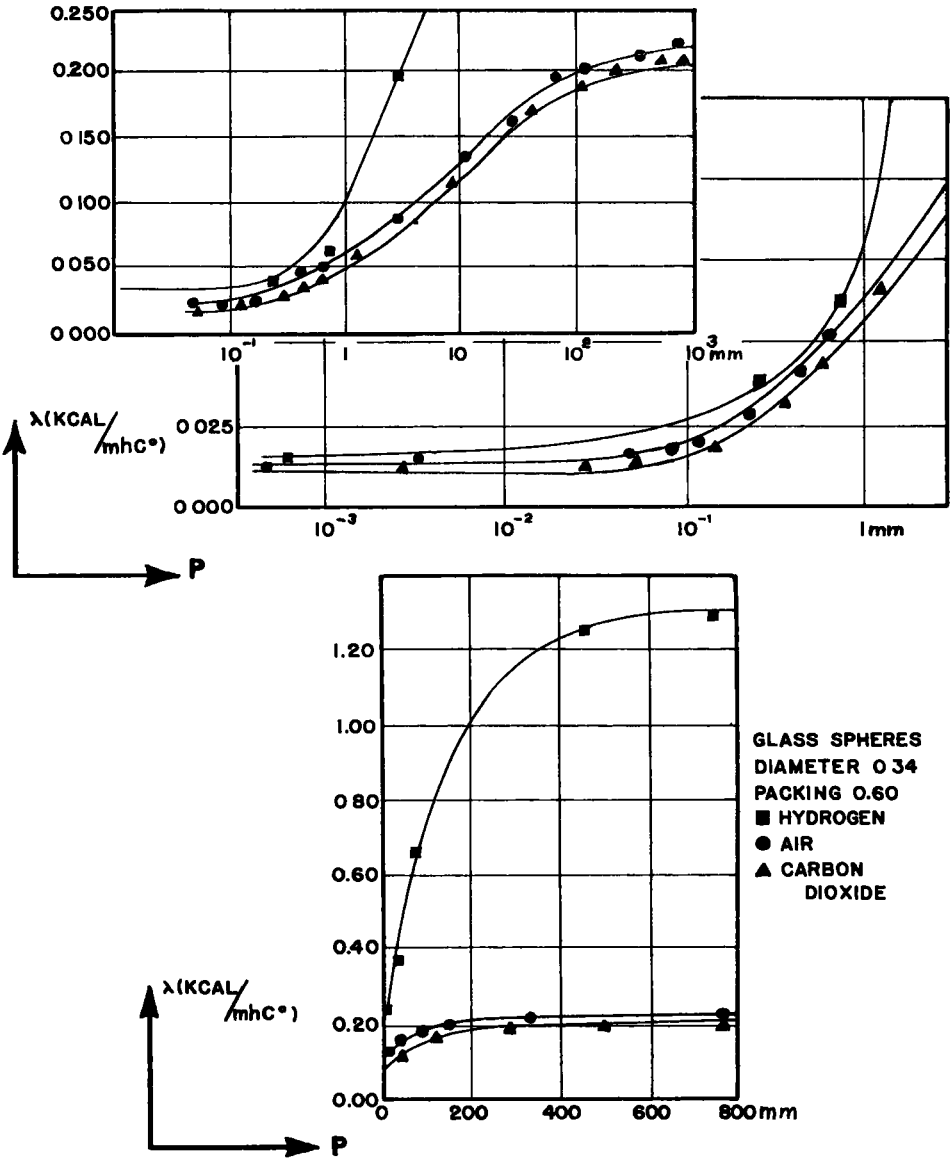

Figure 8. Heat conduction by a powder of glass spheres in different atmospheres at different pressures.

oxide, and by Smith and Wilkes (88) on carbon blacks, that still lower values can be reached when the above materials are used. An aerogel results when a gel is dehydrated without loss of the structure of the solid constituent. The silica aerogel (density 7.49 lb/cu ft) had good mechanical strength (30 pounds per square inch without crushing), a pore size of the order of 10^{-6} cm in diameter and appeared optically empty under the ultra-microscope. Kistler and Caldwell also showed that the thermal conductivity of cork decreases when the pressure is lowered. The zinc oxide powder (density 1.78 lb/cu ft) gave conductivities about the same as air at atmospheric pressure. When the powder was compressed the conductivity increased. Reduction in gas pressure decreased the conductivity. Carbon blacks in the finely divided state have conductivities less than that of still air. For the commercial carbon black pellets (spheron) tested, Smith and Wilkes found a conductivity value close to that of

air. The density was 20.2 lb/cu ft.

From heat conduction measurement on powders in various gaseous atmospheres, Prins et al (77) found some residual conductivity at very low pressure (see Fig. 8). This conductivity was attributed to solid contact of the particles. Magnesium oxide being angular gave a lower residual value than glass spheres. The pressures ranged from 880 mm to 4×10^{-4} mm of mercury. Calculation of the contact radii based on a formula by Hertz gave the right order of magnitude.

De Vries (25) employed a simplified method to calculate theoretically the limits within which the thermal conductivity must lie, taking into account the touching of particles. In an assumed cubical array of spheres the lower limit is obtained when a pile of spheres is divided into concentric cylinders and the cylinders are combined in parallel. The upper limit is obtained when all planes perpendicular to the axis of the sphere pile are considered as isothermal planes – essentially a series treatment. As was observed by the investigator, the values obtained from the two treatments differ widely, thereby limiting its practical value. He believed that the correct value will be close to the lower limit considering test data by Prins and others.

Porous and Loose Materials

In heat insulators use is made of substances composed of small particles with a high percentage of void space between them. The solid material may consist of porous particles (the solid phase being continuous), powders, grains, fibers, etc.

The use of fine powders for heat insulation has been discussed. Insulating materials of fibrous and porous material make use of the insulating value of the air in the material which is kept stationary by the presence of the solid phase. This eliminates convection currents of the air and thereby reduces the conductivity of the material. The fibers themselves may possess a low heat conductivity. However, it has been shown (58, 101) that material of high conductivity, like aluminum foil – plain or crumpled, may be used for insulation. The bright surface reflects the heat and reduces the transmission of heat by radiation. The value of aluminum foil insulation is therefore greater at high temperatures where radiation plays a predominant role in heat transport.

Calculation of Thermal Conductivities

Eucken (31) proposed the following expression for the apparent conductivity k of a material consisting of a medium of conductivity k_s in which small particles of conductivity k_p are dispersed.

$$k = k_s \frac{1 - \left(1 - a\frac{k_p}{k_s}\right)b}{1 + (a - 1)b}$$

where

$$a = \frac{3k_s}{2k_s + k_p}$$

$$b = \frac{V_b}{V_s + V_b}$$

in which

V_b = total volume of dispersed particles

V_s = total volume of medium

The equation can be used only for values of b that are less than 0.5. When the particles in the medium consist of air then k_p will be small compared to k_s, resulting in the equation:

$$k = k_S \frac{1 - b}{1 + \frac{b}{2}}$$

For elliptic or tubular pores the equation becomes:

$$k = k_S \frac{1 - b}{1 + \frac{b}{3}}$$

For plane gaps with one-third of all fissures extending perpendicular to the direction of heat flow, Eucken derived the formula:

$$\frac{1}{k} = \frac{1}{k_S} + \frac{b}{3 k_p}$$

By considering a fissured body as a series of parallel solid plates and air layers of thickness L_{12} and L_{23} respectively, Nusselt (66) derived the following equation taking into account the effect of radiation. Referring to Figure 11(A):

$$k = \frac{L_{12} + L_{23}}{\frac{L_{12}}{k_S} + \frac{1}{\frac{k_p}{L_{23}} + 4\sigma T^3}}$$

in which σ is the radiation constant and T the absolute temperature. For very high temperatures: $4\sigma T^3 \gg 1$, one obtains:

$$k = \frac{L_{12} + L_{23}}{L_{12}} k_S \quad .$$

If radiation is neglected at low temperatures and $k_p \ll k_S$, then the lower limit of the heat conductivity will be:

$$k = \frac{L_{12} + L_{23}}{L_{23}} k_p \quad .$$

From the field of electricity and magnetism, De Vries (25) applied the theories of the behavior of granular media to the problem of thermal conductivity. He considered an isotropic medium with dielectric constant ϵ_0 in which there are grains of different types. All grains having the same dielectric constant and being of the same shape and size are grouped as one type of particle. The volume fraction of grains of the i-type is given as x_i, the volume of the medium is x_0. If there are N types of particles, then:

$$\sum_{1=0}^{N} x_1 = 1$$

The mean apparent dielectric constant of the material is then:

$$\epsilon = \frac{\overline{D}}{\overline{E}} = \frac{\sum_{i=0}^{N} i\, x_i\, \overline{E}_i}{\sum_{i=0}^{N} x_i\, \overline{E}_i} \qquad (A)$$

where:

$\overline{D}$ = mean dielectric displacement,

$\bar{E}$ = mean electric field-strength

$\bar{E}_i = \frac{1}{V_i} \int E_i \, dV_i$ = mean electric field-strength within particle i, and

V_i = volume of particle.

Because of mathematical difficulties equation (A) cannot be solved exactly. To calculate $\bar{E}_i$, it is assumed that all grains of the i-type are surrounded by a homogeneous, isotropic medium with dielectric constant ϵ^1 in which a field-strength E^1 exist at great distance from the particle under consideration.

By means of tensor analysis (74) it is possible to obtain a solution after values for ϵ^1 and E^1 have been selected. The different theories treated by De Vries (25) differ mainly in the selection of ϵ^1 and E^1. The theories are as follows:

(1) Theory of Maxwell (59), Burger (14), Eucken (31).

Assumption: $\epsilon^1 = \epsilon_0$ and $E^1 = \bar{E}_0$; that means, the interaction of the grains is neglected. Maxwell used it in the calculations for spherical grains; Burger extended it to ellipsoidal particles for the electrical conductivity, while Eucken first applied it to thermal conductivity.

(2) Theory of Ollendorf (67)

Assumption: $\epsilon^1 = \epsilon_0$, $E^1 = \bar{E}_p$, where $\bar{E}_p$ is the field which will exist in the space of a removed ellipsoid. It is further assumed that the polarization remains unchanged in the rest of the ellipsoids. Ollendorf then derived a formula for $\bar{E}_p$, the magnetic permeability.

(3) Dielectric constant, Theory of Polder and Van Santen (74)

Assumption: $\epsilon^1 = \epsilon$; $E^1 = \bar{E}$.

(4) Differential Theory of Bruggeman (12) which has been improved upon by De Vries (25).

Assumption: $\epsilon^1 = \epsilon$; $E^1 = \bar{E}$, the same as the previous but in order to get the volume fraction of Δx_1, the grain of the first type is thought to be added in small quantities with volume fraction Δx_1 approaching zero.

In the treatment of Rayleigh (78) the effect of the arrangement of the grains on the conductivity is taken into account. De Vries has shown how the theory could be extended to some other packings as was treated by Rayleigh.

De Vriesthen compares the various theories with each other and also with experimental data on grains of spherical shape. He concludes that for the ratio of particle conductivity k_1 to the conductivity k_0 of the medium $\frac{k_1}{k_0} < 300$ the correct value of the net conductivity k will lie between the theoretical values of Maxwell and Bruggeman while for $1000 < \frac{k_1}{k_0} < 2000$ the value of k will be within 10 percent of the value given by Bruggeman's formula and will be greater. The volume fractions varied from 0.42 to 0.69. The deviation of experimental data obtained for soil from the Maxwell-Burger-Eucken theory is of the same order of magnitude as that for spherical particles. Because of the various assumptions it was pointed out that the treatment is of semi-empirical character.

At an earlier stage we introduced the method of Birch and Clarke for calculating the thermal resistivity of mixed aggregates. In this treatment, heat flow piles one crystal thick are made up of its components arranged in series; each constituent is present in the same proportion in which it occurs in the whole mass. Compare with Figure 9(A)

where

k_g = conductivity of the gas; x_g its volume fraction,

k_W = conductivity of the water; x_W its volume fraction

k_S = conductivity of the solid; x_S its volume fraction.

For the series treatment the effective conductivity k can be calculated from:

$$\frac{1}{k} = \frac{x_g}{k_g} + \frac{x_w}{k_w} + \frac{x_s}{k_s} \tag{1}$$

The parallel treatment results in the equation:

$$k = k_g x_g + k_w x_w + k_s x_s \tag{2}$$

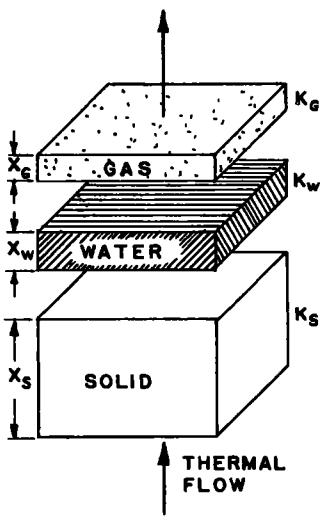

SERIES TREATMENT

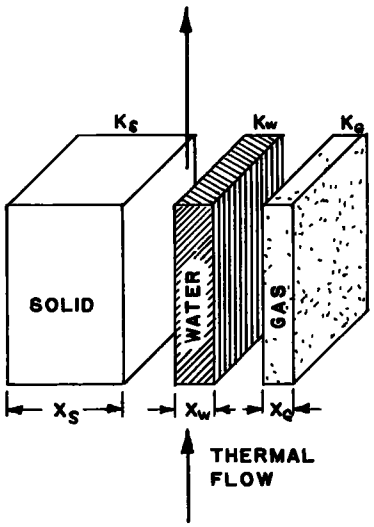

PARALLEL TREATMENT

(A.)

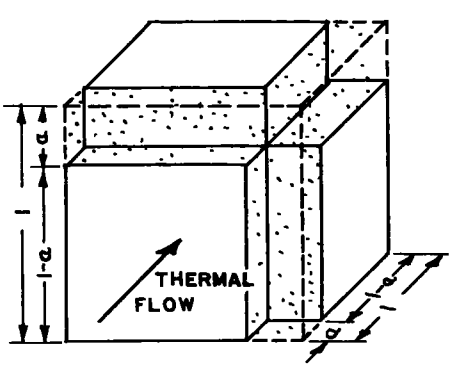

DRY SOIL

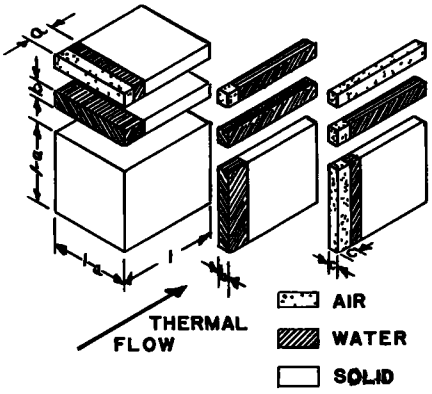

MOIST SOIL

MICKLEY'S MOIST-SOIL MODEL
(B)

Figure 9.

It is obvious that actual values of k will lie somewhere between those given by (1) and (2). The first equation does not take into account intergranular contact while the second one assumes perfect intergranular contact.

Another method of approximating the thermal conductivity of a soil mass is that given by Mickley (61). His picture of the three-component system is as shown in Figure 9(B). The equations derived for the condition shown are as follows: (61)

$$\underline{\text{Completely Dry Soil:}}\quad k = k_g a^2 + k_s (1-a)^2 + \frac{k_s k_g (2a-2a^2)}{k_s(a) + k_g(1-a)}$$

$$\underline{\text{Completely Saturated Soil:}}\quad k = k_w a^2 + k_s (1-a)^2 + \frac{k_s k_w (2a-2a^2)}{k_s(a) + k_w(1-a)}$$

In these equations the volume fraction of the solid $x_s = 1 - 3a^2 + 2a^3$ from which a can be calculated if x_s is known.

Moist Soil:

$$k = k_g c^2 + k_s (1-a)^2 + k_w (a-c)^2 + \frac{2k_w k_g c\ (a-c)}{k_w c + k_g (1-c)} + \frac{2k_s k_w k_g c\ (1-a)}{k_w k_s c + k_s k_g (a-c) + k_g k_w (1-a)} + \frac{2k_w k_s (a-c)(1-a)}{k_s a + k_w (1-a)} \qquad (3)$$

Expressed in volume fractions x_s, x_w and x_g it follows:

$$x_g + x_w = 3a^2 - 2a^3 \quad \text{or} \quad x_s = 1 - 3a^2 + 2a^3$$

$$x_g = 3c^2 - 2c^3.$$

Equation (3) yields the complete dry or saturated soil condition when b = 0 (c=a) or b = a (c=0), respectively. This equation is a means of averaging between equations (1) and (2). As was stated by Mickley, the equation (3) does not hold for dry or nearly dry soil because the contact between grains is not always a face contact. The equations (1), (2) and (3) do not take into account the size, shape and arrangement of the components of the soil.

W.O. Smith (87) took into account the possibility of structure in the soil. His derivation runs similar to that of Mickley for dry or saturated soil except that he assumes a different ratio of voids in series to voids in parallel with the solid and neglects intergranular contact. From Figure 10 the thermal conductivity follows to be:

$$k = k_g \frac{\Sigma A_a}{A} + \frac{\Sigma A_s}{A} \left(\frac{1}{\frac{d_s}{k_s d} + \frac{d_l}{k_g d}} \right)$$

where

k_g = thermal conductivity of air

k_s = thermal conductivity of the solid

A_a = area of the air column

A_s = area of the grain pile column,

d_s = total length of grains in column length d, and

d_i = total length of air gaps between grains in grain column

Further, if

A = total area of the soil sample

P_a = partial volume of all the soil air

P_s = partial volume of the solid framework

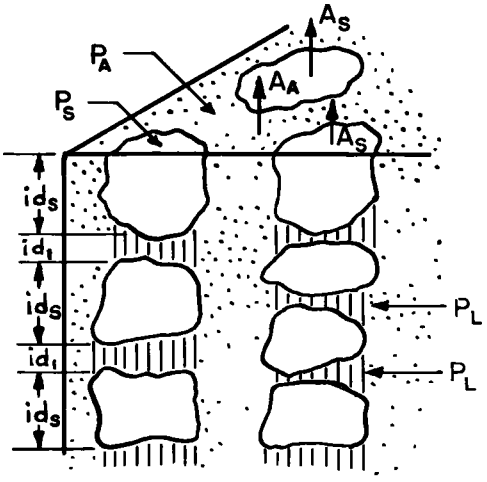

GRAIN PILE FOR DEVELOPMENT OF HEAT FLOW EQUATION

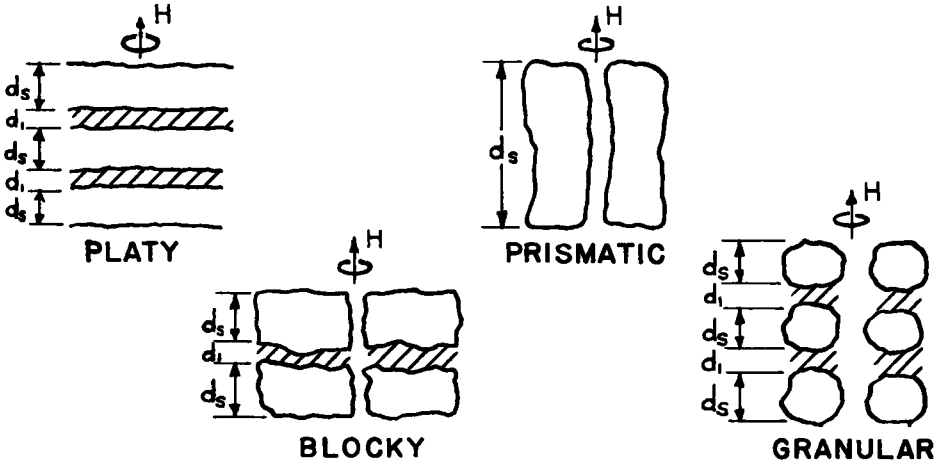

VARIOUS SOIL STRUCTURAL FORMS

Figure 10. Heat conduction in structured soil (after W. O. Smith).

P_i = partial volume of the material in the gaps between the grains in the grain column

$$k = k_g (P_a - P_i) + \frac{P_s + P_i}{\frac{1}{P_s + P_i}\left(\frac{P_s}{k_s} + \frac{P_i}{k_g}\right)}$$

If $k_g P_1$ is neglected (being small) and $a = \frac{P_1}{P_s}$ then

$$k = k_g P_a + \frac{P_s (1 + a)}{\frac{1}{k_s} + \left(\frac{1}{k_g} - \frac{1}{k_s}\right)\left(\frac{a}{1 + a}\right)}$$

This formula may be used for calculating the thermal conductivity of structured soil if a proper value of P_1 is chosen.

P_a denotes the total porosity structural and textural;

P_1 denotes the pore space effective in introducing resistance in series with the grains and will depend on the type of structure;

P_1 can be obtained by calculating values of a from observed data. The equation has the form:

$$k = k_g P_a + k_o P_s \quad \text{or} \quad k_o = \frac{k - k_g P_a}{P_s}$$

where

$$k_o = \frac{1 + a}{\frac{1}{k_s} + \left(\frac{1}{k_g} - \frac{1}{k_s}\right)\left(\frac{a}{1 + a}\right)}$$

and is called the effective conductivity of the soil. From this equation a is calculated if k_o is obtained from experiments on structured soil and from known values of k_a and k_s. A few values of k_o are indicated in Table 18.

Assuming the grains to be spherical and the water collected around the particle

TABLE 18

THERMAL STRUCTURE FACTORS OF DRY SOIL

k_o in 10^{-3} watt/sq cm °C per cm

Soil Structure	Approx. Dimensions cm	Structured $a = \frac{P_1}{P_s}$	k_o	Finely Fragmented $a = \frac{P_1}{P_s}$	k_o
Coarse Blocky		0.036	5.65	0.063	3.80
	1 to 3	0.039	5.30	0.060	3.91
Medium Blocky	0.8 to 2	0.045	4.94	0.072	3.42
	1 to 2.5	0.044	5.00	0.075	3.30
	0.6 to 1.9	0.045	4.81	0.071	3.45
		0.046	4.63	0.071	3.47
	1.3 to 1.9	0.047	4.65	0.058	4.01
		0.059	3.95	0.060	3.92
	1 to 2	0.041	5.15	0.063	3.80
Coarse Platy	0.6	0.041	5.22	0.061	3.90
Medium Platy	0.2 to 0.4	0.051	4.45	0.066	3.68
		0.053	4.37	0.066	3.68
Fine Platy	0.1 to 0.2	0.054	3.96	0.056	4.11
Medium Granular	0.5 to 1.0	0.060	4.15	0.065	3.60
		0.069	3.72	0.074	3.35
Fine Granular	0.1 to 0.3	0.094	2.77	0.075	3.38

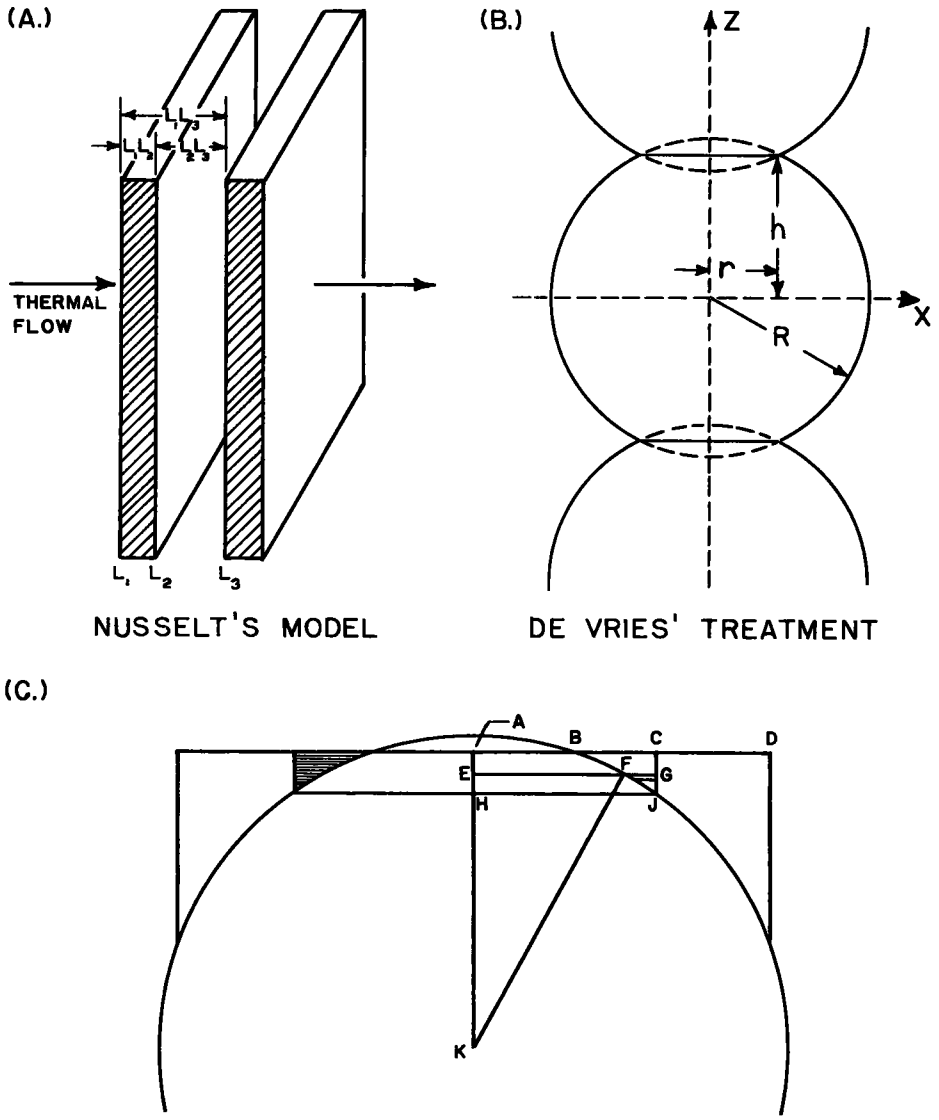

Figure 11.

contacts as shown in Figure 11(C), Gemant (37) derived an approximate formula for the thermal conductivity of moist soil. He neglected the conductivity of the air and the influence of the water rings around the middle four contacts of the grain. Strictly speaking, therefore, his formula only holds for moisture contents up to about 0.2 percent. In the figure: $KH = y_o$; $HJ = x_o$; $AB = a$ = radius of the flat contact surface; $KF = r$ = the radius of the spherical particle. If m is the moisture content and k_s and k_w the thermal conductivities of solid and water, respectively, we have:

$$(2y_o^3 - 3y_o^2 + 1) = 1.272\ m$$

$$f^2 = (1 + a^2)\ k_s - y_o^2 k_w$$

$$g^2 = k_s - k_w$$

$$f'^2 = (1 + 2^2)\, k_s$$

$$g'^2 = k_s$$

The resistivity of the soil is then given as:

$$R = \frac{1}{k} = \frac{2}{\pi fg} \log \frac{(f+g)(f-gy_o)}{(f-g)(f+gy_o)} + \frac{2}{\pi f'g'} \log \frac{f' + g'y_o}{f' - g'y_o}$$

Gemant maintains that this equation gives good agreement with the experimental data above 5 percent moisture. Below 5 percent the experimental data are higher. Unfortunately the formula does not account for variation in densities or in grain sizes.

Making use of a cubical array of spheres, Figure 11(B), and following De Vries' (25) reasoning to calculate the limits of the conductivity when touching of particles occurs, two equations which approximate the dry soil or saturated soil condition are obtained.

For the lower limit De Vries considers the circumscribed cube, and the formula becomes:

$$4R^2k = (4R^2 - \pi R^2)k_g + \int_0^r 2\pi k_s x\,dx + \int_y^R 2\pi \frac{hk_sk_g}{hk_s - 2(k_s - k_g)}\, x\,dx .$$

Integrated it becomes:

$$k = \frac{\pi r^2}{4R^2} k_s + \frac{\pi k_s k_g (R^2 - r^2)}{2R^2 (k_s - k_g)} \left(\frac{k_s}{k_s - k_g} \ln \frac{k_s}{k_g} - 1 \right) + \left(1 - \frac{\pi}{4}\right) k_g .$$

The upper limit is given by the formula:

$$\frac{h}{k} = \int_0^h \frac{dz}{\frac{\pi}{4}\left(1 - \frac{z^2}{R^2}\right)(k_s - k_g) + k_o} ; \quad k = \frac{b\, h\pi (k_s - k_g)}{2R \ln \frac{bR+h}{bR-h}}$$

where:

$$b = \left(1 + \frac{4\, k_g}{\pi (k_s - k_g)}\right)^{1/2} \quad \text{for } k_s >> k_g ;$$

when

$k_g = 0$ the combined equations yield:

$$\frac{\pi r^2}{4R^2} k_s \leq k \leq \frac{\pi h k_s}{2R \ln \frac{R+h}{R-h}}$$

De Vries concluded that the value of the equation is minimized by the fact that the limits are too far apart. Sample calculations for dry soil are given in Table 19.

The examples were taken from experimental work by Kersten (49), Smith (86) (87) and Smith and Yamauchi (84). The table contains the thermal conductivities as determined for the dry soils and also conductivities computed by means of the equations of Eucken (31), Smith (87), Nusselt (which is identical with the Birch and Clarke series treatment), Mickley, and De Vries for the lower limit. The conductivity of dry air k_g was taken as .00024 watt/cm deg C in all cases. The conductivity of the solid particles k_s was taken as given by the investigators whose experimental data were used. The value of k_s for the Chester soil (derived from gneiss) is given by Smith (87) as .025 watt per cm deg C, that of the Miami soils (glacial till) was .0293 watt per cm deg C.

For the soils investigated by Kersten the values were extrapolated to zero void space

TABLE 19

SAMPLE CALCULATION FOR THERMAL CONDUCTIVITIES OF DRY SOIL

Soil	Composition, Percent	Porosity	Thermal Conductivity, watts/sq cm °C per cm						
			Measured	Calculated					
				Smith	Eucken		Nusselt	Mickley	DeVries
Crushed quartz	95 quartz	0.37	0.00429	0.00351	0.0160	(0.00139)	0.00065	0.01076	0.0048
		0.275	0.00720	0.00380	0.0191	(0.00199)	0.00087	0.01345	0.0058
Lowell sand	72 quartz	0.40	0.00271	0.00259	0.0082	(0.00121)	0.0006	0.00975	0.00275
	22 feldspar	0.325	0.00357	0.00290		(0.00155)	0.00074	0.01148	0.00352
	6 pyroxene				0.0093				
Healy clay	23 quartz	0.604	0.00156	0.00166	0.0099	(0.0007)	0.0004	0.00583	0.00217
	55 kaolinite	0.48	0.00296	0.00209		(0.0010)	0.0005	0.0081	0.00352
	22 coal				0.0137				
Chester loam[a]	20-50 sand	0.439	0.00299	0.00295	0.0115	(0.0011)	0.00055	0.0091	0.00348
	20-50 silt								
	20-30 clay								
Miami silty clay[b]	50 sand	0.552	0.00137	0.00137	0.0103	(0.00088)	0.00043	0.00677	0.00268
	20 clay								
Miami silty clay[c]	0-30 sand	0.348	0.00353	0.00354	0.0162	(0.0015)	0.00069	0.01113	0.0048
	50-80 silt								
	20-30 clay								

[a] B horizon, red-brown clay loam

[b] A horizon, dark-brown silt loam

[c] C horizon, olive-drab silty clay loam

using his formula. For crushed quartz: $k_S = .03$; Lowell sand: $k_S = .016$; Healy clay: $k_S = .0327$. The bracketed data in column 6 are calculated assuming the air to be the continuous medium; the figures without brackets, assuming that the solid phase is continuous. De Vries' formula was modified to include the effect of porosity.

The conductivities were computed for a temperature of 50 deg C.

The theory of Maxwell (59) Burger (14) Eucken (31) gives according to de Vries the most promising results of the various theories treated. It assumes $\epsilon^1 = \epsilon_0$ and $E^1 = \bar{E}_0$ in the formula:

$$\epsilon = \frac{\sum_{i=0}^{N} \epsilon_i x_i \bar{E}_i}{\sum_{i=0}^{N} x_i \bar{E}_i}$$

Dividing through by $\bar{E}_0$ it becomes:

$$\epsilon = \frac{\sum_{i=0}^{N} \epsilon_i x_i k_i}{\sum_{i=0}^{N} x_i k_i} \quad \text{where} \quad k_i = \frac{\bar{E}_i}{\bar{E}_0}$$

Because of the tensorial relationship between $\bar{E}_1$ and E^1 the values of k_1 is given by

$$k_i = \tfrac{1}{3} \left(\frac{1}{1 + (\frac{\epsilon_i}{\epsilon_0} - 1) A_1} + \frac{1}{1 + (\frac{\epsilon_i}{\epsilon_0} - 1) A_2} + \frac{1}{1 + (\frac{\epsilon_i}{\epsilon_0} - 1) A_3} \right).$$

For ellipsoidal particles the value of A_1 is given by Scholte (81). Introducing a, b and c for the half-axes of the ellipsoid, we obtain for:

(1) Prolate spheroid: $a > b = c$; $\frac{a}{b} = p$

$$A_1 = \frac{-1}{p^2-1} + \frac{p}{\sqrt{p^2-1}^3} \cdot \ln (p + \sqrt{p^2-1})$$

$$A_2 = A_3 \text{ and } A_1 + A_2 + A_3 = 1$$

(2) Oblate spheroid: $a < b = c$; $\frac{a}{b} = p$

$$A_1 = \frac{1}{1-p^2} - \frac{p}{\sqrt{1-p^2}^3} \cos^{-1} p$$

$$A_2 = A_3 \text{ and } A_1 + A_2 + A_3 = 1$$

(3) Sphere: $a = b = c$

$$A_1 = A_2 = A_3 = \tfrac{1}{3}$$

(4) Long cylinders with elliptical cross sections:

$$a = nb \qquad c = \infty$$

$$A_1 = \frac{b}{a+b}; \quad A_2 = \frac{a}{a+b}; \quad A_3 = 0$$

(5) Laminae: $b = c = \infty$

$$A_1 = 1 \qquad A_2 = A_3 = 0$$

It was indicated that the error will be less than 20 percent using Eucken's formula when the ratio between the heat conductivity of the particles and that of the medium is less than approximately 20. In moist soil the water may be assumed as the medium over a wide range of moisture contents. The solid particles and air bubbles are treated as the inclusions. In this manner the requirements are satisfied. Also for inclusions having conductivities less than that of the medium the theory gives values that are too high and for inclusions having higher conductivity, values that are too low. In moist soil therefore the errors tend to compensate each other.

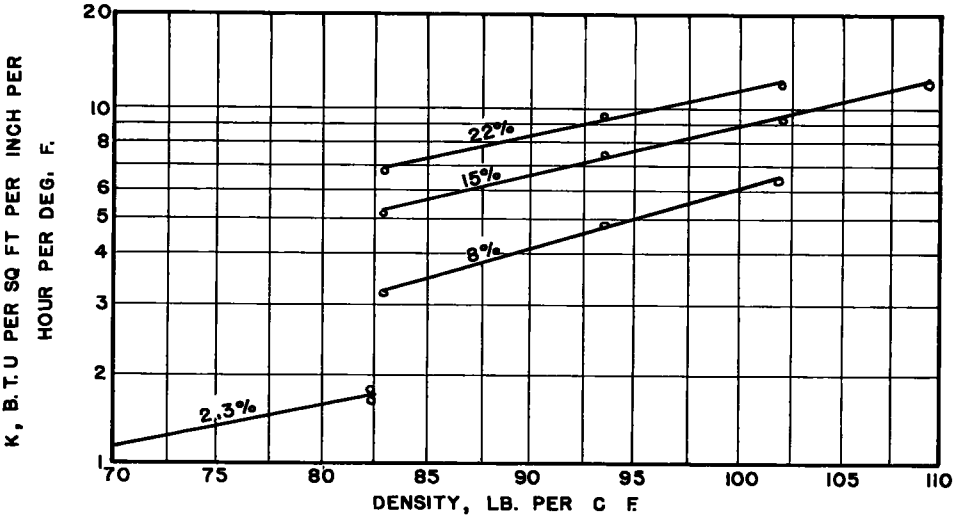

VARIATION OF THERMAL CONDUCTIVITY
WITH DRY DENSITY OF SOIL
VALUES ON CURVES GIVE CONSTANT MOISTURE CONTENT

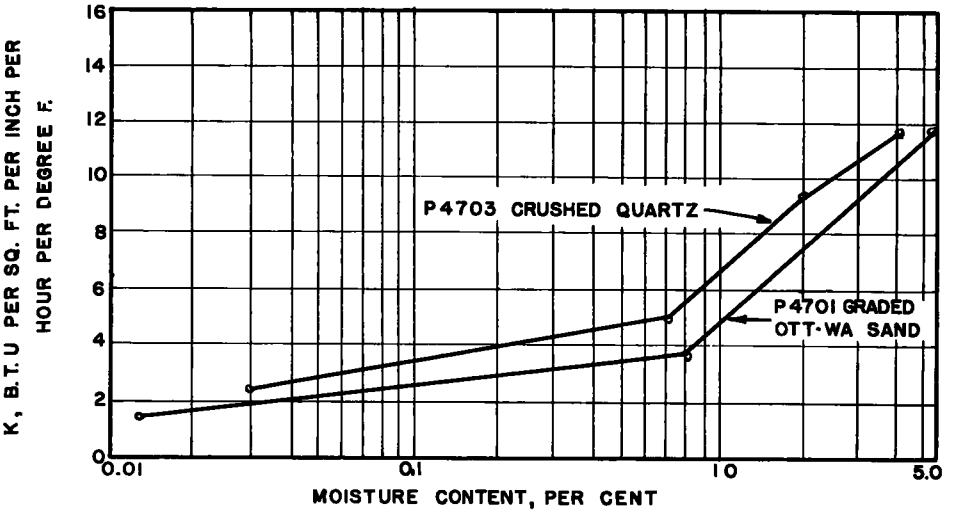

COMPARISON OF THERMAL CONDUCTIVITY
OF TWO QUARTZ SOILS

Figure 12.

The shape of the solid particles is assumed to be ellipsoidical. A_1 is calculated from data obtained from vapor diffusion measurements ($A_1 = 0.144$). In this case "effective flattening" is considered which will not necessarily correspond to the real dimensions of the particles because it includes the effect of angularity and other deviations from ideal ellipsoidal form. The shape of the air particles is also taken as ellipsoidal but it changes with variation in moisture content. The conductivity of the air varies with the amount of free moisture in it and depends, therefore, on the temperature, the moisture content and the soil type. For the calculations of A_1 of soil air De Vries made use of a simple calculation assuming linear interpolation. At 20 deg C and from experimental values of the thermal conductivity of a moist soil ($A_1 = 0.144$ for soil) the formula is derived to be:

$$A_1 = 0.333 - 0.697x_g \text{ for air.}$$

The mean thermal conductivity k_S of the solid constituents is calculated according to their volume fractions and individual mean conductivities. A parallel treatment is assumed leading to the equation for N types of soil minerals.

$$k_S \text{ mean} = \sum_{i=0}^{N} k_i x_i$$

where

k_i = thermal conductivity of the i-type of mineral

x_i = volume fraction of the i-type

From data obtained experimentally on nineteen soils ranging from crushed rock and sand to clay and peat, Kersten (49) derived empirically formulas for calculation of the thermal conductivity of soil when the type of soil, density and moisture content are known. The variation of conductivity with density and moisture content is shown in Figure 12. From these relationships the following equations for prediction of thermal conductivity are derived and given by Kersten:

(1) Silt and clay soils (more than 50 percent silt and clay); unfrozen:

$$k = [1.3 \log (\text{moisture content}) - 0.29)]10^{0.01S-3}$$

(2) Silt and clay soils; frozen:

$$k = 1.44 \times 10^{0.022S-5} + 12.2 \text{ (moisture content)} \times 10^{0.008S-5}.$$

(3) Sandy soils; unfrozen (less than 50 percent silt and clay):

$$k = [1.01 \log (\text{moisture content}) + 0.58]\, 10^{0.01S-3}.$$

(4) Sandy soils; frozen:

$$k = 11.0 \times 10^{0.013S-5} + 4.6 \text{ (moisture content)} \times 10^{0.0146S-5}.$$

In these equations k is in watt/sq cm deg C per cm, S is the dry density in pounds per cubic foot and the moisture content is taken as a percentage of the dry soil weight. The equations for silt and clay are valid for moisture contents of 5 percent or more; for sandy soils at a moisture content, one percent or more. For a sandy soil with fairly high silt and clay content the average obtained from the two equations may be taken. The equations yield, with careful use, values of k within 25 percent accuracy.

In a later article Gemant (35) (36) took into account the effect of density, temperature, composition (sand-clay) and size of particles in developing an equation from a soil grain model shown in Figure 13(A). The temperature determines the amount of water absorbed on the grain m_0 and this has to be subtracted from the total amount of water present to give the water collected between the grains m, taking part in the conduction of heat; a, b and z_w are linear dimensions as shown in the figure. If s represents the density, and w the total moisture content we have:

(A.)

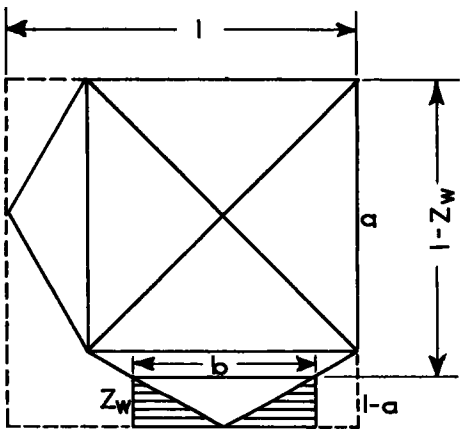

UNITARY CUBE OF MOIST SOIL ACCORDING TO GEMANT

(B.)

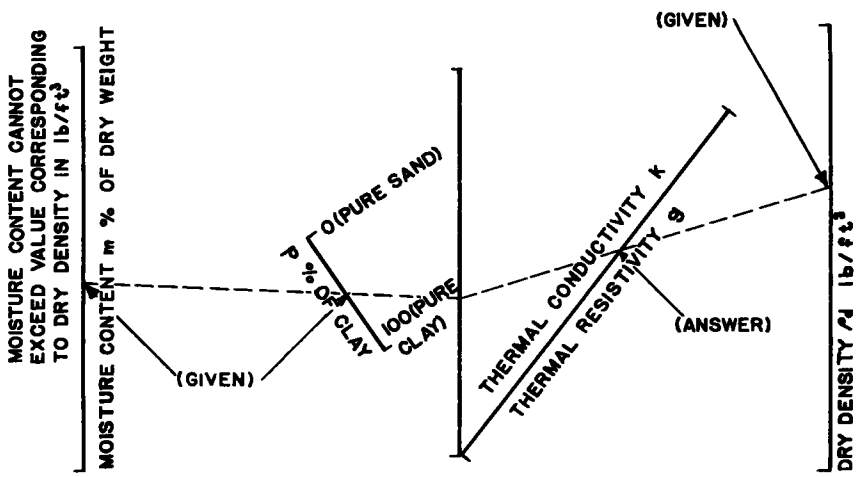

NOMOGRAM FOR DETERMINATION OF THERMAL CONDUCTIVITY AND RESISTIVITY OF SANDY SOIL

Figure 13.

$$a = 0.078\sqrt{s}$$

$$m = 0.16 \times 10^{-3}\, sw - mo$$

$$b^2 = \left(\frac{a}{1-a}\right)^{2/3} \left(\frac{m}{2}\right)^{2/3}$$

$$z_w = \left(\frac{1-a}{a}\right)^{2/3} \left(\frac{m}{2}\right)^{1/3} = \frac{m}{2b^2}$$

Also $k_s = 58.4 - 0.33p$ = thermal conductivity of the solid constituents, where p = percentage of clay in the mixture of sand and clay.

The final equation for the resistivity r of the soil:

TABLE 20

CALCULATED THERMAL CONDUCTIVITIES OF MOIST SOIL
in 10^{-3} °C per cm

Soil	Moisture Content Weight Percent	Volume	Dry Density lb/cu ft	Porosity	Conduct. Meas.	Mickley	Gemant (2nd)	Burger Eucken	Kersten	Nomograph
Crushed quartz	1.9	0.0312	102.8	0.379	13.72	23.1	3.9	18.1	9.13	8.5
	4.3	0.0706	102.7	0.380	18.5	23.5	12.2	18.7	13.0	13.4
	2.1	0.0403	119.6	0.276	23.6	28.5	11.0	24.7	14.2	13.5
	3.7	0.0535	120.2	0.273	30.4	29.1	19.7	25.3	18.3	19.5
Lowell sand	4.1	0.0656	99.8	0.400	12.23	22.5	11.4	11.9	11.9	13.0
	11.8	0.211	111.9	0.329	22.53	27.7	19.9	15.2	21.8	20.0
	14.0	0.253	112.8	0.323	22.22	28.6	16.0	16.8	23.3	21.5
Healy clay	10.7	0.143	83.6	0.482	6.38	12.6	8.4	10.5	7.2	8.8
	22.7	0.304	83.6	0.482	9.11	13.8	11.4	11.7	10.1	11.0
	34.8	0.450	80.6	0.500	12.63	14.6	12.3	12.4	10.2	11.5
Chester loam B-horizon	7.49	0.094	75.5	0.545	2.53	14.1	7.68	8.7	4.8	8.5
	14.8	0.170	69.2	0.583	3.03	13.4	8.92	8.5	6.1	9.0
	25.2	0.324	77.3	0.534	4.28	16.2	13.7	10.4	9.1	12.5
I.S. Clay	30.0	0.337	70	0.575	8.57	10.0	8.26	9.6	8.17	7.65
	50.0	0.560	70	0.575	10.55	11.7	9.80	11.1	9.63	8.8
	18.0	0.318	110	0.331	13.0	16.6	15.80	15.5	16.7	16.2

$$r = \frac{1}{k} = \left[\frac{(1-a)}{a}\right]^{4/3} \frac{\tan^{-1}\sqrt{\frac{k_s - k_w}{k_w}}}{(\frac{m}{2})^{1/3}\left[k_w(k_s-k_w)\right]^{1/2}} + \frac{1-z_w}{k_s a} f\ (\frac{b^2}{a})$$

where:

k_w = conductivity of water = 6

$f(\frac{b^2}{a})$ is an experimental function of given linear dimensions a and b; k, k_s and k_w are all measured in 10^{-3} watt/sq cm deg C per cm.

According to Makowski and Mochlinski (57) the previous formula has the same form as the Kersten formula expressed by them as:

$$k = (a \log_{10} m + b)\, 10^{\frac{s}{100}} - 3 \quad \text{watt/sq cm deg C per cm}$$

in which a and b represent linear functions of the clay content p.

$$a = 1.42408 - 0.00465p \text{ and } b = 0.4192 - 0.00313p.$$

The two authors constructed a nomograph using the Gemant and Kersten formulas from which can be read directly the resistivity or conductivity when the clay content, moisture content and dry density are given. The nomograph is of the form shown in Figure 13(B).

They discussed the Mickley, Gemant and Kersten equations and indicate that Gemant's give the best results for sandy soils, relatively high moisture contents and high densities. It is not reliable for moisture contents below one or two percent and low densities.

Calculated values of the thermal conductivity of moist soil are shown in Table 20. The experimental data used were obtained from the same investigators as for the dry soil computations. The value of k_s used in the calculation of conductivities by the Mickley and Gemant (second equation (35), (36)) equations were computed from the formula (57):

$$k_s = 58.4 - 0.33p \text{ in milliwatts/cm deg C}$$

where p is the percentage of clay in the soil. The conductivity of water was taken as:

$$k_w = 6 \text{ milliwatt/cm}^2 \text{ deg C per cm}$$

In the Mickley and Burger-Eucken equations, the conductivity of air was assumed to be that of moist air at approximately 40 deg C.:

$$k_g = 2.5 \text{ milliwatt/cm}^2 \text{ deg C per cm.}$$

The equation of Burger-Eucken was used following the interpretation of De Vries (25).

DISCUSSION OF RESULTS

In the preceding treatment, the best available theories of thermal conduction in single, di- and multiphase systems have been discussed and the results of their application have been compared with experimental data. The purpose of a theory is, firstly, to permit a visualization of the action mechanism of a physical or chemical phenomenon, preferably in terms of the science of mechanics, and, secondly, to provide a simple mathematical formulation of the phenomenon with the least possible number of physical parameters and of necessary assumptions. In the normal development of a theory, the visualization precedes the mathematical formulation.

The final mathematical formulation may follow immediately the first visualization or may be separated from it by a shorter or longer chain of development. In fact, the latter may be so long that the original visualization is forgotten, or the phenomenon may be so complex that it cannot be completely expressed by a simple picture, but requires a set of differential equations. Whatever be the final mathematical formulation, in the beginning is the picture, and the picture, if it is essentially correct, leads not only to an understanding of the phenomenon and to its expression in mathematical form but also indicates physical or chemical means by which the phenomenon may be changed qualitatively or quantitatively. If such change is the purpose of a study, then a relatively crude visualization may be more important that the refined mathematical formulation.

The picture of the actual thermal phenomena, occurring in soil systems of interest to the engineer, is quite complex with heat conduction, heat convection and material convection taking place in multiphase systems. In order to develop an understanding systematically, the present treatment was restricted to heat conduction. Because of the presence of gaseous, liquid and solid phases in normal soils, the theories of heat conduction in gases, liquids and solids were introduced and discussed before treatment of the more complex granular systems and especially of soils was attempted.

The theory developed for the gaseous phase conforms with the hypothesis of the molecular kinetic theory and is in good agreement with experimental data; in fact, the success of the theory to explain experimental data also in heat conduction was a proof of the kinetic theory of heat. The expression for heat conduction holds for an ideal gas over a large pressure and temperature range. In the case of non-ideal gases or more complex situations the basic concept remains the same but modification has become necessary.

The liquid state is easily recognized and circumscribed in a general way, but it is scientifically more complex than the solid and gaseous states. This is the reason why in its scientific exploration the liquid has been treated for a long time either as an imperfect gas or as a disturbed crystal, or as something intermediate between gas and crystal. Only now is evolving a molecular theory of liquids deserving of its name. Unfortunately, already in its present state this theory has become so abstract and has left its physical model concepts so far behind that its most modern version cannot be profitably applied to our problem. In addition, in soils one is dealing with a very peculiar liquid "water".

The equation derived by Bridgman for the heat conduction in liquids has the advantage of simplicity but gives only approximative results. The average error is 15.2 percent with a maximum error of 39 percent (85). Some assumptions made by Kardos are erroneous as was pointed out by Smith (85) and his equation must be considered as only semi-empirical. However, in view of the close agreement of his calculated values with experimental data some physical significance may be attributed to his concepts. The velocity of sound through the medium may be regarded as a measure of the rate of energy exchange between molecules. To which degree the theoretical equation of Bridgman will correspond with actual values at different temperatures and pressures, is not known because of the inadequate experimental data.

The theory of the crystal state is much more advanced than that of the liquid state; however, no heat conductivity theory has been developed as yet for the solid state of the same validity and simplicity as that of Bridgman for liquids. The expression of Debye with modifications and additions by Peierls (72) (73) and Makinson, involves parameters that cannot be obtained accurately by computation or by direct measurement. Yet evidence is not sufficient to disprove the basic principles on which the theory of Debye is based.

As was pointed out by such investigators as Birch and Clarke, Eucken, De Haas and Biermasz, some additional variables, or different expression of the variables involved, must be taken into account to provide for the differences in experimental data. It is true and also logical that different workers in the field obtain different results, but the data should be within experimental error and should not differ as much as those which are found in the literature for the heat conductivity of crystals. As was mentioned, variation in purity and "micro structure" may account for some of the differences.

The influence of these factors is hard to evaluate because the degree of purity and "mosaic structure" developed is difficult to determine and is usually not given with the other data.

A further test of a theory is to apply it in explanation for the different heat conductivities in different directions occurring in anisotropic crystals. Neither the theory of Wooster (103) which attempts to correlate thermal conductivity with the crystal structure, nor that of Eucken and Kuhn (32) which explains variation in conductivity in crystals in terms of their respective hardness (strength of chemical bonds) appears to be very successful.

This is about as far as any theory went. From Tables 12, and, especially, 13 it must be concluded that Eucken and Kuhn's theory regarding aggregates cannot be valid. The data on mixed crystals presented by Eucken and Kuhn cannot be explained unless the contact between the crystals gives rise to the large deviation from the formulas in Table 14. In contrast to the data in Table 14, the calculated values in Table 15 show reasonable agreement with the experimental data. It must be pointed out, however, that this good agreement is obtained only after adjusting the formulas or after experienced use of the equations and after knowledge of the governing factors in the material under consideration had been obtained.

In glasses, the thermal conductivity increases with increase in temperature. This is the case with all non-crystalline substances including liquids. By following this analogy and by applying Bridgman's formula for liquids the distance between heat propagating units is in the order of the distance between silica atoms in glass. If we consider the silicon atom the center of the "unit cell" (from the crystal concept), the analogy between liquids and glasses becomes more apparent. However, as was pointed out by Birch and Clarke there exist the already mentioned basic differences.

In granular systems the discontinuity of energy and temperature that exists on a solid-gas interface has been recognized and experimentally proven. It is reasonable to assume that a similar phenomenon exists between a solid and a liquid phase. The reduction in conductivity which occurs when an aggregate is substituted for a pure crystal suggests the probability that an interfacial phenomenon exists also on solid-solid phase boundaries. From Kersten's data on the relationship between heat conductivity and crushed quartz content and gradation, it was found that, for the same temperature and the same low moisture content (0.02 percent), the logarithm of the thermal conductivity plotted against density gave two parallel straight lines. The conductivity of the crushed quartz was higher than that of the sand. Since crushed stone sand possesses greater mechanical resistance than rounded natural sand, it is difficult to decide to what extent the increased thermal conductivity of the former at the same density was due to macro-factors of interlocking and contact or to micro-factors such as the different physico-chemical character of the fresh and old grain surfaces, respectively.

The importance of the interfacial resistance has been recognized but not quantitatively evaluated. Even the qualitative picture of what is happening on the boundary between two phases has in many instances defied comprehension. It is felt that a thorough investigation of this point will add markedly to the understanding of soil systems, not only with respect to thermal conductivity but also in regard to most of the important physical characteristics of soils.

The total basic knowledge available on thermal conductivity is not very impressive. No simple equation could be developed even for pure crystals. This situation indicates that a large deal of theoretical work must be accomplished before heat conduction in complex, multiphase systems such as soils can be thoroughly comprehended. On the other hand, the very primitive state in which the theory finds itself gives hope that its further rational development will bear fruits of practical as well as academic importance. At the present time only empirical or semi-empirical equations have been developed to calculate the thermal conductivities of different soil types at different moisture and density conditions. These equations are all based on simplified assumptions concerning the geometry of the grains in contact. They vary from the purely empirical formulas of Kersten to what may be considered the more theoretical equations of De Vries, and Maxwell-Burger-Eucken. Tables 19 and 20 show the reliability

of these approaches. It is obvious that none of the equations is able to give consistently dependable results. The greatest deviation of calculated from experimental values was found for the structured soils – a situation which is likely to be encountered in the field. All the theories mentioned try to express the thermal conductivity of the whole system in terms of the various conductivities of its constituents; however, in their practical use the value of the solid phase conductivity is commonly selected so as to fit the experimental data. This may be practically justified because of temperature discontinuities existing at the boundaries but it stamps the methods as no better than semi-empirical. However incomplete, the equations do give an indication of the order of magnitude of the thermal conductivity of a soil in equilibrium. They are, in a way, all valuable because each makes use of some different approach which may

TABLE 21

VARIATION OF THERMAL CONDUCTIVITY OF CORUNDUM POWDER with Grain Size in 10^{-3} watt/cm^2 ^{0}C per cm

Average Grain Size mm	Measured Density lb/cu ft	Measured Conductivity	Calculated Conductivity at 113.8 16/cu ft Density	
0.60	106.8	3.44	4.28	(4.05)
0.45	113.8	5.89	5.89	(5.89)
0.30	111.6	5.04	5.39	(5.30)
0.175	94.7	3.74	6.27	(5.80)
0.125	103.7	4.17	5.70	(5.27)
0.090	104.4	4.80	6.42	(5.96)
0.075	99.8	4.08	6.30	(5.64)
0.015	66.0	2.14	9.94	(6.44)
0.006	58.5	1.78	9.94	(6.35)

bear fruit in the comprehension of the total situation. The most rapid methods are the nomograms of Makowski and Mochlinski and Kersten's equations. The Maxwell-Burger-Eucken theory has the better mathematical basis, while that of Gemant gives physically the best interpretation. For dry soil the formula of De Vries is considered to be the most representative.

The influence of particle size on conductivity is not clearly pointed out in the formulas treated. Its effect is included in the designation sand, silt and clay (from a size classification). However, the difference in mineralogical character of the different size fractions makes this effect dependent on mineral type as well as on size characteristics. The work of Patten (71) on dry carborundum powder of varying grain sizes produced the first data of real value in this respect. Table 21 gives the variation of the thermal conductivity as a function of the grain size of carborundum powder. The conductivities were calculated back to one density using Kersten's formula for conductivity-density relationships in dry, crushed quartz.

The calculation of the figures in brackets employs the equation found by Kersten for fine crushed quartz. However, the use of the formulas in this respect is somewhat debatable because, as Kersten's formulas show, the particle size has an effect on the influence of the density. The equations can be a useful practical tool in evaluating conductivities but may in certain cases hide the real mechanism of conductivity. Although not quite clear from his data, Patten concludes that for the same moisture content coarse quartz has a higher conductivity than fine quartz flower. He explains it by the assumption that less water is absorbed on the surface of large particles and that the available water can therefore accumulate between the grains and consequently

increase the conductivity. The specific and over-all effect of granulometry still remains to be formulated. Little doubt exists about the importance of size, shape and packing of component particles on the physical properties of soils including their thermal conductivities. Investigation of these granulometric and structural factors will be given primary emphasis in the Princeton research.

ACKNOWLEDGMENTS

This report covers a part of an extensive research project on thermal conductivity and related phenomena in soils and similar granular systems. This research is sponsored by the Insulated Conductor Committee of the American Institute of Electrical Engineers and is guided by a special committee of this organization under the chairmanship of R. W. Burrell of the Consolidated Edison Company of New York. The research is being conducted at the Soil Physics Laboratory, Department of Civil Engineering, School of Engineering, Princeton University. Grateful acknowledgment is made to all those that have aided this work in official and non-official capacity, especially to Admiral W. Mack Angas, Chairman, Department of Civil Engineering, and J.C. Elgin, School of Engineering, Princeton University.

REFERENCES

1. Arrhenius, S., "Über die Reaktionsgeschwindigkeit bei der Inversion von Rohrzucker durch Säuern," Zeitschrift f. physik. Chem., 4: 226-48 (1889).
2. _____, Meddel. Vetenskapsakad. Nobelinst, 3: 20 (1916).
3. Bates, K.O., Hazard, G. and Palmer, G., "Thermal Conductivity of Liquids," Ind. Eng. Chem., 10:6, 314-8 (1938).
4. Bates, K.O., "Thermal Conductivity of Liquids," Ind. Eng. Chem., 28:4, 494-8 (1936).
5. _____, "Thermal Conductivity of Liquids," Ind. Eng. Chem., 25:4, 431-7 (1933).
6. _____, "Thermal Conductivity of Liquid Silicones," Ind. Eng. Chem., 41:9, 1966-8 (1949).
7. Baum, E., "Über den Temperaturkoeffizienten der Viskosität von Flüssigkeiten," Kolloid-Zeitschrift, 135: 176-82 (1954).
8. Birch, F. and Clark, H., "The Thermal Conductivity of Rocks and its Dependence upon Temperature and Composition," Amer. Journ. Sci., 238: 529-58, 613-35 (1940).
9. Bragg, W.H. and Bragg, W.L., "X-Rays and Crystal Structure," 4th Ed., Bell & Sons, Ltd., London (1924).
10. Bridgman, P. W., "The Thermal Conductivity of Liquids," Proc. Nat. Acad. Science, 9: 341-5 (1923).
11. Bromley, L.A. and Wilke, C.R., "Viscosity Behavior of Gases," Journal Engineering Chemistry, 43:7, 1641-48 (1951).
12. Bruggeman, D.A.G., "Berechnung verschiedener physikalischer Konstanten von heterogenen Substanzen," Annalen der Physik, V, 24:636-79 (1935).
13. Buddenberg, J.W. and Wilke, C.R., "Calculation of Gas Mixture Viscosities," Ind. Eng. Chem., 41:7, 1345-47 (1949).
14. Burger, H.C., "Das Leitvermögen verdünnter mischkristallfreier Legierungen," Phys. Zeitsch. 20:73-76 (1919).
15. Chapman, S., "The Kinetic Theory of a Gas Constituted of Spherically Symmetrical Molecules," Royal Society of London Phil. Trans. (a), 211:433-84 (1912).
16. Chapman, S. and Cowling, T. G., "Mathematical Theory of Non-Uniform Gases," Cambridge University Press (1939).
17. "Chemical Engineer's Handbook," McGraw-Hill, N.Y., 824 (1934).
18. Comings, E.W. and Egly, R.S., "Viscosity of Gases and Vapors at High Pressures," Ind. Eng. Chem., 32:5, 714-18 (1940).
19. Cornelissen, J.and Waterman, H.I., Chem. Eng. Science, London, 4:239-46 (1955).

20. Debye, P., "Vorträge über die kinetische Theorie der Materie und Elektrizität," Leibzig und Berlin (1914).
21. De Guzman, J., Annales soc. espan. fis. quim., 353 (1913).
22. de Haas, W.J. and Biermasz, T. "Die Wärmeleitfähigkeit von Kristallen bei tiefen Temperaturen," Physica, 5:320-24 (1938).
23. _____, "The Thermal Conductivity of Diamond and Potassium-Chloride," Physica, 5:47-53 (1938).
24. DeSanarmont, Annalen Chim. Phys., (1848, 1850, 1887).
Poggendorfs Annalen, (1848, 1849, 1850).
Wiedemanns Annalen, (1848, 1850).
25. DeVries, D.A., "Het warmtegeleidings vermogen van grond," Doctor's Thesis. Rijksuniversiteit te Leiden (1952).
26. Drude, P., "Zur Elektrontheorie der Metalle, Annalen der Physik, IV, 1: 566-613 (1900).
27. Eucken, A., "Allgemeine Gesetzmässigkeiten für das Wärmeleitvermögen verschiedener Stoffarten und Aggregatzustände," Forschung a.d. Geb. d. Ingenieurswes, 2:6 (1940).
28. _____, "Die Wärmeleitfahigkeit einiger Kristalle bei tiefen Temperaturen," Phys. Zeitschrift, 12:1005-8 (1911).
29. _____, "Über das Wärmeleitvermögen, die spezifische Wärme und die innere Reibung der Gase," Phys. Zeitsch. 14:324-32 (1913).
30. _____, "Über die Temperaturabhängigkeit der Wärmeleitung fester Nichtmetalle," Annalen der Physik, IV, 34:185-221 (1911).
31. _____, Verein deutscher Ingenieure, Forschungsheft No. 353, Berlin (1932).
32. Eucken, A. and Kuhn, G., "Ergebnisse neuer Messungen der Wärmeleitfähigkeit fester krystallisierter Stoffe bei 0^0 und -190^0 C," Zeitschrift fur phys. Chem., 134:193-219 (1928).
33. Fairbanks, D.F. and Wilke, C.R., "Diffusion Coefficients in Multi-Component Gas Mixtures," Ind. Eng. Chem., 42:3, 471-5 (1950).
34. Gehrcke, E., "Über die Wärmleitung verdünnter Gase," Annalen der Physik, IV, 2:102-114 (1900).
35. Gemant, A., "Die Wärmeleitfähigkeit des Bodens," Archiv der Elektrischen Übertragung, 5:539 (1951).
36. _____, "How to Compute Thermal Soil Conductivities," Heating, Piping and Air Conditioning, 122-123 (Jan., 1952).
37. _____, "The Thermal Conductivity of Soil," Journal of Applied Physics, 21: 750-4 (1950).
38. Glasstone, S., Laidler, K.J. and Eyring, H., "The Theory of Rate Processes," McGraw-Hill, N.Y. (1941).
39. Grunberg, L. and Nissan, A.H., "Viscosity of Highly Compressed Fluids," Ind. Eng. Chem., 42:5, 885-91 (1950).
40. Hildebrand, J.H., "The Liquid State," Proc. Phys. Soc. London, 56:221-39 (1944).
41. Hirschfelder, J.H., Bird, R.B. and Spotz, E.L., "The Transport Properties of Non-Polar Gases," Journal Chem. Phys., 16:968-81 (1948).
42. Ingen-Houtz, J., "Sur les métaux comme conducteurs de la chaleur," Jour. de Phys., 34 (1786).
43. Jakob, M., "Heat Transfer," John Wiley & Sons, 1: (1949).
44. _____, "Warmeleitung," Handbuch der Physik, Band XI (1926).
45. Johnson, A.I. and Huang, C.J., "Thermal Conductivity Chart for Gases," Chem. Eng., 61:204-5 (Feb. 1954).
46. Johnson, E.F., "Molecular Transport Properties of Fluids,"
Ind. Eng. Chem., 46:889-93 (1954).
Ind. Eng. Chem., 47:599-604 (1955).
Ind. Eng. Chem., 48:582-85 (1956).
47. Johnstone, H.F., Jacobson, H.G. and Preckshot, G.W., "Heat Conductivity of Zinc Oxide," Ind. Eng. Chem., 33:1, 106-7 (1941).

48. Kardos, A., "Theorie der Wärmeleitung von Flüssigkeiten," Forschung auf der Gebiete des Ingenieurwes, 5:14 (1934).
49. Kersten, M.S., "Thermal Properties of Soils," Bulletin 28, Eng. Exp. Station, University of Minnesota (1949).
50. Kistler, S.S. and Caldwell, A.G., "Thermal Conductivity of Silica Aerogel," Ind. Eng. Chem., 26:6, 658-662 (1934).
51. Kundt, A. and Warburg, E., "Über Reibung und Wärmeleitung verdünnter Gases," Annalen der Physik (Poggendorffs Annalen), 155: 337 & 525 (1875).
52. Lagemann, R.T., "Molecular Refraction-Viscosity Constant Nomograph," Ind. Eng. Chem., 37:6, 600 (1945).
53. Lasareff, P., "Über den Temperatursprung an der Grenze zwischen Metall und Gas," Annalen der Physik IV, 37. 233-46 (1912).
54. Lindsay, A.L. and Bromley, L.A., "Thermal Conductivity of Gas Mixtures," Ind. Eng. Chem., 42:8, 1508-11 (1950).
55. Loeb, L.B., "Kinetic Theory of Gases," McGraw Hill Book Co., N.Y. (1927).
56. Makinson, R.E.B., "The Thermal Conductivity of Metals," Proc. Camb. Phil. Soc., 34:474-97 (1938).
57. Makowski, M.W. and Mochlinski, K., "An Evaluation of Two Rapid Methods of Assessing the Thermal Resistivity of Soil," Proc. Inst. of Electrical Eng., 103: Part A (1956).
58. Mason, R.B., "Thermal Insulation with Aluminum Foil," Ind. Eng. Chem., 25:3, 245-55 (1933).
59. Maxwell, C., "Treatise on Electricity and Magnetism," Oxford, 365 (1873).
60. Meissner, A., "Leistungssteigerung durch thermische Verbesserung der Isolierstoffe," Elektotech. und Maschinenbau, 53: 25, 289-93 (1935).
61. Mickley, A.S., "The Thermal Conductivity of Moist Soil," Trans. American I.E.E. Tech. Paper 51-326, 70: 1789.
62. Mitra, S.S., "Relation between Vapor Pressure and Viscosity of Liquids," Jour. Chem. Phys., 22: 349-50 (1954).
63. Mitra, S.S. and Chakravarty, D.H., "Vapor Pressure and Viscosity of Liquids," Jour. Chem. Phys., 22: 1775-6 (1954).
64. Moore, W.J., "Physical Chemistry," Prentice-Hall Co., N.Y. (1950).
65. Mukherjee, A.K., Journ. Indian Chem. Soc., 30:725-7 (1953).
66. Nusselt, W., Zeitschrift d. Bayer. Revisionsver. No. 13 & 14 (1913).
67. Ollendorff, F., Arch. fur Elektrotechn., 25:436-447 (1931).
68. Othmer, D.F. and Conwell, J.W., "Correlating Viscosity and Vapor Pressures of Liquids," Ind. Eng. Chem., 37:11, 1112-5 (1945).
69. Othmer, D.F. and Josefowitz, S., "Correlating Viscosities of Gases with Temperature and Pressure," Ind. Eng. Chem., 38: 1, 111-6 (1946).
70. Palmer, G. "Thermal Conductivity of Liquids," Ind. Eng. Chem., 40: 1, 89-92 (1948).
71. Patten, H.E., "Heat Transference in Soils," U.S. Dept. of Agriculture, Bureau of Soils, Bulletin 59 (1909).
72. Peierls, R., "Zur kinetischen Theorie der Wärmeleitung in Kristallen," Annalen der Physik, 3:1055-1101 (1929).
73, _____, "Quelques propriétés typiques des corps solides," Ann. Inst. H. Poincaré, 5:177-222 (1935).
74. Polder, D. and Van Santen, J.H., "The Effective Permeability of Mixtures of Solids," Physica, 12:257-71 (1946).
75. Powell, R.E., Roseveare, W.E. and Eyring, H., "Diffusion, Thermal Conductivity, and Viscous Flow of Liquids," Ind. Eng. Chem., 33:4, 430-5 (1941).
76. Powell, R.W. and Griffiths, E., "The Variation with Temperature of the Thermal Conductivity and the X-Ray Structure of Some Micas," Proc. Royal Society, 163:189-98 (1937).
77. Prins, J.A., Schenk, J. and Schram, A.J.G.L., "Heat Conduction by Powders in Various Gaseous Atmospheres at Low Pressure," Physica, 16:379-80 (1950).
78. Rayleigh, W.R., "On the Influence of Obstacles Arranged in Rectangular Order Upon the Properties of a Medium," Phil. Mag., 34: 481-502 (1892).

79. Riedel, L., Chem. Ing. Tech., 27:209-13 (1955).
80. Sakiadis, B.C. and Coates, J., Paper 39 presented at the Annual Meeting of the Am. Inst. Chem. Engrs. (December 1954).
81. Scholte, Th. G., "A Contribution to the Theory of the Dielectric Constant of Polar Liquids," Physica, 15:5-6, 437 (1942).
82. Schudel, W., Schweiz. Ver. Gas- und Wasserfach, Monats-Bull., 22:112-131 (1942).
83. Schulz, K., "Die Wärmeleitung in Mineralien, Gesteinen und den künstlich hergestellten Stoffen von entsprechender Zusammensetzung," Fortschritte der Mineralogie, Kristallographie und Petrographie, 9:345-535 (1924).
84. Smith, G.S. and Yamauchi, T., "Thermal Conductivity of Soil for Design of Heat Pump Installations," Heating, Piping and Air Conditioning, 129-35 (July 1950).
85. Smith, J.F.D., "The Thermal Conductivity of Liquids," Trans., American Soc. Mech. Engrs., 58:719-25 (1936).
86. Smith, W.O., "Thermal Conductivities in Moist Soils," Proc. Soil Science Society of America, 4:32-40 (1939).
87. _____, "The Thermal Conductivity of Dry Soil," Soil Science, 53:6, 435-59 (1942).
88. Smith, W.R. and Wikes, G.B., "Thermal Conductivity of Carbon Blacks," Ind. Eng. Chem., 36:12, 1111-2 (1944).
89. Smoluchowski, M.R. von Smolan, Wiener Berichte 107 IIA, 304 (1898).
90. _____, Krakauer Anzeiger (A), 129 (1910).
Report on the 2nd International Congress on Heat, 2: 166 Wien (1910).
91. Stokes, G.G., "On the Conduction of Heat in Crystals," Coll. Papers Bd. 3, S. 203, Cambridge University Press (1901).
92. Sutherland, W., "The Viscosity of Mixed Gases," Phil. Mag., 40: 421-31 (1895).
93. _____, "The Viscosity of Gases and Molecular Forces," Phil. Mag., 5(36): 507-31 (1893).
94. Thelen, P., "The Differential Thermal Conductivities of Certain Schists," University of California Publication, Bulletin of the Dept. of Geology, 4:11, 201-26 (1904-06).
95. Thiesen, M., "Zur Theorie der Diffusion," Verhandl. deut. physik. Ges., 4:348-60 (1902).
96. Uyehara, O.A. and Watson, K.M., National Petroleum News, 36: 764 (1944).
97. Voigt, W., "Lehrb. d. Kristallphysik," Leibzig und Berlin, B.G. Treubner, 403 (1910).
98. Wassiljewa, A. "Wärmeleitung in Gasgemischen," Physik. Zeits, 5: 737 (1904).
99. Wilke, C.R., "Diffusional Properties of Multi-Component Gases," Chem. Eng. Prog., 46: 95-104 (1950).
100. _____, "A Viscosity Equation for Gas Mixtures," Jour. Chem. Phys., 18:517 (1950).
101. Wilkes, G.B., "Reflective Insulation," Ind. Eng. Chem., 31:7, 832-8 (1939).
102. Wood, W.A., "The Variation with Temperature of the Thermal Conductivity and the X-Ray Structure of Some Micas," Proceedings, Royal Society, 163:199-204 (1937).
103. Wooster, W.A., "Thermal Conductivity in Relation to Crystal Structure," Zeitschrift für Kristallographie, 95: 138-49 (1936).

THE NATIONAL ACADEMY OF SCIENCES—NATIONAL RESEARCH COUNCIL is a private, nonprofit organization of scientists, dedicated to the furtherance of science and to its use for the general welfare. The ACADEMY itself was established in 1863 under a congressional charter signed by President Lincoln. Empowered to provide for all activities appropriate to academies of science, it was also required by its charter to act as an adviser to the federal government in scientific matters. This provision accounts for the close ties that have always existed between the ACADEMY and the government, although the ACADEMY is not a governmental agency.

The NATIONAL RESEARCH COUNCIL was established by the ACADEMY in 1916, at the request of President Wilson, to enable scientists generally to associate their efforts with those of the limited membership of the ACADEMY in service to the nation, to society, and to science at home and abroad. Members of the NATIONAL RESEARCH COUNCIL receive their appointments from the president of the ACADEMY. They include representatives nominated by the major scientific and technical societies, representatives of the federal government, and a number of members at large. In addition, several thousand scientists and engineers take part in the activities of the research council through membership on its various boards and committees.

Receiving funds from both public and private sources, by contribution, grant, or contract, the ACADEMY and its RESEARCH COUNCIL thus work to stimulate research and its applications, to survey the broad possibilities of science, to promote effective utilization of the scientific and technical resources of the country, to serve the government, and to further the general interests of science.

The HIGHWAY RESEARCH BOARD was organized November 11, 1920, as an agency of the Division of Engineering and Industrial Research, one of the eight functional divisions of the NATIONAL RESEARCH COUNCIL. The BOARD is a cooperative organization of the highway technologists of America operating under the auspices of the ACADEMY–COUNCIL and with the support of the several highway departments, the Bureau of Public Roads, and many other organizations interested in the development of highway transportation. The purposes of the BOARD are to encourage research and to provide a national clearinghouse and correlation service for research activities and information on highway administration and technology.